ROLE OF TISSUE TRANSGLUTAMINASE INDUCED INTEGRIN TRAFFICKING IN KIDNEY CANCER METASTASIS

by
Ayca Zeynep İlter Akülke

Submitted to Graduate School of Natural and Applied Sciences
in Partial Fulfillment of the Requirements
for the Degree of Doctor of Philosophy in
Biotechnology

Yeditepe University
2016

ROLE OF TISSUE TRANSGLUTAMINASE INDUCED INTEGRIN TRAFFICKING IN KIDNEY CANCER METASTASIS

APPROVED BY:

Assoc. Prof. Dr. Dilek Telci .....
(Thesis Supervisor)

Prof. Dr. Asıf Yıldırım .....

Prof. Dr. Gamze Köse .....

Assoc. Prof. Dr. Damla Arısan .....

Assist. Prof. Dr. Hüseyin Çimen .....

DATE OF APPROVAL: ..../..../2016

This thesis is dedicated to my
aunt Necla Nesrin İlter ...

ACKNOWLEDGEMENTS

First of all, I would like to thank to my supervisor Assoc. Prof. Dr. Dilek Telci for her support, encouragement, for proofreading of hundreds of my thesis drafts, and giving a chance to work with her throughout my PhD period. I also wish to express my gratitude to Prof. Dr. Fikrettin Şahin for his continuous material and moral supports.

I am deeply grateful to my thesis committee members, Prof. Dr. Gamze T. Köse, Assoc. Prof. Ömer Faruk Bayrak and Assoc. Prof. Damla Arısan for sharing their experiences and for their inputs during my thesis. My sincere thanks go to Prof. Dr. Bayram Yılmaz, Prof. Dr. Mustafa Çulha and Assist. Prof. Hüseyin Çimen for sharing their labs and valuable experiences. I am really thankful to Dr. Mehveş Arıoğul Poda and Dr. Marco Sifringer who inspired me to go after my dream of being a scientist.

I am so thankful to my lab partners Merve Erdem, İnci Kurt, Hande Nayman, Halime İlhan, Bürge Ulukan, Polen Koçak and Zeynep Bolat for helping and supporting me whenever I needed. I wish to express many thanks to Siğnem Eyüboğlu for her understanding and assistance during my thesis. I would also like to thank my best friends Çiğdem Aysel, Fatma Hicran Özcan, Selen Beytekin, for their endless support and patience during my whole education life. I warmly thank to my friends, İrem A. Altınışık, Eray Şahin, Şeyma Yıldırım, Elif Kon, Oya Arı, Melis S. Söğüt, Elif Yavaş, Özlem Şilan Çoşkun, Bihter Yavuz, İlker Kanbağlı, Mine Altunbek, Cansu T. Tunç, Ceren Koyuncu, Safa Aydın, Selami Demirci, Ayşegül Doğan, Burçin K. Asutay, Esra A. Çoban and Mustafa Yoğutçu for their continuous support.

Lastly but most importantly, I owe my loving thanks to my parents Hilal İlter and Nevzat İlter, my grandmother Cemile Bal, my aunt Nalan Yerebasan, my brother İlker İlter, Mr. Mete Girayalp, my spiritual sister Pınar Akülke Durmaz and my best friend, my soul mate and the love of my life, my husband Murat Akülke. They have given the at most support during my research. Without their encouragement and understanding it would have been impossible for me to finish this work.

ABSTRACT

ROLE OF TISSUE TRANSGLUTAMINASE INDUCED INTEGRIN TRAFFICKING IN KIDNEY CANCER METASTASIS

Integrins plays an important role in metastasis formation by orchestrating the cell adhesion and cytoskeletal dynamics together with the surrounding extracellular matrix. Tissue transglutaminase (TG2) is the ubiquitously expressed member of transglutaminase family which is able to catalyze Ca^{+2} dependent cross-linking by forming an intermolecular ε-(γ-glutamyl)-lysine isopeptide bond between proteins. Recent study demonstrated that regardless from its enzymatic activity, the upregulation of TG2 along with ITGβ1 and SDC4 can be a new diagnostic marker in the metastatic state of renal cell carcinoma (RCC), a notoriously radio-resistant and chemoresistant cancer. To date, integrin targeted therapeutic agents is not able to stabilize the metastatic progress of RCC therefore this study seeks to understand whether TG2 together with SDC4 may behave as a central player during the endo/exocytic cycle of β1 integrins. For this purpose, crosstalk between TG2 and cell surface receptors SDC4, ITGβ1 was investigated in RCC cell lines using co-immunoprecipitation (IP) assay followed by the measurement of cell attachment and spreading potential of TG2 downregulated RCC cells on β1 integrin substrates. In order to clarify the role of TG2-SDC4 interplay in integrin internalization and recycling a biotinylation-based IP and Flow Cytometry assay using active integrin binding antibody was performed, respectively. Results from this study showed that TG2 was associated with ITGβ1&SDC4 in all four primary and metastatic site RCC cell lines with the highest interaction affinity detected for the metastatic Caki-1 cells. Cell adhesion assays suggested that TG2 is a major component that mediates the RCC cell adhesion as the silencing of TG2 in all four RCC cell lines resulted in a marked decrease in their adhesion potential on β1 integrin substrates. The analysis of the role of TG2 and SDC4 in integrin β1 trafficking in Caki-1 cells using shRNA technology suggested that TG2 together with SDC4 contributes to the β1 integrin internalization and recycling. These findings support a role for TG2 in association with SDC4 in the development of RCC metastases through regulation of the cell adhesion and β1 integrin trafficking.

ÖZET

DOKU TRANSGLUTAMINAZ GÜDÜMLÜ INTEGRIN TRAFİĞİNİN BÖBREK KANSERİ METASTAZI ÜZERİNE ETKİSİ

Kanser hücrelerinin kontrolsüz migrasyonu sırasında hücre adhezyonu ve hücre iskeleti dinamikleri integrinler tarafından kontrol edilmektedir. Doku transglutaminazı (dTG), transglutaminazlar arasında dokularda en yaygın ifade edilen protein olmakla beraber dTG, Ca^{+2} varlığında proteinler arasında ε-(γ-glutamil)-lisin izopeptidi oluşturarak proteinler arası çapraz bağ kurduğu bilinmektedir. Son yapılan çalışmalar göstermiştir ki ileri renal hücreli böbrek kanseri (RHBK) tümörlerinde dTG seviyesi, ITGβ1 ve SDC4 proteinleri ile beraber artmakta bu nedenle kemoterapiye dirençli olan RHBK için yeni bir teröpatik markör olarak öne sürülmektedir. RHBK tedavisinde integrine spesifik tedavi ajanlarının yetkin etki göstermemesi dTG'nin sindekan-4 (SDC4) ile birlikte β1 integrinlerin hücre içine alımı ve dışarı çıkarılması mekanizmasında rol oynadığını öne sürmüş ve bu tezin hipotezini oluşturmuştur. Bu sebeple RHBK hücre hatlarında dTG ve ITGβ1&SDC4 arasındaki interaksiyon immün çökertme metodu ile belirlenmiş olup dTG ifadesi azaltılmış RHBK hücrelerinin β1 integrin matrislerine yapışma ve yayılma potansiyelleri incelenmiştir. dTG ve SDC4'ün ITGβ1'lerin hücre içine alınması belirlemek için hücre yüzeyindeki ITGβ1'ler biyotinlenerek immün çökerme uygulanmış; ITGβ1'lerin dışarı verilmesindeki rolünün belirlenmesi için ise ITGβ1'e özgü antikor ile etiketlenen integrinlerin hücre yüzeyi seviyesi akış sitometresi ile yapılmıştır. dTG seviyesi azalmış RHBK hücrelerinin integrin β1 matrislerine yapışması ve yayılmasında önemli ölçüde azalma bulunarak dTG' nin hücre adhezyonundaki görevi tespit edilmiştir. İncelenen dört farklı RHBK hücre hattından dTG ile ITGβ1 ve SDC-4 etkileşiminin Caki-1 metastatik hücre hattında en yüksek düzeyde olduğu bulunmuştur; bu nedenle shRNA teknolojisi ile dTG ve SDC4 proteinleri baskılanarak β1 integrinlerinin hücre içine alınması ve dışarı çıkması döngüsündeki rolü Caki-1 hücre hattında tespit edilmiştir. Sonuçlarımız ışığında dTG' nin SDC4 ile ITGβ1'nin hücre yüzeyindeki deviniminde rol oynadığı tespit edilerek RHBK metastazı nedeni olan hücre göçünde önemli rol oynayabileceği ortaya atılmıştır.

TABLE OF CONTENTS

LIST OF FIGURES

LIST OF TABLES

LIST OF SYMBOLS/ABBREVIATIONS

ADAM	A disintegrin and metalloproteinase
ADMIDAS	Adjacent to metal-ion dependent adhesive site
ALIX	ALG-2 interacting protein
AKT	Protein kinase B
APS	Ammonium persulfate
ATTC	American type culture collection
BSA	Bovine serum albumin
CASK	Calcium/calmodulin serine protein kinase
CDC42	Cell division cycle 42
cDNA	Complementary deoxyribonucleic acid
CHIP	Carboxy-terminus of Heat shock protein-70 interacting protein
CHO	Chinese hamster ovary
CLCA	Chloride channel calcium activated
COL1	Collagen Type 1
CSF	Colony stimulating factor
DAG	Diacylglycerol
DMEM	Dulbecco's modified Eagle's medium r
DMSO	Dimethyl sulfoxide
DTT	Dithiothreitol
ECM	Extracellular matrix
EDTA	Ethylenediaminetetraacetic acid
EEA	Diabetic foot ulcer
EGF	Epidermal growth factor
EGFR	Epidermal growth factor receptor
EMT	Epithelial mesencyhmal transition
ERK	Extracellular signal-regulated kinases
ESCRT	Endosomal-sorting compex required for the transport
FAK	Focal adhesion kinase
FAT	Focal adhesion targeting domain
FBS	Fetal bovine serum

FERM	Four point one, ezrin, radixin, moesin
FGF	Fibroblast growth factor
FGFR	Fibroblast growth factor receptor
FN	Fibronectin
GAG	Glycosaminoglycan chains
G (D/T) P	Guanosine (di/tri) phosphate
GFFKR	Glycine-Phenylalanine- Phenylalanine-Lysine-Arginine
GIT	G protein-coupled receptor kinase interacting protein
GPCR	G protein coupled receptor
HIF	Heparin binding epidermal growth factor
HYB	Hybrid
HRP	Horse-radish peroxidase
IAA	Iodoacetamide
IP3	Inositol triphosphate
ILK	Integrin linked kinase
ITGβ1	Integrin Beta 1
LM	Laminin
LPA	Lysophosphatidic acid
LRP	Lipoprotein receptor related protein
M	Molar
ml	Milliliter
µl	Microliters
mM	Millimolar
MAPK	Mitogen activated protein kinase
MEK	Mitogen-activated protein kinase kinase
MESNA	Sodium 2-mercaptoethane sulfonate
MLC	Myosin light chain
MLCK	Myosin light chain kinase
MLCP	Myosin light chain phosphatase
MIDAS	Metal ion-dependent adhesion site
MMP	Matrix metalloproteinase
MTOR	Mammalian target of rapamycin
MVB	Multivesicular bodies

NMR	Nuclear magnetic resonance
PAX	Paxillin
PDGF	Platelet derived growth factor
PDGFR	Platelet derived growth factor receptor
PDK	Phosphoinositide-dependent protein kinase
PDZ	Post synaptic density protein of 95, Discs large zonula occludens
PH	Plexirin homology
pH	Negative log of hydrogen ion concentration
PKC	Protein kinase C
PI3K	Phosphoinositide 3-kinase
PMA	Phorbol myristate acetate
PLC	Phospholipase C
PSI	Plexin-semaphorin-integrin
PTB	Phosphotyrosine binding
RAB	Ras-related proteins in brain
RCC	Renal cell carcinoma
RGD	Arginine-Glycine-Asparagine
RIAM	Rap1-GTP-interacting adaptor molecule
ROCK	Rho-associated protein kinase
P/S	Penicillin, streptomycin
QPCR	Quantitative polymerase chain reaction
RhoGDI1	Rho guanine dissociation inhibitor 1
RT	Reverse transcriptase
S.D.	Standard Deviation
SDC	Syndecan
SDS-PAGE	Sodium dodecyl sulfate polyacrylamide gel electrophoresis
SFK	Src family kinase
SNARE	Soluble N-ethylmaleimide-sensitive factor attachment protein receptor
siRNA	Silencing Ribonucleicacid
shRNA	Short hairpin Ribonucleicacid
c-Src	Proto-oncogene tyrosine-protein kinase
TEMED	N,N,N’,N’- Tetramethylethylenediamine

TG	Transglutaminase
TG2	Tissue transglutaminase
TG2 o/e	Tissue transglutaminase overexpressed
TGF-β1	Transforming growth factor beta1
TIMP	Tissue inhibitors of matrix metalloproteinase
TKI	Tyrosine kinase inhibitors
TNF-α	Tumor necrosis factor alpha
TM	Transmembrane
uPa	Urokinase plasminogen activator
VEGF	Vascular endothelial growth factor
VEGFR	Vascular endothelial growth factor receptor 1
VHL	Von Hippel Lindau
WASH	Wiskott–Aldrich Syndrome protein family homolog
WASp	Wiskott–Aldrich Syndrome protein
WST-	Water soluble tetrazolium salt

1. INTRODUCTION

Most of the cells are enclosed by extracellular matrix (ECM), which functions as a supporting nonliving material that is able to regulate the dynamic interactions of the cell. ECM is composed of fibers (collagen, elastin), adhesive glycoproteins (FN, laminin, vitronectin), glycosaminoglycans and proteoglycans [1]. The main structural proteins; elastin and collagen serve as a linker between other ECM proteins. The major collagen types that are found in ECM and basement membrane are collagen I, III, IV, V and the glycosaminoglycan-containing IX [2]. FN and laminin glycopoteins act as glue between cells and ECM. Besides through its cell to ECM adhesion function, vitronectin modulates plasminogen activator system that takes role in the progression of invasion and the metastasis of cancer cells [3,4]. Aside from constituting the structural framework for the cells, ECM proteins do also coordinate the biological functions such as cellular migration, proliferation, differentiation and apoptosis [5] through binding to other ECM proteins, signaling receptors, growth factors and adhesion molecules. Compare to other ECM proteins, FN provides a binding site for collagen and several integrin receptors, heparan sulphate proteoglycans that acts as main regulators of cell-ECM interactions. The functional FNIII domains include a RGD motif which is composed of arginine-glycine-aspartic acid amino acids that serves as a central binding ligand for many different types of integrin molecules [6].

When cancer cells become metastatic they change their affinity and avidity to their ECM [7]. The phenotypic changes in cancer cells begin with the alterations in the expression of cell surface molecules, mainly in integrins followed by an increase in matrix metalloproteinase activity, necessary for ECM remodeling, and the deposition of newly synthesize ECM molecules. Functions of these activated signaling pathways are critical to regulate the gene expression, cytoskeletal organization, cell adhesion, proliferation and survival. Finally, cancer cells can gain the function of invasive migratory capability as well as the ability to adopt to different microenvironments to survive [7]. Owing to their unique ability to connect ECM to the cytoskeleton, integrins are essential to regulate the intracellular pathways, which controls the cytoskeletal shape, force generation necessary for the cell translocation, cell growth and survival [8].

1.1. Integrin Structure and Activation

Integrins were first discovered by Hynes *et al* in 1986 and denote its name from being an integral membrane protein [9]. They are the main cell surface receptors, which take role in the assembly of functional extracellular matrix and are capable of facilitating the directional cell migration to the correct tissue location. Although integrins are not able to directly respond to the intracellular or extracellular stimuli by growth factors, they are perfectly evolved to convey bidirectional signaling across the membrane [9,10].

Integrins are type I transmembrane heterodimeric glycoprotein cell surface receptors, which regulate a diverse array of cellular functions including the cell adhesion, motility, migration, differentiation, apoptosis and survival through a bidirectional signaling between the extracellular and intracellular environments [10].

In vertebrates, there are 18 α- and 8 β-subunits, which can form at least 24 different non-covalently associated αβ pairings or heterodimers out of 144 possible combinations with distinct binding properties [10] and different tissue distributions [11].
As a mechanical linker between the cell inner and outer environments, integrins can be divided into subgroups based on their ligand specificity (Figure 1.1) and subunit composition (Table 1.1) [12].

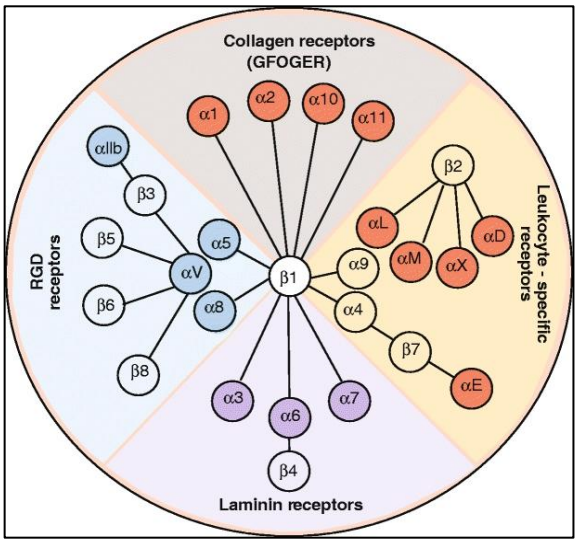

Figure 1.1. Integrin family members and their ligand specifity [12].

Table 1.1 Spesific ligands of integrin heterodimers,
adapted from Johnson *et al* 2009 [12]

Integrin Heterodimers	**Ligands**	**Integrin Heterodimers**	**Ligands**
α1β1	Collagens, Semaphorin 7A, (laminins)	αDβ2	ICAM, VCAM
α2β1	Collagens, tenascin C, (laminins)	αMβ2	ICAM, VCAM, iC3b, factor X, fibrinogen
α3β1	Laminins (Collagen)	αLβ2	ICAM
α4β1	FN, VCAM	αXβ2	Fibrinogen, plasminogen, heparin, iC3b
α5β1	FN (RGD)	αVβ3	Fibrinogen, FN, vitronectin, tenascin C, osteopontin, bone sialoprotein (RGD), MMP-2
αVβ1	FN, Vitronectin	αIIbβ3	Fibrinogen (RGD, GAKQAGDV), FN (RGD), vitronectin
α6β1	Laminins, ADAMs	α6β4	Laminins
α7β1	Laminins	αVβ5	Vitronectin (RGD)
α8β1	FN, Vitronectin, Tenascin C, osteopontin, nefronectin (RGD)	αVβ6	FN, TGF-β-LAP (RGD)
α9β1	Tenascin C, osteopontin, ADAMs, factor XIII, VCAM, VEGF-C, VEGF-D	α4β7	FN, VCAM, MadCAM
α10β1	Collagens	αEβ7	E-cadherin
α11β1	Collagens	αVβ8	Vitronectin (RGD)

The α and β subunits define the characteristic feature of integrin binding to the extracellular matrices. α1β1, α2β1, α10β1, and α11β1 integrins correspond to the primary collagen receptors whereas α3β1, α6β1, α6β4 and α7β1 serve as the main laminin receptors, while α5β1, α8β1, αIIbβ3 and αvβ integrins interact with the ECM in a RGD-depended manner. Most of the integrins are widely expressed regardless of the tissue

distribution except for (i) α6β4, which is unique to keratinocytes, (ii) αIIbβ3, which is only found on platelets surface, (iv) αDβ2, αMβ2, αLβ2, αXβ2 integrins that are restricted to leukocytes and (v) αEβ7 and α4β7 integrins, which are expressed on the surface of lymphocytes and circulating T cells, respectively [12].

Structurally, α and β heterodimers are composed of a N-terminal extracellular multidomain followed by a transmembrane region and short C-terminal cytoplasmic sequences (10-70 amino acids) except for β4, which uniquely has a long cytoplasmic domain of over 1000 amino acids [13,10].

The extracellular domain of α subunit comprised of a seven-bladed β propeller domain, thigh and two calf domains. In addition, 9 of the 18 α subunits (α1, α2, α10, α11, αD, αE, αL, αM, and αX) contain an α-I domain inserted within the β-propeller domain, which serve as an exclusive ligand binding site [10]. The α-I domain contains five β sheets surrounded by seven α helices with a characteristic divalent cation-binding (Mg^{+2}) sequence motif of DxSxS in a conserved metal-ion dependent adhesive site (MIDAS) [14].

The β subunit has the same I domain (β-I) next to the a hybrid (Hyb) domain respectively followed by a plexin-semaphorin-integrin (PSI) domain, four cysteine rich epidermal growth factor (EGF) repeats and a proximal membrane β tail (β-T). β-I domain includes Mg^{+2} coordinating MIDAS and an inhibitory Ca^{+2} binding adjacent site next to the MIDAS (ADMIDAS). ADMIDAS site is also crucial for Mn^{+2} binding to regulate the conformational change resulting in the active form of integrin [15]. Both β-I and α-I domain responsible from the extracellular ligand binding and subsequent integrin activation, especially in the absence of α-I domain, β-I domain takes a crucial role in the activation of integrins.

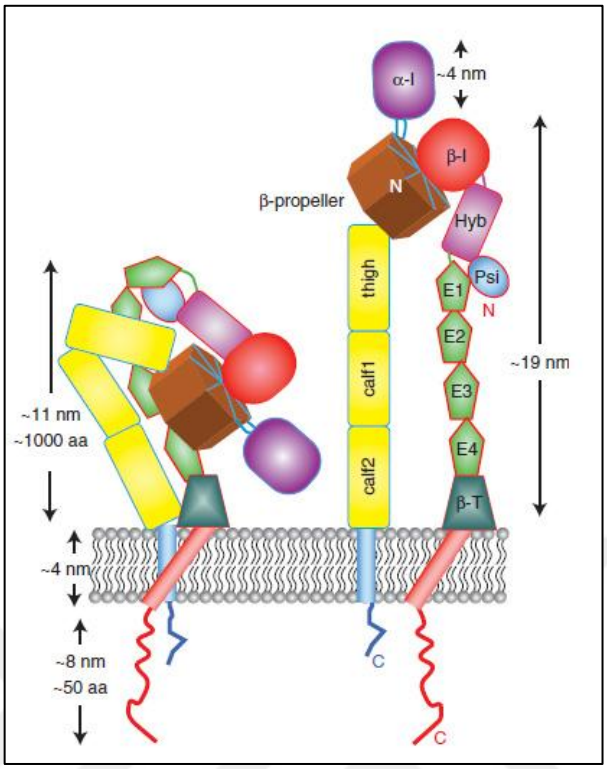

Figure 1.2. Schematic structure of αxβ2 integrin. Left panel represents inactive (bent) conformation whereas right panel shows the active (extended conformation), adapted from Campbel *et al*. 2011 [11].

When the extracellular domains are unbound to their ligand, integrins are at the resting low affinity state corresponding to the bend conformation. Upon activation, the extracellular domains become stabilized in the extended form representing the active conformation state (Figure 1.2) [16]. While this conformational change increases the affinity of ligand to the external-ligand binding site, the binding of ligand leads to the transmission of signals from outside to inside of the cell.

Two models were proposed to explain the conformational changes; "*switchblade*" model states that integrins need to be presented in the extended form for the ligand binding. According to this model, TM and cytoplasmic domains of α and β dissociate from each other, which in turn leads to the dislocation of epidermal growth factor (EGF)-like repeat in the β stalk. This translocation results in the extension of head region in a switchblade-like movement. The "*dead-bold*" model suggested that the active integrin state occurs in a bent conformation and subsequent piston-like movements of the transmembrane regions

lead to sliding of the extracellular stalks. As a result of these movements, the α and β subunits become apart and extension takes place following the ligand binding [17]. Both models come up with the conformational change that exposes the head domain for the ligand binding.

Transmembrane domains are single pass spanning structures composed of an approximate of 29 amino acid residues. Referring to detailed structural NMR analysis of αIIbβ3, GFFKR (Glycine- Phenylalanine, Phenylalanine, Lysine, Arginine) motif in the distal region is highly conserved and takes role in the shift from the resting to active state [18]. Rather than cytoplasmic domains, TM domains take part in the activation of integrins. Three models have explained the role of TM domains in the separation of integrin α and β subunits during activation; in piston model, TM domains act like a piston, move vertically resulting in the shortening of TM domain [19], in scissors model, the angle of TM domains increases [20] and in separation model, there is a physical separation of TM domains of α and β subunits [20]. Regardless to their way of function, all models predict the disengagement of α and β subunits, which results in the integrin activation [21].

Similar to transmembrane domains, cytoplasmic domains have not been clearly resolved in high resolution yet, since the only NMR data was obtained from cytoplasmic tail of αIIbβ3 [22]. Although most of the cytoplasmic domains are comprised of 20-70 amino acids, β4 cytoplasmic domain contains more than 1000 amino acids. The α and β subunits have conserved GFFKR (Glycine- Phenylalanine, Phenylalanine, Lysine, Asparagine) and HDR(K/E) (Histidine-Aspartic acid-Arginine-Arginine/Lysine-Glutamic acid) sequences inserted in the membrane proximal region of cytoplasmic domain, which take part in the formation of a salt bridge between arginine and aspartic acid, respectively [18]. Hughes *et al* demonstrated that the salt bridge is a physical regulator between αIIb and β3 during the establishment of active and inactive integrin conformation by means of maintaining the inactive state of integrins. However, in β1 subunit point mutation studies, the salt bridge did not show an apparent function under the *in vivo* physiological conditions [23]. Therefore, the main function of the salt bridges has not been detected so far.

β tails are highly conserved and flexible compared to α tails thereby β tail interactions are better investigated [24,25]. There are two well defined motifs identified as NpxY and NxxY in the membrane proximal and distal region of β subunit, respectively, which

interacts with the phosphotyrosine (PTB) domains of several integrin binding adaptor proteins [26]. According to their binding specificity α tails are primarily determinant for extracellular ligand, whilst β tails are the main mediators for the intracellular interactions especially for adhesome components such as talin, paxillin, filamin, integrin-linked kinase (ILK) and focal adhesion kinase (FAK) [25].

1.2. Integrin signaling

Although, integrins have no kinase activation, its cytoplasmic tail provides a connection between the ECM and cytoskeleton proteins in other words; it permits a bidirectional signaling (inside-out, outside-inside) through the cell membrane [10].
This signaling cascade triggers major cellular processes such as migration, survival, differentiation, apoptosis and transcriptional control [4,27,28]. Integrin activation process arises from inside-out or outside-in signaling. A signal generated from inside the cell leading to a conformational change is defined as inside-out activation which increases the extracellular ligand binding affinity of integrin ectodomains for further outside-in activation. This bidirectional signaling leads to the integrin clustering and facilitate the formation of adhesome complexes [23].

1.2.1 Inside-out signaling

The alterations of integrin affinity for their extracellular ligand was first investigated in blood cells since their integrin-dependent cell adhesion should be restricted to avoid the formation of thrombosis [29].

Under normal physiological conditions, integrins of circulating platelets and leukocytes are found in an inactive conformation state, unable to bind to their receptors. Although platelets express different cell surface integrins such as αvβ3 (vitronectin receptor), α2β1 (collagen receptor), α5β1 (FN receptor), α6β1 (laminin receptor), the fibrinogen receptor αIIbβ3 is highly expressed compared to the other integrins [30], therefore most of the integrin activation studies were carried out to analyze the activation of αIIbβ3 integrins [31,28].

Ligand binding such as thrombin, sphingosine-1 phosphate, lysophosphatidic acid (LPA) or phorbol myristate acetate (PMA) to G protein coupled receptors (GPCR) on cell the surface of platelets triggers PLC (phospholipase C) to induce the hydrolysis of phosphatidylinositol 4 5-bisphosphate (PIP2) to inositol triphosphate (IP3) and diacylglycerol (DAG). Increased Ca^{+2} and DAG leads to the activation or translocation of active- GTP bound Rap-1 to the plasma membrane via activation of PKC or GEFs (Guanine exchange factors) [32]. IP3 binds to the IP3 receptor located on ligand gated Ca^{+2} channel of endoplasmic reticulum surface and releases Ca^{+2} ions to cytoplasm. Increased Ca^{+2} induces the exchange of Rap-1-GDP (GDP bound Ras related protein-1) to Rap-1 GTP (GTP bound Ras related protein-1) under catalysis of CalDAG-GEF (Calcium and DAG-regulated guanine nuclear exchange factor) [33]. Activated Rap-1-GTP interacts with RIAM (Rap-GTP interacting adaptor molecule), which translocates Rap-1 GTP to the plasma membrane via its PH (pleckstrin homology) and RA (Ras-association)- like domain [16] RIAM adaptor protein acts like a scaffold, connects the membrane targeting sequence in Rap-1 to talin thereby recruiting talin to the plasma membrane [34] hence induce a subsequent integrin activation (Figure 1.3.) .

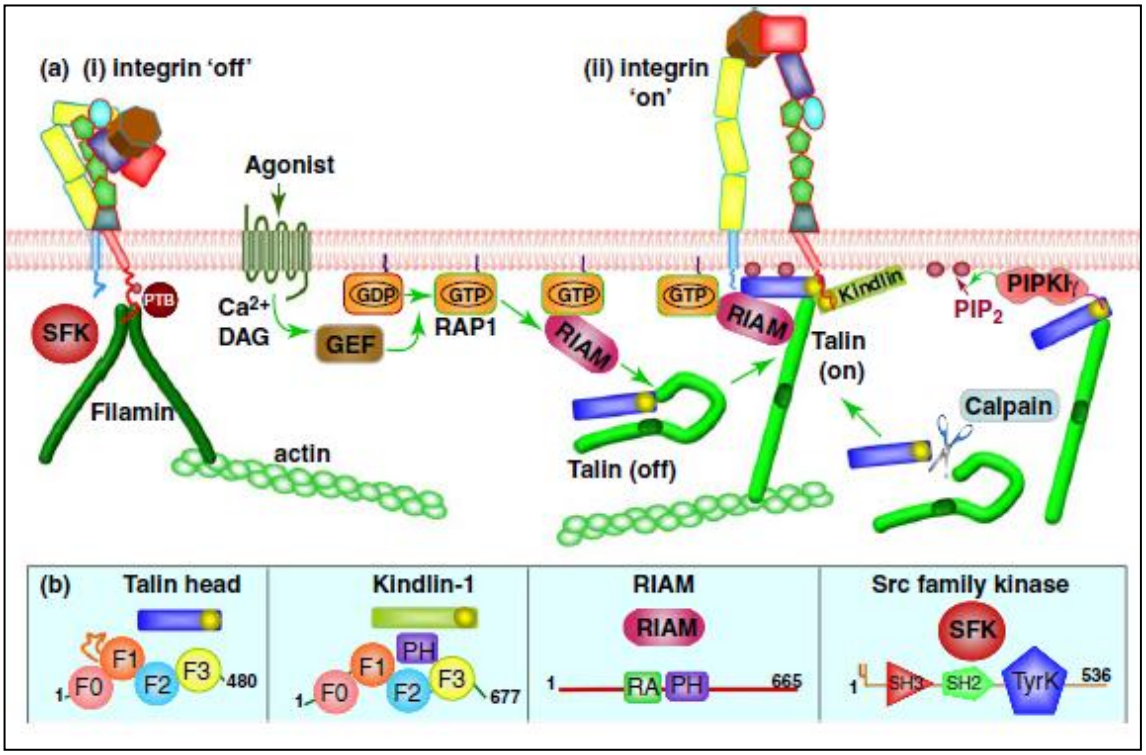

Figure 1.3. Integrin activation by talin [16].

Talin acts as a linker between integrins and actin cytoskeleton protein during the integrin-mediated cell adhesion and regulates the integrin activation by stimulating the integrin inside-out signaling [35,36]. Talin is composed of an antiparallel homodimer consisting of a N-terminal head domain (~47 kDA) and a large tail rod region (~220 kDA). N- terminal is composed of FERM (four point one, ezrin, radixin, moesin) domain containing F1, F2, F3 subunits and regulates the affinity of integrins to ECM ligands by binding to the NPxY motif on the cytoplasmic tails of β integrins [13,28].

Another activation pathway is regulated by PIP2 and calpain. Inactive talin possess an auto conformation state, in which C-terminal domain interacts with the phosphotyrosine binding domain (PTB) thereby blocks the integrin binding pocket. Increased local concentration of PIP2 by PtdIns (4,5) P2 producing enzyme named as phosphate kinase type Iγ (PIPKIγ), results in the release of talin autoinhibition. PIPKIγ also takes role in the recruitment of talin to the membrane through the interaction between PIPKIγ C terminal region and talin F3 domain. Talin contains a C- terminal calpain (Ca^{+2} stimulated protease) cleavage site which removes the talin rod region from the head domain. By itself the head domain is able to activate integrins alone hence the rod domain is necessary for the integrin connection to cytoskeleton proteins and the focal adhesion formation [37]. Crystal structure of αIIBβ3 TM domain analysis showed that once talin binds to NPxY motif, the inner membrane clasp generated by a consecutive pair of Phenylalanine residues against TM helix, which promotes a salt bridge formation by regulating the electrostatic interaction between D723 and R995 residues, is disrupted. This conformational change exposes extracellular domain for the ligand binding and initiates the subsequent integrin activation [38].

Kindlin, an adaptor protein important in integrin activation, comprises of an evolutionary conserved three proteins kindlin-1, kindlin-2 and kindlin-3 and takes its name from a rare autosomal recessive congenital skin disease called Kindler syndrome [39]. Although kindlin-1 mainly expressed in the epithelial cells and kindlin-3 expression is restricted to the hematopoietic cells, kindlin-2 is ubiquitously expressed in many tissues [40,41]. Kindlin has a FERM domain which possesses a similar sequence to talin and contains typical F1, F2 and F3 subdomains. Similar to talin, PTB binding domain of kindling is located at F3 domain and interacts with the membrane-distal NxxY motif found in the cytoplasmic β1, β2, β3 integrin tails [42]. From these distinct regions, both kindlin and

talin regulate integrin activation hence kindlin alone is not sufficient to switch integrins to the extended active state [43,44]. The importance of synergistic interaction between talin and kindlin in integrin activation was demonstrated by *in vitro* studies which showed that co-transfection of talin and kindlin-2 increased the integrin activation whereas siRNA silencing of kindlin-2 decreased the talin-induced αIIbβ3 activation in CHO (chinese hamster ovary) cells [45].

In adherent cells integrin activation is triggered by a cytoskeletal tension, which is generated via a complex containing FN, α5β1 integrin, talin and actin-myosin-II proteins. Regulation of mechano-sensing through α5β1 interaction with different substrates is required for many biological responses [46].

1.2.2. Outside-in signaling

Outside-in signaling requires an inside-out activation induced by the binding of integrin activators to the cytoplasmic tail of integrins in order to fine-tune the affinity of integrin through alteration of the integrin extracellular domain for a subsequent ligand binding. Upon ligand binding, the headpiece in the extracellular domain changes its conformation by inducing a shift in the β-I-domain, which leads to the integrin clustering at the plasma membrane and endorses the assembly of actin filaments [47]. Different from inside-out activation this conformational change does not induce any structural modifications in the transmembrane and intracellular domains [48]. Ligand bound active integrins form nascent adhesions (a dot like adhesion), which are relatively unstable structures and further disassemble or re-organize into large stress fibers to form the mature adhesion complexes [49]. Focal adhesions are dynamic protein complexes initiated by the integrin-ECM binding along the cell periphery at the leading edge [50]. The talin by binding to the integrin cytoplasmic tail via through its head domain and binding to the actin via its rod region, mediate a direct link between integrins and cytoskeleton [51]. Following vinculin recruitment to nascent adhesions, talin also binds to vinculin, which in turn leads to the vinculin binding to α-actinin and actin [52]. Hence, vinculin stabilizes actin-talin interactions by acting like a crosslinker [53]. This mechanism shows that talin could link to actin in multiple ways [54].

Talin forms a platform for the recruitment of paxillin to the adhesion sites [55]. In the cytoplasm, integrin-linked kinase (ILK), isoforms of particularly interesting Cys-His-rich protein (PINCH) and parvin form the IPP complex are simultaneously recruited to the focal adhesion complex where they interact with paxillin, which are together recruited to the focal adhesion complex [56]. Paxilin functions as a switch in the adhesion turnover and signals for the activation of Rac and Rho GTPases [47]. Phosphorylation of different sites on paxilin regulates the RhoGTPases. For example, Tyr31 and Tyr118 phosphorylation of paxilin by FAK or Src leads to the recruitment of Crk-II and p130CAS adaptor proteins, which establishes a complex to activate Rac via the Rac GTP exchange factor DOCK180 [57,58]. On the other hand, the phosphorylation of paxilin by FAK on Ser 273 forms another complex by recruiting G-protein adaptor proteins GIT1-GIT2 and Rac GTP exchange factor βPIX to activate Rac and regulates the accurate position of p21-activated kinase-1 (PAK-1) in the cell protrusions [59,60,56]. As an effector of Rac, PAK-1 phosphorylates the myosin light chain kinase (MLCK) from Ser 439 and 991 [61] resulting in the inactivation of myosin II, which in turn endorses the membrane protrusion and cell movement instead of the adhesion growth [62]. Activated Rac regulates actin polymerization through Arp2/3 complex via the Scar/WAVE family of activator proteins [47]. Arp2/3 interacts with FAK and vinculin to promote actin polymerization (Figure 1.4.) [63].

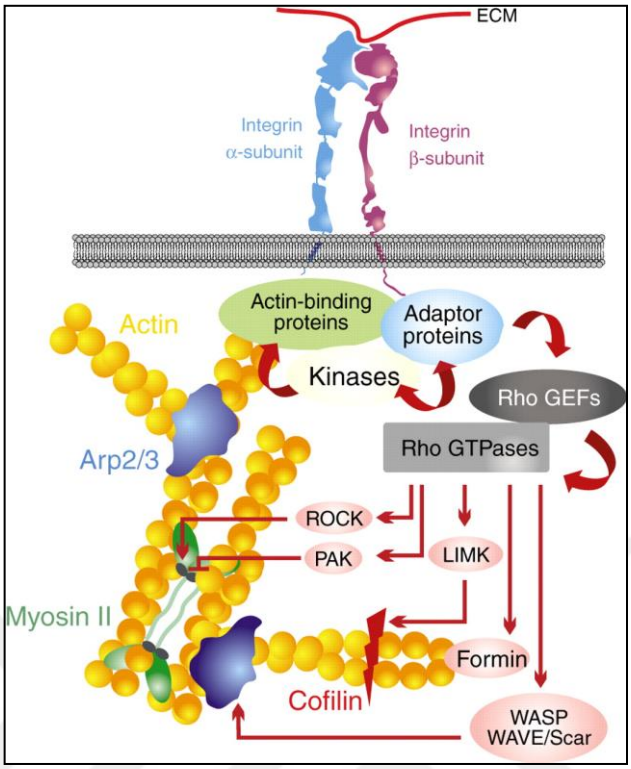

Figure 1.4. Formation of focal adhesion complexes upon integrin engagement [47].

Integrin signaling regulates Rho GTPase family members Rac1, Cdc42, and RhoA, which are the regulators of actin dynamics as well [63]. The small GTPase RhoA activates ROCK (Rho associated coiled coil containing protein kinase), which in turn phosphorylates myosin II regulatory light chain (R/MLC) and myosin light chain phosphatase to activate myosin II. Activation of myosin II inhibits protrusion while tightly bundling with actin filaments and resulting in the formation of stable adhesions [47].

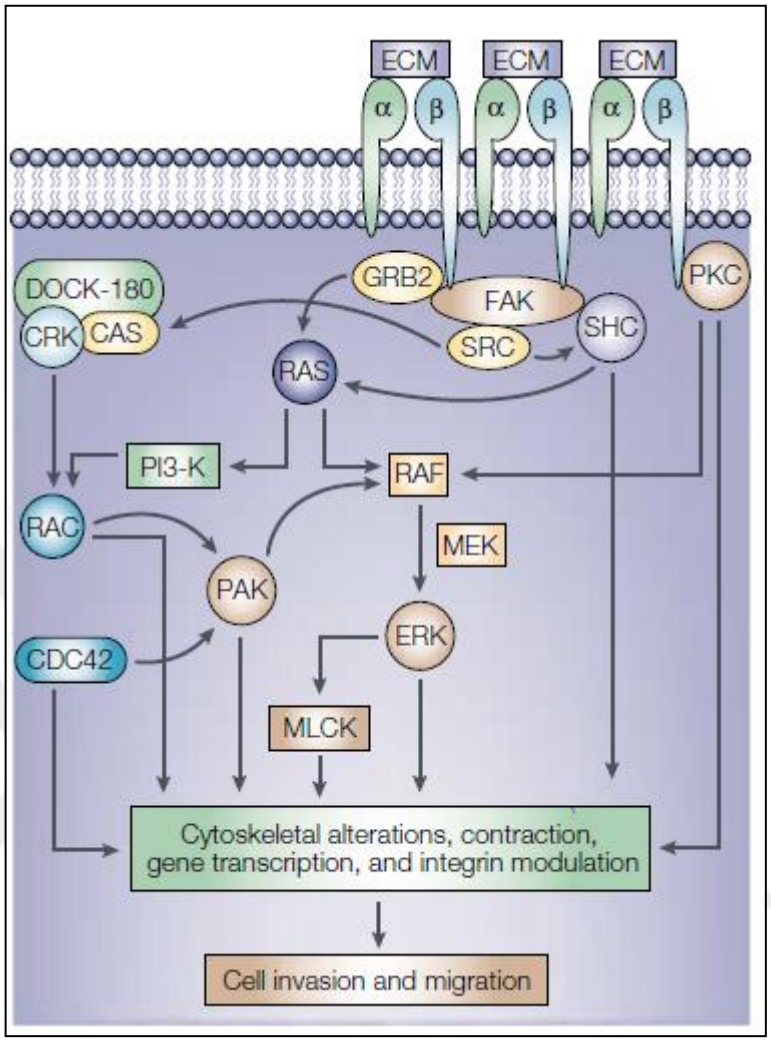

Figure 1.5. Downstream signaling events of FAK [64].

Further FAK (focal adhesion kinase) recruitment to adhesion complex activates Rho GTPases, which is crucial for cell migration, adhesion turnover, crosstalk between growth factor signaling and integrins. The structure of FAK comprises N terminal FERM domain, a central kinase domain, proline rich regions and C terminal focal adhesion targeting domain (FAT), which serves as a binding site for talin and paxilin [65]. Following integrin clustering the autophosphorylation of FAK from tyrosine 397 residues reveals docking sites to kinases containing SH2 binding domain such as Src that leads to a constant and elevated activation of Src-FAK complex [66]. Growth factor induced integrin-Src-FAK complex transmit the signals through RAS-MEK-MAPK pathway which regulate focal adhesion dynamics and cell survival. Another target of FAK is the Rho family GTPases

including Rac, cell division cycle 42 (Cdc42), and RhoA, which can regulate the rapid polymerization of actin filaments at the cell edge, the extension of lamellipodium and the membrane ruffling processes during the cell cycle [67]. Rac and Cdc42 are activated by binding to the integrin, whereas Rho activation is not only regulated by integrins but also by syndecan-4 heparan sulfate proteoglycans and additional cell surface receptors [68]. FAK can also phosphorylate p85 subunit of PI3K; activated PI3K is then recruited to the focal adhesion points and induce AKT serine/threonine kinase, which regulates integrin mediated cell survival (Figure 1.5) [4].

Integrins can be phosphorylated from the serine residue of β-tail by PKC (protein kinase C) in response to the phorbol ester treatment, which is a potent activator of PKC. Following phorbol ester treatment of B lymphoblastoid cells showed that β1 integrin tail was phosphorylated at S785 which is the only serine residue at amino acid 785 in the β1 integrin tail [69]. Apart from serine/tyrosine residues, β tails can be phosphorylated at the threonine residues (T788/789), which are located between the serine/threonine rich intervening sequences in membrane proximal and distal NxxY motifs. Point mutation experiments revealed that threonine phosphorylation regulates morphological characteristics and cytoskeleton organization rather than the integrin activation [70].

1.3. Integrins in cancer

Cancer is defined as a group of diseases that is characterized by abnormal cell growth, invasion and metastatic dissemination of neoplastic cells. Cancer types are classified by the origin of the tissue such that; carcinoma is derived from the epithelial tissue, sarcoma is derived from the non epithelial (mesenchymal) tissue, adenocarcinoma is derived from the glandular tissues [71], leukemias or lymphomas are derived from the hematopoietic or lymphoid cells. During the multistep development of tumor formation, the hallmark traits are required to gain metastatic capability. These hallmarks are listed as; (i) sustaining proliferative signaling, (ii) evading growth suppressors, (iii) resisting cell death, (iv) enabling replicative immortality, (v) inducing angiogenesis and (vi) activation of invasion and metastasis [72]. In addition to these mechanisms, genomic instability and mutation and tumor promoting inflammation have been added as the enabling characteristics together with the reprogramming energy mechanism, evading immune destruction that are excepted

as the emerging hallmarks. Acquisitions of these hallmarks determine the cancer cell phenotype and constitute the tumor microenvironment through directing the signaling interactions [72]. Once cells have undergo neoplastic cell transformation they become ECM independent to sustain their survival and proliferation [25]. Although cancer cells exhibit an anchorage independent growth, they still promote integrin signaling during tumor initiation and progression [73,74]. It has been revealed that neoplastic cells increase the integrin expression to promote their cell growth, proliferation and migration [75]. Under normal conditions, β1 integrins together with α6, v, 2, 3 dimers and α6β4 integrins are low level expressed proteins in adult epithelial cells. However in many cancer types a significant overexpression of these heterodimers were remarkably detected (Figure 1.6) [76].

Tumour type	Integrins expressed
Melanoma	αvβ3 and α5β1
Breast	α6β4 and αvβ3
Prostate	αvβ3
Pancreatic	αvβ3
Ovarian	α4β1 and αvβ3
Cervical	αvβ3 and αvβ6
Glioblastoma	αvβ3 and αvβ5
Non-small-cell lung carcinoma	α5β1
Colon	αvβ6

Figure 1.6. List of overexpressed integrins in different cancer types, adapted from Desgrosellier *et al*. 2010 [76].

Cancer cell invasion and metastasis involve multiple distinct steps starting from (i) loss of cell adhesion, degradation of basement membrane and transmigration through interstitial stroma, (ii) tumor angiogenesis and following transendothelial migration into blood vessels and lymphatic vessels which is known as intravasion, (iii) survival in the circulation, (iv) extravasion, (v) colonization in the target organ (Figure1.6) [77]. Briefly, metastatic cells initially loosen their adhesions by disruptions of E-cadherin mediated cell-cell attachment to reach neighboring cells. Following the degradation of basement membrane, angiogenesis endows metastatic cells to enter into circulating system. Leucocytes maintain

proteolytic enzymes and cytokines to facilitate extravasion from blood vessels. Metastatic cells adhere to leukocytes and platelets via their selectins to form emboli for the subsequent adaptation on the target organ.

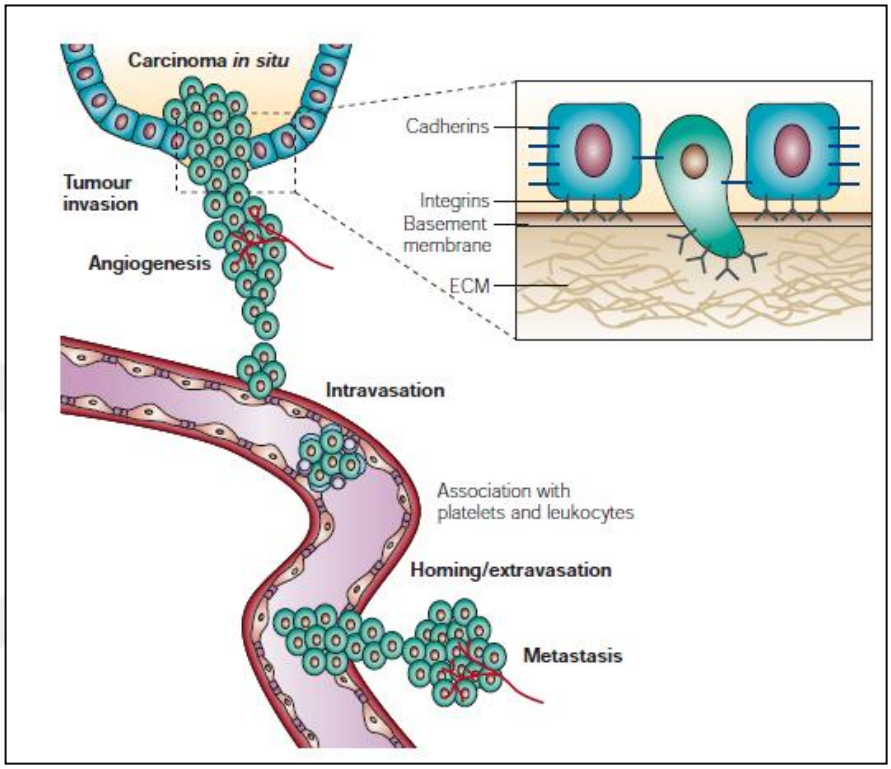

Figure 1.7. Schematic view of metastatic cascade [75].

1.3.1 Role of integrins in metastatic cascade

In the first step of metastasis, disruption of cell-cell interaction with loss of E-cadherin function is required for malignant formation. Dysregulated integrin-receptor tyrosine kinase signaling assists the loss of cell-cell interactions in metastatic cells [75]. One of the study showed that breast cancer cells in matrigel embedded system which were defined as disorganized aggregates of non-polarized cells were re-gained their adherent junction following the treatment with antibody blocking β1 integrin. By this way, cells re-gained their organized cytoskeleton structure and stop growing [78]. Sonnenberg *et al* used β1 knockout epithelial cells of neural origin GE11 and fibroblast-like GD25 cells to showed that cell response is related with ECM and specific integrins on its surface which may

show differences in different steps of metastatic cascade. In this study GE11 epithelial cells "knocked in" to express β1 could only respond to laminin-1 as they expressed α6β1 the major laminin-binding β1 integrin by interrupting the cadherin mediated cell-cell adhesion and scattering [79].

Two main mechanisms were purposed [75] to explain the cell-cell adhesion dysregulation via abnormally increased RTK activity along with integrins. Excessively activated RTKs or src family tyrosine kinases (SFKs) stimulate the phosphorylation of β-catenin and intra-cytoplasmic tail of E-cadherin. E-cadherin/β-catenin was recognized by Hakai (the Cbl-like E3 ubiquitin ligase) which regulated the transfer of ubiquitin chains to E-cadherin/β-catenin complex and induced the degradation of the complex in proteasome. However the balance between ubiquitination and de-ubiquitination mechanism may lead to the endocytosis of E-cadherin/β-catenin and resulted in the loss of E-cadherin function once more [80].

In colon cancer cells the over-experssion of v-Src and subsequent phosphorylation of FAK by β1 integrin signaling led to the disruption of E-cadherin localization which showed that FAK phosphorylation via integrin signaling is necessary for Src-related deregulation of E-cadherin [81].

Integrins regulate epithelial mesencymal transition (EMT) during tumor progression by contributing to the activation of TGFβ which represses the proliferation of epithelial cells and induce primary cancer growth. In order to display its biological activity, TGFβ needs to be incorporated with its propeptide, LAP (the latency-associated peptide) and form a small latent complex [82].

αvβ6 was found to be able to activate TGFβ while depending on whether LAP was immobilized on ECM or given as soluble ligand [83]. In the further stages of tumor development LAP could induce αvβ6 dependent cell movement via increasing MMP-9 expression [83]. Interestingly compare to other subunits of integrin only β8 subunit could activate TGFβ via a metallopreotease dependent way in colon and lung adenocarcinoma, fibrosarcoma and liver cancer cell lines [84].

The essential function of integrin was elucidated in cell migration where it orchestrates the majority of the metastasis progression. The steps of migration can be summarized as; (i)

extension of filapodia in order to direct the cell migration, (ii) formation of lamellipodium (iii) nucleation of focal adhesions in lamellipodium and subsequent actin stress fibre formation and (iv) contraction of stress fibres to generate the pushing the forces which is required for cell movement [85]. Providing the anchorage is the critical function of integrin to regulate the cytoskeleton and maintain migration. Upon induction by growth factors, integrins convey pro-migratory signals by subsequently inducing FAK to regulate the actin cytoskeleton formation and cell motility [75].

FAK leads to the recruitment of SFKs to induce the phosphorylation of p130 CAS and paxillin which recruits Crk-DOCK180 complex for the following activation of Rac. Rac induces the lamellipodia formation through activation of WASp whereas another member of RhoGTPase Cdc42 stimulates the filapodia formation through the activation of SCAR/WAVE. Through their VCA domain at C-terminal region, WASp/Scar family proteins bind and activate Arp2/3, which nucleates and crosslinks new actin filaments. Besides, Rac and Cdc42 induce p21-activated kinases PAK1 and PAK4, respectively, which promote the actin polymerization by activating LIM kinase. While Cdc42 and Rac take role in the actin polymerization at the leading edge, Rho kinase (ROCK) and mammalian diaphanous (mDIA) increase the actomyosin contractility for the trailing-edge detachment. ROCK promotes the phosphorylation of myosin light chain (MLC) by decreasing the myosin light chain phosphatase (MLCP) activity. Integrin regulated Rho-ROCK signaling take part in carcinoma dissemination which is the key for cancer cell invasion through 3D matrices through amoeboid movement [86]. Finally integrins can stimulate downstream signaling of RAS via activation of SFK/Shc signaling as ERK/MAPK activates MLCK via phosphorylation and leading to an actomyosin based contractility [87].

Integrins takes a partial role to facilitate the remodeling of ECM by matrix metalloproteinases (MMPs) necessary for the cell penetration through basement membrane [75]. αvβ3 integrin was found to be upregulated in glioblastoma and melanoma which can also activate MMP2 (a gelatinase enzyme coded by MMP2 gene) and plasmin for the degradation of the interstisyel basement membrane. Following the MM2 interaction with its inhibitor tissue inhibitors of MMP-2 (TIMP-2), the transmembrane matalloproteinase MT1-MMP translocates the MMP2-TIMP2 complex to cell membrane and cleaves the pro-domain of MMP-2 [88]. αvβ3 cooperates with partially activated MMP2 and a generate

fully active MMP2. αvβ3 can also associate with urokinase plasminogen activator receptor (uPAR) [89]. Interaction with uPAR and its activator uPA lead to the conversion of plasminogen to plasmin. In turn plasmin can directly induce ECM degradation by activating the pro-MMPs [90].

Although integrin functions in angiogenesis have not been clearly identified yet, it was found that αvβ3 and its ligand vitronectin facilitate the formation of a tumor vascularization in the high-grade glioblastomas [91]. Besides another study claimed that formation of β1 integrin/hERG1 (human ether-a-go-go related protein 1 channel) complex through FN stimulation induced PI3K-Akt pathway which resulted in the generation of the HIF-1α-induced VEGF secretion factor. As a result, VEGF-A secretion stimulated the angiogenesis formation in the colorectal cancer [92].

In order to survive in different microenvironments, anoikis resistance is an important key for the formation of micrometastasis. EGFR mediated β1 integrin engagement induced BCL-2 expression, reduced its inhibitor pro-apoptotic BIM expression and facilitated ERK activation in the epithelial cells suggesting that integrins together with BCL-2 may coordinate the tumor progression [93]. A more recent work showed that chronic lymphotic leukemia B cell adhesion on FN via α4β1 integrin upregulated Bcl-2 expression and reduced Bax expression which resulted in an enhanced the anti-apoptotic effect [94].

Following micrometastatis, macrometastatis formation which is defined as colonization of tumors in different organs is interdependent with integrins interdependent regulation [75]. Importance of αvβ3 integrin upregulation and binding to platelets by their selectins for better adaptation on new microenvironment is indicated in Figure 1.6 [75]. A recent study indicated that α6β4 association with CLCA (chloride channel calcium activated) in pulmonary endothelial cells assisted cancer cells to target microvascular bed of the lung [95]. In addition αvβ3 interaction with the endothelial cell adhesion molecule L1 endorsed the transmigration of melanoma cells across the endothelium [96]. A new highlighted work proposed that α6β4 and α6β1 expressing tumor exosomes could interact with fibroblasts and epithelial cells in the lung. Once these exosomes were uptaken, cellular morphology changed and this mechanism promoted the metastatic cell colonization and organ specific metastasis [97].

Overall in each step of metatasic cascade integrins takes a crucial role to promote the cell proliferation, cell migration and survival thus many inhibitors and drugs has been developed to target specific integrins in order to block their functions. Vitaxin/Etaracizumab, Volociximab and ATN-161 PHSRN mimetic were designed for anti-renal cell cancer therapy in order to block αvβ3 and α5β1 respectively [98]. A humanized antibody Volociximab is designed against integrin FN recognition motif RGD as an antiangiogenic inhibitor. Volociximab is a chimeric monoclonal antibody, which is composed of 82 per cent human 18 per cent murine and developed as anti-angiogenic inhibitor. Several studies were carried out to determine the function of Volociximab as an angiogenesis blocking antibody [99,100]. Preliminary studies performed on human umbilical vein endothelial cells (HUVEC) showed that an anti α5β1 integrin antibody prevented the tube-like vessel structures in 3D fibrin gel matrices even in the presence of stimulators for new blood vessel formation such as VEGF and bFGF ([100]. Another study showed that function blocking anti α5β1 integrin antibody inhibited the tumor associated blood vessel formation using chorioallantoic xenograft membrane model, which was generated using HT20 colon carcinoma cells [99]. Further studies were focused on the anti-cancer effect of volociximab [101]. In a phase I study on 21 patients with advanced solid malignancies of various cancer types such as RCC, colorectal cancer, melanoma, esophageal cancer, hepatocellular carcinoma, breast, prostate, pancreas, thyroid cancer, salivary gland carcinoma and non-small cell lung cancer [101], showed that out of 21 patients one patient with a RCC showed a minor response and one patient with melanoma displayed a stable disease. As a result, six patients out of 21 acquired clinical benefit and were suggested as candidates for future phase II studies. In another single arm phase II study performed on ovarian cancer patients, out of the 14 patients, CA125 tumor marker was decreased in 12 patient, while 13 patients showed no response against the therapy [102]. In these patients, Volociximab treatment decreased the circulating endothelial progenitor cells (CEPB) which takes role in the progression of macrometastasis and endorse the revascularization subsequent to cytotoxic therapy [103,104]. A more recent study was carried out on 33 patients with advanced solid tumors for the first time using a human integrin monoclonal antibody, PF-04605412. Although the pharmacokinetic of previous studies suggested the use of 15 mg/kg chimeric volociximab antibody during the therapy, this study was not able to achieve the same pharmacokinetic results using 15 mg/kg and indicated the need for five-fold higher dose for an effective treatment. Since 75

mg/kg of was higher than the maximum tolerated doses for the administration of human integrin monoclonal antibody, the use of this drug for cancer treatment became clinically impossible. Therefore, no significant difference by means of anti-tumor activity was obtained from the study [105].

1.3.2. Integrin traffic

Cell migration happens through a series of distinctive phases leading to a net cell-body movement. Firstly CLCA (chloride channel calcium activated), cell becomes polarized meaning that the cell front and rear gets distinct from each other. Following polarization, cell extends protrusions, which could be in a broad lamellipodia or spike-like filopodia structure in the direction of migration at the leading edge. Protrusions are localized by integrins, integrin linked cytoskeletal proteins and receptors for the chemotactic molecules at the leading edge, thereby form a traction site to direct the migration. Cell moves over the tractions site by releasing at the trailing edge or rear later [64,8]. Adhesions in these protrusions are constructed by integrins, which are able to link the extracellular matrix to cytoskeletal proteins [10].

Accumulating evidence showed that the changes in the adhesion traits of neoplastic cells help them to acquire invasive and migratory capabilities [106-108]. The alterations in the expression and function of integrins take part in each step of the tumor development, dissociation of tumor cells from primary site, invasion of the surrounding basement membrane, penetration into bloodstream, transport through circulation, extravasion into parenchyma of distant organs and the formation of new colonies [109]. The organization of cell polarity, adhesion, migration and the related signaling pathways during migration, proceeded perfectly under the control of integrin trafficking consisted of endocytosis and recycling pathways [110].

Elevated expressions of certain integrin levels leads to the deregulation of endocytosis and recycling pathways and consequently leads to the formation of aggressive, invasive, motile cancer cell type formation [38,111]. Among 24 integrin heterodimers, α5β1, α6β4, αvβ3, and αvβ6 have been associated with the cancer progression [112]. Except for α6β4¸ the integrins α5β1, αvβ3, αvβ6 recognizes the RGD sequences and function as FN receptor [10]. Along with α5β1, syndecan-4 heparan sulphate proteoglycans are involved in the

formation of focal adhesion by directly binding to heparin binding domain of FN and consequently regulating the actin cytoskeleton organization, which is a crucial process for cell migration [113,53,114].

1.3.3. Internalization of integrins through different routes

The process involving the management of integrin internalization and recycling cycles might coordinate the distribution of integrins from one part to another in the cells so that migrating cells can remove the integrins from the cell rear and re-introduce them into the cell front in order to regulate the cycles of adhesion assembly and disassembly, which in turn, endow a forward-directed cell movement [110]. To facilitate the coordinated cell motility, the endocytosis and recycling cycles control the localization of integrins at plasma membrane. Endocytosis is defined by the internalization of receptor proteins from the plasma membrane. Enclosed in an endosome these receptor proteins then pass through internal compartments in order to be conveyed to different cellular locations. Endocytic routes are defined as; clathrin mediated endocytosis (CME), clathrin-independent endocytosis, which is mediated by the dynamin-dependent caveolar endocytosis [115] and dynamin-independent macropinocytosis [116]. The clathrin dependent and caveolar endocytosis are driven by dynamin-2 (dyn-2) GTPase which surrounds the neck of budding vesicles to pinch off the membrane [117]. Dyn-2 is recruited by FAK via Src in a PIP2 dependent manner for the destabilization of cell-ECM contact and to facilitate the subsequent microtubule dependent focal adhesion turnover [117]. Dab2 and Numb proteins have been implicated as clathrin dependent endocytosis regulators which have PTB binding domains recognizing the NPxY or NxxY motifs in the integrin β tails [118]. Dab2 and Numb localizes at different cell adhesion sites and directly regulates the integrin internalization and focal adhesion turnover together with clathrin and dynamin [119,120]. As both active and inactive integrins can be internalized, the mechanism of internalization might depend on the localization of adhesion and cell type [120,121]. Together with Eps15 (Epidermal growth factor receptor pathway substrate-15) accessory protein, Dab-2 leads to the clathrin mediated internalization of inactive α1/2/3β1 integrins internalization in conjunction with clathrin from the apical surface to the basal plasma membrane in order to create a new adhesion cites [122].

KIF15 coordinates the localization of Dab-2 to the basal surface of the cell. Along with AP-2 or another clathrin adaptor ARH, KIF15 localized Dab-2 regulates the focal adhesion turnover, which is already localized at the sub-central region of the cell in the large focal adhesions [123]. Par-3-atypical protein kinase (Par-3) phosphorylation and dephosphorylation cycles of Numb regulates the endocytosis of β1 and β3 integrin internalization together with adaptor protein-2 (AP-2) to promote the disassembly of focal adhesion complex, which in turn facilitate cell migration but not cell spreading [119]. Recent studies showed that Arf GTPases also regulates the integrin internalization in coorperation with guanine nucleotide exchange factors. Activation of ubiquitously expressed BRAG-2 (brefeldin-resistant Arf GEFs) catalytic activity by PIP2, which is mostly found in coated pits, subsequently activates Arf5 and Arf6 together with clathrin and its adaptor AP-2. Arf5 promotes β1 integrin internalization whereas Arf6 induces Rac1 activation and lamellipodia formation upon β1 integrin activation [124].

Caveolae are uncoated invaginations constituted by cholesterol and sphingolipids in the plasma membrane, which regulates the clathrin-independent and dynamin-dependent integrin internalization [125]. Caveolar mediated integrin endocytosis has been demonstrated in fibroblast and leukocyte cells. In leukocyte cells, GPCR induced αLβ2 internalization is regulated by the caveolar endocytosis, which promotes the ICAM-1 mediated transmigration of leukocytes [126]. A more recent study on fibroblasts showed that syndecans, specifically syndecan-4, was depicted as an important player in the clathrin-independent and dynamin-dependent integrin internalization. This study suggested that syndecan-4 binding to FN resulted in the syndecan-4 signaling pathway and induced a PKCα dependent activation of RhoG, which in turn led to dynamin and caveolin-dependent α5β1 integrin internalization and promoted the wound healing *in vivo* [127].

Unlike from receptor mediated endocytosis, macropinocytosis is activated by growth factor stimulation such as PDGF (platelet derived growth factor), macrophage colony-stimulating factor (CSF-1), epidermal growth factor (EGF) or phorbol myristate acetate known as tumour-promoting factor, which lead to the uptake of non-selective solute molecules, antigens and nutrients in an actin-dependent process [128]. PDGF stimulation led to accumulation of β1 and β3 integrins at the apical surface of the cell before they are engulfed via macropinocytosis in fibroblast. Formation of integrin pool via PDGF

stimulation may accelerate integrins recycling, which endorses the formation of new adhesion sites [129].

Regardless of the route for integrin internalization, Rab GTPases (Ras superfamily of monomeric G proteins) coordinates the vesicular trafficking of variable cellular cargos through vesicular coat components, intracellular motors, and soluble *N*-ethylmaleimide-sensitive factor attachment protein receptors (SNAREs) [130]. Rab21 directly interacts with β1 integrin to facilitate the endocytosis from plasma membrane to EEA1 (early endosomal autoantigen-1) containing early endosome vesicles [131] though binding a conserved sequence WKLGFFKR [10], mostly found in integrin α tails in a manner insensitive to monodansyl cadaverine. p120RasGAP (RASA-1) competes with Rab21, which binds to the same conserved domain in α tails via its GAP domain, leads to active return of integrin β1 from the EEA1 containing endosomes to the plasma membrane, which is necessary for the directional cell motility in PC-3, MDA-MB-231 and NCI-H460 cells [132]. Rab5 regulates microtubule-dependent adhesion disassembly through mediating active β1 integrin internalization especially on FN-coated substrates [133].

1.3.4 Integrin recycling

In line with endocytosis, recycling provides new adhesion sites along by supporting the formation of cell-matrix adhesion formation. Aside from the regulation of cell adhesion capacity, integrin trafficking can also change the downstream signaling of other receptors to promote the cell migration [134]. Similar to the other cargos, following the endocytosis, integrins mainly recycled back to the plasma membrane via recycling endosomes or trafficked to late endosomes/lysosomes depending on the sorting decisions [135]. For example, sorting nexins 17 and 31 prevent the lysosomal degradation of integrins by binding to the membrane-distal NPxY motif in cytoplasmic β tail via its FERM domain in early endosomes [136,137]. Besides, Wiskott–Aldrich syndrome protein and SCAR homolog (WASH) activates the Arp2/3 complex and regulates the recycling of internalized α5β1 integrin to the plasma membrane and endorse the cell invasion through FN-rich matrixes [138].

The most characterized integrin recycling pathways are defined as Rab-4 dependent fast (short loop) and Rab-11 dependent slow (perinuclear recycling compartment, long loop) routes (Figure 1.8.). Rab-4 dependent short loop recycling pathway controls the integrin recycling in growth factor or serum stimulated cells [139]. Inactive β1 integrin heterodimers are recycled from the plasma membrane in an actin and a Rab-4a-dependent manner via Arf6 while active β1 integrins are recycled through Rab-11 dependent manner back to the plasma membrane [140,141]. Additionally, ligand bound active α5β1 integrins that are directed to lysosomes can be transported back to plasma membrane in a retrograde manner through Rab25 and CLIC-3 (Chloride intracellular channel protein 3) dependent pathway on FN rich matrixes in cancer cells [135]. Rab5 and Rab21 belong to Rab5 family GTPases; Rab5 takes role in β1 integrins endo/exocytic cycle while Rab21 is essential during cytokinesis [131,142].

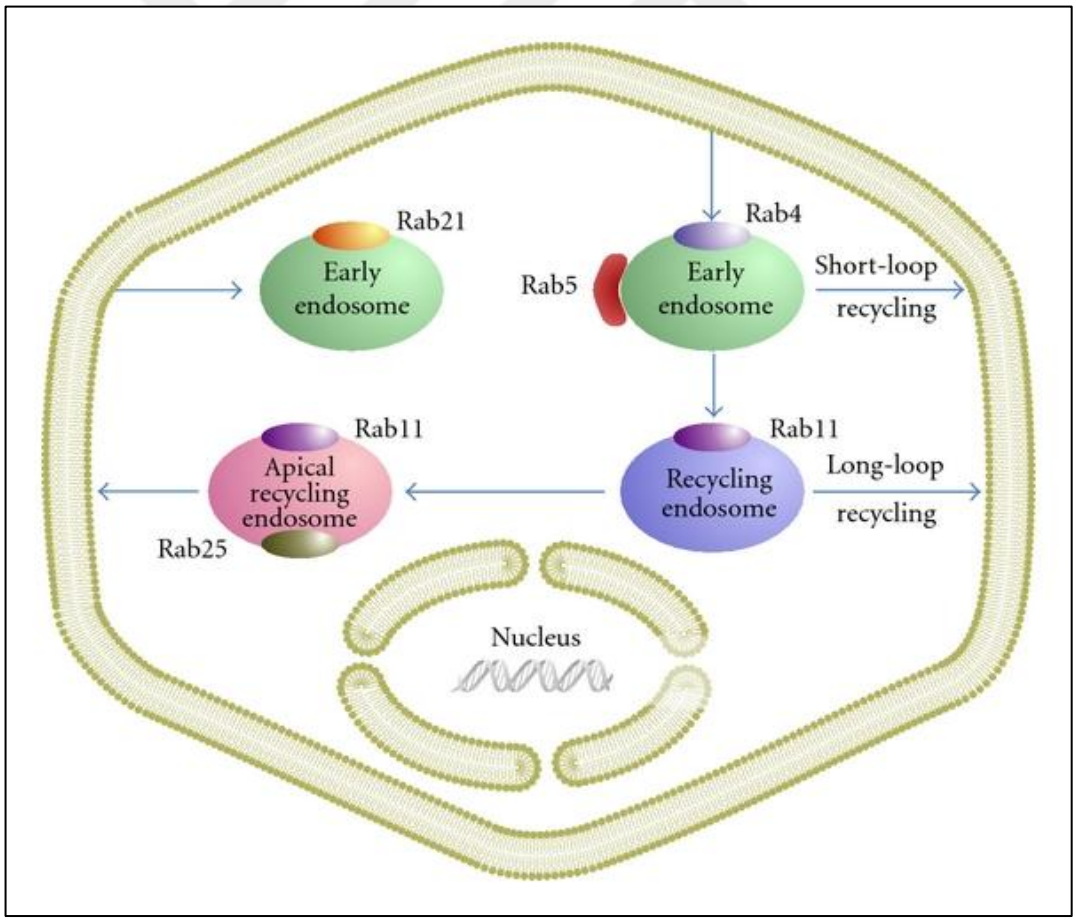

Figure 1.8. Role of Rab family GTPases in integrin internalization and recycling [131].

1.4. SYNDECANS

In mammals there are four types of cell surface syndecans belonging to heparan sulphate proteoglycan family [143]. Based on their protein sequence homology, syndecans are grouped in two pairs in means of sequence identity; syndecan-1&3 and syndecan 2&4. Due to the tissue distribution, syndecan-1 is mostly expressed in mature epithelial cells and takes part in the developmental processes [144]. Syndecan-2, known as "fibroglycan", is mainly produced by mesenchmal cells but also abundant in the liver and neuronal cells and not expressed by the epithelial cell lines. Syndecan-3 is named as "N-syndecan", which is a "neural syndecan" mainly expressed in the major axonal and neuronal migratory pathways in the developing brain but also expressed in some stratified epithelia and in the differentiating cartilage [145] and finally syndecan-4 is, an "amphiglycan" named by David *et al.* 1992, a ubiquitously expressed protein both in the developing and adult tissues [146,147]. Syndecans are typical single *type I transmembrane membrane-spanning proteins* with covalently attached heparan sulphate chains on their extracellular domains, although syndecan 1 and 3 might also contain chondroitin and dermatan sulphate chains. Each syndecan consists of an extracellular domain with glycosaminoglycan chains (GAG), a core protein with a modest size (20-45 kDa), a transmembrane domain and a short cytoplasmic domain that lacks of an intrinsic kinase activity [148]. Although the function of chondroitin sulphate chains remain unclear, heparan sulphate chains are not only involved in the interaction with the heparin binding growth factors such as fibroblast growth factors (FGFs) platelet-derived growth factor (PDGF), transforming growth factor-β (TGF-β) and vascular endothelial growth factors (VEGFs) [149] but also promote interactions with the extracellular matrix protein FN and the plasma protein antithrombin-1 [149].

The cytoplasmic domain consists one variable (V) region, which is unique to each syndecan and two conserved membrane distal and proximal common regions (C1 and C2), respectively. Membrane proximal C1 region have a serine and tyrosine, whereas C2 region includes a EFYA sequence (Glutamic acid, Phenylalanine, Tyrosine, Alanine) at C terminus that is the specific binding site for PDZ (Post synaptic density protein of 95, Discs-large and Zonula occludens-1) domain containing scaffold proteins four of which was identified as the syndecan interacting PDZ domain–containing proteins; syntenin, synectin, synbindin, and calcium/calmodulin dependent serine protein kinase (CASK). C1

domain might involve in syndecan dimerization in order to allow binding several cytoplasmic proteins including ezrin, tubulin, Src kinase, and cortactin while C2 region organizes the clustering of receptors and maintain the connection with actin cytoskeleton (Figure 1.9). Of the syndecans, the variable region is well-studied in syndecan-4 (SDC-4) and regulates the mechanism of syndecan-4-cytoskeleton interactions during cell migration and matrix assembly [149,150]

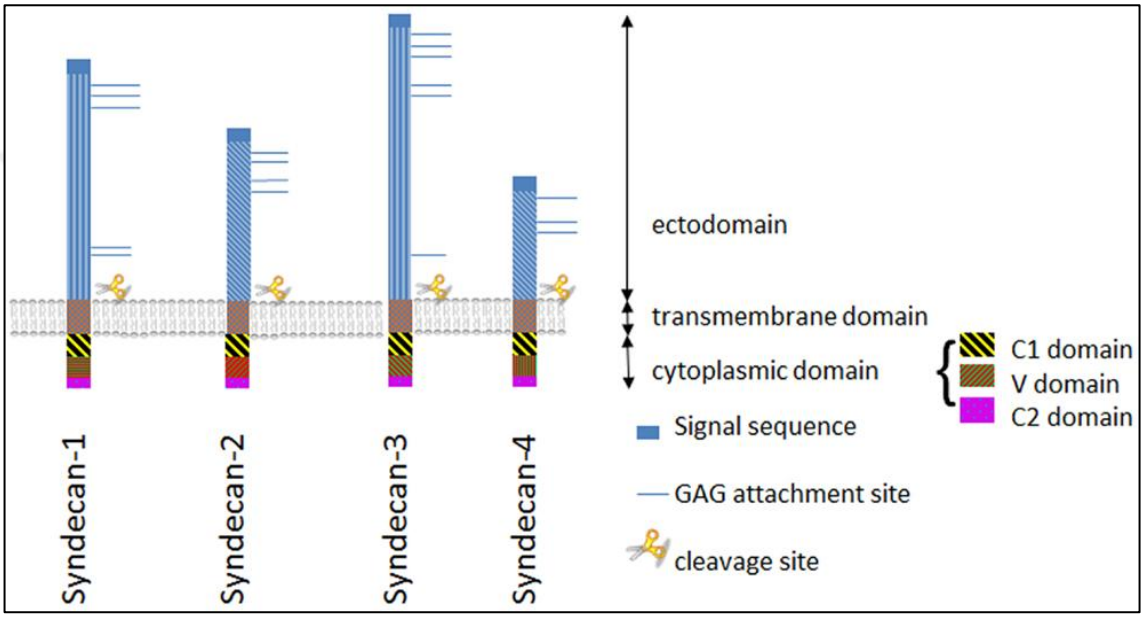

Figure 1.9. Schematic view for two subfamilies of syndecans; syndecan 1-3 and syndecan 2-4. Syndecans have variable ectodomain structure except GAG chain binding sites whereas well conserved cytoplasmic region contains C1, C2 and variable region. Figure was adapted from Szatmari *et al* 2015 [151].

1.4.1. Syndecan-4 signaling

SDC4 is ubiquitously expressed and has a wide range of tissue distribution. According to its functionality, SDC4-driven signaling mechanisms can be divided into extracellular, membrane-based and intracellular signaling pathways [152]. As an example to extracellular signaling, SDC4 extracellular domain is cleaved by matrix metalloproteinases (MMPs) and this cleavage leads to the shedding of its extracellular domain resulting in the release of soluble SDC4 fragments into extracellular matrix with covalently attached GAG chains that are still capable of binding to growth factors. In addition, the shedding of SDC4

extracellular domain can form external points for cell attachment in the surrounding matrix leading to a direct connection with the extracellular matrix protein such as FN. These interactions generate focal adhesion points and give a direction to a guided cell migration both of which occur during inflammation and in tumor cell biology [153].

Upon ligand binding, syndecan-4 multimers are clustered at cholesterol and sphingolipid-rich regions known as lipid rafts which is necessary for its signaling functions at the cell membrane [154]. In addition, though its heparan sulfate chains SDC4 is required to stabilize the interaction between FGFs and its receptor FGFRs and strengthen the receptor-ligand interaction resulting in the activation of FGFRs even at low ligand concentration [155,156]. Independent from FGFR, SDC4 has the ability to activate MAPK signaling pathway via mediating the binding of FGF2 to FGFR by its heparan sulphate chains [157]. Apart from other syndecans, SDC-4 is the unique member of the family as it is co-localized with α5β1 integrin on focal adhesions and takes role in the stress fibre formation when bound to FN [158]. It was shown that SDC-4 can induce PKC-α kinase activity in a ternary complex with PIP2 (phosphatidylinositol 4,5-bisphosphate) [159,160] which facilitates the PKC-α and β1 integrin interaction during cell migration to different ECM matrixes [161]. A recent work postulated that SDC4 mediated activation of PKC-α regulates the integrin β1 internalization and controls focal adhesion formation [162]. PKC-α activation is dependent on PIP2 binding to SDC4 cytoplasmic tail whereas PKCδ prevent this activation via inducing the phosphorylation of Ser183 located at SDC4 intracellular domain [163]. Ser183 phosphorylation of SDC4 prevents the binding of syntenin to SDC4 PDZ binding domain, which disturbs the SDC4 oligomerization [164]. Hence this inhibition mechanism favors the synergestic signaling with SDC4 and α5β1 on FN matrix [165] which in turn activates FAK (focal adhesion kinase) and supports the focal adhesion stabilization by recruiting the cytoskeletal proteins such as α-actinin, vinculin and paxilin [166].

Upon phosphorylation of SDC4 by Src, syntenin binds to PDZ-domain of SDC4 and activates SDC4 recycling by subsequent suppression of small GTPase ARF6 activity which leads to the endocytosis and degradation of α5β1 integrin also the upregulation of αVβ3 at the cell membrane [167].

SDC4 driven intracellular signaling encompasses a broad range of cellular mechanisms such as Rho GTPase regulation, macropinocytosis, caveolin-dynamin dependent β1 integrin internalization, exosome formation and mTOR pathway regulation [168-172]. In the absence of growth stimulation, together with PDZ binding domain protein synectin, syndecan-4 sequesters RhoG by binding to Rho guanine dissociation inhibitor I (RhoGDI1) and subsequently repress of Rac-1 GTPase activity which is necessary for the directional cell migration. In spite of RhoG and Rac1 inhibition, RhoA is activated in the presence of low serum conditions by PKC-α mediated RhoGDI1 phosphorylation at serine 34 residue and facilitate a low rate of migration together with syndecan-4 [170]. In case of growth factor stimulation, syndecan-4 oligomerization induces PKC-α activation and resulting in the phosphorylation of RhoGDI1 at serine 96, which in turn lead to RhoG induced Rac1 activation by forming a trimeric complex with ELMO1 and DOCK180 [173]. Activation of Rac1 by RhoG-ELMO1-DOCK180 complex leads to the polarized cell migration [152]. Besides the control of directional cell migration, SDC-4 is necessary to establish the location of RhoG and Rac1 activation and provide a spatial control of Rac1 activity to determine the cell polarity [150,174]. In addition to the control of cell polarity and migration, SDC4 also regulates the macropinocytosis and subsequent internalization of cell surface proteins through the regulation of RhoG and Rac1 mediated membrane ruffling [175]. SDC4 induces integrin trafficking through PKC-α, which triggers Rho activation and leads to the integrin internalization in a dynamin-caveolin- dependent manner (Figure 1.10) [127].

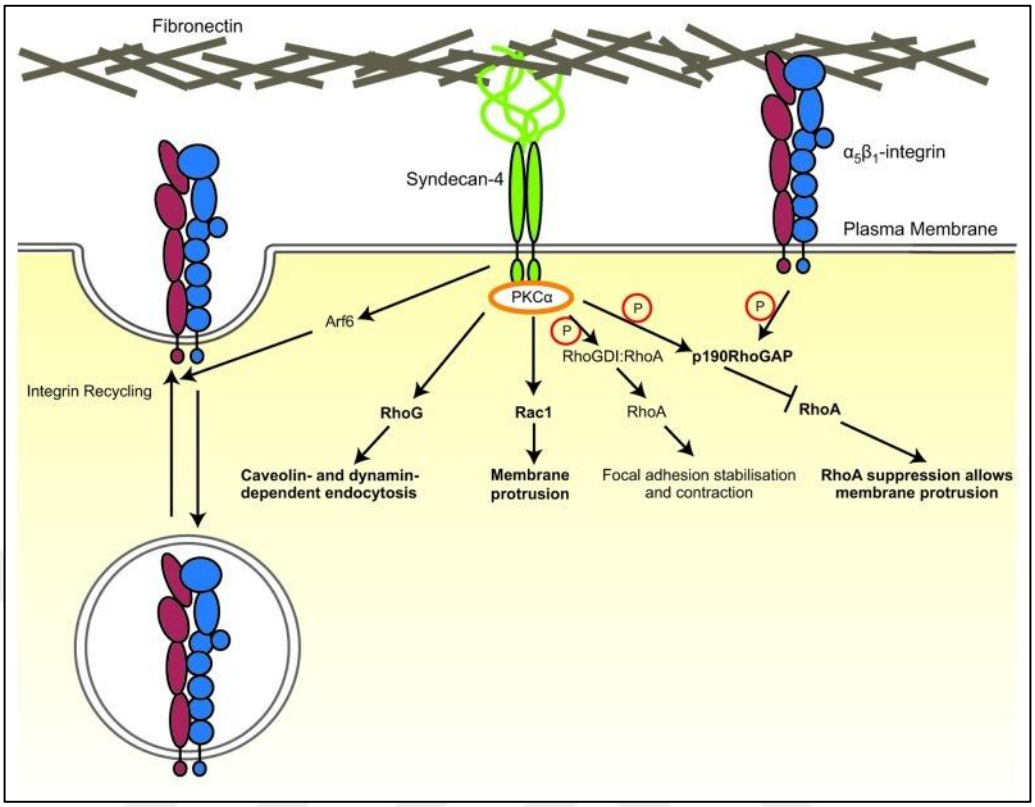

Figure 1.10. Activation of GTPases and integrin recycling by SDC4 [170].

Recent reports take into account SDC-4 role in the biogenesis of intraluminal vesicles (ILVs) of endosomal multivesicular-bodies (MVBs) known as exosomes [176]. Function of membrane proteins are terminated by ubiquitination and their sorting into intraluminal vesicles, which is initiated with the recruitment of an adaptor protein named as ALG-2-interacting protein X (ALIX) to SDC-4-syntenin complex. This protein complex in turn enrolls the endosomal-sorting complex required for the transport III (ESCRT-III) to cytoplasmic vesicles to promote the formation of multivesicular-bodies (MVBs). These MVBs fuse with cell membrane and release their content into the extracellular milieu [172]. Recent evidence showed that exosomes have ability to determine the organ-specific metastasis [177].

The final mechanism for intracellular signaling of SDC-4 is the establishment of mTORC2 complex assembly. Upon PKC-α activation with SDC-4-PIP2 complex, PKC-α recruits mTORC2 members (mSin-1, mLST8, and rictor translocation) and facilitate Akt translocation to cell membrane. Once in the membrane Akt is phosphorylated at Thr308 by PDK1 and Serine 473 by PDK2 known as mTORC2. SDC-4 deletion in endothelial cells

induced the disruption of mTORC2 complex formation and lead to systemic hypertension and decreased endothelial cell size via decreasing FoxO1/3a and eNOS phosphorylation [169].

1.5. TRANSGLUTAMINASE

Transglutaminases (TGs; Enzyme Commision System of Classification 2.3.2.13) are ubiquitously found enzymes in micro-organisms, plants, fish, invertebrates and vertebrates [178]. TGs are responsible for the Ca^{+2} dependent posttranslational modification of proteins by introducing protein-protein crosslink between ε-lysine and γ-carboxamide groups of protein-bound glutamines [179]. To date nine distinct TG genes have been identified [180] in humans while the eight of them; the circulating zymogen factor XII (FXIII), the keratinocyte transglutaminase (TG1), tissue transglutaminase (TG2), the epidermal transglutaminase (TG3), prostate transglutaminase (TG4), transglutaminase X,Y,Z (TG5, TG6, TG7) respectively are catalytically active whereas the erythrocyte membrane protein band 4.2 is the only catalytically inactive member [180,181]. All transglutaminase share the same aminoacid sequences of Tyrosine-Glycine-Glutamine-Cysteine-Tryptophan-Valine-Phenylalanine-Alanine in the catalytic core for the transamidation activity except band 4.2 has Alanine instead of Cysteine. TGs are secreted in unconventional manner to ECM which lack defined amino-terminal hydrophobic leader sequence [182,178]. Characteristics of nine different transglutaminases by means of chromosome location, protein function and distribution are summarized in the Table 1.3 [183].

Table 1.2 Characteristics of Transglutaminases

Gene/Protein	**Chromosome location**	**Function**	**Tissue distribution**
TGM1/TG1 (Keratinocyte TG)	14q11.2	Cornified envelope formation during keratinocyte differentiation	Stratified squamous epithelia of skin, in the lower female genital tract, upper digestive tract
TGM2/TG2 (Tissue TG)	20q11-12		Ubiquitously expressed, located at membrane, cytosol, mitochondria, nucleus
TGM3/TG3 (Epidermal TG)	20q11-12	Cornified envelope formation during keratinocyte differentiation	Brain, testis, intestine, spleen, kidney, hair follicles, epidermis (Hitomi *et al*, Kim *et al* 1999)
TGM4/TG4 (Prostate TG)	3q21-22	Copulatory tract formation, masking the antigenicity of the male gamete in rats	Prostate glands, prostatic fluids, seminal plasma
Gene/Protein	Chromosome location	Function	Tissue distribution
TGM5/TG5	15q15.2	Not defined	Foreskin keratinocytes, skeletal muscle, epithelial barrier lining
TGM6/TG6	20q11	Not defined	Mice brain, human testes and lungs
TGM7/TG7	15q15.2	Not defined	Testes, lungs, brain
F13A1/ FXIIIa	6q24-25	Blood clot formation, wound healing	Platelets, monocytes, macrophages, megakaryotcytes, placenta, uterus, prostate, liver, placenta, synovial fluid, chondrocytes, astrocytes, osteoclasts and osteoblasts
EPB42/ Band 4.2	15q15.2	Regulation of erythrocyte shape, maintenance of erythrocyte membrane stability	Human erythrocyte membrane, spleen, bone marrow, fetal liver

1.5.1 Enzymatic functions of transglutaminases

TGs mediate Ca^{+2} dependent protein cross-linking reaction between the γ-carboxamide group of glutamine (Gln) residue of acceptor protein and ε- amino group of lysine residue of donor protein in order to form an ε-(γ-glutamyl)-lysine isopeptide bond [178]. Ca^{+2} ion is an essential molecule to induce catalytic activity to expose active-site cysteine residue. TG-mediated transamidation results in the release of ammonia molecule as a byproduct and lead to an establishment of a proteolysis-resistant covalent bonds between cross-linked proteins [184]. TGs also catalyse protein aminylation and deamidation reactions for primary amines and polyamines such as; putrescine, spermine and histamine. Protein aminylation reaction occurs via the incorporation of an amine (H_2NR) to polypeptide-bound Gln residue in the acceptor protein. However in the absence of a suitable amine cosubstrate or under lower physiological pH, TG converts Gln residue to Glu residue in the reactive protein which is known as deamination reaction (Figure 1.11.) [178,185].

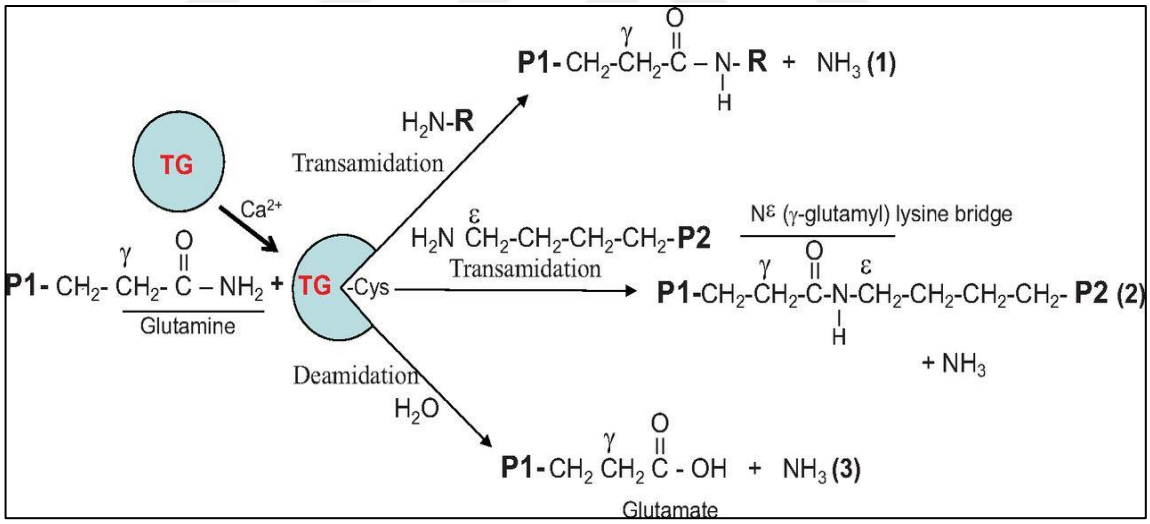

Figure 1.11. Enzymatic functions of transglutaminases. Acceptor protein is represented as *P1* and protein bound amines are represented as *P2*. TG transamidase activity is regulated in the presence of Ca^{+2}. TG can covalently link primary amines or protein bound amines to the glutamine residue of acceptor protein and release ammonia as a byproduct. Protein-protein crosslink can be generated by the formation of ε-(γ-glutamyl) lysine isopeptide bond. Under low pH conditions, TGs can use water molecule as an acyl-acceptorand convert Glu residue to Gln residue by deamination [183].

TGs are associated with several diseases such as neurodegenerative disorders (Huntington, Alzheimer's, Parkinson's, Amyothropic lateral sclerosis), skin diseases (Lamellar ichtyosis), celiac disease, autoimmune disease, fibrosis and cancer [186,187].

Tissue transglutaminase was the first identified member of transglutaminase family, however its physiological functions remain elusive. Compared to other members of the family, TG2 has distinguished characteristics such as ubiquitous expression and extensive tissue distribution [183]. Accumulating evidences showed that TG2 takes role in various stages of tumor progression and drug resistance in many cancer types including breast, melanoma, ovarian, lung, glioblastoma and pancreatic cancer [188-195]. Interestingly recent studies showed the elevated expression levels of TG2 in renal cell carcinoma as well [196,197].

1.5.2 Tissue Transglutaminase

Tissue TG (tTG or TG2) named as TGc or Gh is widely expressed member of the TG family in the body therefore called as tissue transglutaminase [178]. Owing to its unusual multifunctionality TG2 is able to catalyze Ca^{+2} dependent cross-link activity and Ca^{+2} independent GTP hydrolysis [183,179]. Three dimensional structure of TG2 revealed four domains composed of NH_2 -terminal β sandwich domain containing integrin and fibronectin binding sites (residues 1-138) followed by a α/β catalytic core domain (residues 139-471) for acyl transfer reaction and two C-terminal β-barrels (Figure 1.12). Despite of all other transglutaminases, TG2 has an additional guanine binding ability, which is positioned in the cleft between catalytic core and the first β-barrel. TG2 is predominantly found in the cytoplasm while it could be located at cell membrane, mitochondria and nucleus or can be externalized from the cell and deposited in the ECM [178,198].

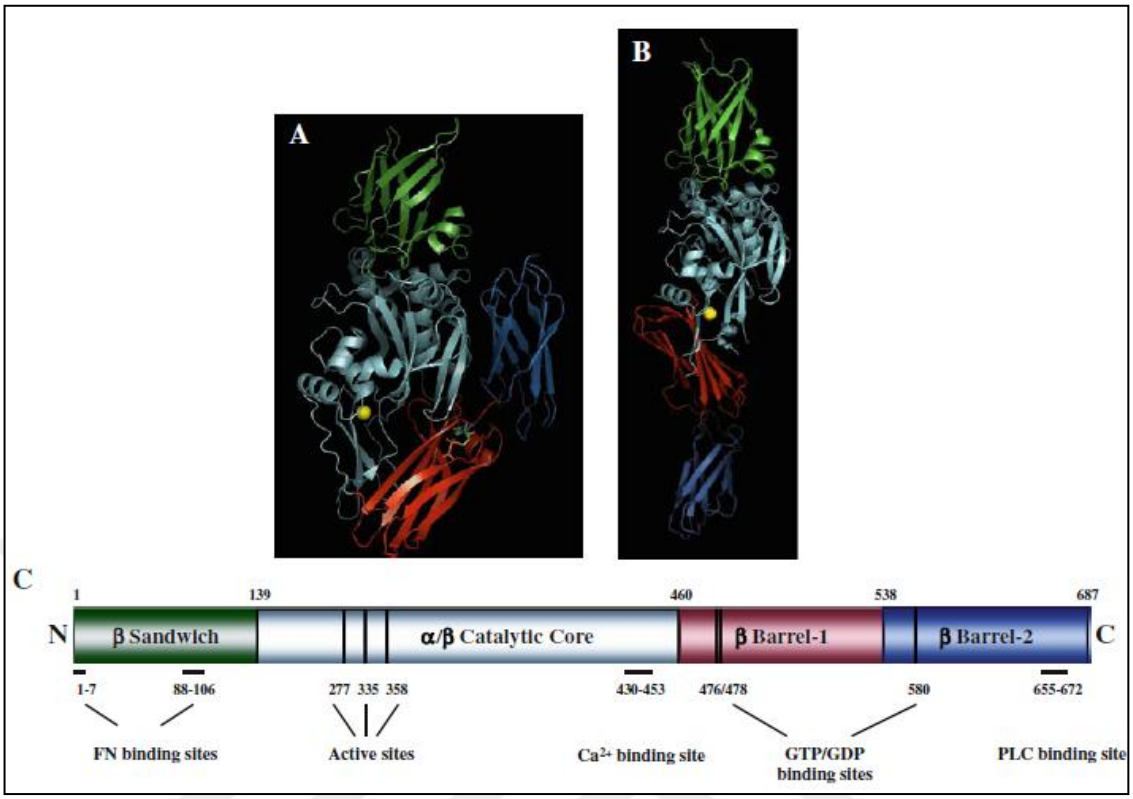

Figure 1.12. Molecular structure (A, B) and schematic presentation of functional domains. Yellow ball represents Ca^{+2} ion. A represents catalytically inactive TG2 which is bound to GTP and B shows the active, extended form of TG2. Four distinct domain of TG2 is shown in C schematically. N terminal β sandwich domain has FN binding site which regulates cell adhesion to extracellular matrix. Catalytic core domain is responsible for enzymatic activity. β barrel domain has GTP/GDP binding sites and C terminal β barrel 2 domain is able to interact with phospholipase C in the absence of Ca^{+2}, which promotes pro-inflammatory functions by introducing crosslinking activity of TG2. Adapted from Wang *et al* 2012 [199].

TG2 multifunctionality is tightly controlled under physiological conditions in the intra- and extracellular environments [200]. Transamidation activity occurs in the presence of Ca^{+2} and inhibited by GTP, GDP and GMP. Although crosslinking activity is observed under high Ca^{+2} concentrations with 90μM of ionization constant, GTP-bound TG2 with a 1.6μM ionization constant, is not able to crosslink proteins [201]. Under normal conditions, TG2 is mainly GTP/GDP bound form and Ca^{+2} concentration is at low levels inside the cell, which means TG-dependent crosslinking is physiologically inactive. This probably

explains why the overexpression of TG2 levels is not correlated with the enhanced crosslinking activity [183].

Interestingly, while extracellular environment conditions contains low GTP and high calcium levels, extracellular TG2 found catalytically inactive [202]. It is indicated that oxidative conditions regulates TG2 activity [183]. Among three triad of cysteine residues; Cys 370, 371 and 230, Cys230 is discovered as the key redox sensor which leads to inactivation of TG2 transamidation activity under oxidizing conditions [203]. In addition to that, nitric oxide induces the nitrosylation of several Cys residues which again induce the the inactivation of TG2 catalytic activity [204]. Besides, TG2 phosphorylation from its serine 216 residue by protein kinase A prevents transamidase function and drives the kinase activation of TG2 [205]. Given that, extracellular oxidation conditions, nitrosylation and phosphorylation reactions regulates the allosteric regulation of TG2 activity.
Independent from its transamidation activity TG2 also has PDI (protein disulphide isomerase) activity through TG2 is able to convert reduced or denaturated inactive RNAse A into active enzyme by catalyzing the formation of correct disulphide bonds [206]. This reaction did not require Ca^{+2} also was not hampered by nucleotides as well [183].

It is known that nucleotide concentration is high and Ca^{+2} levels are low in the cytosol, it was offered that PDI function of TG2 may be active in mitochondria [206]. Studies focused on mitochondrial TG2 showed that in TG2 -/- mice disulphide bond content of mitochondrial complexes I,II and V was decreased and ATP levels in cardiomyocytes and skeletal muscle cells of TG2 -/- mice was diminished as well [207]. Recent studies revealed an interaction between TG2 and ANT1 (adenine nucleotide translocator-1), which is a permeability transition pore protein of mitochondria [208].

1.5.3 TG2 mediated cell adhesion signaling

As mentioned before ECM is a prominent component which can regulate the interactions between the cell and its microenvironment to determine cell behavior or cell fate such as proliferation, migration, survival and apoptosis [1]. The preliminary work implying the association of TG2 in cell-matrix adhesion was performed by Gentile *et al* 1992 [209] and revealed that TG2 over-expressing fibroblast cells gained trypsin resistance whereas TG2 down-regulation or activity inhibition by mABs decreased the cell attachment and

spreading of endothelial cells [209-211]. A follow up study showed that melanoma cells displaying a resistance to fluid shear stress in circulating blood and was able to adhere subendothelial FN via TG2 crosslinking activity [212]. Taken together these studies placed the investigation of TG2-FN in the center of investigation. Erythrocyte TG2 bound to FN with a stoichiometry about 2:1 in the absence of Ca^{+2} which provided that TG2-FN interaction is independent from its enzymatic activities such as transamidation and G-protein function [213,214].

Akimov *et al*. in 2001 [215] showed that during the monocyte differentiation into macrophage, TG2 co-localized with β1 and β3 integrins increasing their cell surface adherence on FN. Down-regulation cell surface of TG2 or reducing its activity with function-blocking antibody led to a marked decrease in adhesion and spreading of monocytes to FN especially on the gelatin binding fragment. FN gelatin binding domain is comprised of four type I and two type II modules. The unique interaction site for TG2 was determined as $I_6II_{1,2}I_{7,8,9}$, domain where I_7 and I_8 modules serves actual TG2 binding while II_2, I_9 modules stabilize the FN-TG2 interaction [216].

Although collagen binds to $I_{6\text{-}9}$, $II_{1,2}$ modules of FN, it was claimed that TG2 binding does not affect the collagen-FN binding therefore collagen-FN and TG2 can form a tertiary complex. More importantly, FN-binding integrins do not interfere TG2 binding sites on FN hence during cell adhesion, TG2 and integrin can collaborate to enhance the cell adhesion due to having different binding sites on FN [217].

The location of integrin binding site on TG2 has not been revealed but it was proposed that it could be placed within the first and the fourth strand of TG2. However integrin-FN binding is a weak interaction, TG2 serves as a bridge between integrin and FN and enhances their binding interaction. Since cell surface TG2 can interact with β1 and β3 integrin subunits, TG2-integrin association did not interfere with integrin-FN interaction therefore TG2-FN-integrin can form a ternary complex. which is necessary to regulate cell adhesion and migration events [215].

Increased levels of cross-linking mutant TG2 on cell surface promotes integrin clustering which triggers RhoA activation by inducing FAK and suppressing Src- p190RhoGAP inhibitory pathway [215,218]. It was known that the heparan sulphate proteoglycan SDC-4

interacts with Hep-2 region of fibronectin and promote RhoA dependent focal adhesion, stress fiber formation and actomyosin contraction together with integrins [219].

Upon TG2 binding to FN, SDC-4 interacts though its heparan sulphate proteoglycan chains to conserved ^{261}LRRWK^{265} heparin binding site of TG2 [220]. This interaction drives PKCα binding to cytoplasmic tail of integrin β subunit. Following the integrin-PKCα interaction, FAK is phosphorylated at Tyr397 and at Tyr861 and stimulates ERK activation [113] through integrin inside-out activation and this interaction regulates integrin distribution on cell surface.

In the presence of FN-TG2 heteorcomplex, SDC4 activated PKCα which subsequently induced syndecan-2 (SDC-2) to modulate actin cytoskeleton organization through the ROCK pathway via RGD independent manner in mouse embryonic fibroblasts (MEFs). This study also indicates SDC4 mediated PKCα signaling induces α5β1 integrin instead of β3 integrin (Figure 1.13) [221].

Role of TG2 interaction with platelet derived growth factor receptors (PDGFR) was identified in fibroblast. In response to PDGF, TG2 promotes complex formation between PDGFRβ and integrins which further induces the phosphorylation of PDGFR downstream signaling members such as; Shp-2 phosphatase at Tyr-542 and Akt1 at Thr-308 and leading to fibroblast proliferation and migration [222].

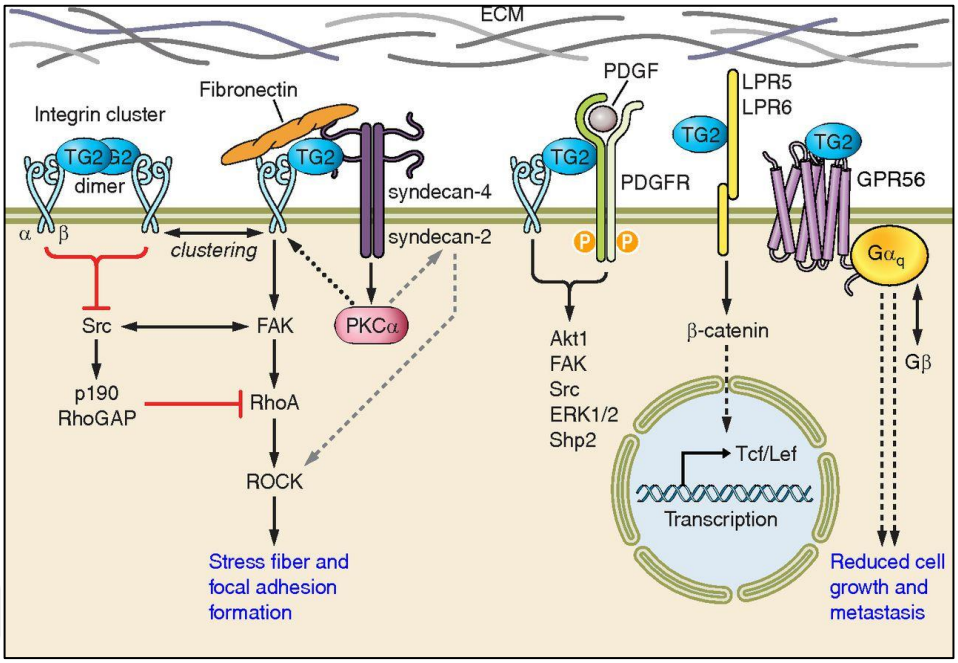

Figure 1.13. Schematic representation of cell surface TG2-mediated cell adhesion signaling [183].

From the previous studies it was shown that the plasma membrane transglutaminase, thrombin-activated FXIII (FXIIIA-subunit), activates vascular endothelial growth factor receptor (VEGFR-2) by crosslinking αvβ3 integrin and facilitate angiogenesis. Recent studies also indicate that TG2 covalently crosslinks VEGFR-2 in endothelial cells and mediates its translocation through nucleus which results in increased VEGF induced ERK activation [223,224].

In addition to integrin binding and modulation of growth factor receptors, TG2 is able to interact with low density lipoprotein receptor related proteins 5 and 6 (LRP5/6) which induces the translocation of β-catenin to nucleus and regulates the expression of Tcf/Lef transcription. Following Tcf/Lef expression $p21^{Cip1}$ levels decreases and vascular smooth muscle cell calcification occurs [225]. Only one study claimed that cell surface TG2 took role as an atypical G-protein coupled receptor (GPR5) ligand and supported the suppressive role of GPR56 in stroma cells [226]. A more recent study emphasized on the potential of TG2 in stimulating the survival signals in cancer cells via microvesicle (MV) formation. The study demonstrated that in cancer cell-derived MVs, crosslinking of FN by TG2 might not only induce mitogenic survival signaling in cancer cells but also contribute to the tumor cell differentiation [227].

1.6. RENAL CELL CARCINOMA

Kidney cancer is the sixth leading cause of cancer deaths and the most lethal urological cancer, which leads to over 102.000 worldwide deaths annually [228]. Men are at higher risk to develop kidney cancer which shows 12/100.000 incidence whereas in women 5/100.000 incidence has been recorded in the developed nations [229]. Kidney cancer is comprised of two main cancer types which are renal cell carcinoma (RCC) and renal pelvis carcinoma [230]. The majority of kidney cancer is related to RCC which is accounting for 90per cent of kidney cancers and in that of 90 per cent, 33 per cent diagnosed cases are being metastatic [230]. Active and passive smoking, obesity, hypertension, continued misuse of pain medications are listed as risk factors in addition to patients with end-stage renal failure, renal cyctic disease and tuberous sclerosis who have higher potential to develop renal cell carcinoma [231-233]. RCC is derived from the proximal renal tubular epithelium of nephron and includes variety of cells such as clear cells, granular cells and spindle cells. The proximal renal tubule regulates the pH, salt and glucose concentration by reabsorption in the process of filtration or excretion of urine [234].

The most common tumor cell type exhibited by RCC is the clear cell RCC (ccRCC) detected in 75 per cent of RCCs. Other tumor cell types are listed as, type I (5 per cent), type II (10 per cent), papillary chromophobe (5 per cent) and oncocytome (10 per cent) [234]. There are sporadic and inherited forms of ccRCC, which are tightly associated with the mutations in von-Hippel-Lindau (VHL) gene located on the chromosome 3 (3p25-26) [234]. Patient with familial VHL- related ccRCC, which has autosomal dominant pattern, inherit a one defective allele and the other allele acquires mutations during development/growth [235]. This type of renal tumor has a more rapid oncogenic transformation. Inherited VHL-related ccRCC usually occurs at a young age and characterized by the presence of multiple primary tumors. Hence non-inherited, sporadic ccRCC tumors acquire defects in each VHL alleles, which leads to VHL protein dysfunction. Non-inherited ccRCC is mostly seen as a late onset case and characterized by a single primary lesion [236]. VHL is a tumor suppressor gene and encodes a component of an E3 ubiquitin-ligase complex named as VHL protein which targets hypoxia inducible factor (HIF), a transcription factor, for proteosome mediated degradation. Under hypoxic conditions or in case of biallelic inactivation of VHL, HIF1-α is not hydroxylated thus

cannot be ubiquitinated by VHL protein complex including elongin B, elongin C, and cullin-2 and Rbx1 [237]. Once stabilized, HIF1-α translocates to the nucleus and forms a complex with HIF1β to become an active transcriptional factor as HIF-1 dimer. HIF1 activates hypoxia-inducible genes which are vascular endothelial growth factor (VEGF), epidermal growth factor receptor (EGFR), platelet derived growth factor (PDGF), glucose transporters, transforming growth factor-α (TGF-α) and erythropoietin. These proteins takes role in angiogenesis, cell growth and survival, glucose metabolism and pH control [238]. Upon growth factor binding to tyrosine kinase receptors on cell membrane HIF1-α protein levels increases through 3 pathways; PI3K/Akt/mTOR, PI3K/RAS/RAF/MEK and integrin driven PI3K activation leading to Akt/mTOR pathway induction (Figure 1.13). Understanding the function of VHL and HIF related pathways takes priority to develop novel targeted therapies against RCC [239].

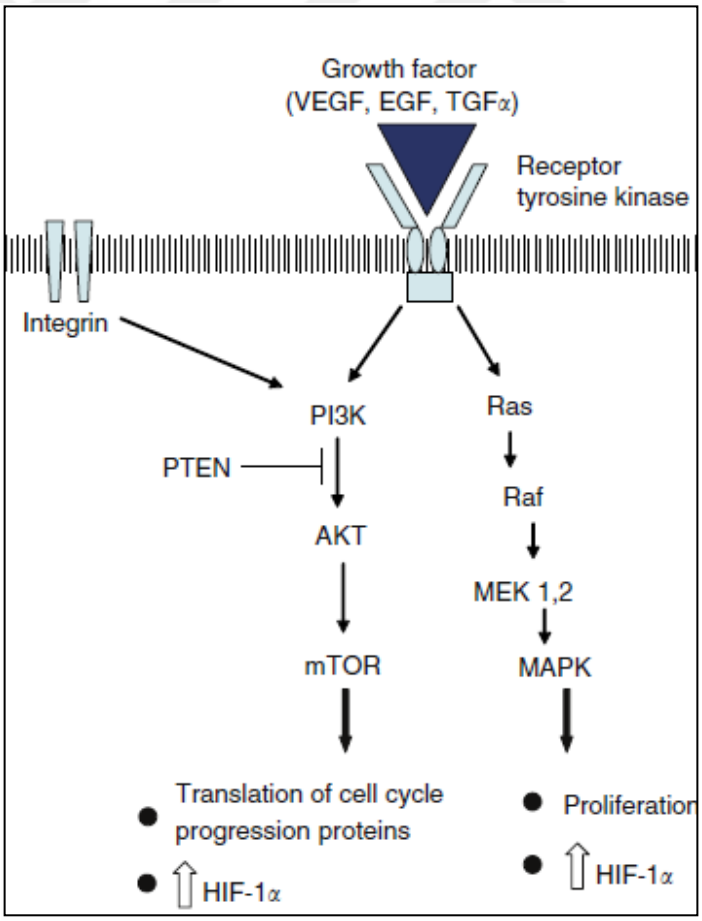

Figure 1.14. Schematic view of signal transduction pathways which leads to increment of HIF-1α adapted from Patel et al. 2006 [229].

Although kidney cancer is resistant to chemotherapy [240] there are other treatment options, which are determined by considering several factors such as stage of the cancer, possible side effects and patient's preferences. Surgical therapies are listed as, (i) radical nephrectomy (removal of large tumors together with the entire kidney, surrounding tissue and lymph nodes), (ii) partial nephrectomy (surgical removal of the tumor which is at 4 cm size or less), (iii) laparoscopic and robotic surgery (radical or partial nephrectomy can be performed) [241]. In addition to surgical therapies there are currently available targeted therapeutic agents for ccRCC. Treatment of intermediate risk ccRCC consists of interferon small molecule VEGFR tyrosine kinase inhibitors (TKI); sunitinib, pazopanib or VEGF targeted monoclonal antibody, bevacizumab together with (IFN-α). Sunitinib and pazopanib are commonly used drugs for the first line therapy at the intermediate risk level since 25 per cent of the patients do not respond against these drugs therefore sorafenib is still an option for the patients resistant to the selective therapy [236]. At the high risk of RCC, intravenously injected mTOR inhibitor temsirolimus is preferred whilst as a second line therapy together with VEGF inhibitors, mTOR inhibitor everolimus and orally administrated TKI axitinib can be selected [242]. In comparison with other TKIs, axitinib has a higher potency and selectivity against VEGF receptors which is able to recognize VEGFR 1, 2, 3 even at nanomolar concentrations [243]. However, the efficacy of VEGF and mTOR inhibitors differs from patient to patient also the combinations of the agents may lead to prohibitive toxicities, therefore exploring novel biomarkers and developing inhibitors beyond VEGF/mTOR signaling appears to be more promising [244].

1.6.1 Tissue transglutaminase in RCC

Pioneering work by Erdem *et al* in 2014 showed that TG2 along with ITGβ1-SDC4 is related with the tumor aggressiveness suggesting that TG2 interaction with ITGβ1-SDC4 could be a novel biomarker for the detection of metastasis in RCC [196]. In this paper, experiment was carried out with 95 samples together with autologous healthy kidney samples. Although there was no correlation detected in the expression levels of TG2, ITGβ1 and SDC4 by means of metastasis, microvascular invasion and histopathology which was analyzed with Fuhrman grade method, a remarkable negative correlation was detected between tumor necrosis and expression levels of TG2, ITGβ1 and SDC4. Results indicated that 70.5 per cent of RCC tumors displayed a 2.9 fold decline in *TGM2* Results

indicated that 70.5 per cent of RCC tumors displayed a 2.9 fold decline in *TGM2* expression whereas TG2 catalytic activity was decreased in the tumor body of randomly selected samples by an average of 87.5 per cent. In comparison with control epithelial cells, primary and metastatic site RCC cells showed a higher *TGM2* mRNA levels. In both primary and metastatic cell lines TG2 activity was significantly decreased compared to control cells. Since TG2 down-regulation and loss of TG2 activity facilitate tumor growth rather than being an ECM stabilizer TG2 interaction with ITGβ1 and SDC4 put forward the necessity of TG2 as a cell adhesion protein during tumor progression. Results depicted from study indicated that TG2 interaction with ITGβ1 and SDC4 is obligatory because neither TG2 nor ITGβ1 or SDC4 increment lead to the development of RCC metastasis by themselves. In a follow-up study carried out between metastatic and primary RCC tumor tissue samples *(n=33)* where gender, age, nuclear grade and pathologic T stages paired within tissue samples, an increase in TG2 protein levels in the primary tumors of metastatic patients was evident along with a decrease in the disease-free survival rates suggesting that the initial increment of TG2 expression in primary site tumor cells could be a predictive marker during the diagnosis [197]. Different form Erdem *et al*. 2014 in the study by Park *et al*. 2015 comprising higher specimen number of 638, it was reported that the expression levels of TG2 in primary site tumor samples was not only related to ccRCC tumor aggressiveness but also with higher values of pathological grades [245]. By the same research group, a new partner of TG2 in kidney cancer, named as CHIP was introduced, (carboxyl-terminus of HSP70-interacting protein) stating that owing to its ubiquitin ligase activity CHIP targets TG2 to proteosomal degradation and the reduced the levels of TG2 leads to down regulation the tumor growth in RCC [246].

In addition to the prognostic significance of TG2 in RCC tissue samples, TG2 was found to be important in the control of apoptosis [247]. Study demonstrated that TG2 silencing stabilized p53 expression and led to an increase in the apoptosis of 768-O, A-498, Caki-1 and ACHN cells. Besides, TG2 was able to crosslink the DNA binding domain of p53 in TG2 -/- mouse embryonic fibroblast (MEF) cells [248]. Further study was focused on the detailed molecular mechanism of TG2 dependent p53 degradation. Under starvation conditions using aminoacid free Earle's Balanced Salt Solution (EBSS), TG2 was able to interact with p53 and p62 concurrently regardless from the ubiquitin-dependent recognition of p62. The study revealed that p62 binding domain of PB1 (Phox and BEM1p-1)

interacted with β-barrel domain of TG2 whereas HDM2 (human double minute 2 humolog)-binding domain of p53 interacted with N-terminus domain of TG2. Moreover, in xenograft animal models the use of TG2 inhibitors together with DNA targeted anti-cancer drug doxorubicin decreased the tumor size [248].

Overall accumulating evidences point at the importance of TG2 and interaction with its partners which should be investigated in detail to develop a novel diagnostic biomarker in kidney cancer.

1.7. AIM OF THE STUDY

cRCC is the most malignant type of kidney cancer with high mortality rate due to chemo- and radio-resistance and insufficient targeted drug therapies particularly in metastatic stage [236]. Owing to increased expression of integrins in various cancer types, a chimeric antibody Volociximab has been developed as a commercial drug in order to prevent tumor-related angiogenesis by targeting α5β1 integrins [101]. Although *in vitro* studies performed using Volociximab in endothelial cells showed a reduced level of blood vessel formation even in the presence of growth factors [78], the clinical trials in advanced solid tumors especially in RCC did not lead to a significant change during the cancer progression [101]. Unfortunately, recent study carried out using a human monoclonal integrin β1 antibody also indicate that previous pharmacokinetic studies was not sufficient to determine the accurate dosage to decrease or prevent the cancer progression since the therapeutically effective dosage should be increased 5 times more than tolerated dosage, which may lead to a subsequent cytokine mediated infusion reaction [105].

Recent studies highlighting the involvement of TG2, a ubiquitously expressed protein, in RCC suggested that together with ITGβ1 and SDC4 TG2 can be a prognostic marker for this cancer type due to the high level expression in the primary site tumor samples that has displayed metastatic properties [196]. In addition, TG2 takes a role in the crosslinking of the DNA binding domain of p53 which subsequently results in p53 degradation leading to increased tumor survival via evasion of apoptosis [247,248]. Moreover together with TG2 inhibition, DNA targeted anti-cancer reagents decreased the tumor volume in the xenograft models [248].

Given the proposed role of TG2 in cRCC tumor metastasis, this study aims to investigate the role of TG2 in SDC-4 driven integrin turnover [113] using cRCC cell lines. Although SDC4 has been shown to induce integrin trafficking [53], the role of TG2, one of the novel cell surface partners of SDC4, in this process has not been demonstrated yet. Recent study demonstrated by Telci *et al* 2008 showed that TG2-FN heterocomplex induced TG2/SDC-4 interaction, which in turn activated PKC α through binding to β1 integrin and subsequently triggered the integrin dependent survival signals in RDG-independent manner [113]. Although at the time the proposed activation of this mechanism defined as a novel integrin inside-out signaling pathway, the recent finding of SDC-4 driven integrin turnover suggests that the observed effect could be due to TG2 mediated SDC4 activation leading to increased turn-over of β1integrins.

In the light of these evidences this thesis seeks to understand the importance of TG2 in the cell adhesion of primary and metastatic site cRCC cancer cells on β1 integrin matrices by focusing on the interplay between the cell surface TG2 partners ITGβ1 and SDC4. The second aim of this study is to investigate the role of TG2 in ITGβ1 internalization and recycling using TG2 down-regulated and over-expressed metastatic Caki-1 cells. Finally in order to understand the role of SDC4 in this mechanism, SDC4 was stably down-regulated in TG2 overexpressed Caki-1 cells using lentiviral particles.

2. MATERIALS

2.1. INSTRUMENTS

The instruments used in this study were as follows:

- Laminar flow cabinet (ESCO Labculture Class II Biohazard Safety Cabinet 2A, Singapore)
- CO_2 incubator (Nuaire NU5510/E/G, USA)
- Centrifuge (Hettich mikro 22R and SİGMA 2-5 centrifuge, Germany)
- Vortex (Stuart SA8, UK)
- pH meter (Hanna instruments PH211, Germany)
- Mini-PROTEAN Tetra Cell Electrophoresis System (Bio-Rad 165-8001, USA)
- ChemiDOC XRS+Gel Imaging System (Biorad Universal Hood 2 (USA)
- Mini Trans-Blot Cell Blotting System (Bio-Rad 170-3935, USA)
- Heater (Bioer,MB102, China)
- 80 °C freezer (Thermo Forma -86 C ULT Freezer, USA)
- ELISA plate reader (Bio-Tek EL x 800, USA)
- Magnetic Stirrer(Heidolph MR 3004, Germany)
- FACS Calibur (BD Biosciences, USA)

2.2. EQUIPMENTS

The laboratory equipments used in this study were as follows:

- Serological pipettes 25, 10, 5, two ml (Grenier-Bio or Axygen, USA)
- Micropipettes 10µL, 20µL, 100µL, 200µL, 1000µL (Eppendorf Research, Germany)
- Polypropylene centrifuge tubes, 50 ml, 15 ml, two ml, one ml, 0.5 ml (Isolab, Germany)

- Cell culture flasks, T-25, T-75, T-150, multiple-well cell culture plates, and cryovials (TPP Switzerland or Grenier-Bio, Germany)
- Electronic pipette (CAPP aid, Denmark)
- Pipette tips 10 µL, 100µL, 200, 1000 µL (CAPP Expell Plus, Denmark)
- Filter 0.22 µm (TPP, Switzerland), 0.45 µm (Santorium Stedim_Biotech, Germany)
- Bright-Line™ Hemacytometer (Sigma Aldrich, Z359629, USA)
- Cover Slip (Sigma Aldrich, Z375357, USA)
- Graduated Cylinder 50 mL, 250 mL, 500 mL, 1000 mL (Isolab, Germany),
- Whatman paper (Isolab, Germany)

2.3. CHEMICALS

2.3.1. Cell Culture Media:

- Dulbecco's Modified Eagle's Medium, high glucose (Gibco 41966)
- McCoy's 5A Medium (PAN Biotech P04-00501)

2.3.2. Growth Supplements:

- Fetal Bovine Serum (FBS) cell culture tested (Sigma F9665, Germany)

2.3.3. Other Reagents:

- 2-propanol (AppliChem A3928, Germany)
- Absolute Ethanol (AppliChem A3678, Germany)
- Acrylamide/ Bis-acrylamide (29:1) (Sigma A3574)
- Ammonium Persulfate (APS) (BioRad, 1610700, USA)
- Bovine Serum Albumin (Santa Cruz, sc-2323, USA)
- Collagen Type-I from Human Placenta (Sigma C7774)
- Dimethyl sulfoxide (Santa Cruz sc-202581, USA)

- Dithiothreitol (DTT) (Applichem A1101, USA)
- Dulbecco's Phosphate Buffered Saline (DPBS) (PAN Biotech P04-53500, Germany)
- Ethylenediaminetetraacetic acid (EDTA) (Merck, K40173218 946, Germany)
- Ethylene glycol tetraacetic acid (EGTA) (Fluka 03779, USA)
- ExtrAvidin Peroxidase (Sigma, E2886)
- Fibronectin from Human Plasma (Sigma F0895)
- Glycine (Merck 104169)
- 4-(2-hydroxyethyl)-1-piperazineethanesulfonic acid (HEPES) (Multicell 600-032-EG, Canada)
- Laminin from Human Placenta (Sigma L6274)
- Methanol 99per cent (Sigma, 34885, USA)
- Phenylmethanesulfonylfluoride (PMSF) (Sigma 78830, USA)
- Protease Inhibitor (PI) (Sigma, P8340, USA)
- Penicillin-streptomycin (Thermo Scientific SV30010 or Biochrom A2213, Germany)
- OPD Substrate Tablets (o-phenylenediamine dihydrochloride) (Invitrogen, 34006)
- Protein Assay Reagent A (BioRad, 5000113)
- Protein Assay Reagent B **(**BioRad, 5000114)
- Puromycin dihidrochloride (Santa Cruz, sc-108071)
- Polybrene (Santa Cruz, sc-134220)
- Sodium orthovanadate (Na_3VO_4) (Sigma, S6508, USA)
- N,N,N′,N′-Tetramethylethylenediamine (TEMED) (Sigma, T7024, USA)
- Trypsin-EDTA (Biochrom L2153, Germany)
- Tris-base (Merck 108387)
- Tris-HCl (Merck 108219)
- Triton-100X (Biomatik Corporation, A4025)
- Trizol (Invitrogen, 15596-018)
- Tween-20 (Merck, 822184)

2.4. KITS and SOLUTIONS

- Amersham Hybond- ECL Nitrocellulose Membrane (GE Healthcare RPN303D)
- Amersham Rainbow Protein Marker (GE Healthcare RPN800E)
- Bovine Serum Albumin, Protein Standard (Sigma P0834)
- Clarity™ Western ECL Substrate, (BioRad, 1705061,USA)
- RIPA Lysis Buffer (Santa Cruz sc-24948, USA)
- Hs_TGM2_1_SG QuantiTect Primer Assay (QT00081277, USA)
- Hs_ITGB1_1_SG QuantiTect Primer Assay (QT00068124, USA)
- Hs_SDC4_1_SG QuantiTect Primer Assay (QT01008126, USA)
- Hs_RRN18S_1_SG QuantiTect Primer Assay (QT00199367, USA)
- Hs_TGM2_1 FlexiTube siRNA (20nmol/tube) (Qiagen SI00743715, USA)
- Hs_TGM2_6 FlexiTube siRNA (20nmol/tube) (Qiagen SI03055465, USA)
- AllStars Negative Control siRNA (20nmol/tube) (Qiagen 1027281, USA)
- RNAifect Transfection Reagent (Qiagen 301605, USA)
- Hiperfect Transfection Reagent (Qiagen, 301704, USA)
- PVDF membrane 0.45 μm, 26.5 cm x 3.75 m (ThermoFisher Scientific, 88518 , USA)
- Protein G Plus Agarose bead (Santa Cruz, sc-2002, USA)
- Protein A Agarose bead (Santa Cruz, sc-2001, USA)
- Syndecan-4 shRNA (human) lentiviral particles (Santa Cruz, sc-36588-V, USA)
- TG2 shRNA (human) lentiviral particles (Santa Cruz, sc-37514-V, USA)
- Control shRNA lentiviral particles (Santa Cruz, sc-108080, USA)
- copGFP Control Lentiviral Particles (Santa Cruz, sc-108084, USA)
- QuantiTect SYBR Green PCR Kit (Qiagen, 204145, USA)
- Sensiscript RT Kit (Qiagen, 205213, USA)

2.5. ANTIBODIES

2.5.1. Primary Antibodies

- Mouse- anti-TG2 Antibody (ThermoFisher Scientific, Labvision Cub 7402, MS-224-P, USA)
- Monoclonal Anti-β-Actin antibody produced in mouse (Sigma,)
- Polyclonal rabbit anti- Integrin β1 Antibody (Santa Cruz, sc-8978, USA)
- Anti-Syndecan 4 antibody (Abcam, ab24511, USA)
- Active human integrin β1 from 12G10 clone (MCA 2028, BioRad, USA)

2.5.2. Secondary Antibodies

- Anti- rabbit IgG Peroxidase Conjugate (Sigma A0545)
- Anti- mouse IgG Peroxidase Conjugate (Sigma A4416)
- Alexa Fluor® 488 Goat Anti-Mouse IgG (H+L) 2mg/ml (ThermoFisher Scientific, 35502, USA)
- Pierce High Sensitivity Streptavidin (Thermo Scientific, 21130 USA)

2.6. CELL LINES

- A-498, Primary Human Kidney Epithelial Carcinoma, Adherent (ATCC Number: HTB-44)
- ACHN, Metastatic Renal Cell Adenocarcinoma (Lung), Adherent (ATCC Number: CRL-1611)
- Caki-1, Metastatic Kidney Clear Cell Carcinoma (Skin), Adherent (ATCC Number: HTB-46)
- Caki-2, Primary Clear Cell Carcinoma of Human Kidney, Adherent (ATCC Number: HTB-47)

3. Methods

3.1. Cell Culture Methods

3.1.1. Cell types and culturing conditions:

Caki-2, A-498, Caki-1 and ACHN Renal cell carcinoma cell lines were obtained from ATCC (American Type Cell collection. ACHN and A-498 cells were cultured in Dulbecco's Modified medium and Caki-1 and Caki-2 cells were maintained in McCoy's 5A medium, both of which were supplemented with 10 per cent (v/v) FBS (Fetal Bovine Serum), 100 units/ml Penicillin and 100µg/ml Streptomycin. Cell line description, growth properties, ATCC catalog number and characterization according to VHL gene mutation were listed in Table 2.1.

Table 2.1. Primary and metastatic site cell lines

Cell Type	**ATCC number**	**Growth Properties**	***VHL* gene mutations**
Caki-2, primary clear cell carcinoma of human kidney	HTB-47	Adherent	-/-
A-498, human kidney carcinoma	HTB-44	Adherent	+/+
Caki-1, human kidney carcinoma derived from skin metastatic site	HTB-46	Adherent	-/-
ACHN, human kidney carcinoma derived from pleural effusion metastatic site	CRL-1611	Adherent	-/-

3.1.2. Cell passaging

Cell passaging was performed when RCC cells reached to a 70 per cent confluency. Briefly cells were rinsed with 1X DPBS (Dulbecco's Phosphate-Buffered Saline) pH 7.4 and dislodged using 0.05 per cent (w/v) trypsin, 5 mM EDTA solution in PBS pH 7.4. Trypsin activation was neutralized using 10per cent FBS (v/v) containing medium to give approximately a 1:3 final volume ratio of trypsin to medium. Cells were precipitated by centrifugation at 300 *xg* for 5 minutes and resuspended in their pre-defined growth medium.

3.1.3. Determination of cell number

Cell were detached from cell culture plates and collected in 15 ml tubes as described above (Section 3.1.2). 10 µl aliquots of the cell suspension were loaded onto BrightLine hemocytometer. The middle area of hemocytometer was determined as the cell counting area by using the inverted light microscope (Nikon Eclipse TS100). The cell number per milliliter was calculated according to the formula ‘‘counted number of cells x dilution factor/ mm2 x chamber depth’’.

3.1.4. Cryopreservation of cells

Cells were trypsinized and counted as described above (Section 3.1.3). Counted cells were centrifuged at 300 *xg* for five minutes. Density of cell number per one cryovial was determined as $1x10^6$ cells/mL and cells were resuspended in 1 milliliter freezing mixture containing 10 per cent (v/v) DMSO (Dimethyl sulfoxide) and 90 per cent (v/v) FBS. Cells were then frozen at -80°C and transferred to a liquid nitrogen container in the following day for the long-term storage.

3.1.5. Thawing mammalian cells

Stock cells were taken from the liquid container and quickly warmed up to 37°C. Cell suspension was collected into a sterile 15ml tube and 5ml growth media was added drop

wise onto the cell suspension with continuous mixing to avoid harming the cells with a sudden increase in the osmotic pressure. Cell suspension was centrifuged at 300 *xg* for 5 minutes to remove DMSO containing freezing mix. Cell pellet was resuspended in growth medium and transferred into a tissue culture plate. The medium was then changed in the next 12-24 hours to remove the rest of the DMSO, which is a toxic substance. Cells were passaged at least once before the experiment begins.

3.2. DETECTION OF GENE EXPRESSOIN LEVELS OF TG2, SDC4, INTEGRIN β1 IN RCC CELL LINES

3.2.1. RNA isolation

Caki-2, A-498 and Caki-1, ACHN cells were counted and seeded into 6 well plates at 200.000 cells/well and 300.000 cells/well density respectively, in 10 per cent (v/v) FBS, 1 per cent Pen/Strep containing relevant complete medium. Following day, cells were incubated with 2 per cent (v/v) FBS containing medium for 16 hours to induce quiescence. Samples were collected in 500µl of Trizol reagent into sterile 1.5ml tubes and incubated at room temperature for 5 minutes to dissociate the nuclear complexes. 100 µl of chloroform was added on the samples and mix well for 15 seconds then incubated at room temperature for 15 minutes. Samples were centrifuged at 12.000 *xg* for 15 minutes at four degree and the upper aqueous phase containing the RNA was transferred into a fresh 1.5ml tube, mixed with equal quantities of isopropanol subsequently and incubated on ice for 15 minutes. Following incubation samples were centrifuged at 12.000 *xg* for 15 minutes to obtain the RNA precipitate which was a white-yellow pellet at the bottom. Pellet was cleared with 75 per cent (v/v) ethanol and centrifuged at 7.000 *xg* for 10 minutes. Supernatant was discarded and remaining ethanol was removed by air-drying. Pellet was dissolved in RNase-DNase free water and incubated at 55°C for 30 minutes. RNA concentration was measured using Nanodrop Spectrophotometer. The RNA concentration was calculated according to formula “Concentration of RNA sample (ng/µl) = 40 x A_{260} x dilution factor”.

3.2.2. Reverse transcriptase polymerase chain reaction

cDNA products were reverse transcribed using Sensiscript Reverse Transcriptase from QIAGEN. PCR reaction was carried out at 37°C for 60 minutes according to manufacturer's protocol (Table 2.2). cDNA samples were measured using NanoDrop 1000 Spectrophotometer.

Table 2.2. RT-PCR reaction mix

Reagents	**Volume per reaction**
10x Buffer	2 µl
dNTP (5mM)	2 µl
Oligo-dT primer (10 µM)	2 µl
Senscript Reverse transcriptase enzyme	1 µl
Rnase-Dnase free water	variable
Template	variable
Total reaction volume	20 µl

3.2.3. Quantitative polymerase chain reaction

The mRNA expression levels of *TGM2*, *SDC4* and *ITGβ1* genes were analyzed using Qiagen SYBR Green PCR Kit (cat no: 204143). Reaction mixture contains 6.25µl Syber green PCR mix, 1.25µl universal primer, 3µl Rnase-Dnase free water and 500 ng for each sample, according to the reaction conditions listed in Table 2.3.

Table 2.3. Quantitative PCR conditions

Cycle	Temperature	Time	Phase
1	94°C	15 min	
2	95°C	5 min	Initial denaturation
3 (39 repeat)	95°C	60 sec	Denaturation
	55°C	60 sec	Annealing
	72°C	60 sec	Extension
4	72°C	10 min	Final extension
5 (80 repeat)	50-80°C 0.5 °C increase /12 sec		Melt curve
6	4°C	∞	Cooling

Samples were studied in triplicate. During the analysis relative quantification was normalized using 18S rRNA reference gene and absolute quantification was analyzed using the standard curve.

3.3. MEASUREMENT OF TG2 AND INTEGRIN B1 PROTEIN LEVELS IN RCC CELL LINES

3.3.1. Preparation of cell lysates

Caki-2 and A-498 (200.000 cells/well) and Caki-1, ACHN (300.000 cells/well) cells were counted and seeded into 6 well plates. Cells were brought to the quiescent state by incubation in 2 per cent (v/v) FBS containing medium for 16 hours. Next, cells were immediately placed on ice and scraped from the surface using RIPA (Radioimmunoprecipitation assay) lysis buffer (50 mM NaCl, 1 per cent (v/v) Igepal CA-630, 0.5 per cent (w/v) sodiumdeoxycholate, 0.1 per cent (w/v) SDS in 50 mM Tris pH 8.0) containing 1mM Na_3VO_4, 2 mM PMSF and 1 per cent (v/v) protein inhibitor cocktail. Following the mechanical shearing of DNA that was carried out by 4 cycles of sonication

at 60 per cent power with three second pulses on ice, cell lysates were cleared from DNA by centrifugation at 12.000 *xg* for 10 mins at four degree.

3.3.2. Determination of protein concentration by Lowry method

Protein content of cell extracts was determined using a colorimetric kit, Bio-Rad Lowry Assay. Five µl of BSA standards ranging between 0.05-0.75mg/ml and one µl of 1:5 diluted cell lysates dissolved in four µl of dH_2O were added into the well of 96 well plate in duplicate. Samples were mixed with 25 µl of Lowry Assay A solution and 200 µl of B solution subsequently and mixture was incubated for 15 minutes at room temperature. The absorbance values were taken using Elisa Microplate reader at 750 nm to draw a calibration graph.

3.3.3. Sodium dodecyl sulfate-polyacrylamide gel electrophoresis (SDS-PAGE)

Denatured proteins were separated due to their molecular weight using SDS-PAGE method. Four per cent (w/v) polyacrylamide stacking gel and six, eight or 10 per cent (w/v) polyacrylamide separating gels were prepared according to Table 2.4.

Table 2.4. The ingredients of stacking and separating polyacrylamide for two gels

	Stacking Gel	**Separating Gels**		
Stock solutions	**4 per cent**	**6 per cent**	**8 per cent**	**10 per cent**
30 per cent (w/v) acrylamide / 0.8 per cent bisacrylamide	0.65 ml	3 ml	4 ml	5 ml
0.5 M Tris-HCl containing 0.4 per cent (w/v) SDS, pH 6.8	1.25 ml			
1.5 M Tris-HCl containing 0.4 per cent (w/v) SDS, pH 8.8		3.75 ml	3.75 ml	3.75 ml
dH_2O	3.05 ml	8.25 ml	7.5 ml	6.25 ml
10 per cent (w/v) APS	25 µl	100 µl	100 µl	100 µl
TEMED	5 µl	20 µl	20 µl	20 µl

Equal amount of proteins from cell extracts were prepared 1:1 ration in 2x Laemmli buffer (125 mM Tris-HCl, pH 6.8, 20 per cent (v/v) glycerol, four per cent (v/v) SDS, 10 per cent (v/v) 2-β-mercaptoethanol and 0.004 per cent bromophenol blue) and stored at -20°C until used. The sample volume did not exceed 30 µl. SDS-PAGE was carried out using Bio-Rad Mini-PROTEAN Tetra cell Electrophoresis System. The gel was prepared as four per cent (w/v) polyacrylamide stacking gel and six, eight or 10 per cent (w/v) separating gel. The stacking gel was prepared using 0.5M Tris-HCL, 0.4 per cent SDS stock solution pH 6.8 whereas the separating gel was composed of 1.5M Tris-HCL, 0.4 per cent (w/v) SDS stock solution, pH 8.8. Preparation of stacking and separating gels were shown in Table 2.4. Polymerization of acrylamide was initiated by the addition of 10 per cent (w/v) ammonium persulphate (APS) and N,N,N',N'-Tetramethylethylenediamine (TEMED) was added to accelerate the process at the given volumes. The separating gel (80x60x1.0) was poured to casting gel and allow to polymerize at room temperature for 20 minutes and water saturated isopropanol was poured onto the top of the gel to avoid oxidation and facilitate the formation of an even gel surface. Following the polymerization, isopropanol was removed and the gel surface was washed with dH_2O until isopropanol discarded completely and the excess amount of the water was gently taken from the edges of gel with the help of filter paper. The stacking gel was directly poured on the separating gel and 10-well combs with 1.0 mm thickness were placed into the stacking gel carefully by avoiding the formation of air bubble between the teeth of the comb. Following the gel polymerization at room temperature, the comb was carefully removed and wells were washed with Tris-Glycine electrode running buffer pH 8.5 (25 mM Tris, 192 mM glycine, and 0.1 per cent (w/v) SDS). Protein samples were loaded to wells along with three µl of full range molecular weight marker (GE healthcare). Gel plates were placed into the frames and then positioned into gel-casting apparatus where the short glasses were faced to the inner side of the module. The gel-casting apparatus was placed into U shaped electrophoretic apparatus and filled with running buffer (25 mM Tris, 192 mM glycine, and 0.1 per cent (w/v) SDS). Electrophoresis was performed in the running buffer at 70V through the stacking gel for 15 minutes and 90V until the Bromophenol Blue sodium salt tracking dye front reached to the bottom of the separating gel.

3.3.4. Western blotting

After resolving the proteins with SDS-PAGE, samples were transferred onto nitrocellulose membrane with 0.45µm pore size using Bio-Rad wet blot system electrophoretically. Whatmann papers, fiber pads and nitrocellulose membrane were soaked in ice-cooled in transfer buffer pH 8.3 (25 mM Tris-Base, 192 mM glycine and 20 per cent (v/v) methanol) at least 15 minutes. Gel sandwich was prepared on the black side of gel cassette in the following order; fiber pad, two layers of wetted Whatmann paper, resolving gel, nitrocellulose membrane, two layers of wetted Whatmann paper and fiber pad. The blocking cassette was then inserted into the U shaped blocking apparatus in a position that membrane was faced to the anode electrode. The blocking apparatus was filled with 1 liter of ice-cooled transfer buffer and a frozen ice container was also placed in apparatus to avoid overheating. The electro transfer of the proteins was performed at 150 mA for 90 minutes on ice. The success of transfer was confirmed by the transfer of high weight molecular markers on the nitrocellulose membrane. Membrane was blocked with five per cent (w/v) non-fat milk in TBS-Tween, pH 7.4 for 1 hour than probed either with mouse monoclonal anti-TG2 Cub7402 or anti-mouse integrin β1 antibody dissolved in 5 per cent (w/v) non-fat milk in TBS-Tween, pH 7.4 or rabbit anti-syndecan-4 antibody prepared in 3 per cent BSA in TBS-Tween, pH 7.4. Membrane was incubated overnight at four degree. Following incubation, membrane was washed three times with TBS-Tween, pH 7.4 for five minutes and equilibrated with PBS, pH 7.4 for 10 minutes. The immune-detection of blots were accomplished using Amersham ECL Advance Western Blotting Detection Kit. Equal amounts from each A and B solution were mixed in a sterile eppendorf tube then added onto the membrane. Membrane was incubated with ECL mixed solution for at least 30 seconds (500µl from solution A and 500µl from solution B). After incubation the access amount of detection mix was removed carefully with the help of a tissue or a filter then membrane was placed between two clear acetate sheets. The signal was detected using Bio-Rad Chemiluminescent Imaging Systems.

3.4. DETECTION OF TG2ASSOCIATION WITH ITGβ1 AND SDC4 USING CO-IMMUNOPRECIPITATION ASSAY

RCC cells were seeded on 6 wells plates described in Section 3.2.1 and incubated with 2 per cent FBS (v/v) containing media for 16 hours. Cells were detached from their substratum using three different methods including non-enzymatic 2 mM PBS.EDTA (w/v), enzymatic 0.05 per cent (w/v) Trypsin or direct gently scraping in 200µL/well immunoprecipitation buffer containing 0.25 per cent (w/v) sodium deoxycholate, 150 mM NaCl, 0.1 mM phenylmethylsulfonyl fluoride, 1 per cent (v/v) protein inhibitor mixture (v/v), 50 µM TG2 specific inhibitor (ZDON) in 50 mM Tris-HCl, pH 7.4. Cells were dislodged with non enzymatic or enzymatic methods were centrifuged at 300 *xg* for 5 minutes and the pellet was resolved in immunoprecipitation buffer. Mechanically dislodged cells were directly lysed in immunoprecipitation buffer. Protein content was determined using Lowry assay and 150 or 200 µg of protein from each samples were pre-cleared by incubating the samples first with 0.5 µg of rabbit IgG for 1 hour and then 50 µl of protein A-Sepharose bead slurry for 90 minutes. Any possible non-specific protein-protein interactions were eliminated by spinning down the A-Sepharose bead slurry at 600 *xg* for one minute and transferring the cell lysates into fresh 1.5 tubes. Pre-cleared cell lysates were next probed with 0.5 µg of polyclonal rabbit anti-integrin ß1 or rabbit polyclonal anti-syndecan 4 for 90 minutes at four degree. Immune complexes were collected with 50 µl of protein A-Sepharose slurry for 2 h at four degree and beads were treated with 2x Laemmli sample buffer and stored at -20 °C until used. Proteins were extracted via heating the samples to 95 °C for 5 minutes and loaded into 8 per cent SDS PAGE gel for electrophoresis. Proteins were transferred to nitrocellulose membrane and probed with mouse monoclonal anti-TG2 Cub7402 antibody. Immune detection was obtained as described in Section 3.3.4.

3.5. SILENCING OF TGM2 USING siRNA TRANSFECTION AND shRNA TRANSDUCTION METHODS

3.5.1 Small interfering (siRNA) RNA transfection

Cells were transfected with non-silencing control siRNA (AllStars Negative Control siRNA, SI03650318) human TGM2 targeting siRNAs (FlexiTube siRNA: Hs_TGM2_1, SI00743715 and Hs_TGM2_6 siRNA, SI03055465) using Qiagen Hiperfact and RNAifact transfection kits. A-498, Caki-2 cells were seeded in 200.000/well and Caki-1, ACHN cells were seeded in 300.000/well density in 6 well plate and allowed to attach overnight in the mammalian incubator. Following day, cells were deprived of serum to drive them into the quiescent for at least 16 hours. Next, siRNAs were diluted either in Buffer ECR or serum free growth media and cells were transfected with TGM2 siRNA and Negative Control siRNA in 2 per cent (v/v) FBS containing medium using transfection reagents for 36 hours and calculations were done according to the Tables 2.5 and 2.6.

Table 2.5. RNAifect transfection reagent calculations

Plate type: 6 well plate	**Transfection reagent: RNAifect reagent**
Amount of TG2 siRNA (20 µM)	5 µg (19,23µl)
Volume of transfection reagent	30 µl
Buffer EC-R	80,77 µl
Volume of medium on cells	1900 µl

Table 2.6. Hiperfect transfection reagent calculations

Plate type: 6 well plate	**Transfection reagent: Hiperifect reagent**
Amount of TG2 siRNA (2 µM)	12 µl (150ng)
Volume of transfection reagent	12 µl
Serum Free Medium	100 µl
Volume of medium on cells	2300 µl

3.5.2. Determination the toxicity of puromycin and blasticidine components using cell viability assay (WST-1)

Toxicity of blasticidine and puromycin was determined using WST-1 (4-(3-(4-Iodophenyl)-2-(4-nitrophenyl)-2H-5-tetrazolio)-1.3-benzene disulfonate) cell viability assay which is a colorimetric assay and used for the non radioactive quantification of cell proliferation, cell viability and cell toxicity. The assay procedure is based on the tetrazolium salts which are cleaved to formazan molecule by the mitochondrial enzymes. Increasing number of viable cells is correlated with the increase in the mitochondrial dehydrogenase activity resulting in the formation of formazan dye in viable cells, which is related with the number of metabolically active cells.

In order to analyze toxicity of puromycin and blasticidine, wild type RCC cells were seeded on 96 well plate at 7500 and 5000 cells/well density for Caki-2 and A-498, respectively, while for Caki-1 and ACHN cell density was determined as 10000/well. Cells were allowed to attach overnight and treated with 100µl/well growth media containing 0.5-5 µg/ml puromycin with 0.5µg/ml increasement in the concentraiton. 1-10µg/ml blasticidine concentration was applied to the cells with 1µg/ml dosing intervals for 10 days. Media was discarded in every 3 days and cells were incubated with fresh media containing the indicated concentrations of puromycin and blasticidine.

To determine the cell viability, 5 µl WST-1 solution was dissolved in 45 µl growth medium and 50 µl of final volume was added to the each well of 96 well tissue culture plate. After addition of WST-1, cells were incubated for one hour in dark at 37°C. The absorbance of each sample was measured at 450 nm using 630 nm as reference wavelength with an ELISA plate reader. The cell viability obtained for the non-treated RCC was accepted as the control and the absorbance value was represented as 100 per cent cell viability. The values obtained for treatments were normalized against the control in all experiments. The minimal effective dose for these antibiotics was set for the concentration where 100 per cent cell death was observed.

3.5.3. Short hairpin RNA (shRNA) transduction

A-498 and Caki-2 cells were seeded as 20.000 cells /well and ACHN and Caki-1 cells were seeded as 25.000/well in 24 well tissue culture plate. After the overnight incubation cells were treated with 8 µg/ml polybrene in two per cent (v/v) FBS and one per cent (v/v) pen/strep (v/v) containing growth media for 12 hours. Following the polybrene incubation, lentiviral particles were added with a multiplicity of infection (MOI) of 2 for Caki-2, A-498, ACHN cells and 4 for Caki-1 cells in two per cent (v/v) FBS and one per cent (v/v) pen/strep containing growth media and incubated for 24 hours. Stably transduced cells were selected by the addition of puromycin in 10 per cent (v/v) FBS one per cent (v/v) pen/strep containing growth media. Puromycin concentrations were determined as; 2.5 µg/ml for Caki-2 & Caki1 2.5 µg/ml for A-498, 3 µg/ml for ACHN cells. Growth media were then replaced in every 3 days with puromycin containing fresh medium until the cells reached to 75 per cent confluency, which was followed by their transfer into the 6 well plates or T25 flasks. For TG2 overexpression, the packaging plasmids used in HEK293 transfection to obtain human *TGM2* gene carrying lentiviral particles were kindly provided by Assoc. Prof. Dr. Ömer Faruk Bayrak and produced by Hande Nayman according to Messner *et al.* [249]. The plasmid OHS6085-21357963 comprising human *TGM2* gene was purchased from Thermo Scientific. Following the generation of lentivirus using HEK 293T cells, viral particle containing media was collected at 24 and 48 hours, filtered through 0.45um filter. Lentiviral particle containing medium was given to Caki-1 Wt cell in 1:2 ratio. Caki-1 Wt cells were incubated with lentiviral particles for 3 hours and then fresh lentiviral particle containing medium (1:2 ratio) was added onto Caki-1 Wt cells. Lentiviral transduction was performed together with 8µg/ml polybrene. Following another 3 hours incubation media was removed and cell monolayer was washed using DPBS twice, then growth medium was added on Caki-1 cells. TG2 protein levels of each cell line were determined using Western Blot and QPCR method as described in the Section 3.2.3.

3.6. CELL ADHESION ASSAY

3.6.1. Coating plates with β1 integrin substrates

The wells of 96 well plate was coated with β1 integrin substrates. Briefly, human plasma fibronectin (FN) was dissolved in 50 mM Tris.HCL pH 7.4 buffer and used at 5µg/ml final concentration to perform substrate coating overnight at 4°C [250]. Human placenta Collagen type-1 (Col1) was solubilized in 0.2M acetic acid and neutralized using 5:3:2 ratio of Collagen: 2xDMEM: 0.2M NaOH buffer, pH 7.2 [251]. Wells were coated with ColI at 40µg/ml for 2 hours at 37 °C. Laminin derived from human placenta was dissolved in 1xDPBS pH 7.4 and used to coat 96 well plates at 10µg/ml final concentration with a 2 hour-incubation of the plate at 37°C. Coating of the wells was achieved using 50 µl/well from each ITGβ1 substrate at the given concentrations.

3.6.2. RCC cell adhesion on β1 integrin substrates

AllStars Negative Control and TG2 siRNA treated RCC cells lines were dislodged using 0.05 per cent trypsin. EDTA (v/v) solution, collected in the FBS containing medium to neutralize trypsin.EDTA activation (Section 3.1.2) and washed twice with serum free medium to remove FBS. Cells were then seeded on β1 integrin substrate coated wells at 20.000/well density and incubated at mammalian incubator at early (30 mins for FN and LM, and 60 mins for Col1) and late (60 mins for FN and LM, and 90 mins for Col 1) time points in order to analyze both cell adhesion and spreading morphology. Cells were fixed, permeabilized and stained as described previously [113]. Briefly, cells were then washed once with DPBS, pH 7.4 and fixed in 3.7 per cent (w/v) paraformaldehyde in DPBS, pH 7.4. Following two DPBS, pH 7.4 washes, cell membrane was permeabilized using 0.1 per cent (v/v) Triton-X-100 in DPBS pH 7.4. Following another set of washes with DPBS, pH 7.4, May Graünwald and Giemsa co-staining processes were employed to stain both cytoplasm and nucleus respectively. Images were taken from the central portion of each well as non-overlapping fields using Zeiss light microscopy at 40x magnification. At least 9 images of different fields per sample were quantified using Scion image analysis programme. In each field the number of adhered cells were analyzed by “threshold” and

“particle analysis” whereas spread cells were measured by "density slicing" options of the Scion Image Analysis program.

3.7. ACTIVE ITGβ1 INTERNALIZATION AND RECYCLING METHODS

3.7.1. Internalization of biotinylated cell surface integrin ß1

Caki-1 cells were seeded on 6 well plates at 250.000 cells/well density. Next day, cells were serum starved using 0.01 per cent (w/v) BSA containing serum free media overnight at 37°C. Following the incubation, cell surface proteins were labeled using 0.5 mg/ml NHS-SS biotin (750µl/well) which is covalently attached to proteins, in DPBS, pH 7.4 for 30 mins at 4°C. After labeling, cells were incubated at 37°C for 10, 20 and 30 minutes using 10 per cent (v/v) FBS containing media (2mls/well) to induce the integrin internalization. Following the incubation, the covalently attach NHS-SS biotin on the cell surface was removed using reducing agent, 750µl/well of 60 mM MesNa in 50mM Tris pH 8.6 containing 100 mM NaCl, 1 mM EDTA for 30 mins at 4°C. Next, MesNa was quenched by addition of 750µl/well of 100mM Iodoacetamide prepared in DPBS, pH 7.4 for 15 mins at4°C. Cells were collected in 150µl of immunoprecipitation buffer containing 50mM Tris-HCL pH 7.4, 150Mm NaCl, 0.25 per cent (w/v) sodium deoxycholate, one per cent (v/v) Triton X-100, one (v/v) per cent protease inhibitor cocktail and 0.1mM PMSF by gentle scraping. Cell lysates were centrifuged at 12.000 *xg* for 3 minutes. Proteins were measured using Lowry assay for equal protein loading. The positive control sample, which represents all biotinlylated integrins on cell surface before the initiation of internalization, was not subjected to MesNa and IAA treatment. Volume density of internalized samples were divided to only cell surface labeled, not MesNa and IAA treated samples, in order to evaluate the ITGβ1 internalization ratio.

3.7.2. Detection of internalized active ß1 integrins using immunoprecipitation assay

Equal amount of protein from each sample were precipitated using mouse anti-human CD49 12G10 clone integrin ß1. 100-120µg proteins were used during the experiment. Non-spesific IgG binding was pre-cleared using 0.5 µg of normal mouse IgG for 1 hour at 4 °C and possible non-specific protein-protein interactions were removed following the

incubation with 20 µl of protein G-Sepharose bead slurry for 90 minutes at 4 °C. Pre-cleared cell lysates were then probed with 0.75µg of mouse anti-human 12G10 clone integrin ß1 antibody for 18 hours at 4°C. Immune complexes were collected in 35 µl of protein G-Sepharose slurry for 3 hours at 4 °C and beads were treated with non-reducing 2x Laemmli sample buffer and stored at -20 °C until used. Proteins were extracted via heating the samples to 95°C for 7 minutes and samples were loaded to six per cent SDS PAGE gel for electrophoresis (Section 3.3.3) than transferred to PVDF membrane with 0.45µm pore size (Section 3.3.4). Membrane was blocked in three per cent (w/v) BSA in 1x TBST pH 7.4 for 1 hour at room temperature than probed with HRP-conjugated Streptavidin (Thernoscientific) in 3.5:1000 ratio in 1x TBST, pH 7.4 then incubated 20 hours at 4°C. Following the incubation membrane was rinsed using 1x TBST, pH 7.4 four times for 5 minutes and equilibrated in DPBS pH 7.4 for 10 minutes.

3.7.3. Measurement of ß1 intergin internalization using capture ELISA method

Caki-1 cells were seeded on 6 well plate at 250.000 cells/well density. Next day, cells were serum starved using 0.01% (w/v) BSA containing McCoy's 5A for 16 hours at 37°C. Following the incubation, cell surface proteins were labeled using 0.5 mg/ml NHS-SS biotin in DPBS, pH 7.4 for 30 mins at 4°C. After labeling cells were incubated with 0.01% (w/v) BSA containing McCoy's 5A for 6 hours at 37°C to allow the internalization of all biotin labeled proteins. Following the incubation, the remaining biotin on cell surface was removed using reducing agent, MesNa and followed by quenching Iodacetamide in DPBS pH 7.4 as described in Section 3.7.1. Cells were lysed by in 200µl of lysis buffer containing 200mM NaCl, 75mM Tris pH 7.4, 15mM NAF, 1.5mM NA_3VO_4, 7.5mM EDTA, 7.5mM, EGTA, 1.5 per cent (v/v) Triton-x-100, 0.75 per cent (v/v) Igepal 630 and 1 per cent (v/v) protease inhibitor cocktail. Following the mechanical sharing of DNA that was carried out by 4 cycles of 60 per cent with three second pulses on ice, Lowry assay was performed for equal protein loading. One day before the experiment wells of 96 well plate were coated with 5µg/ml anti-β1 integrin (MCA2028, clone 12G10), prepared in 0.05 M Na_2CO_3 buffer, pH 9.6 and left to incubation for 16 hours at 4°C. Following day, coated wells were washed with 100µl of DPBS containing 0.05 per cent (v/v) Tween-20 then blocked with DPBS, pH 7.4 containing five per cent (w/v) BSA and 0.05 per cent Tween-20 (100µl/well) for one hour at room temperature. Next, coated wells were washed twice

with DPBS, pH 7.4 and 30µg of protein samples were seeded on 5µg/ml anti-β1 integrin coated wells in 50µl then incubated at 4°C for 20 hours. On the next day, cell monolayers were washed three times with 100µl of DPBS containing 0.05 per cent (v/v) Tween-20 for five minutes and labeled biotins were corporate with HRP-conjugated Extravidin in 1:500 ratio using DPBS, pH 7.4 containing one per cent (w/v) BSA and 0.05 per cent Tween-20 for 1.5 hour at room temperature. The wells were washed twice with DPBS, pH 7.4 and then pre-equilibrated with 0.05M Phospate-Citrate buffer containing 30% of H_2O_2 pH 5.0. Biotin-avidin complexes were visualized using a HRP substrate, o-phenylenediamine (OPD) tablets, dissolved in 0.05M Phospate-Citrate buffer containing 30% of H_2O_2 pH 5.0 (1 tablet per 10 ml buffer). 200µl of developing buffer containing OPD tablet was added to the wells and following the color change the reaction was terminated using 3M H_2SO_4. Absorbance was taken at 492nm in microplate reader. Non-MesNa treated samples were assigned as total biotinylated cell surface β1 integrins of each sample (w/oMesNa).

3.7.4. Analysis of integrin ß1 recycling using Flow Cytometry

Cells were seeded on 12 well plate at a 125.000 cells/well density in the complete medium. On the following day cells were serum starved using 0.01 per cent (w/v) BSA containing serum free media for 16 hours at 37°C. After incubation, cells were labeled using 5µg/ml β1 integrin antibody (MCA2028, clone 12G10) or isotype control (whole mouse IgG) as a negative control in 30mM HEPES and 0.01 per cent (w/v) BSA containing DMEM (400µl/well) for one hour at 4°C. Positive and isotype controls were then fluorescently labeled using mouse Alexa-conjugated 488 secondary antibody in 1:100 ratio using 30mM HEPES, 0.01 per cent (v/v) BSA containing DMEM (400µl/well) on ice for 45 minutes.
Cells were washed twice with DPBS and cell surface proteins were induced to internalize using 10 per cent (v/v) FBS containing media for 20 minutes at 37°C. Following internalization, FBS containing medium was removed and cell monolayers were washed twice with DPBS, pH 7.4. Remaining antibody-bound β1 integrin on cell surface was stripped off using 0.1M glycine, 0.5M NaCl, pH 3.0 (400µl/well) twice for 45 seconds. Glycine solution was removed and acidic conditions were neutralized washing twice with HBSS media and once with 0.01 per cent (w/v) BSA containing McCoy's 5A medium (500µl/well). After the removal of media from the wells, integrin recycling was triggered by the addition of 1ml/well of serum free media containing 10µg/ml human placenta

fibronectin for 60, 90 and 120 mins at 37°C. Upon completion of time points, cell were deattached using 300 µl/well of 0.05 per cent (w/v) trypsin.EDTA and trypsin activation was inhibited using 300 µl of trypsin inhibitor (1mg/ml) per well. Cells were centrifuged at 400 *xg* for 5 minutes and pellet was washed with 30mM HEPES, 0.01 per cent (v/v) BSA containing serum free media. Cell surface integrins were labeled using mouse Alexa-conjugated 488 secondary antibody in 1:100 ratio using 400 µl of 30mM HEPES and 0.01 per cent (v/v) BSA containing DMEM on ice for 45 mins. After incubation cells were washed once with 500 µl of DPBS, pH 7.4 and then dissolved in 500 µl of 0.5 per cent (v/v) formaldehyde in DPBS pH 7.4. At least 10.000 events were acquired using a Becton Dickinson FACSCalibur™ flow cytometer and results were analyzed with the CellQuestPro Program.

3.8. DENSITOMETRIC ANALYSIS OF BLOTS

Western Blot images were captured by a supersensitive 16-bit CCD camera using ChemiDOC XRS+Gel Imaging gel imaging system. In internalization assay, the densitometric analysis of chemiluminescence-detected biotin labeled β1 integrin signals were quantified with Image Lab software supplied by BioRad. Each biotin signal was normalized against the relative amounts of biotin signal of total cell surface β1 integrins (positive control samples). The final relative quantification of TG2, ITGβ1 and SDC4 protein levels were determined as the net area values of the band divided by the corresponding β-actin loading control.

3.9. STATISTICAL ANAYSIS

Represented data were derived from at least three independent experiments and showed as the mean ± standard deviation (S.D). The comparison between samples were analyzed using One-way ANOVA followed by Tukey post multicomparison tests provided by GraphPad Prism version 5.03 for Windows, Graphpad Software, San Diego California USA. P values under 0.05 were considered as statistically significant.

4. RESULTS

4.1. PROTEIN EXPRESSION LEVELS OF TG2, ITGβ1 AND SDC4 IN RCC CELL LINES

The protein expression levels for TG2, ITGβ1 and SDC4 in RCC cell lines were determined by Western Blot analysis as mentioned before in Section 3.3.1. RCC cell lysates were collected in RIPA buffer containing protease inhibitors and used in analysis. Experiments were conducted at least three different times and volume density measurement of protein bands were performed using Image Lab program described in Section 3.7.

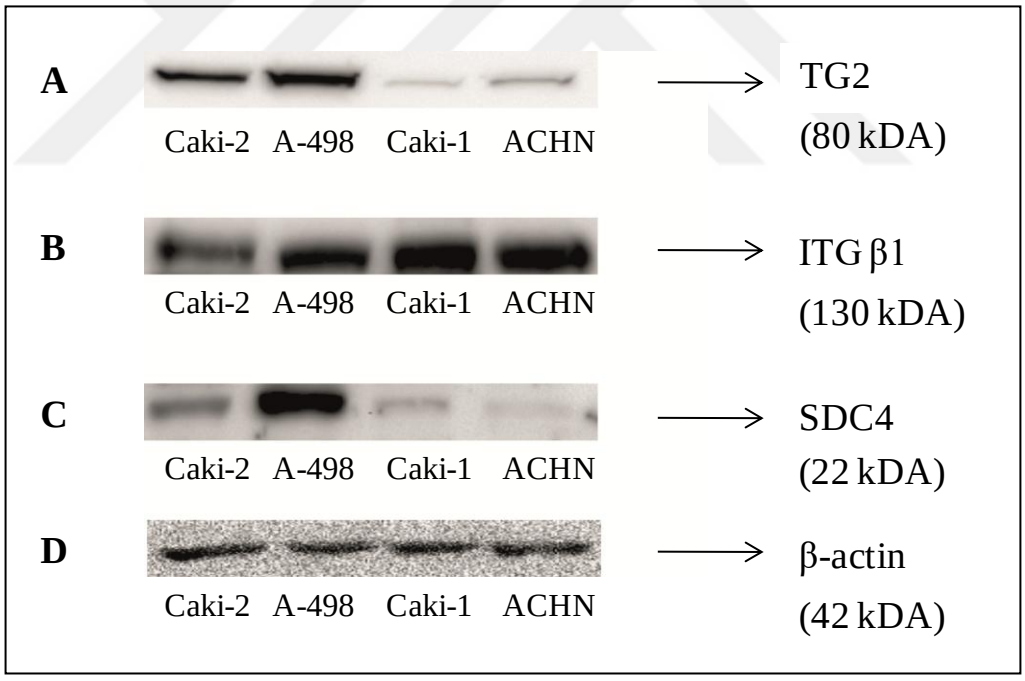

Figure 4.1. Western blot analysis in RCC cell lines for the expression of TG2 (**A**) Integrin β1 (**B**) SDC4 (**C**) and β-actin (**D**) levels. Mouse monoclonal TG2 cub7402 (1:10.000 dilution), mouse monoclonal anti-β1 integrin antibody (1:10.000 dilution) and rabbit polyclonal SDC4 (1:5000 dilution) were used to detect TG2, ITβ1 and SDC4 levels respectively. Protein levels were normalized against β-actin (1:5000 dilution) levels.

In comparison to metastatic site RCC cells Caki-1 and ACHN, TG2 protein expression was found higher in the primary site RCC cells, Caki-2 and A-498. A-498 cells displayed the highest TG2 protein expression level among the four RCC cell lines. In that, A-498 cells have 1.7 fold higher TG2 protein level than Caki-2 cells, while 19.6 fold and 7.3 fold more TG2 protein expression was present in A-498 cell when compared to Caki-1 and ACHN cells, respectively ($p<0.05$). Interestingly, there was no significant difference in TG2 protein expression levels between ACHN and Caki-1 when the mean of three experiment was taken into account ($p<0.05$, Figure 4.1 and 4.2).

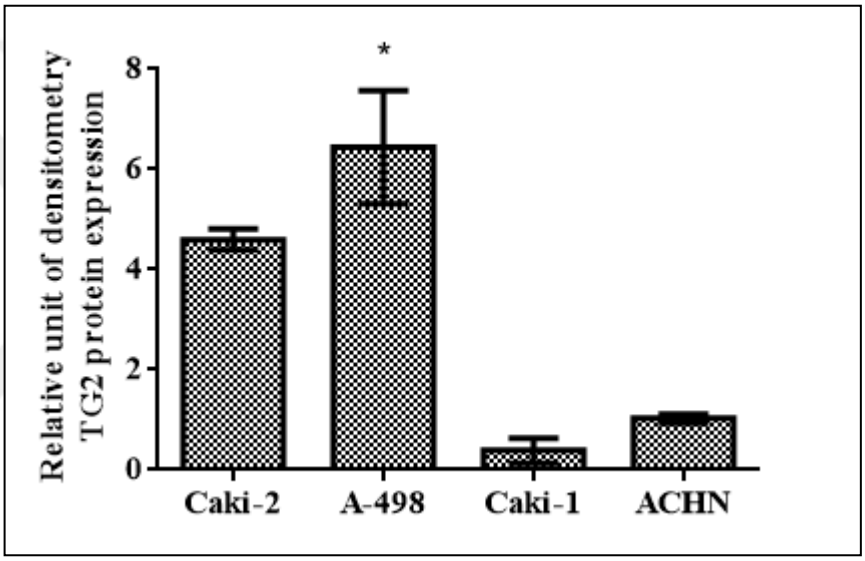

Figure 4.2. Total TG2 level of RCC cell lines was quantified by Image Lab volume intensity analysis. Relative density of TG2 was obtained by dividing that of actin levels in each cell line.

In contrast to lower TG2 levels, ITGβ1 protein expression levels were shown to be elevated in metastatic cells compared to primary site cells. Statistically no significant difference was detected between Caki-2, A-498 and ACHN cell by means of ITGβ1 protein expression levels compared to each other, while a 3 fold increase in ITGβ1 expression level was detected in Caki-1 cells in comparison to A-498, Caki-2 cells and ACHN ($p<0.05$) (Figure 4.1 and 4.3).

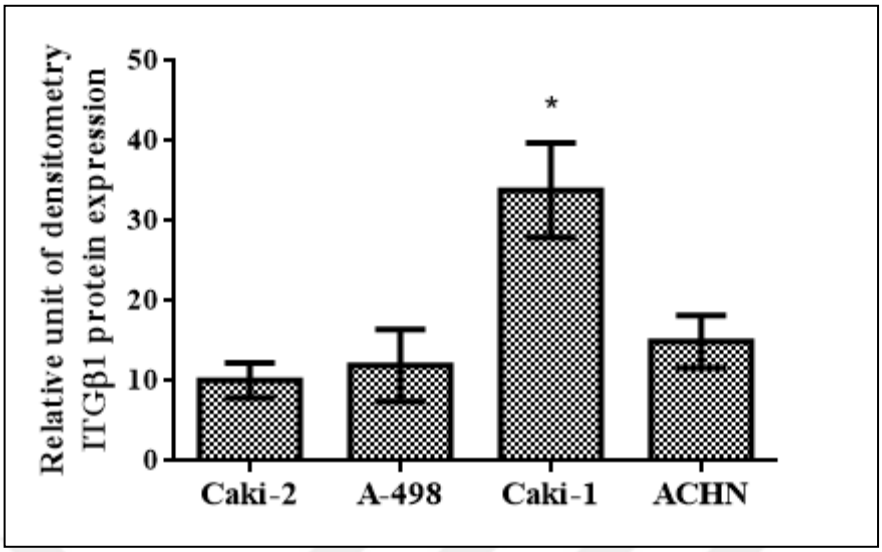

Figure 4.3. Total ITGβ1 level of RCC cell lines was quantified by Image Lab volume intensity analysis. Relative density of ITGβ1 was obtained by dividing that of actin levels in each cell line.

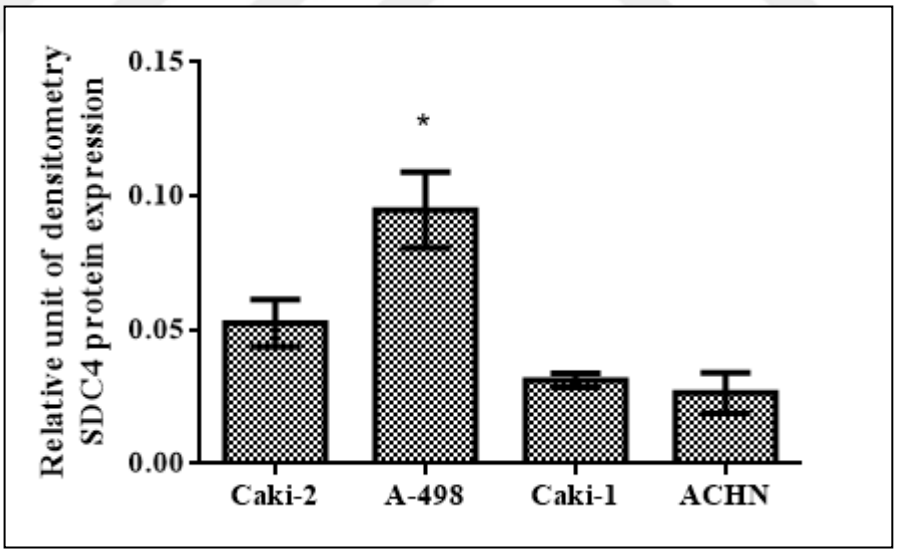

Figure 4.4. Total SDC4 level of RCC cell lines was quantified by Image Lab volume intensity analysis. Relative density of SDC4 was obtained by dividing that of actin levels in each cell line.

Similar to TG2 protein expression levels, A-498 cells displayed the highest SDC4 protein expression levels. While SDC4 core protein was barely detected in Caki-1 and ACHN cells, A-498 cells demonstrated seven fold more SDC4 protein expression level when compared to Caki-1 cells ($p<0.05$). Caki-2 cells possessed approximately 1.6 fold higher SDC4 protein expression level in comparison to Caki-1 and ACHN cells. The SDC4 protein levels were statistically non-significant between Caki-1 and ACHN cells (Figure 4.1 and 4.4).

4.2. DETECTION OF TG2 INTERACTIONS WITH ITGβ1 AND SDC4 USING CO-IP METHOD

In order to analyze the direct interaction of TG2 with ITGβ1&SDC4, RCC cells were collected either by with gentle scraping or using trypsin.EDTA. Regardless of cell disassociation procedure, cells were centrifuged and the pellets were dissolved in IP buffer (0.25 per cent (w/v) sodium deoxycholate, 150 mM NaCl , 0.1 mM phenylmethylsulfonyl fluoride, 1 per cent (v/v) protein inhibitor and 50 μM TG2 specific inhibitor (ZDON) in 50 mM Tris-HCl, pH 7.4) as described in Section 3.4.

Among four RCC cell lines Caki-1 demonstrated the highest interaction of TG2-ITGβ1 with almost 1:1 association between these proteins; whereas, Caki-2 showed 18 per cent (~1:6), A-498 cells demonstrated 15 per cent (~1:7) and ACHN cells displayed 6 per cent (~1:16) interaction between TG2 and ITGβ1 when these cells were collected directly in IP buffer. Interestingly when trypsin was used, Caki-2 cells and A-498 cells demonstrated a two fold increase in TG2-ITGβ1 interaction with a 30 per cent (~1:6) and 26 (~1:4) per cent association with ITGβ1, respectively. In contrast to primary site cells, using trypsin to harvest the cells led to a decrease in TG2-ITGβ1 interaction in metastatic cells since the TG2-ITGβ1 interaction was found as five per cent and two per cent in Caki-1 cells and ACHN cells, respectively (Figure 5A).

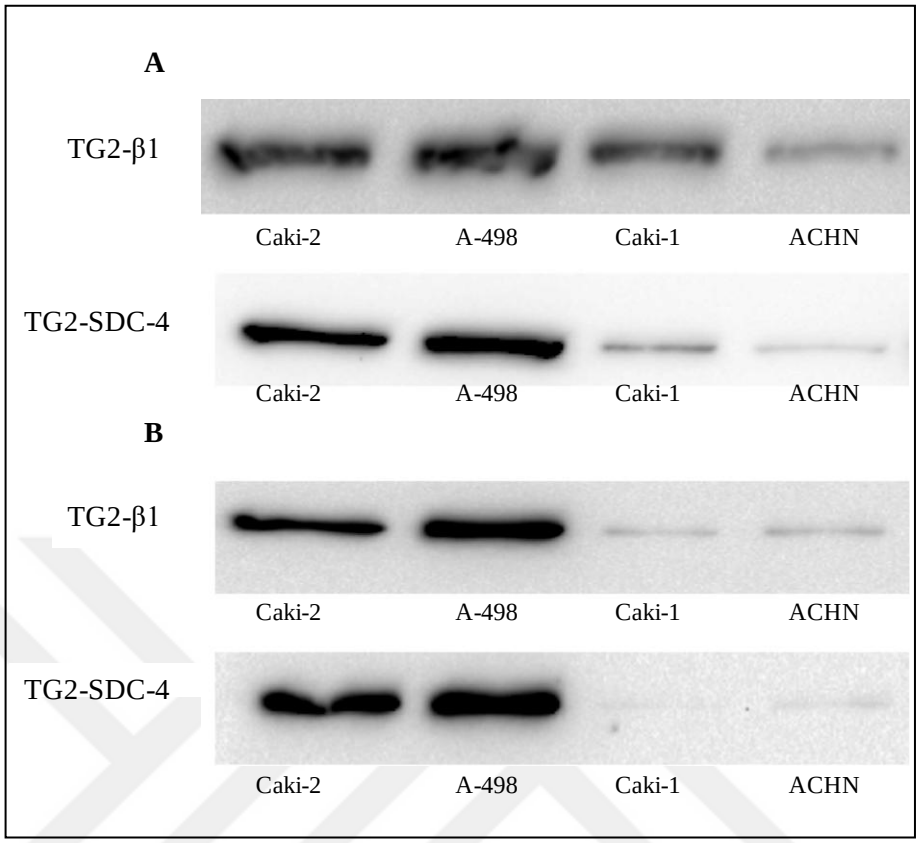

Figure 4.5. TG2 interaction with ITGβ1 and SDC4. Cells collected in IP buffer (**A**) and using Trypsin (**B**). Proteins were pulled down with rabbit anti-ITGβ1 and rabbit anti-SDC4, Western blot was performed using mouse TG2 cub7402 antibody (1:10.000). Results were normalized against TG2 protein levels of each RCC cell line.

Given that TG2 interaction depends on heparan sulphate chains of SDC4 [220], the interaction ratio between TG2 and SDC4 core protein may not represent the actual association between these two proteins. Indeed, Caki-1 cells collected in IP buffer, displayed the highest interaction level between TG2-SDC4, which was evident as 34 per cent, however when trypsin was used, the ratio of the interaction was decreased to four per cent (Figure 4.4). ACHN cells showed a lower interaction potential compared to other four RCC cell lines which was analyzed as 3.5 per cent and one per cent for IP buffer and trypsin treatment. Caki-2 and A-498 cells demonstrated 31 per cent and 28 per cent association with TG2-SDC4 in IP experiments performed with direct cell collection in IP buffer treatment, whereas in the case of trypsin treatment 45 per cent and 38 per cent

association between TG2 and SDC4 was detected in Caki-2 and A-498 cells, respectively (Figure 5B).

4.3. ANALYSIS OF siRNA MEDIATED TGM2 SILENCING IN RCC CELL LINES USING QPCR

To avoid from the possible siRNA off-target effects and to obtain a significant siRNA silencing two different siRNAs targetting different regions on *TGM2* gene were used. siRNA1 (siR1) targeted the sides 1200 to 1600, while siRNA6 (siR6) targeted the sites 1600 to 2000 within the open reading frame of *TGM2* gene. In order to eliminate non-specific effects of transfection a non-silencing siRNA (NS) that does not target any known mamalian gene, was purchased from Qiagen and used as the negative silecing control. As described in Section 3.5.1, RCC cell were treated with siR1, siR6 and NS for 36 hours following the serum starvation. QPCR analysis showed a drastic decrease in TGM2 mRNA level in siR1 and siR6 treated RCC cell lines while no statistically significant difference was recorded between NS treated and non-treated control cells. Analysis of TGM2 mRNA levels with qPCR showed that when compared to the non treated control cells, TGM2 mRNA levels in siR1 and siR6 treated Caki-2 cells were decreased to 6 per cent and 18 per cent of either non-transfected or NS transfected control cells, respectively (Figure 4.5). TG2 down-regulation with siR1 in A-498 cells showed a decline, which was recorded as 59 per cent whereas siR6 treatment led to a 33 per cent reduction in A-498 TGM2 mRNA levels. In Caki-1 cell siRNA treatment led to a marked decrease in TG2 mRNA levels, which was evaluated as 94 per cent for siR1 treated and 95 per cent for siR6 (Figure 4.7). Similar to Caki-2 and Caki-1 cells TG2 silencing led to a respective 90 per cent and a 80 per cent reduction in TG2 mRNA levels in siR1 and siR6 treated ACHN cells (Figure 4.8).

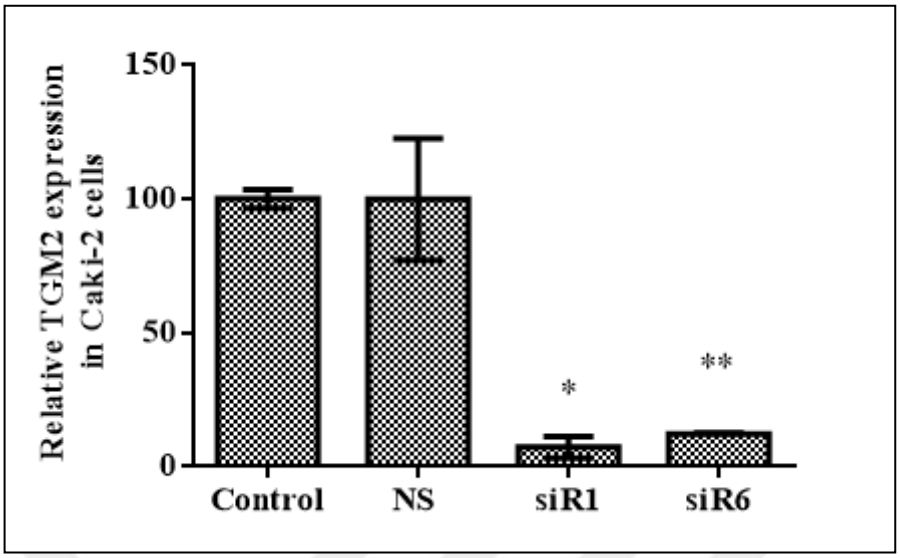

Figure 4.6. Effect of siRNA treatment in Caki-2 cells was evaluated using qPCR. *TGM2* mRNA levels were normalized against 18s rRNA expression levels. * $p < 0.05$ shows the significant difference against control or NS treated cells.

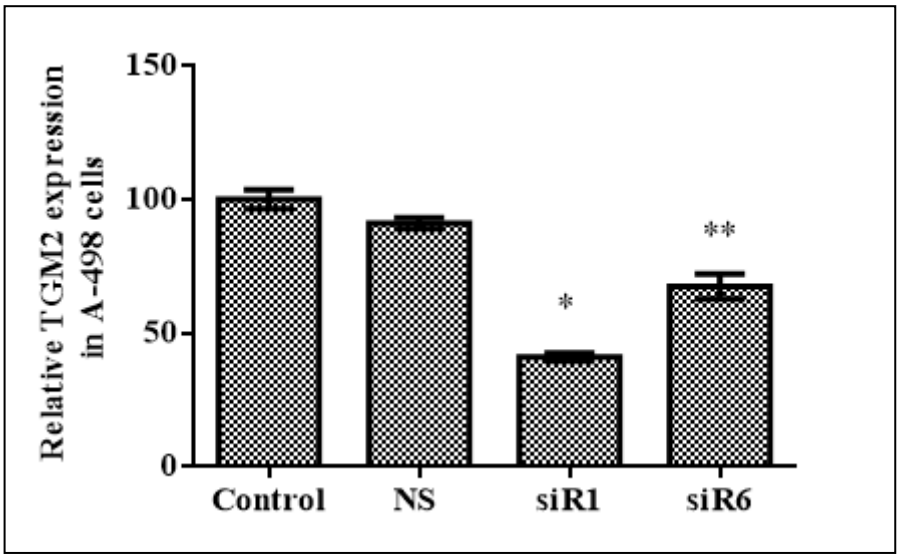

Figure 4.7. Effect of siRNA treatment in A-498 cells was evaluated using qPCR. *TGM2* mRNA levels were normalized against 18s rRNA expression levels. * $p < 0.05$ shows the significant difference against control or NS treated cells.

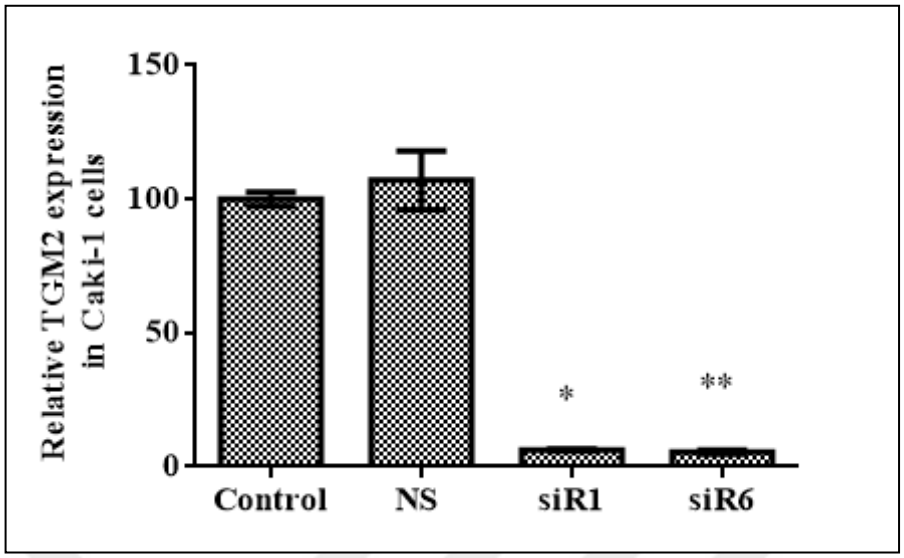

Figure 4.8. Effect of siRNA treatment in Caki-1 cells was evaluated using qPCR. *TGM2* mRNA levels were normalized against 18s rRNA expression levels. * $p < 0.05$ shows the significant difference against control or NS treated cells.

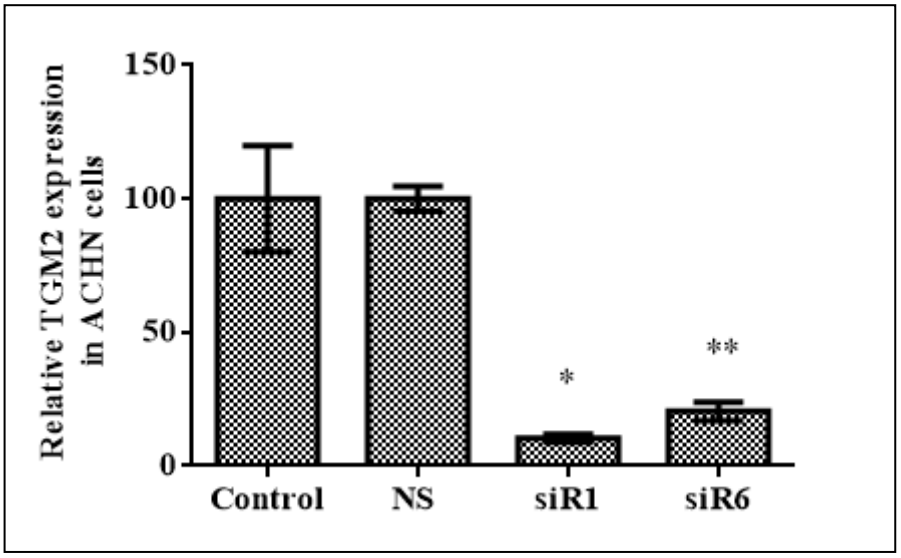

Figure 4.9. Effect of siRNA treatment in ACHN cells was evaluated using qPCR. *TGM2* mRNA levels were normalized against 18s rRNA expression levels. * $p < 0.05$ shows the significant difference against control or NS treated cells.

Previous literature demonstrated that TG2 in complex with the ITGβ1 integrin substrate FN was able to enhance cell adhesion and survial through SDC4 and/or ITGβ1 in a RGD-dependent [215] or independent manner [113]. A more recent study determined a correlation between the up-regulation of TG2 together with ITGβ1 and SDC4 and RCC metastasis development [196]. One of the study showed that primary MEF cells isolated from β1 integrin and SDC4 knockout mice displayed an impaired cell attachment and spreading on FN coated matrices [113]. In agreement with this study, it was shown that SDC4 silencing by siRNAs led to a significant decrease in human osteoblast cell adhesion on FN and TG-FN complex was remarkably restored the loss of osteoblast cell adhesion [252]. Together with these findings to point out the significance of, ITGβ1 and SDC4 levels in the cell adhesion process, therefore before assessing the importance of TG2 in cell adhesion to ITGβ1 substrates the levels fo *ITGβ1* and *SDC4* in TG2 silenced cells were determined using QPCR analysis. Results depicted from the Figure 10A showed no significant decrease in *ITGβ1* level in the primary site and metastatic RCC cell lines following the siR1 and siR6 treatment. Likewise, *SDC4* gene expression levels were not affected by the downregulation of TG2 by siRNA silencing in Caki-2, A-498, ACHN and Caki-1 cells (Figure 10B).

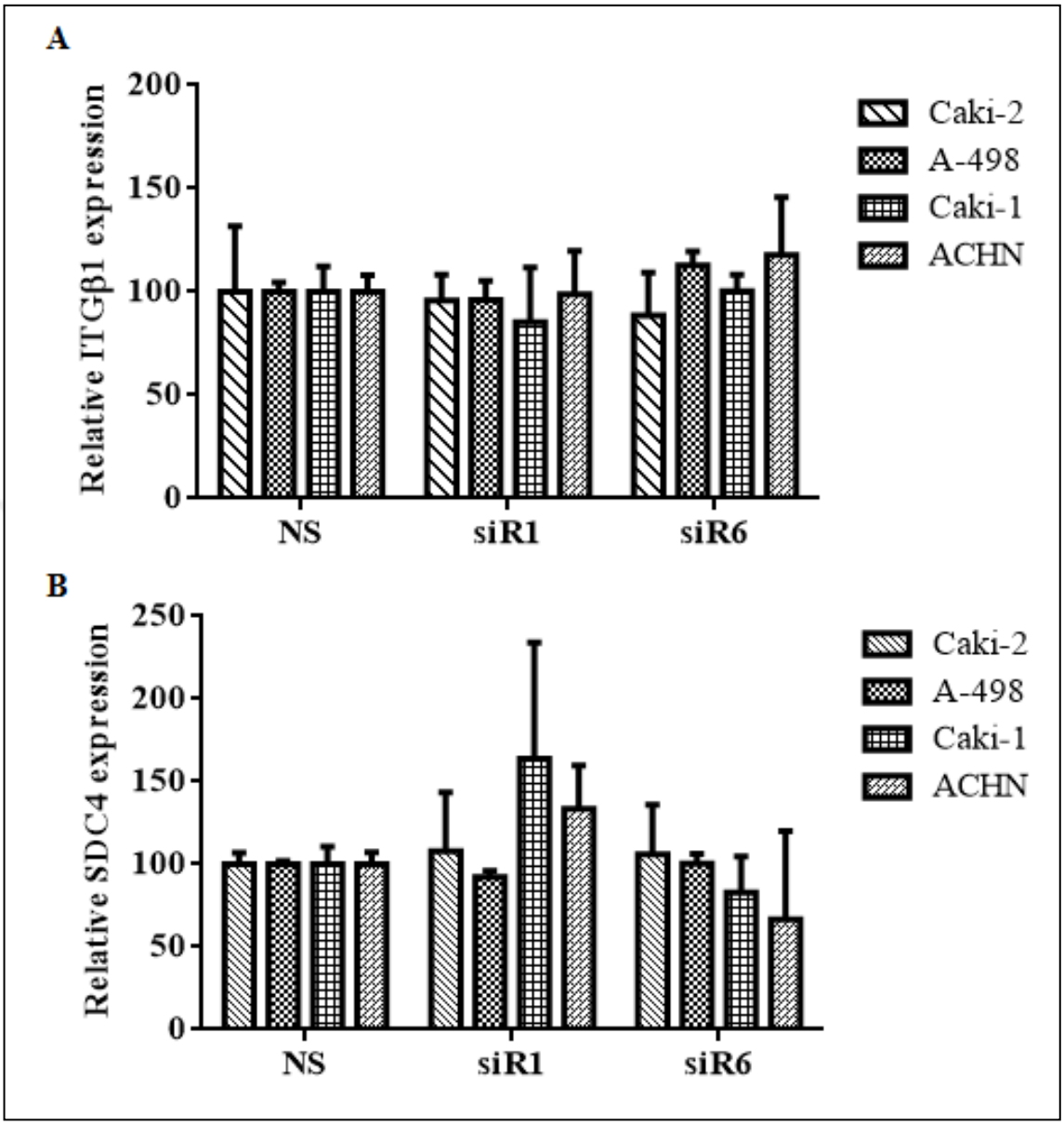

Figure 10. Relative *ITGβ1* (**A**) and *SDC4* (**B**) mRNA expression levels of NS control, siR1 and siR6 treated four RCC cell lines

4.4. DETECTION OF RCC CELL ADHESION POTENTIAL ON β1 INTEGRIN MATRIX SUBSTRATES

Beside its transamidating activity, non-enzymatic functions of TG2 have been implicated to play an important role in the regulation of cell adhesion [221,253]. TG2-FN heterocomplex binding to SDC4 [113] and TG2 interaction with β1 and β3 integrins [215] could promote cell adhesion to ECM by maintaining an integrin induced cell survival signaling pathway [250]. In agreement with these findings, the increased expression of TG2 together with β1 integrin up-regulation was found to be associated with RCC metastasis [196], which drives us to seek the cell adhesion potential of RCC cell lines onto β1 integrin substrates. In order to investigate the necessity of TG2 during cancer cell migration, RCC cells were seeded on FN, ColI and LM pre-coated wells without serum supplementation following the treatment with siRs (Section 3.5). To detect the time point for the initiation of focal contacts and the formation of mature focal adhesions, early and late time points were determined through previously performed optimization experiments as 30 and 60 mins for FN, LM and 60 and 90 mins for ColI substrates. As statistically no significant difference between non-treated control and NS treated cells was detected in the gene expression and cell adhesion levels, graphs were constructed as per cent cell attachment and per cent cell spreading of NS treated cells together with siR1 and siR6 treated cells. The per cent cell adhesion (attachment and spreading) recorded at the late time point for NS was considered as 100 per cent.

4.4.1 Attachment and spreading of TG2 silenced Caki-2 primary site cancer cells on β1 integrin substrates

Caki-2 cells were seeded at 200.000 cells/well density in 6 well plate and transfected with TGM2 siR1 and TGM2 siR6 for subsequent downregulation of TG2. Following the siR treatment, cells were dislodged and seeded on FN (Figure 4.11 A), Col1 (Figure 4.11 B) and LM (Figure 4.12).

NS treated Caki-2 cells showed an 80 per cent cell attachment and 74 per cent spreading on FN at the early time point of 30 mins, when compared to the cell adhesion recorded for the late time point of 60 mins. siR1 and siR6 treated Caki-2 cells led to an average of 48 per cent decrease in the attachment on FN-coated wells at the early time point while ~42 per

cent reduction in Caki-2 cell attachment was recorded for the late time point following the siR1 and siR6 treatment. TG2 down-regulation by siR1 and siR6 showed a respective 56 per cent and 61 per cent decrease in Caki-2 cell spreading on FN in 30 mins whereas a 47 per cent and 51 per cent reduction was achieved at the late time point.

Similar to FN, NS treated control cells demonstrated a 84 per cent cell attachment and 78 per cent cell spreading on Col1 at the early time point of 60 mins, while for the late time point of 90 mins cell attachment and spreading values on Col1 were detected 100 per cent and 90 per cent, respectively. siR1 and siR6 treated Caki-2 cells displayed a respective 42 per cent and 45 per cent decrease in the cell attachment on Col1 matrix compared to control cells at the early time point. TG2 silencing with siR1 showed a 43.5 per cent decrease while 46.8 per cent reduction in Caki-2 cell attachment on Col1 was recorded for the late time point when compared to control cells.TG2 down-regulation in Caki-2 cells led to a 62 per cent loss of cell spreading following to siR1 treatment whereas 68 per cent reduction in the cell spreading of siR6 treated Caki-2 on Col1 matrix was detected at the early time point. At the late time point of 90 mins a 51 per cent and a 60 per cent decrease in cell spreading on Col1 matrix was detected following the siR1 and siR6 treatment in Caki-2 cells, respectively.

In contrast to FN and Col1, a lower cell adhesion on LM was observed for Caki-2 cells such that 76 per cent attachment and 48 per cent spreading was evaluated at the early time point of 30 mins whilst at the late time point 90 per cent cell spreading was detected. At the early time point, TG2 silencing led to a 42 per cent and 36 per cent decrease in cell attachment of siR1 and siR6 treated cells respectively, where as a 29 per cent reduction in the attachment was recorded at the late time point for both siR1 and siR6 treated Caki-2 cells. When compared to control cells, TG2 down-regulation following both siRs treatment resulted in 25 per cent and 52 per cent cell spreading in Caki-2 cells at 30 and 60 mins, respectively.

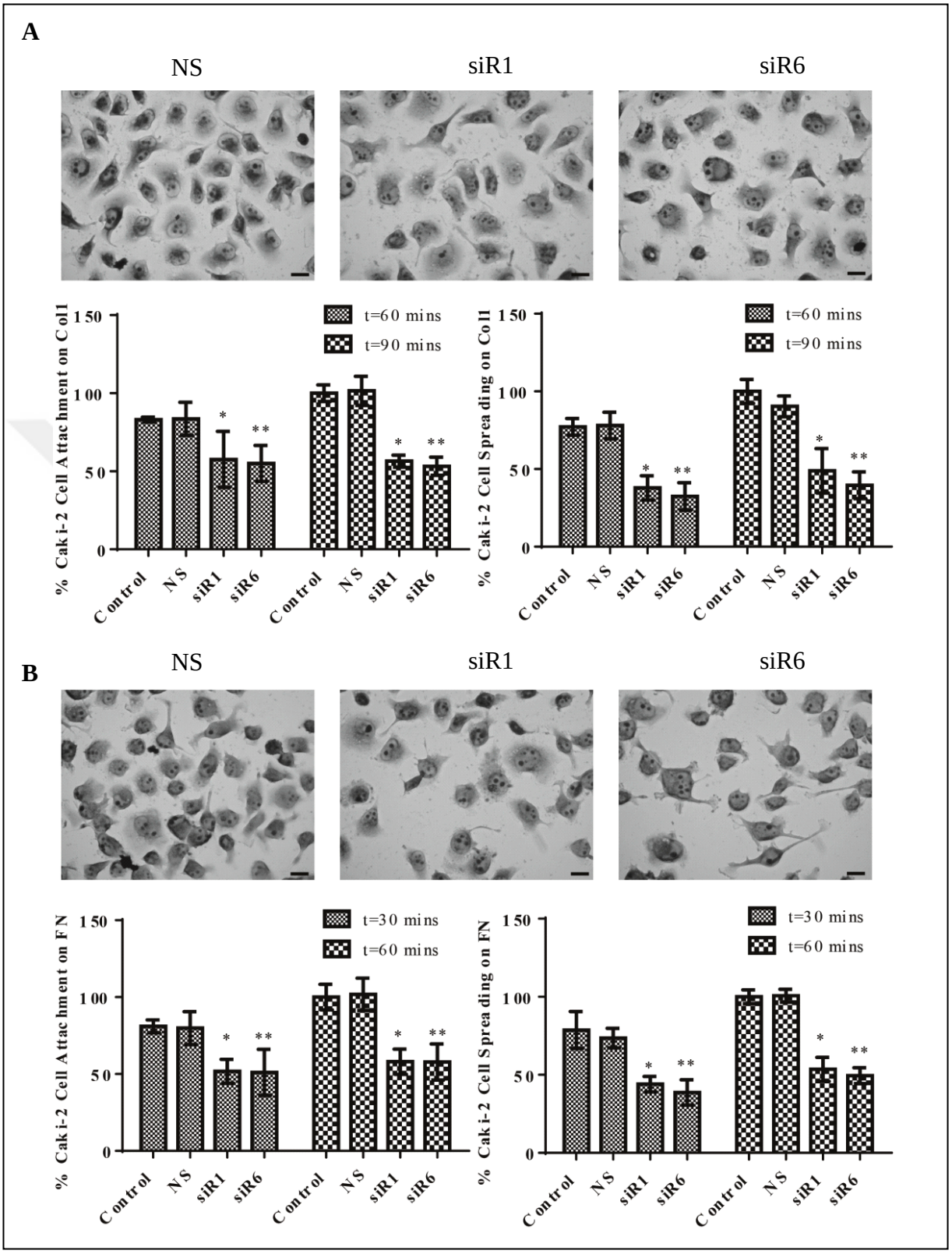

Figure 4.11. Detection of cell adhesion potential of primary site Caki-2 cells on FN (**A**) and Col1 (**B**) matrices. Bars, 20 μm.

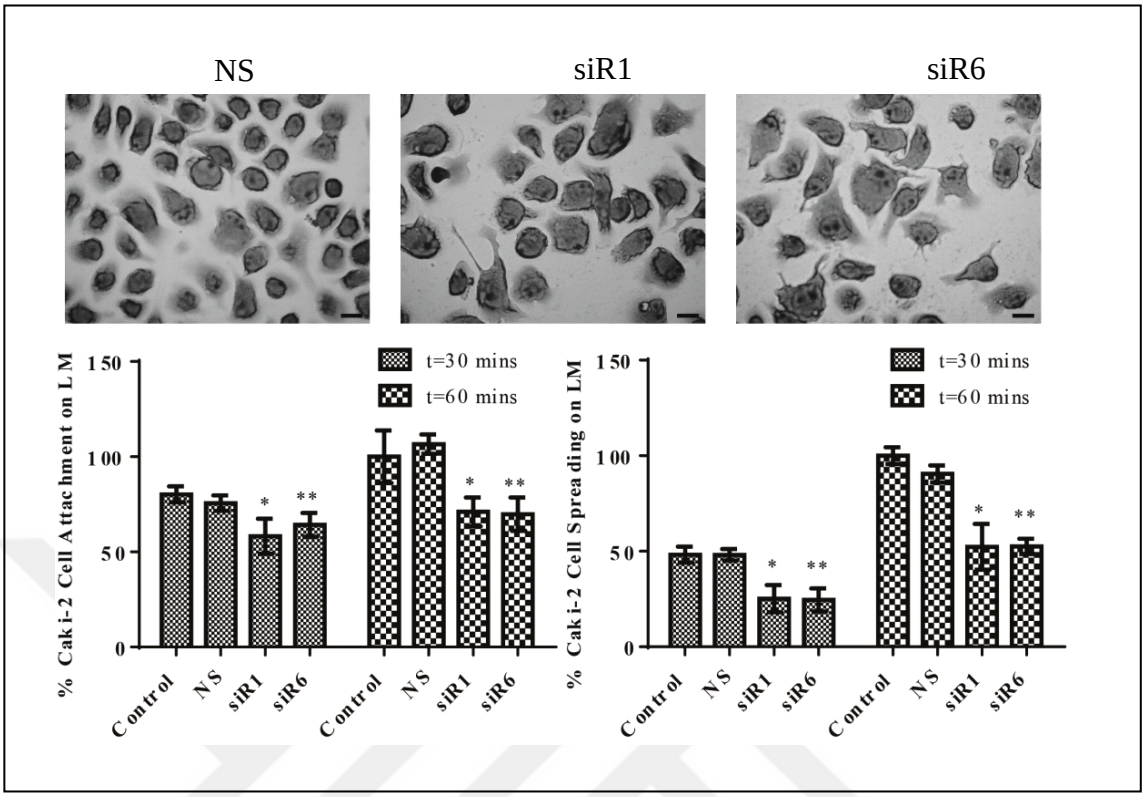

Figure 4.12. Detection of cell adhesion potential of primary site Caki-2 cells on LM. Bars, 20 μm.

4.4.2 Attachment and spreading of TG2 silenced A-498 primary site cancer cells on β1 integrin substrates

Similar to primary site Caki-2 cells, A-498 cells were seeded at 200.000 cells/well density on 6-well plate and the down-regulation of TG2 was performed using siR1 and siR6. TG2 silenced A-498 were seeded on FN, Col1 and LM to detect the TG2 mediated cell adhesion on these β1 integrin substrates (Figure 4.12- 4.13).

NS treated A-498 cells displayed 77 per cent cell attachment and 68 per cent cell spreading on FN at the early time point of 30 mins when compared to cell attachment and spreading recorded for the late time points. TG2 silencing led to a loss of 42 per cent cell attachment at the early time point while a respective 32 per cent and 36 per cent decrease in cell attachment was recorded for the late time point in both siR1 and siR6 treated A-498 on FN coated matrices. Silencing of TG2 resulted in 54 per cent decrease in cell spreading of siRs

treated A-498 at the early time point whereas 45 per cent reduction was detected in both siR1 and siR6 treated A-498 cells on FN at the late time point (Figure 4.13A).

NS treatment showed ~82 per cent cell attachment and 81 per cent cell spreading on Col1 matrix at the early time point in comparison to late time point. TG2 down-regulation of A-498 cells resulted in a loss of 44 per cent cell attachment and spreading in both siR1 and siR6 treated A-498 cells at the early time point while only a 65 per cent and a 60 per cent cell attachment was recorded for the late time point in siR1 and siR6 treated A-498 cell respectively. Following siR1 and siR6 treatment the late time point cell spreading was evaluated in TG2 silenced A-498 cells as 61 per cent (Figure 4.13B).

NS treated A-498 cells showed 82 per cent and 90 per cent cell attachment at the early and late time point on LM matrix, in that order, whereas 68 per cent cell spreading was detected at the early time point when compared to the spreading of NS treated cells at the late time point. TG2 silencing led to 41 per cent reduction in the attachment of siR1 treated A-498 cells whereas a 38 per cent decrease in cell attachment was evaluated in siR6 treated A-498 cell at the early time point of 30 mins. At the late time point only a 4 per cent increase in cell attachment was detected in siR1 and siR6 treated A-498 cells. Interestingly at the early time point of 30 mins, no significant difference in cell spreading of siRs treated and NS treated cells was detected as the analysis indicated a 50 per cent cell spreading for siR1 and 44 per cent cell spreading for siR6 treated A-498 cells. However at the late time point of 60 mins, the cell spreading for siR1 and siR6 treated A-498 cells was respectively recorded as 64 per cent and 56 per cent while control NS cells displayed a 100 per cent cell attachment (Figure 4.13).

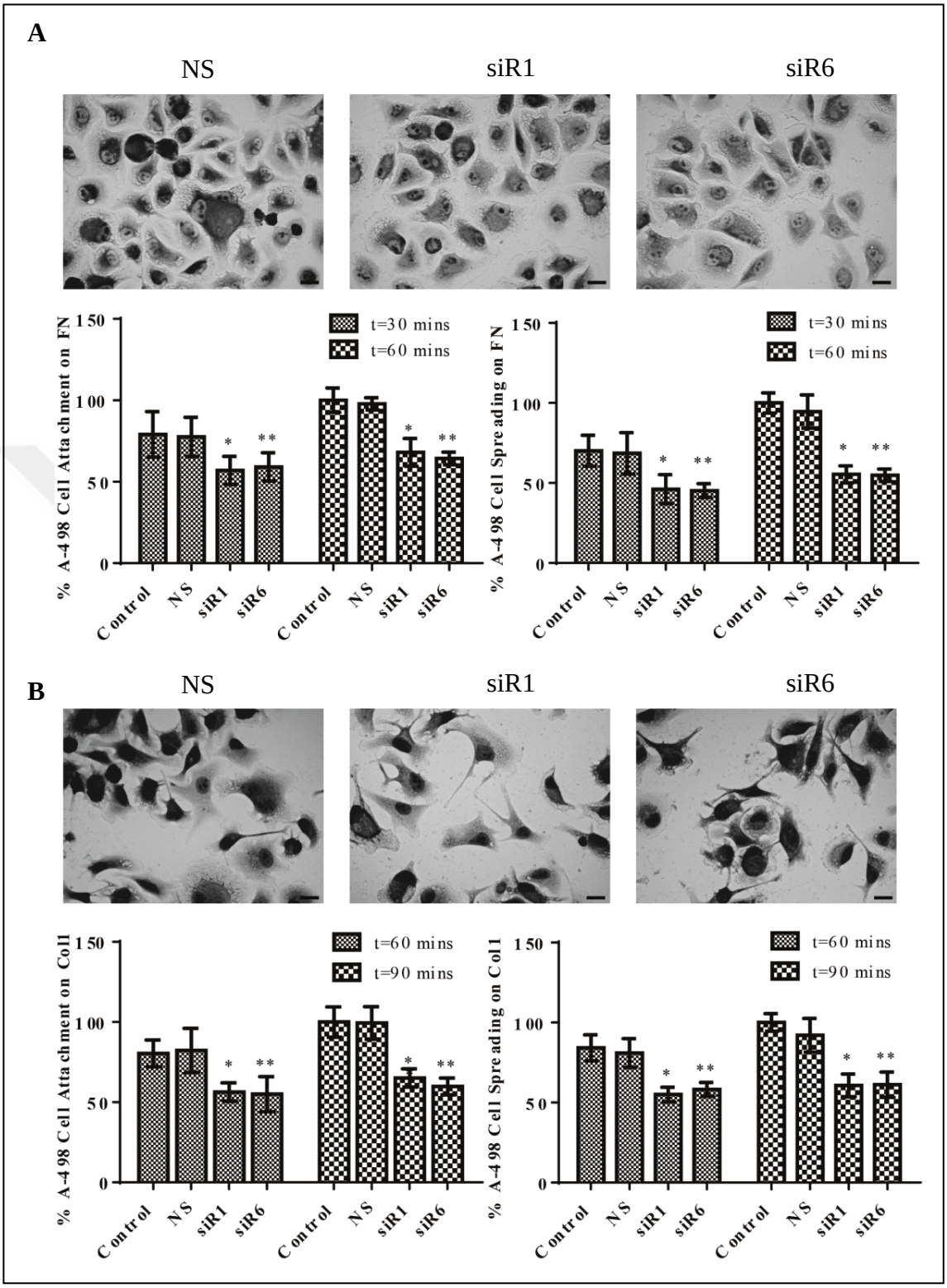

Figure 4.13. Detection of cell adhesion potential of primary site A-498 cells on FN (**A**) and Col1 (**B**). Bars, 20 μm.

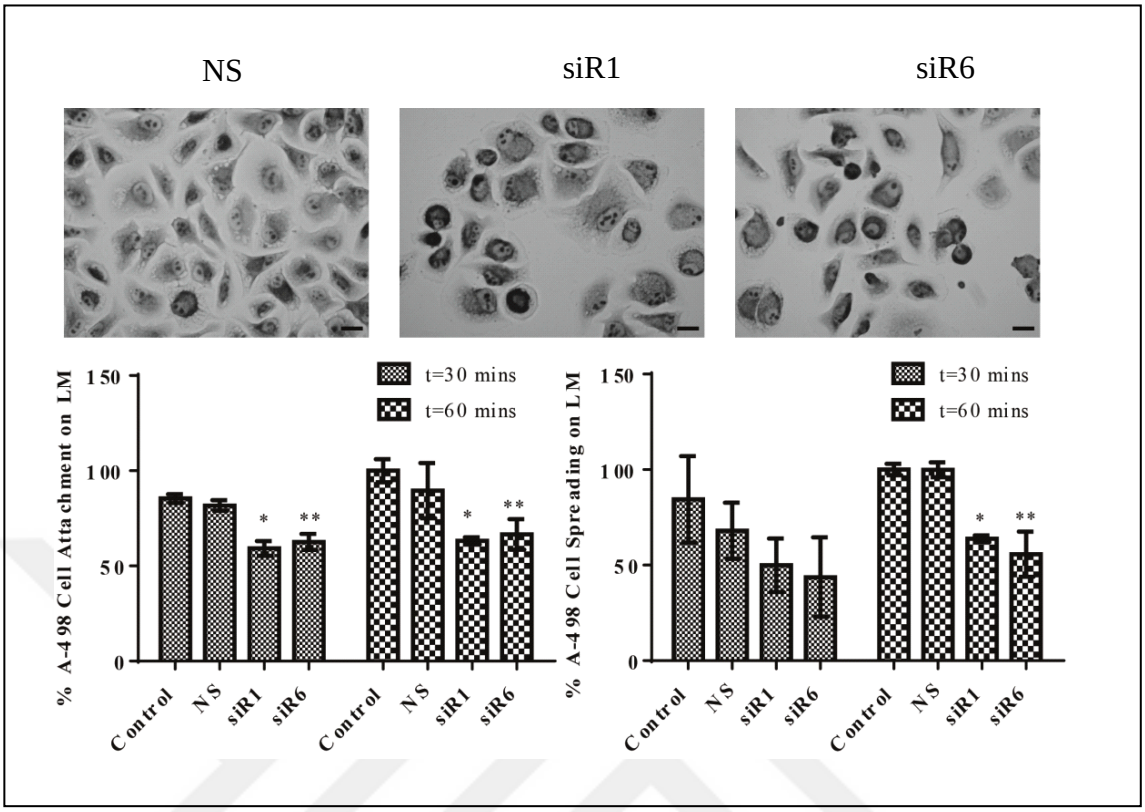

Figure 4.14. Detection of cell adhesion potential of primary site A-498 cells on LM. Bars, 20 μm.

4.4.3 Attachment and spreading of TG2 silenced Caki-1 metastatic site cancer cells on β1 integrin substrates

Similar to primary site cancer cells, TG2 was demonstrated to be necessary for the metastatic site cell attachment and spreading on β1 integrin matrix substrates. For this purpose cell adhesion assay of Caki-1 cells was demonstrated following TG2 silencing TG2 downregulated Caki-1 cells were seeded on FN, Col1 and LM matrices (Figure 4.15-16) as described in Section 3.5.1 and 3.6.1.

When compared to three RCC cell lines, Caki-1 cells showed the highest cell adhesion level on FN which was recorded as 92 per cent for cell attachment and 82 per cent for spreading at the early time point. Interestingly, siR1 treatment decreased the cell attachment to 61 per cent and siR6 reduced the cell attachment to 57 per cent in both early and late time points, which clearly showed that the cell adherence potential of siR treated

Caki-1 cells on FN matrix substrate did not change over the time. Similar to cell attachment results, silencing of TG2 led to an ordered 52 per cent and a 60 per cent decrease in cell spreading of siR1 and siR6 treated Caki-1 cells on FN when compared to the cell spreading recorded for the late time of NS treated control cells. At the late time point of 60 mins, TG2 downregulation reduced the cell spreading potential of siR1 and siR6 treated Caki-1 cells to 56 per cent and 61 per cent, respectively (Figure 4.15 A).

NS treated Caki-1 cells showed an 81 per cent cell attachment and 88 per cent cell spreading on Col1 at the early time point of 60 mins. TG2 downregulation decreased the cell attachment levels to 53 per cent in each siR1 and siR6 treated Caki-1 cells at 60 mins whereas 60 per cent cell attachment was detected for each siR1 and siR6 treated cells at the late time point of 90 mins. Silencing of TG2 in Caki-1 cells with siR1 and siR6 treatment resulted in 52 per cent and 43 per cent cell spreading at 60 mins, in that order, while a respective 57 per cent and 46 per cent cell spreading was recorded for siR1 and siR6 treated Caki-1 cells at 90 mins. However, the extra 5 per cent increase seen in cell attachment and spreading at the late time point was not significant (Figure 4.15 B).

NS treated Caki-1 cells displayed 82 per cent cell attachment and 77 per cent cell spreading on LM matrix substrate. Following siR1 and siR6 mediated TG2 silencing, cell attachment on LM was recorded as 54 per cent and 60 per cent, respectively, at the early time point of 30 mins, whereas a 60 per cent cell attachment was recorded at the late time point of 60 mins for both siR1 and siR6 treated Caki-1 cells. TG2 downregulation led to a respective 45 per cent and 51 per cent reduction in siR1 and siR6 treated Caki-1 cells at the early time point while a 40 per cent decrease was recorded in TG2 silenced Caki-1 cell spreading on LM at the late time point (Figure 4.16).

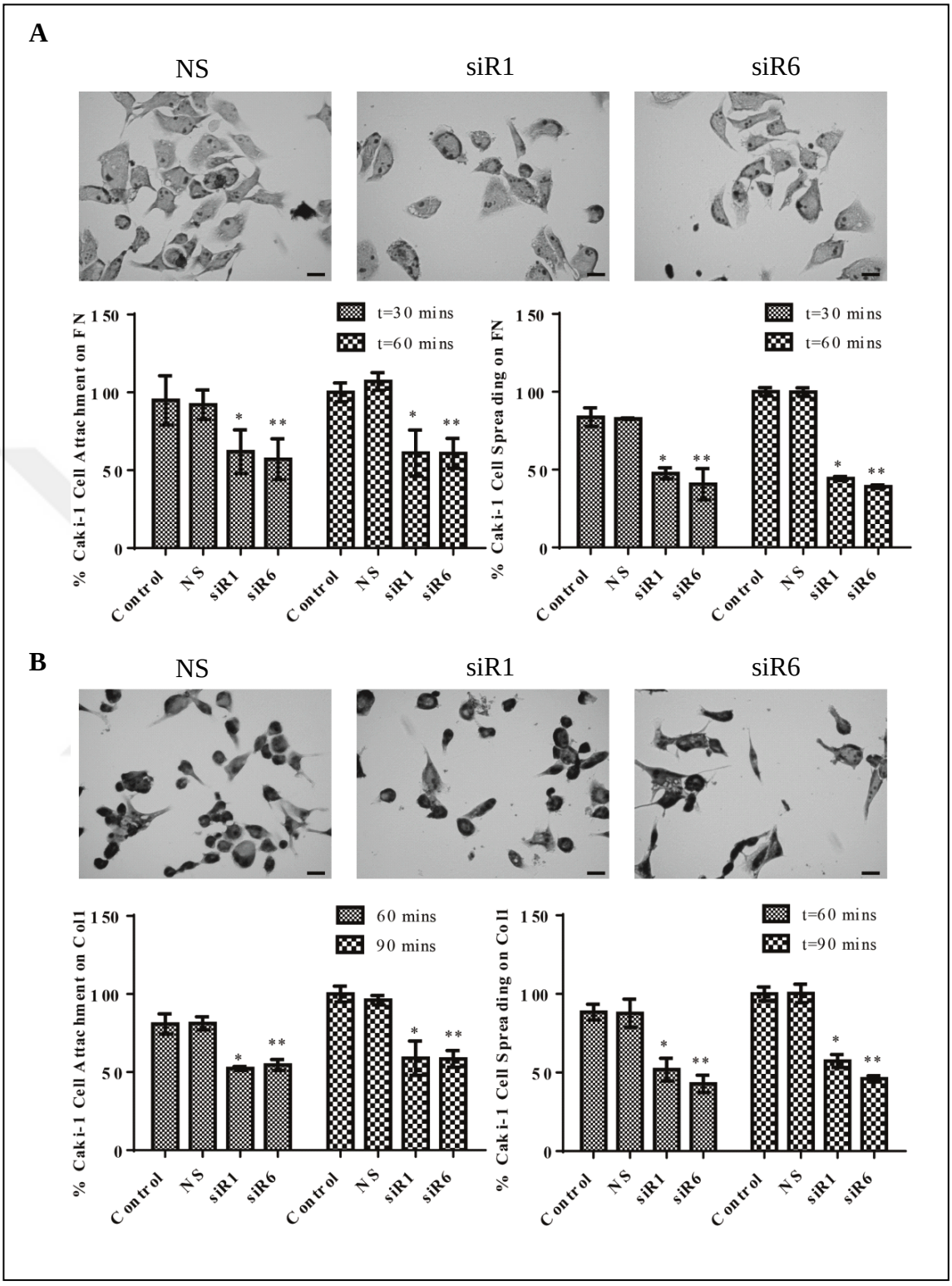

Figure 4.15. Detection of cell adhesion potential of primary site Caki-1 cells on FN (**A**) and Col1 (**B**). Bars, 20 μm.

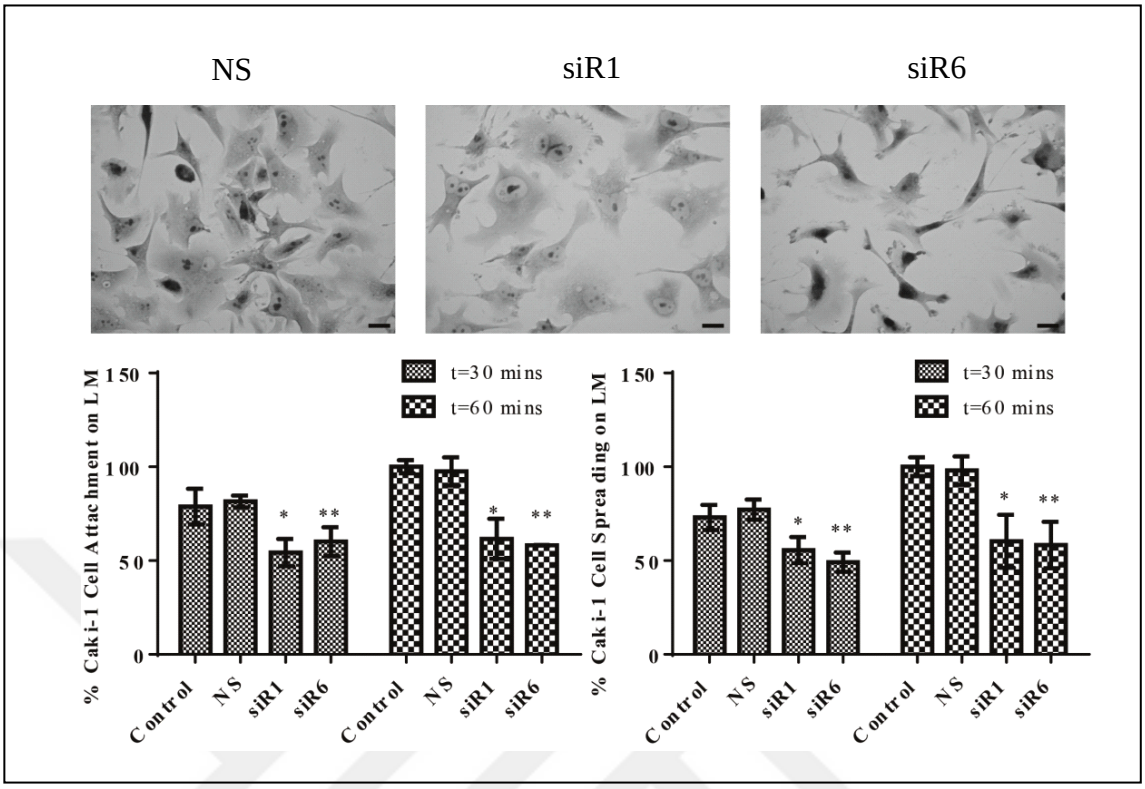

Figure 4.16. Detection of cell adhesion potential of primary site Caki-1 cells on LM. Bars, 20 μm.

4.4.4 Attachment and spreading of TG2 silenced ACHN metastatic site cancer cells on β1 integrin substrates

In order to demonstrate the effect of TG2 in ACHN cell adhesion on β1 integrin matrices, TG2 downregulated and control NS ACHN cells were seeded on FN, Col1 and LM substrates as described in Section 3.5.1 and 3.6.1 (Figure 4.17-18).

NS treated ACHN cells showed a 76 per cent cell attachment and spreading on FN matrix substrate at the early time point of 30 mins when compared to the NS treated control cells at the late time point of 60 mins. TG2 down-regulation led to a 48 per cent decrease in siR1 and a 44 per cent reduction in siR6 treated ACHN cells at 30 mins whereas 40 per cent reduction in cell attachment to FN matrix was recorded for both siR1 and siR6 treated ACHN at the late time point of 60 mins. Silencing of TG2 showed a 46 per cent decrease in cell spreading at the early time point, while a respective 40 per cent and 50 per cent reduction in cell spreading was detected in siR1 and siR6 treated ACHN cells at 60 mins

(Figure 4.17 A). In comparison to three RCC cell lines, ACHN cells displayed the lowest cell adhesion potential onto Col1 matrix substrate, which was recorded as 60 per cent for cell attachment and 52 per cent for cell spreading compared to NS treated control cells at the late time point. TG2 downregulation displayed 40 per cent cell attachment on Col1 in each siRs treated ACHN cells at the early time point of 60 mins, while ~55 per cent cell attachment was evident for each siR treated ACHN cells at the late time point of 90 mins. Silencing of TG2 led to a respective 23 per cent and 31 per cent cell spreading of siR1 and siR6 treated ACHN and a further 30 mins incubation increased the cell spreading to 51 per cent for siR1 and 43 per cent for siR6 treated ACHN cells (Figure 4.18 B).

Similar to Caki-2 cells, ACHN cells had a lower adhesion potential on LM matrix substrate compared to A-498 and Caki-1 cells, since only 65 per cent cell attachment and 51 per cent cell spreading was evaluated for NS treated ACHN cells. TG2 down-regulation with siR1 led to a 52 per cent reduction in ACHN cell attachment on LM at the early time point of 30 mins, whereas 55 per cent cell attachment was recorded in siR6 treated ACHN cells at 30 mins. Comparison of the late time point to early time point showed only 11 per cent increase in cell attachment of siR1 and siR6 treated ACHN cells on LM (Figure 4.16). Results of spreading assay for ACHN has given similar values with that of A-498 cells as TG2 down-regulation did not lead to a significant change in the cell spreading potential of ACHN cells on LM matrix substrate at 30 mins. The siR1 and siR6 treated ACHN cells displayed a 29 per cent cell spreading, while a 49 per cent cell and 43 per cent cells spreading was detected in that order for the late time point of 60 mins (Figure 4.18).

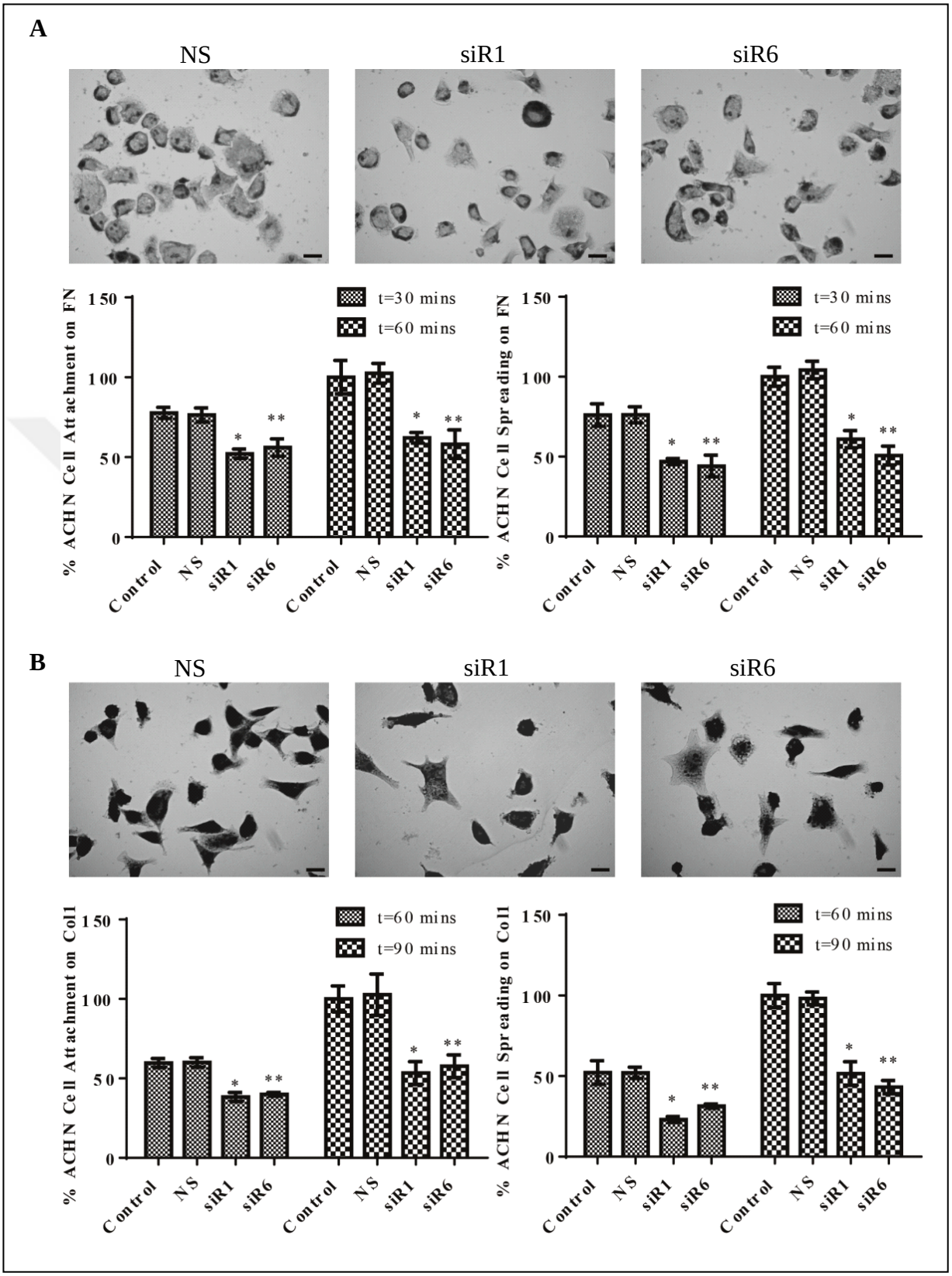

Figure 4.17. Detection of cell adhesion potential of primary site ACHN cells on FN (**A**) and Col1 (**B**). Bars, 20 μm.

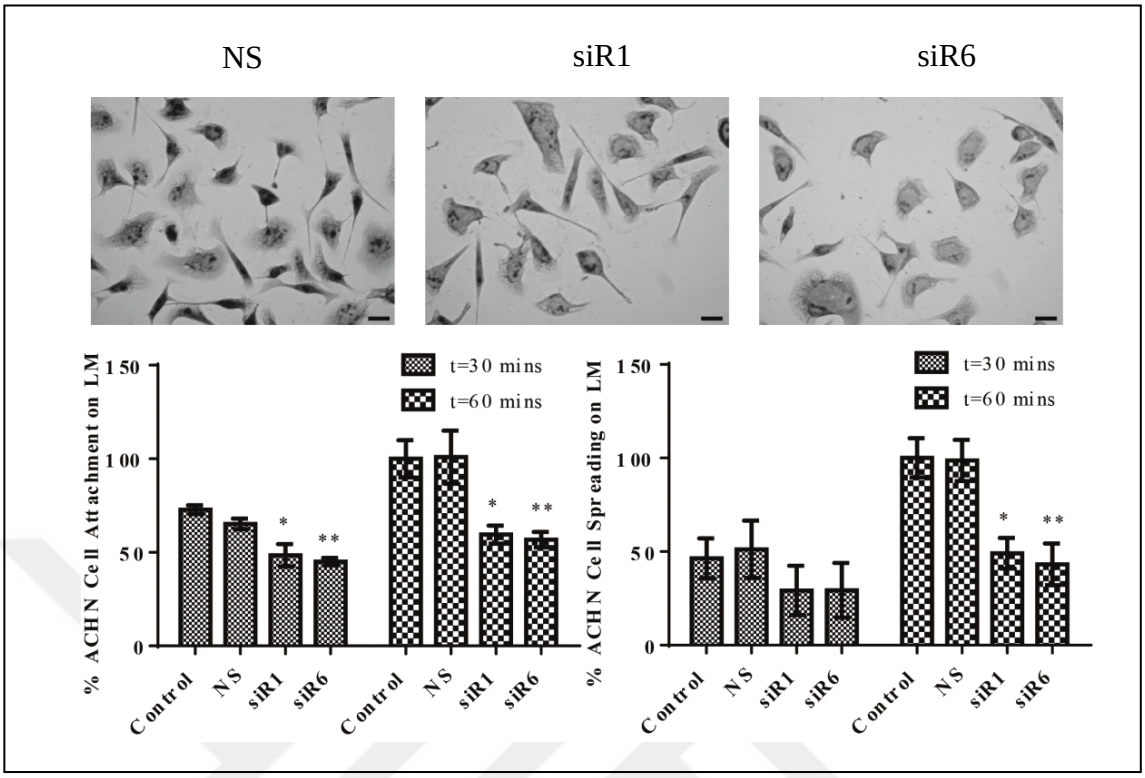

Figure 4.18. Detection of cell adhesion potential of primary site ACHN cells on LM. Bars, 20 μm.

4.5. STABLE SDC4, TG2 DOWNREGULATION AND TG2 OVEREXPRESSION IN CAKI-1 CELLS USING LENTIVIRAL PARTICLES

In order to analyze the effect of TG2 down-regulation and overexpression in integrin β1 trafficking, Caki-1 cells were treated with human shRNA lentiviral particles containing puromycin selection gene obtained from Santa-Cruz (scrambled control, sc-108080 and human shTG2, sc-37514-V). Caki-1 cells were treated with lentiviral particles as described in Section 3.5.3. Caki-1 cells treated with lentiviral particles were selected by the addition of puromycin and blasticidin. In order to determine the minimum effective dose for blasticidin and puromycin, Caki-1 Wt cells were subjected to puromycin between the range of 0.5-5μg/ml or blasticidin between the range of 1-8 μg/ml. The cell medium was changed in every three days with fresh media containing the indicated antibiotics. The minimal effective dose which led to 100% toxicity was determined for the selection.

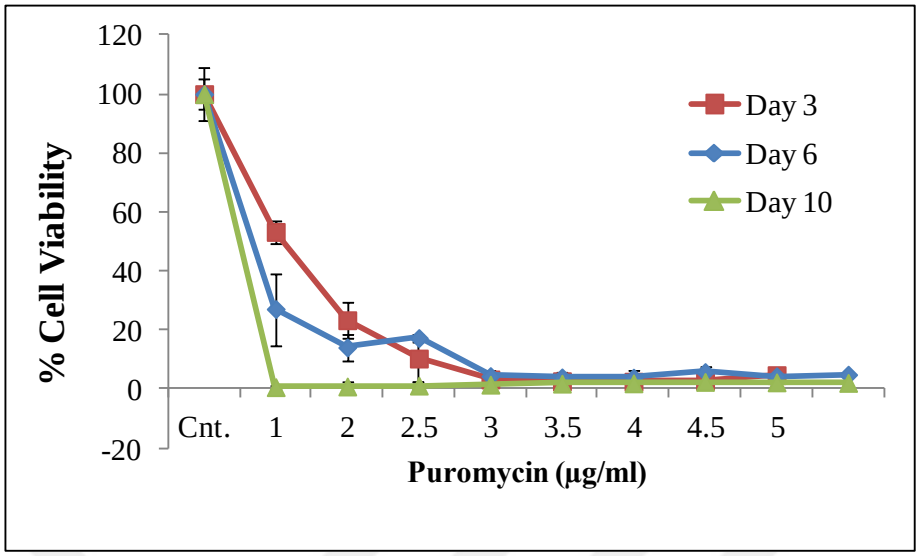

Figure 4.19. WST-1 Cell Viability assay showing the toxicity of puromycin on Caki-1 Wt cells.

Results obtained from Figure 19 showed that at the day 3, 2.5µg/ml puromycin led to a 90% decrease in the cell viability while 4.7 per cent cell viability was detected at the day 6. At the end of the 10 day WST-1 assay results confirmed 100% decrease in the cell viability in the presence of 2.5µg/ml puromycin therefore 2.5µg/ml puromycin was selected as the minimum effective dose and used in shRNA transduced cell selection in order to avoid a possible antibiotic resistance.

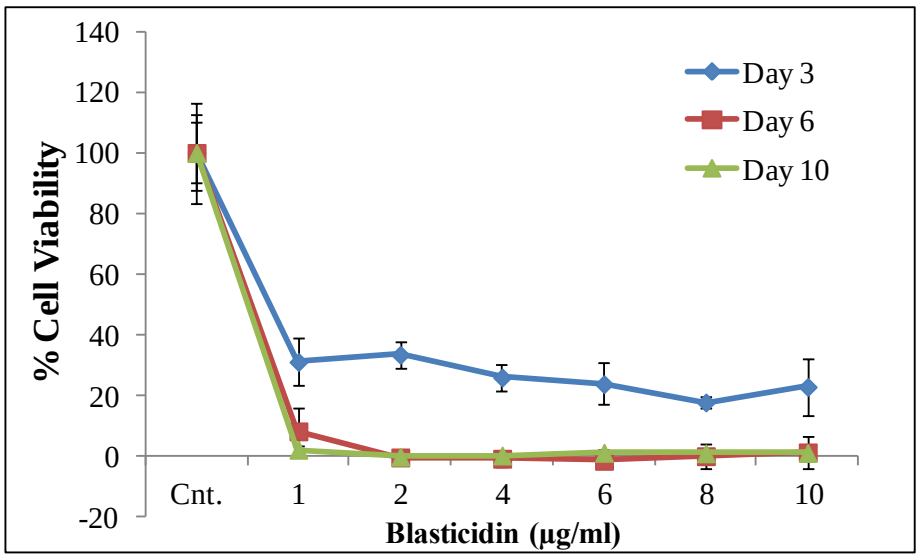

Figure 4.20. WST-1 Cell Viability assay showing the toxicity of blasticidin on Caki-1 Wt cells.

Following the treatment of Caki-1 Wt cells with blasticidin, at the 3rd day cell toxicity was detected 31.1, 33.4, 25.9, 23.8, 17.7 and 22.8 per cent for 1-10µg/ml blasticidin respectively. After 3 days, blasticidin was effectively showed its toxicity where nearly 100 per cent cell death was detected. However under microscope a few cells were detected to be alive and attached in the presence of 1-7µg/ml blasticidin therefore 8µg/ml blasticidin concentration was chosen to be used in the antibiotic selection (Figure 20).

Next, transduction efficiency of TG2 downregulation and over-expression were analyzed using qPCR and Western Blot as described in Section 3.2.3 and 3.3.4. In comparison to wild type cells shTG2 Caki-1 cells showed 87 per cent decrease in TG2 protein whereas 2.25 fold increase in the protein level of TG2 was detected in Caki-1 TG2 overexpressed cells (TG2 o/e) (Figure 21A). Statistical analysis showed no difference between wild type (Wt) and scrambled control (Scr) cells by means of TG2 protein expression. Next, mRNA levels in Caki-1 shTG2 and TG2 o/e was detected by using qPCR analysis (Figure 21B). In parallel with the Western Blot experiments 86.1 per cent reduction in *TGM2* mRNA levels was detected in shTG2 Caki-1 cells whereas a 3.9 fold increase of TG2 expression was obtained for TG2 o/e cells when compared to Caki-1 Wt cells. No significant difference between Wt and Scr cells obtained from the results of qPCR analysis.

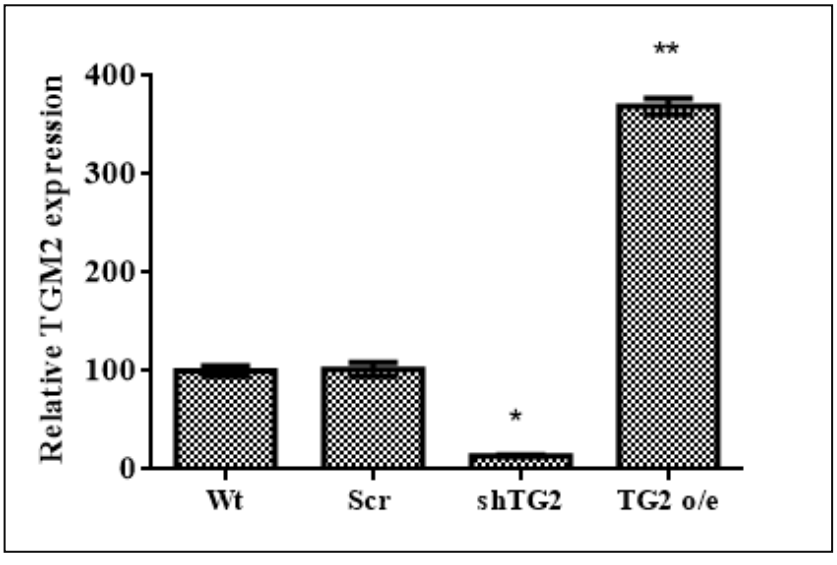

Figure 4.21. Effect of TG2 down-regulation and overexpression was detected using qPCR analysis. *TGM2* mRNA levels were normalized against 18s rRNA expression levels. * $p < 0.05$ shows the significant difference against Wt cells.

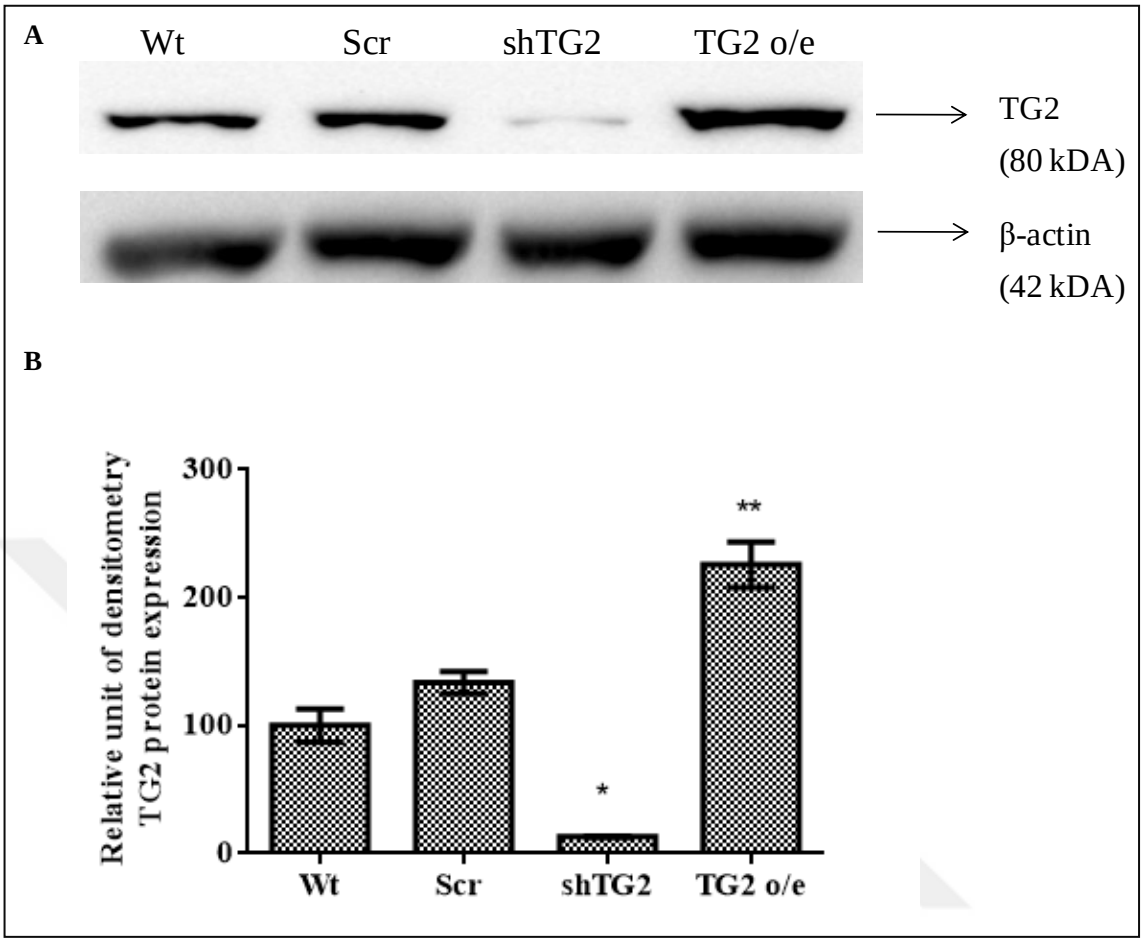

Figure 4.22. (**A**) Western Blot analysis of TG2 downregulated and overexpressed Caki-1 cells. (**B**) Total TG2 level of Caki-1 Wt, Scr, shTG2 and TG2 o/e cells were quantified by Image Lab volume intensity analysis. Relative density of TG2 was obtained by dividing that of actin levels in each cell line.* $p < 0.05$ shows the significant difference against Wt cells.

In order to analyze the role of SDC4 in integrin β1 trafficking, SDC4 in TG2 overexpressed Caki-1 cells was silenced using SDC4 targeted shRNA lentiviral (shSDC4 TG2 o/e cell) as described in Section 3.5.3. Although SDC4 was expressed in a very low quantity in Caki-1 cell, the efficiency of SDC4 silencing was determined by performing qPCR analysis. In order to rule out the off-target effects of silencing procedure, following TG2 and SDC4 silencing TG2, ITGβ1 mRNA expression levels were detected in Caki-1 Wt, Scr, shTG2, TG2 o/e, shSDC4 TG2 o/e and shSDC4 cells (Figure 23). In addition, *TGM2* mRNA levels (Figure 4.23) were detected in Caki-1 shSDC4 TG2 o/e and shSDC4 cells followed by the analysis of SDC4 mRNA levels in Caki-1 Wt, Scr, shTG2 and TG2 o/e cells (Figure 4.25).

Results depicted from Figure 22 showed that SDC4 silencing did not decrease the TGM2 mRNA levels in TG2 o/e Caki-1 cells where more than 3.5-fold increase was still detected in *TGM2* levels when compared to Caki-1 Wt cells. There was no statistically significant difference detected among Wt, Scr and SDC4 silenced (shSDC4) cells by means of *TGM2* mRNA expression (Figure 4.23). Next, ITGβ1 mRNA levels were analyzed and according to the statistical analysis no significant change among Caki-1 Wt, Scr, shTG2, TG2 o/e, shSDC4 TG2 o/e and shSDC4 cells was detected (Figure 24). In parallel with ITGβ1 levels, no significant difference was detected in the *SDC4* mRNA expression levels of Caki-1 Wt, Scr, shTG2 and TG2 o/e (Figure 4.25). However, SDC4 silencing led to a significant and respective 80 per cent and 70 per cent decrease in SDC4 expression in TG2 o/e cells silenced with SDC4 shRNA lentiviral particles (shSDC4 TG2 o/e) and wild type cells treated only with SDC4 shRNA particles (shSDC4). Statistical analysis showed no differences between shSDC4 TG2 o/e and shSDC4 by means of SDC4 mRNA expression levels (Figure 4.25).

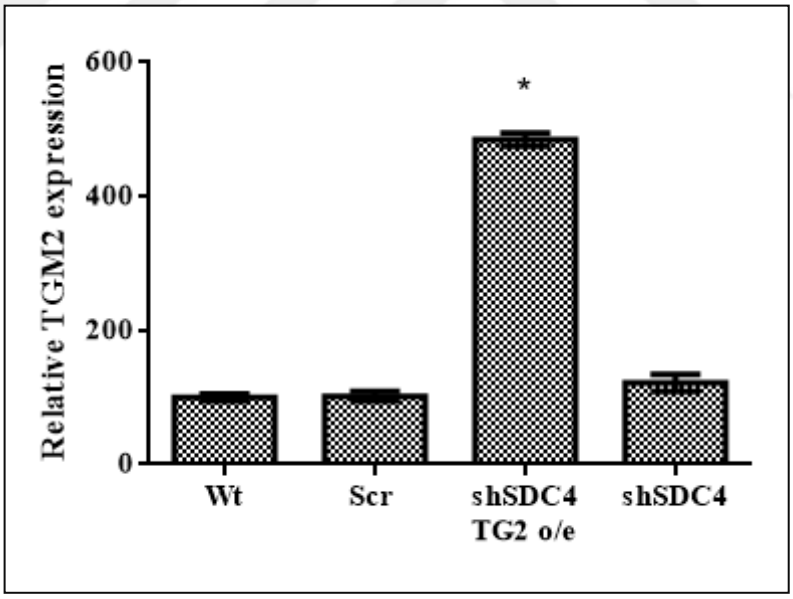

Figure 4.23. Effect of TG2 overexpression was detected in Caki-1 Wt, Scr, shSDC4 TG2 o/e and shSDC4 cells using qPCR analysis. TGM2 mRNA levels were normalized against 18s rRNA expression levels. * $p < 0.05$ shows the significant difference against Caki-1 Wt cells.

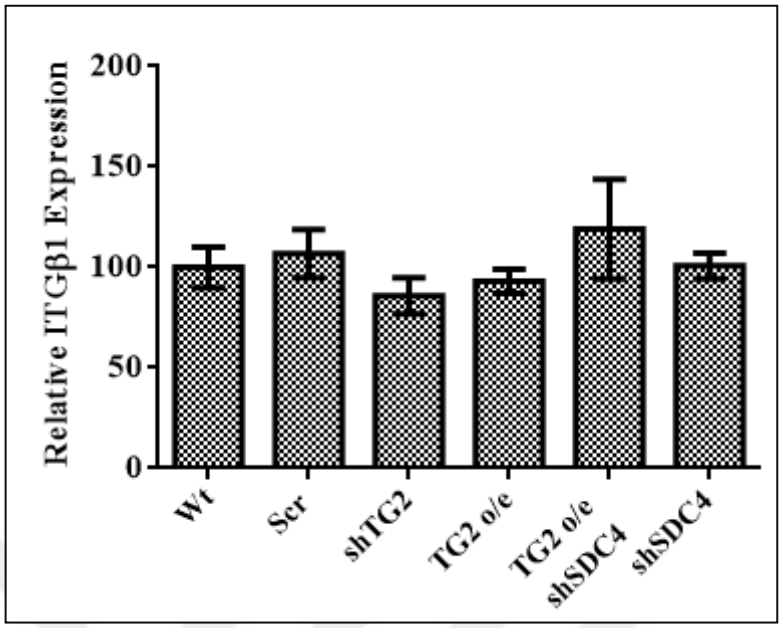

Figure 4.24. Relative ITGβ1 mRNA expression levels in Caki-1 Wt, Scr, shTG2, TG2 o/e, shSDC4 TG2 o/e cells and shSDC4 cells. ITGβ1 mRNA levels were normalized against 18s rRNA expression levels.

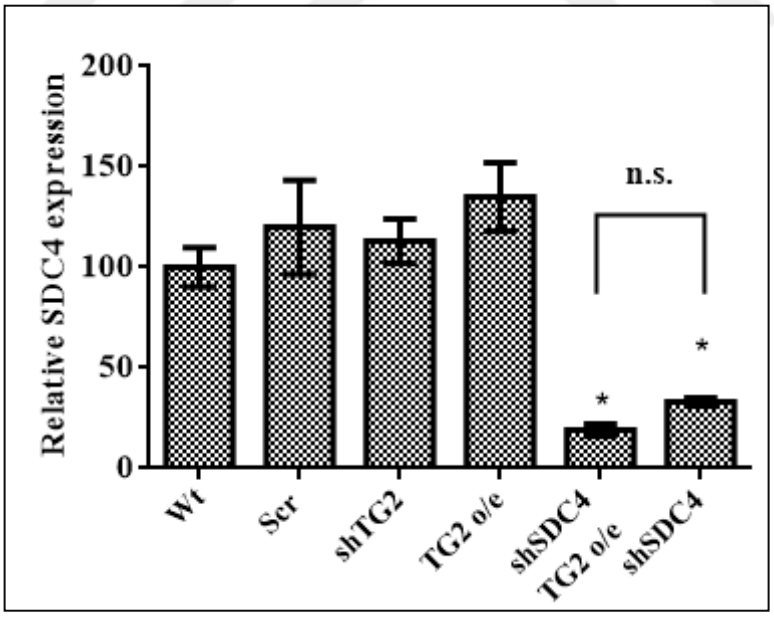

Figure 4.25. Relative SDC4 mRNA expression in Caki-1 Wt, Scr, shTG2, TG2 o/e, shSDC4 TG2 o/e cells and shSDC4 cells. SDC4 mRNA levels were normalized against 18s rRNA expression levels. * $p < 0.05$ shows the significant difference against Caki-1 Wt cells. No significant difference (n.s) was detected in the expression levels of *SDC4* between shSDC4 TG2 o/e and shSDC4 cells.

4.6. β1 INTEGRIN BASED INTERNALIZATION AND RECYCLING ASSAY OPTIMIZATION

Integrin endo/exocytosis cycles defines the signaling pathways regulating integrin-mediated cell to ECM interaction in order to maintain cell adhesion, migration and survival mechanisms [112]. De-regulation of integrin internalization and recycling may lead to an abnormal cell migration and subsequent tumor progression. Since integrin trafficking takes priority during tumor progression and cancer metastasis, various experiments were performed to enlighten the molecular machinery responsible for the integrin internalization and recycling in migrating cells [138,254]. However, in the literature different methods were developed for each cell type hence it is almost impossible to rely on one method to detect the integrin internalization and recycling machinery [140,254-256]. Therefore, initial part of this project was focused on the optimization of the method to detect the integrin trafficking in the metastatic cancer cell line Caki-1, which possessed the highest ITGβ1 expression and ratio of TG2 association (Figure 4.5).

Upon activation via inside out or outside-in signaling mechanisms, integrins shift their conformations from the inactive state with a closed headpiece to the active extended state with an open headpiece. Since its discovery several antibodies were produced to recognize inactive integrin β1 (mAb13, K20, JB1B) or active (12G10, 8A2, TS21/6) β1 integrins [257]. Although it is claimed that β1 integrins primarily located on the cell surface remains in the inactive state, a recent study showed that the active integrin internalization rates were higher when compared to inactive integrin β1 internalization rates in PC-3, NCI-H460, MDA-MB-231 cancer cell lines. This study therefore clearly demonstrated that cancer cells used active β1 integrins to facilitate cell migration [141]. The first method to analyze the integrin traffic was optimized by Roberts *et al*. in 2001 [254], using a method similar to pulse-chase experiments where biotinylated of cell surface integrins were chased when internalized through capture ELISA and/or immunoprecipitation method. For the recycling experiments, antibody-based integrin recycling assay were first developed by Pardi *et al*. in 1995 [258]. For this study the method using MCA2028 clone 12G10 antibody labeling the active cell surface integrins before the acid rinse was adopted from Jovic *et al*. 2007 [255].

4.6.1 Assay development to detect the β1 integrin traffic in RCC cells

In order to detect the recycling of active β1 integrins, integrin β1 on cell surface was labeled using 5µg/ml active MCA2028 clone 12G10 antibody for 1 hour under the conditions abrogating the integrin internalization (non-internalized conditions), which was achieved by incubating samples at 4°C or on ice. Following the incubation, cell surface β1 integrins were induced to be internalized by using 0.5 per cent (w/v) BSA in serum free media for 2 hours at 37°C. Next, non-internalized β1 integrins on cell surface was removed using 0.5 per cent (v/v) glacial acetic acid and 0.5 M NaCl pH 3.0 containing acid rinse solution. In this particular acid rinse protocol, cells were incubated with acid rinse solution 2 times for 45 sec then washed twice with DPBS pH 7.4 and once with serum free medium to neutralize acidic conditions. Integrin β1 recycling was next achieved by incubating the acid rinsed cell monolayer with 10 per cent (v/v) FBS containing medium for 120 mins at 37°C. Recycled β1 integrins were captured by labeling the recycled cell surface β1 integrins with Alexa-488 conjugated secondary antibody for 30 mins on ice. Flow Cytometry was then performed as described in Section 3.7.3. In order to eliminate the non-specific binding of mouse IgG on cell surface proteins, Caki-1 cells incubated with IgG antibody were used as a gating control. Following acetic acid treatment one of the samples were immediately labeled using Alexa-conjugated secondary antibody to detect the efficiency of acid rinse used in this particular experimental conditions.

Results from the recycling experiment showed no evidence of significant difference in ITGβ1 turn-over among scrambled control (Scr), TG2 silenced (shTG2) and overexpressed (TG2 o/e) Caki-1 cells. Only acetic acid treated Caki-1 wild type cells showed approximately 6 per cent higher β1 integrin recycling compared to Caki-1 Wt, Scr and shTG2 cell lines (Figure 4.26).

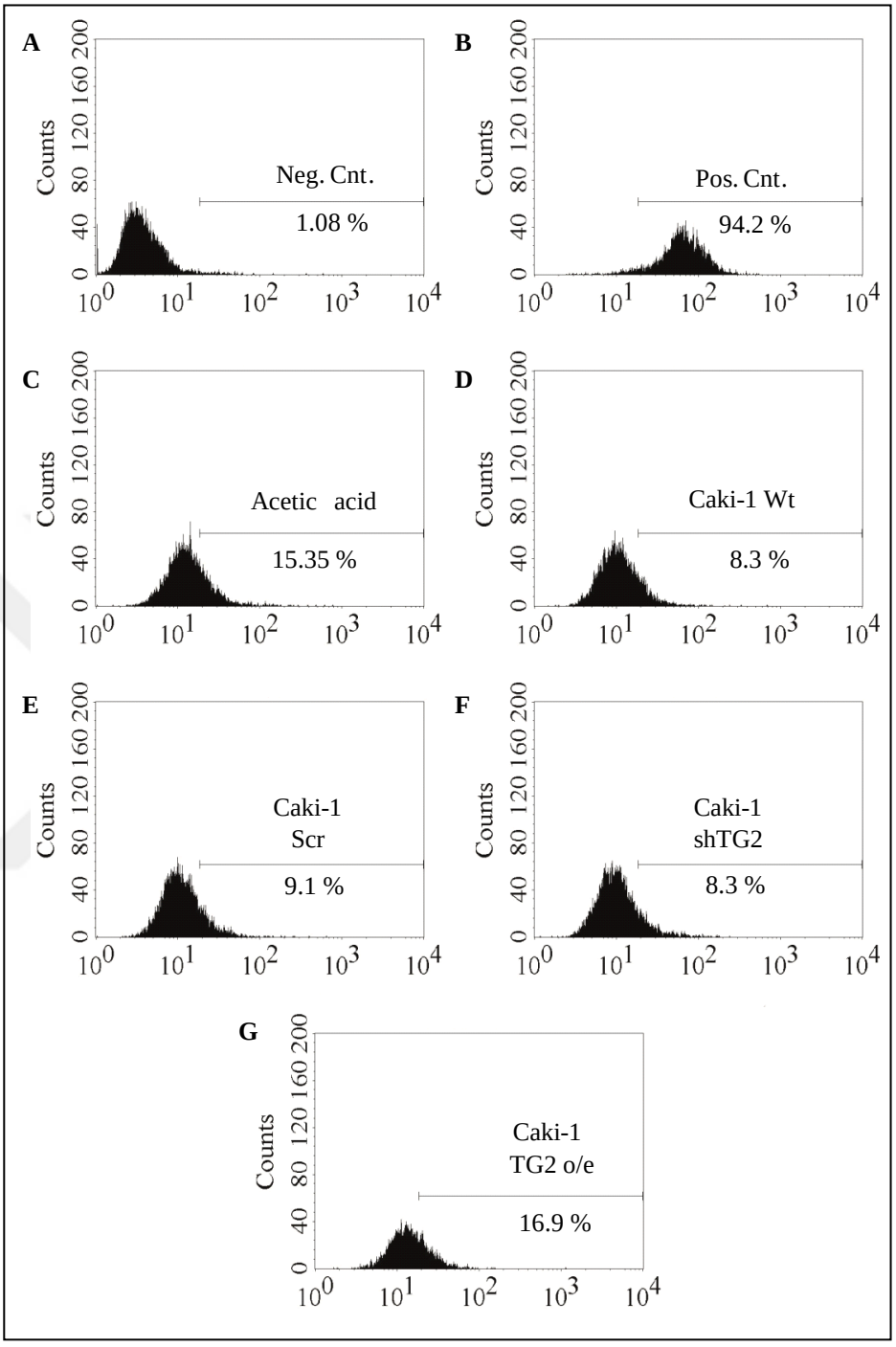

Figure 4.26. Flow Cytometry results of Caki-1 integrin β1 recycling (**A**) Negative Control (Neg.Cnt) Caki-1 cells labeled with mouse IgG isotype control (**B**) Caki-1 wt cells labeled with 12G10 followed Alexa-488 secondary antibody without acid rinse (**C**) Caki-1 wt cells labeled with 12G10 followed Alexa-488 secondary antibody with acid rinse before the recycling induction with FBS (**D-G**) Caki-1 Wt, Scr, shTG2 and o/eTG2 cells labeled with 12G10 followed Alexa-488 secondary antibody with acid rinse.

These preliminary experimental results suggested that there might be a problem either in the induction of ITGβ1 internalization or efficiently striping the 12G10 labeled ITGβ1 through acid rinse. Since these data pointed out two different problems in the optimization of internalization conditions and antibody stripping conditions, initially we aimed to optimize the conditions to increase the internalization rates using (i) AIM-V medium with or without soluble fibronectin, (ii) serum free McCoy 5A medium containing soluble fibronectin, and (iii) McCoy 5A medium containing FBS. AIM-V is a commercially available serum free medium which contains fatty acids, cholesterol, transferrin, iron salt and insulin like growth factors, and principally used in culturing immune system cells. Since all proteins in AIM-V medium are of human origin, it could be mimicking an environment necessary to induce the integrin internalization. The concentration of FN was determined from the study, which showed that FN RGD-impared FN fibril deposition was only facilitated in the presence of 50 nM biotinylated if the cells were seeded on a TG2-FN matrix [221]. Finally, FBS was considered as it includes several growth hormones, cholesterol, vitamins, enzymes, glucose and inorganic salts, which are essential for cell growth and has been widely used to stimulate integrin internalization and recycling experiments [140,141] In order to detect integrin internalization using flow cytometry, cells were labeled as described in Section 3.7.3 than internalization was induced using AIM-V, AIM-V+50nM soluble FN, McCoy5A medium containing 50 nM soluble FN, and McCoy5A medium containing 10 per cent (v/v) FBS for 1 hour at 37°C. Following the internalization, non-internalized β1 integrins on cell surface was labeled using Alexa-conjugated secondary antibody. Caki-1 Wt cells treated with the isotype control represented the case if all β1 integrins were internalized and in negative control, cells labeled with 12G10 antibody without being subjected to any inductive medium conditions, represented the case where the integrin internalization was kept in bare minimum. Hence the integrin internalization was taken as 99.8 per cent in isotype control (Fig 4.27A) while the integrin internalization rate in negative control was accepted as 3.7 per cent (Fig 4.27B). Therefore, in our experimental set-up the shift from the left side through the right side of the histogram gave the percentage of internalized integrins. According to the results induction of integrin internalization using the AIM-V only and AIM-V with 50nM soluble FN resulted in a similar percentage of integrin internalization with 36.1 and 34.5 percent (Figure 4.27 C-D). When McCoy 5A containing 50 nM soluble FN was used 33.1 of the ITGβ1 was found to be internalized (Figure 4.27E). Similarly when 10 per cent (v/v) FBS

was used instead of FN 35.8 per cent of cell surface ITGβ1 was internalized (Figure 4.27F).

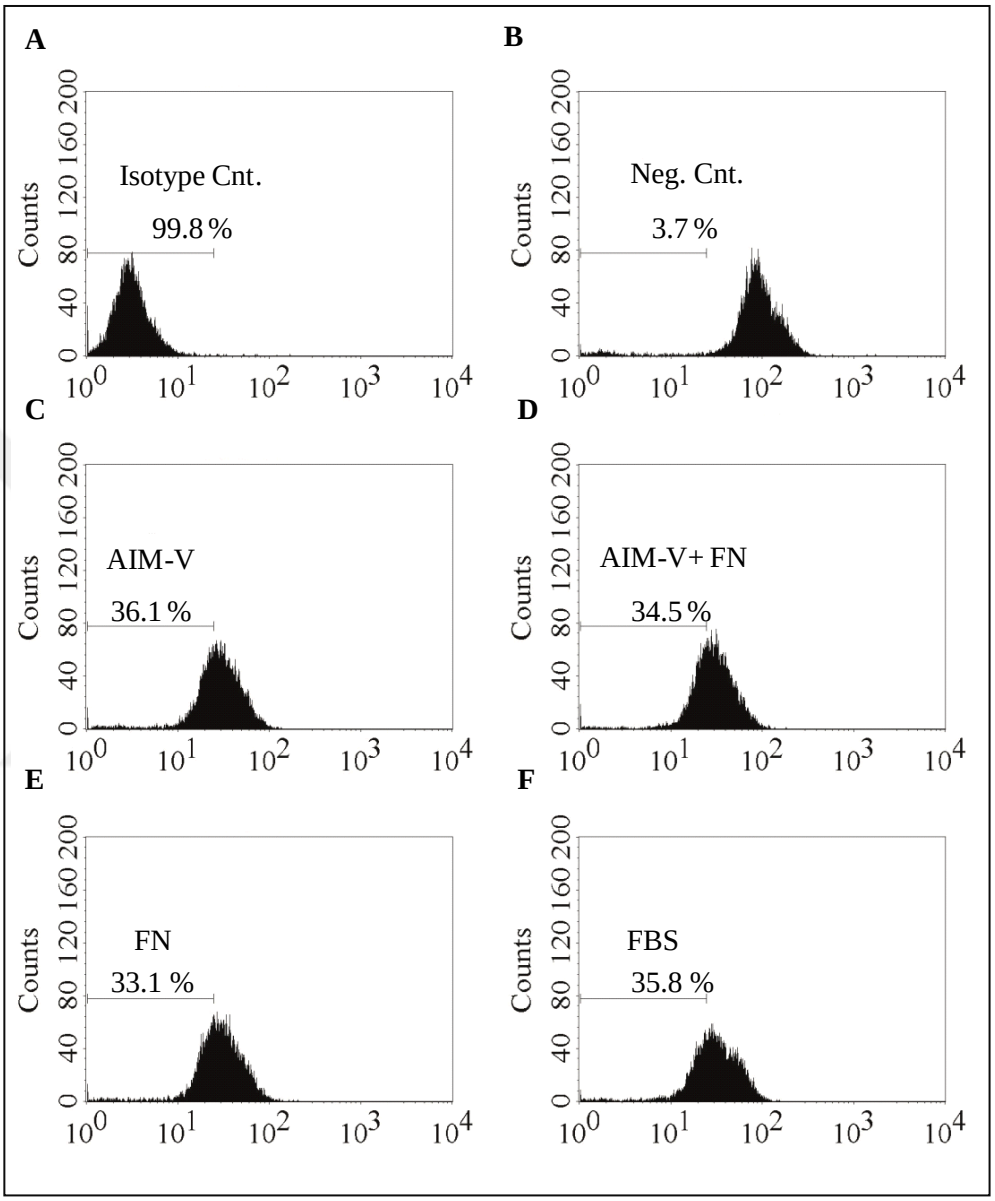

Figure 4.27. Detection of integrin β1 internalization with Flow Cytometry using different inducers. (**A**) Negative Control (Neg. Cnt) Caki-1 cells labeled with mouse IgG isotype control (**B**) Caki-1 Wt cells labeled with 12G10 followed Alexa-488 secondary antibody without acetic rinse (**C-F**) Caki-1 cells stimulated with AIM-V, AIM-V+50nM FN, 10 (v/v) per cent FBS and serum free medium containing 50nM soluble FN respectively.

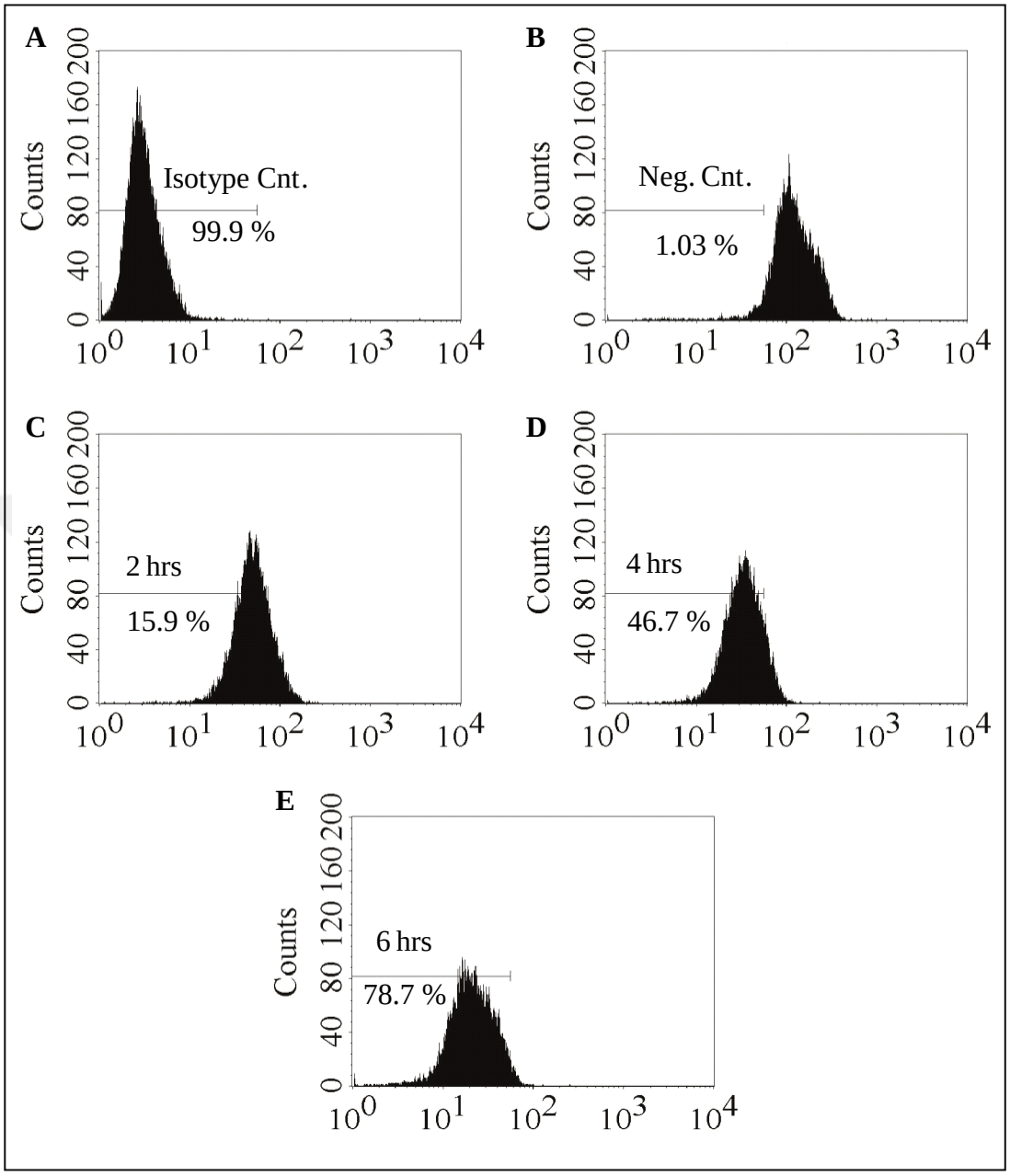

Figure 4.28. Detection of integrin β1 internalization using 0.01 per cent BSA (w/v) at different time points. (**A**) Negative Control (Neg. Cnt) Caki-1 cells labeled with mouse IgG isotype control (**B**) Caki-1 Wt cells labeled with 12G10 followed Alexa-488 secondary antibody without acetic rinse (**C-E**) Caki-1 cells stimulated with 0.01 per cent BSA for 2, 4 and 6 hours respectively.

In order to increase the internalization efficiency, a different experimental method was adopted from Powelka and Hsu *et al*. 2004 [140], in which cells were serum starved the overnight in serum free medium containing 0.01 per cent (w/v) BSA to enrich the

intracellular pool of β1 integrins. In this protocol, following the Caki-1 cell surface labeling of ITGβ1, the internalization was induced using 0.01 per cent (w/v) BSA for 2, 4 and 6 hours at 37°C. At the end of the each incubation period the remaining non-internalized β1 integrins on the cell surface were labeled using anti-mouse Alexa-488 conjugated secondary antibody. Results depicted from Figure 4.24 showed in Caki-1 cells incubated with 0.01 per cent (w/v) BSA for 2 hours 15.9 per cent of cell surface β1 integrins were internalized, while incubation for 4 and 6 hours led to a significant increase in integrin internalization with 46.7 and 78.7 per cent, respectively (Figure 4.28).

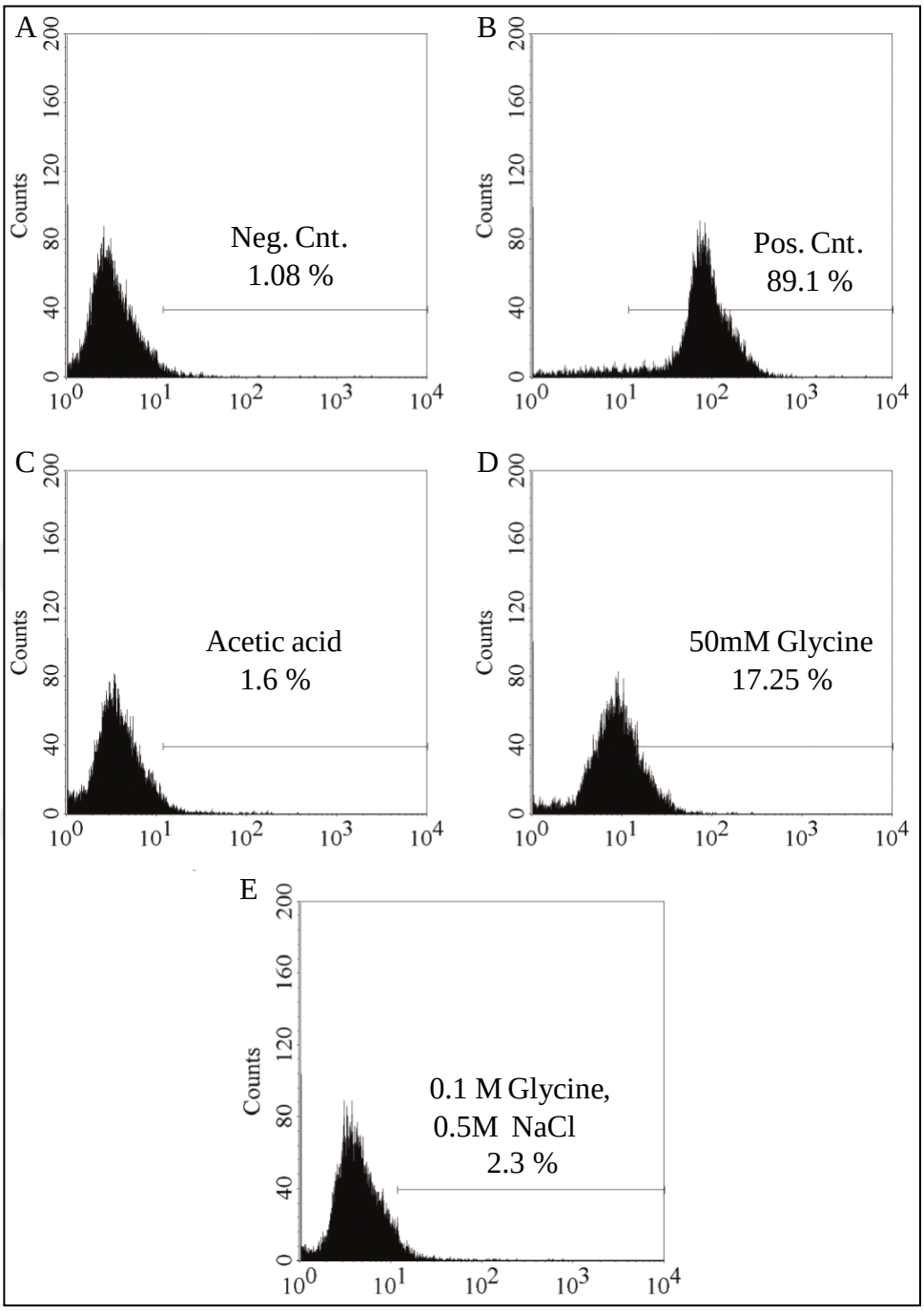

Figure 4.29. Acid rinse optimization using Caki-1 Wt cells (**A**) Negative Control (Neg. Cnt) Caki-1 wt cells labeled with mouse IgG isotype control (**B**) Caki-1 Wt cells labeled with 12G10 antibody without any acid rinse (**C-E**) Caki-1 Wt cells labeled with 12G10 antibody which was flowed by (**D**) 0.5 per cent (v/v) acetic acid solution pH 3.0 rinse (**E**) 50 mM glycine solution pH 2.5 rinse (**F**) 0.1 mM Glycine solution pH 3.0 rinse before the labeling with Alexa-488 secondary antibody

To eliminate the non-specific cell surface 12G10 antibody labeled integrin β1 following acid rinse treatment different rinse solutions with low pH were introduced into the experimental set-up. In the literature, 50 mM glycine rinse solution with a pH of 2.5 was used during the investigation of JAM-A protein induced-integrin β1 recycling in HL60 neutrophil cells [259]. Another study was suggested the use of 0.1M glycine, 0.5M NaCl containing solution with a pH 3.0 which was utilized in the recycling of LM binding integrins in NIH 3T3 fibroblast and DU145 prostate cancer cells [260]. Both of these rinse solutions were compared with 0.5 per cent acetic acid rinse treatment where the incubation time of acetic acid treatment was increased from 45 seconds to 90 seconds. All acid rinse solutions were applied to Caki-1 cells right after cell surface ITGβ1 labeling using active integrin β1 antibody 12G10. Caki-1 cells were treated with these different rinse solutions twice for 45 seconds, a total of 90 seconds. Results achieved from the new acid rinse treatment showed a remarkable decrease in cell surface labeled ITGβ1 stating that increase in time of rinse incubation was effective in the stripping of 12G10 antibody from the cell surface non-internalized β1 integrins. As stated in Figure 4.28, the level of labeled ITGβ1 after the rinse was detected as 1.26 for 0.5 per cent acetic acid and 2.3 per cent for 0.1M glycine and 0.5M NaCl rinse solutions, while 17.25 per cent ITGβ1 level was detected after the rinse with 50 mM glycine. When the morphological changes in Caki-1 cells were observed following the low pH rinse treatments under the light microscope, it was seen that 0.1M glycine, 0.5 M NaCl containing rinse solution caused the least morphological change while other rinse solutions lead to the detachment of cells from their substratum therefore 0.1M glycine, 0.5M NaCl containing rinse solution was used for the subsequent experiments (Figure 4.29).

Together with the results obtained from Figure 4.28 and 29, the conditions for the recycling experiments were set as; 0.01 per cent (w/v) BSA to induce internalization, 0.1M glycine, 0.5M NaCl, pH3.0 to stripe the non-internalized integrins after the BSA induction, and 10 per cent (v/v) FBS treatment for 120 mins to induce the recycling of active β1 integrins.

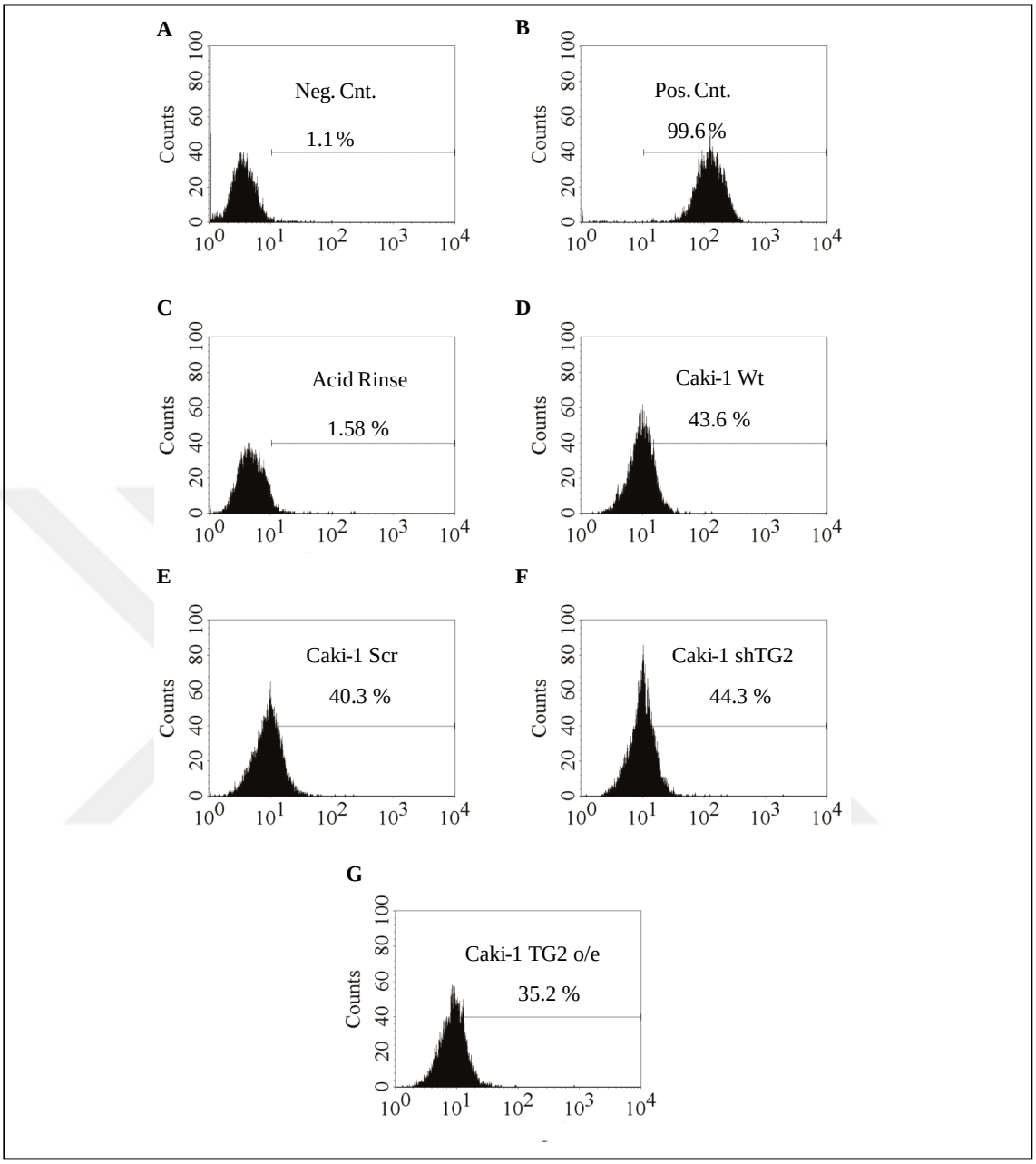

Figure 4.30. Flow Cytometry results of Caki-1 integrin β1 recycling adapted from Jovic *et al*. 2006 method with the changes in rinse treatment. (**A**) Negative Control (Neg.Cnt) Caki-1 cells labeled with mouse IgG isotype control (**B**) Caki-1 Wt cells labeled with 12G10 followed Alexa-488 secondary antibody without acid rinse (**C**) Caki-1 Wt cells labeled with 12G10 followed Alexa-488 secondary antibody with acid rinse before the recycling induction with FBS (**D-G**) Caki-1 Wt, Scr, shTG2 and o/eTG2 cells labeled with 12G10 followed Alexa-488 secondary antibody with acid rinse.

Results obtained from Figure 30 demonstrated no evidence of significant difference between Wt, Scr and shTG2 cells which were evaluated as 43.6, 40.3, 44.3 per cent respectively and an interesting 5 per cent decrease was detected in TG2 o/e cells.

In order to analyze whether the new conditions set for recycling experiments does indeed enable us to visualize the difference in the recycling ITGβ1 levels, experiments were performed on Caki-1 cell clones Wt, Scr, shTG2 and TG2 o/e cells. Unfortunately, results obtained from Figure 29 demonstrated no significant difference in the recycled levels of ITGβ1 among Wt, Scr and shTG2 cells, which were evaluated as 43.6, 40.3, 44.3 per cent respectively, however an interesting 5 per cent decrease was detected in TG2 o/e cells.

In order to confirm the ITGβ1 internalization results of Flow Cytometry analysis (Figure 28) the internalization rates for Wt, Scr, shTG2 and TG2 o/e cells were measured using capture ELISA method, which is commonly used in the detection of integrin internalization [254,256,261,262]. To optimize capture ELISA method, surface proteins of Caki-1 cell were labeled using 0.5 mg/ml NHS-SS biotin and internalization was induced using 0.01 per cent (w/v) BSA containing McCoy's 5A for 6 hours. To remove the covalently bound NHS-SS biotin on cell surface proteins following the internalization, the cell monolayers were treated with MesNa and IAA as described in Section 3.7.3. Absorbance values for Non- MesNa treated samples were assigned as total biotinylated integrins (w/o MesNa) present on the cell surface (Section 3.7.3). Internalization percentages were calculated by dividing absorbance value of MesNa treated sample to the non-MesNa treated sample (Figure 4.30).

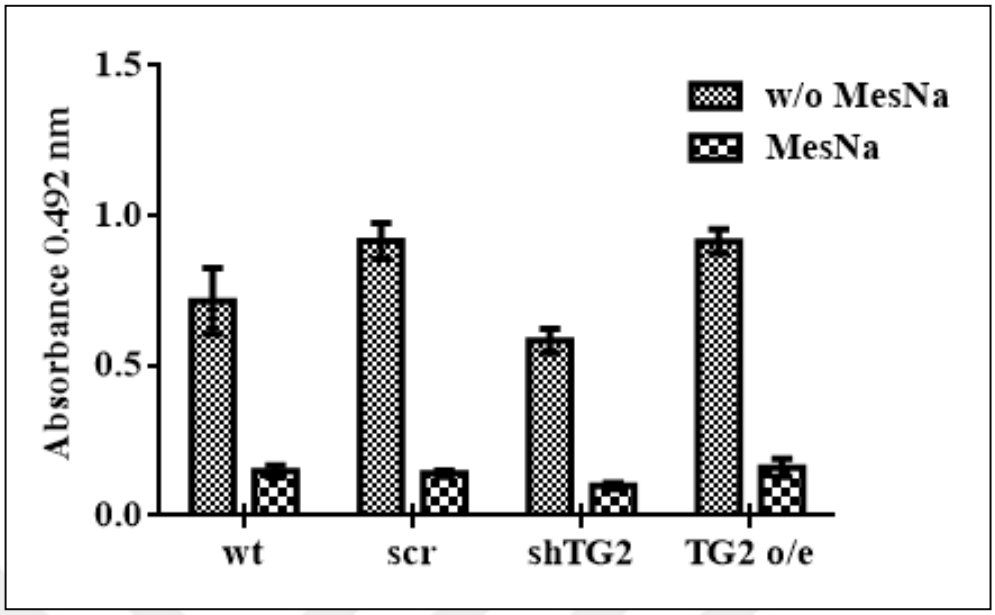

Figure 4.31. Detection of β1 Integrin internalization in wild type (Wt), TG2 silenced (shTG2) and TG2 overexpressed (TG2 o/e) cells using capture ELISA assay

In contrast to Flow Cytometry results shown in Figure 4.28, internalization rates were detected almost 50 per cent less when capture-ELISA method was performed. Results in Figure 4.30 showed that ITGβ1 internalization ratio for Caki-1wt cells was detected as 20 per cent and ITGβ1 internalization rates of Scr, shTG2 and TG2 o/e cells showed more or less the same results evaluated as 15.2, 17 and 17.4 per cent, respectively, indicating that capture-ELISA assay may not be a suitable method to detect the integrin internalization of Caki-1 cells (Figure 31).

A thorough search of the literature suggested that the internalization of integrins can also be analyzed using immunoprecipitation assay [141,142,254]. Therefore, the same experimental set-up was established and ITGβ1 internalization was induced using 0.01 per cent (w/v) BSA for 6 hours at 37°C. Following the internalization, cells surface proteins were labeled using NHS-SS biotin as described in Section 3.7.1. then cell lysates were collected in IP buffer containing 50mM Tris-HCL pH 7.4, 150Mm NaCl, 0.25 per cent (w/v) sodium deoxycholate, 1 per cent (v/v) protease inhibitor cocktail and 0.1 mM PMSF. Cell lysates were sonicated at 60 per cent power by four cycles and followed by Lowry assay for equal protein loading. Active ITGβ1 was pull down for 1.5 hour at 4°C and immune complexes were collected using protein G agarose beads for 2 hours. In the

first trial, proteins were extracted using 2x Laemmli buffer containing β- mercaptoethanol via heating and proteins were transferred using nitrocellulose membrane in Western Blot. Following the transfer the membrane was probed by HRP-conjugated extravidin peroxidase (Figure 4.32).

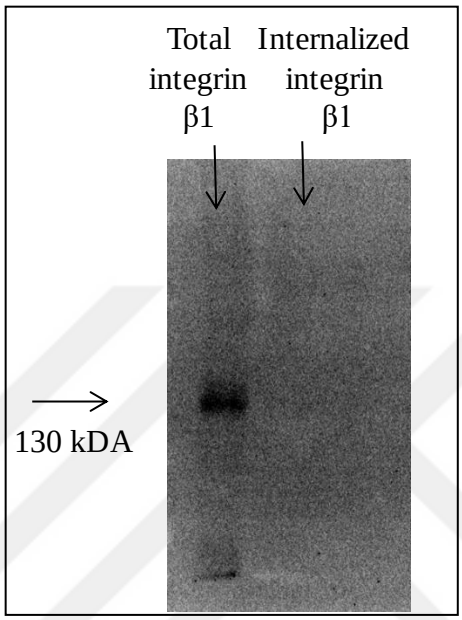

Figure 4.32. Biotin-based IP method optimization to detect internalized active β1 integrins of Caki-1 Wt cells. Total integrins samples were not subjected to either MesNa or IAA and represents biotin labeled cell surface β1 integrins. Internalized β1 integrins detected with IP method. First line total cell surface β1 integrins pulled down with 12G10 ITGβ1 antibody integrin and second line demonstrated the internalized β1 integrins pulled down with 12G10 ITGβ1 antibody.

Results demonstrated that although the total cell surface biotinylated β1 integrins were clearly detectable by this method (Figure 4.32 first lane), the integrin internalization was not detectable under these conditions (Figure 4.32 second lane), suggesting that the need for further optimization.

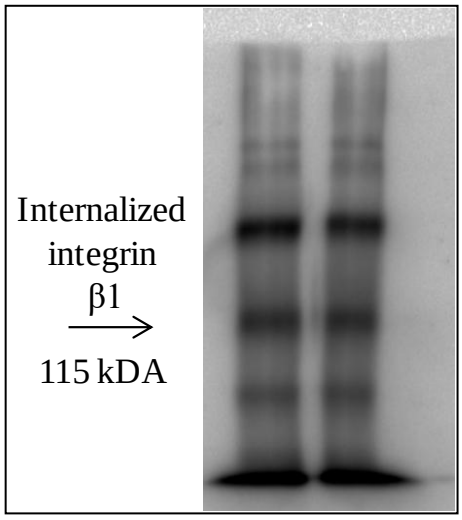

Figure 4.33. Biotin-based IP method optimization to detect internalized active β1 integrins of Caki-1 Wt cells. Total integrins samples were not subjected to either MesNa or IAA. Internalized β1 integrins detected with IP method. First line showed the β1 integrins pulled down with 12G10 ITGβ1 antibody and second line demonstrated the β1 integrins pulled down with rabbit polyclonal β1 integrin antibody.

In order to visualize the internalized β1integrins a few changes were made in the conditions of internalization, IP and Western Blot protocol. Since TG2 in complex with FN was shown to induce cell adhesion and integrin activation in various cell lines [113], FN was used instead of BSA to induce the internalization at 10μg/ml for 2 hours. Following the labeling of cells surface proteins using NHS-SS as described in Section 3.7.1. β1 integrins were allowed to be internalized for 2 hours using soluble FN as described above then to solubilize integral membranes of the organelles particularly the endosomes, a new IP buffer, which was described in Section 3.7.1, was introduced and used in cell lysis. Following the collection of cell lysates, samples were frozen in liquid nitrogen and thawed back in water bath at 37°C for 5 minutes in thrice, then the cell slurry was homogenized using a pestle homogenizer which was applied to each sample for 1 minute in ice-cold conditions. Proteins were precleared by centrifugation and protein quantity was measured using Lowry assay for equal protein loading (Section 3.3.2). 100-120 μg proteins were used for each sample during the experiment. Incubation of cell lysates with 12G10 antibody was increased to 20 hours as described in Section 3.7.2. After the collection of antibody-bound proteins by protein agarose G beads for 4 hours at 4°C, beads were mixed

with 2 x non-reducing Laemmli sample buffer which did not contain any β-mercaptoethanol. Western Blot was performed according to the protocol in Section 3.3.4 and 3.4 (Figure 4.32). Following the membrane development, bands were visualized at ~115kDA which is the molecular weight of non-reduced β1 integrins. As clearly seen in Figure 31B, using the new method, internalized β1 integrins could be detected. Besides, when compared to β1 integrins precipitated by rabbit β1 integrin antibody, active ITGβ1 antibody showed 23 per cent more sensitivity.

Once the IP method was optimized to visualize internalized β1 integrins the next question is whether soluble FN or FBS is an optimal inducer to detect a TG2 induced ITGβ1 internalization. For this purpose, Caki-1 Scr, shTG2 and TG2 o/e cells were treated with 10µg/ml of soluble FN or 10 per cent (v/v) FBS containing media to induce ITGβ1 internalization for 2 hours at 37°C. Following the incubation cells were collected as described in Section 3.7.1 and IP was performed using 140µg proteins (Section 3.7.4).

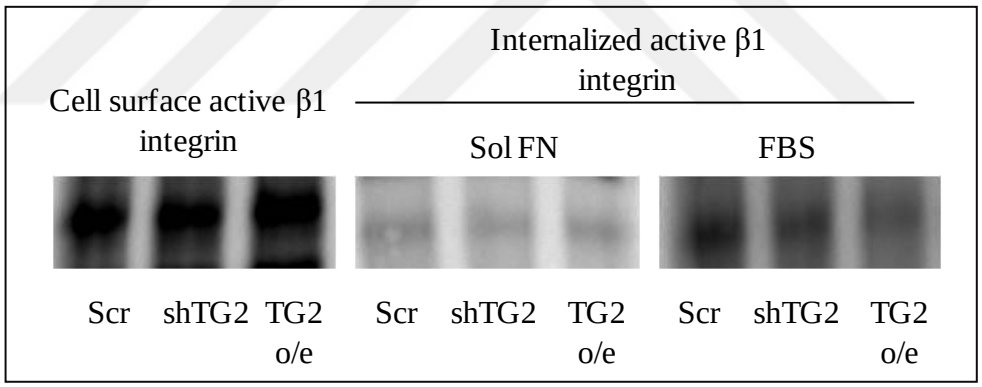

Figure 4.34. Biotin based IP experiment results of internalized ITGβ1 using Sol FN and FBS in Caki-1 Scr, shTG2 and TG2 o/e cells

Analysis showed that no significant difference by means of β1 integrin internalization, was detected between Scr, shTG2 and TG2 o/e cells following the treatment with soluble fibronectin. Internalization rates were analyzed by dividing the samples to that of cell surface β1 integrins and revealed a respective 12, 10 and 7 per cent integrin internalization for Scr shTG2 and TG2 o/e. On the other hand, use of FBS treatment as inducer led to a 67 per cent of ITGβ1 internalization in Caki-1 Scr control cells. The integrin internalization level for shTG2 and TG2 o/e cells was detected as 39 and 29 per cent, respectively. Results

suggested that the downregulation of TG2 by shRNA led to at least a 30 per cent decrease in ITGβ1 internalization rate; however, an unexpected 38 per cent decrease was analyzed in internalization rate for TG2 o/e cells (Figure 4.34).TG2 o/e cells might have increased rate of recycling hence undergone a second round of integrin internalization.

Following the optimization of acid rinse treatment and integrin internalization conditions, recycling experiment were performed to detect if seeding cells on a immobilized FN matrix led to a change in the ITGβ1 recycling rate. In Figure 35, Caki-1 cells Wt and shTG2 were seeded on 5μg/ml FN coated plates and ITGβ1 integrin internalization was induced using 10 per cent (v/v) FBS for 30 mins. Following the internalization remaining antibody on cell surface was stripped of using 0.1M Glycine, 0.5M NaCl containing acid rinse solution pH 3.0, then recycling was performed by using 10 per cent (v/v) FBS for 120 mins. As can be seen from the Figure 4.35, FN matrix did not induce a sufficient integrin recycling rate as the percentages for ITGβ1 recycling was detected as only ~3 and 13% more than the negative control for Wt and shTG2 Caki-1 cells.

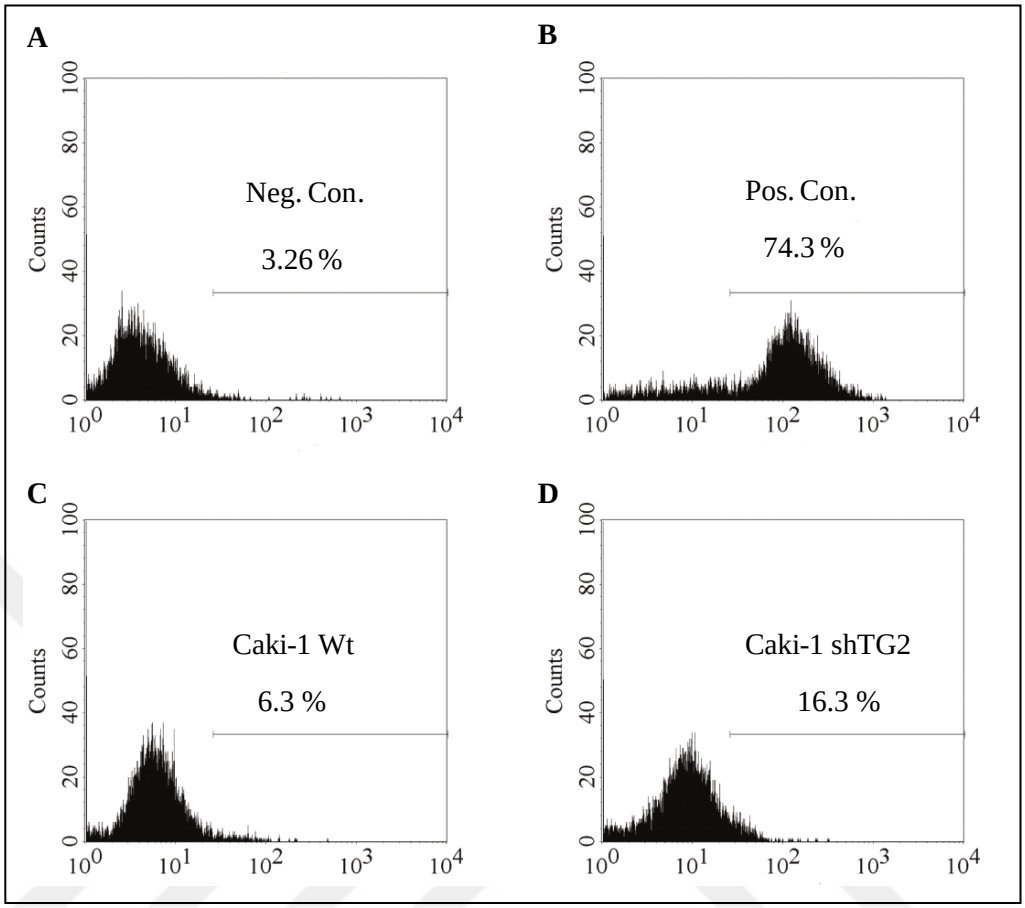

Figure 4.35. Flow Cytometry results of Caki-1 integrin β1 recycling on immobilized FN coated plates. (**A**) Negative Control (Neg.Cnt) Caki-1 cells labeled with mouse IgG isotype control (**B**) Caki-1 wt cells labeled with 12G10 followed Alexa-488 secondary antibody without acetic rinse (**C**) Caki-1 Wt and shTG2 cells (**D**) in which ITGβ1 internalization was induced using 10 per cent (v/v) FBS for 30 mins and recycling was stimulated using 10 per cent (v/v) FBS for 120 mins after the acid rinse treatment

In order to detect if the use of soluble FN rather than immobilized FN was more sufficient to induce integrin recycling, soluble FN was introduced following the FBS internalization for 30 mins as described in Section 3.7.4. The incubation of Caki-1 wt cells with soluble FN led to 51.78 per cent of integrin recycling, a rate which was acceptable when compared to integrin β1 internalization by PDGF which was resulted as~50 per cent [254]. A significant 24 per cent difference was detected between wild type and shTG2 cells following the 120 mins recycling of β1 integrins using 10μg/ml soluble FN (Figure 36).

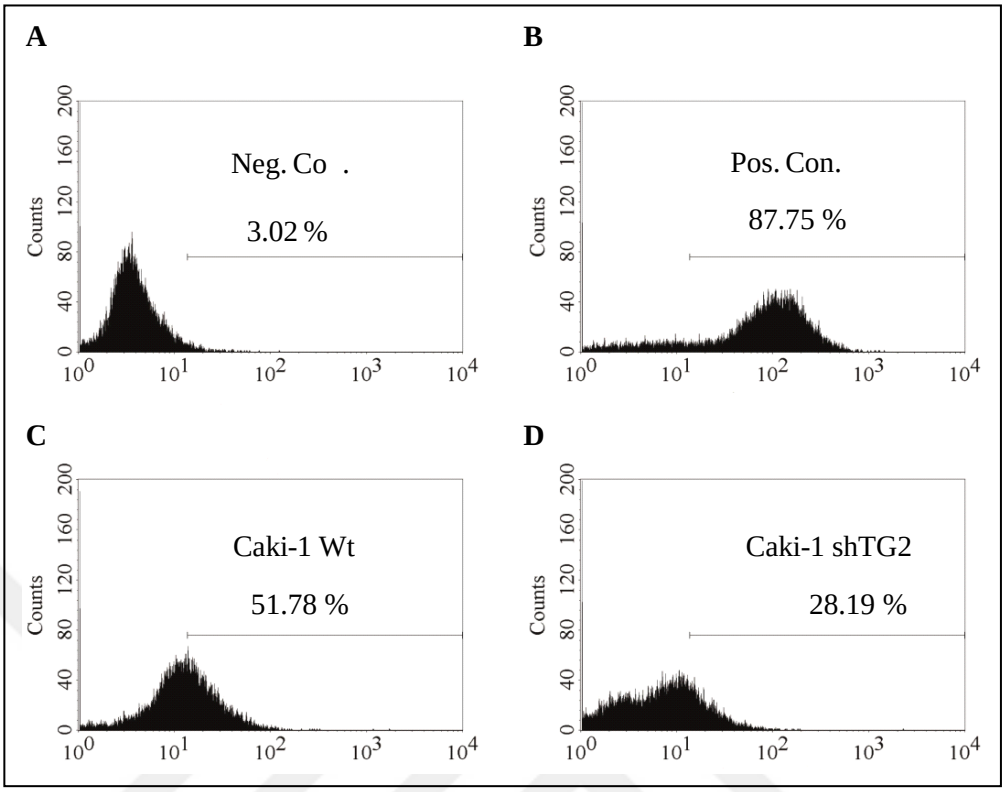

Figure 4.36. Flow Cytometry results of Caki-1 integrin β1 recycling using soluble FN (**A**) Negative Control (Neg.Cnt) Caki-1 cells labeled with mouse IgG isotype control (**B**) Caki-1 Wt cells labeled with 12G10 followed by Alexa-488 secondary antibody without acid rinse (**C**) Caki-1 Wt and shTG2 cells (**D**) in which ITGβ1 internalization was induced using 10 per cent (v/v) FBS for 30 mins and recycling was stimulated using 10 μg/ml soluble FN for 120 mins

4.7. β1 INTEGRIN TRAFFICKING IN RCC CELL LINES

Although in the Section 4.6, 10 per cent (v/v) FBS was determined as the internalization inducer for further experiments, the internalization time point was still required an optimization. For this purpose, four RCC cell lines were subjected to 10 per cent (v/v) FBS treatment for 30, 60, 90 and 120 mins and cell surface proteins were then labeled as described in Section 3.7.1 followed by IP was performed using 100-120μg proteins. The relative amount of biotin labeled internalized integrins was normalized against total cell surface β1 integrins.

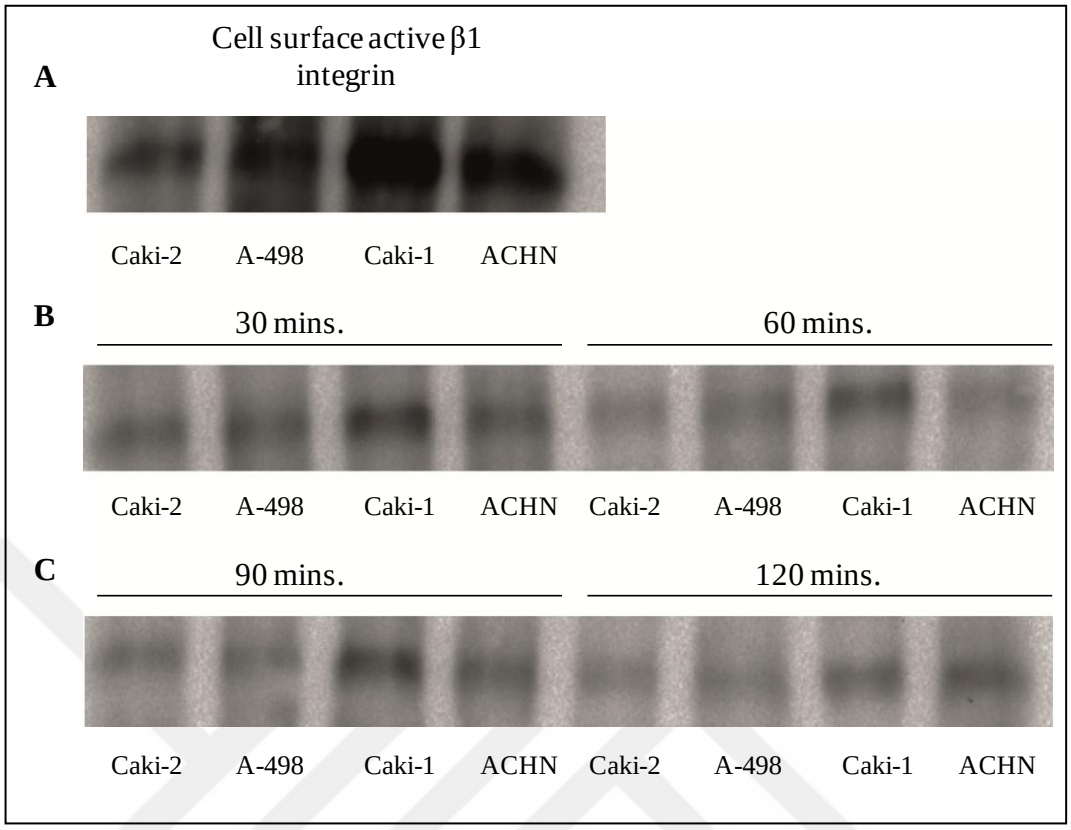

Figure 4.37. Detection of Integrin β1 internalization at 30, 60, 90 and 120 mins using 10per cent (v/v) FBS on RCC cell lines. (**A**) Total biotinylated cell surface ß1 integrin levels of RCC cells. (**B)** Internalized ß1 integrin levels of RCC cells following 30 and 60 minutes, (**C)** Internalized ß1 integrin levels of RCC cells following 90 and 120 minutes.

Following the internalization using 10 per cent (v/v) FBS, a primary site Caki-2 cells displayed a constant rate of internalization at each time point which was detected as 19, 19.6, 18.1 and 15 per cent for 30, 60, 90 and 120 mins, respectively. Another primary site cell A-498 cells showed an elevated level of ITGβ1 integrin internalization compared to Caki-2 cells which was evaluated as 29 per cent for 30 mins, 35.6 per cent for 60 mins, 28 per cent for 90 mins and 22.3 per cent for 120 mins (Figure 36 B). After 60 mins incubation with FBS, ITGβ1 internalization rates were declined gradually in each cell line (Figure 36 B, C and Figure 37). In metastatic site cells, Caki-1 displayed a higher integrin β1 internalization compared to other RCC cell lines such that 36.6 per cent internalization rate was detected for Caki-1 cells at 30 mins while a 37, 36.5 and 24.03 per cent internalization was evident at 60, 90 and 120 mins respectively. In contrast to Caki-1 cells, the other metastatic cell line ACHN cells displayed lower β1 integrin internalization rates

as 27 per cent internalization was detected for 30 mins, which was decreased to an average of 16 per cent at 60, 90 and 120 (Figure 36C and 37).

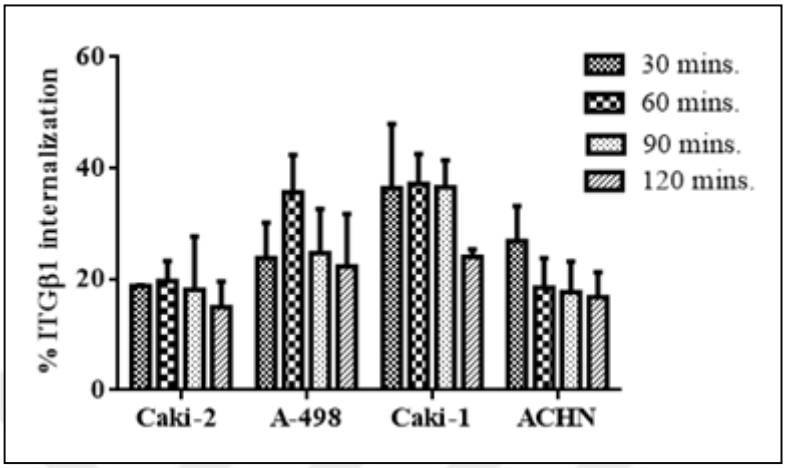

Figure 4.38. Analysis of β1 integrin internalization rates of Caki-2, A-498, Caki-1, and ACHN cell lines. The relative amount of biotin labeled internalized integrins were normalized against total cell surface β1 integrins.

A statistically significant difference in the endocytosis rate for active β1 integrin was only detected for A-498 at the 60 min-time points, while other RCC cells displayed a similar rate of β1 integrin internalization at the determined time points. Therefore, in order to compare the recycling potential of all four RCC cell lines, 30 mins time point was determined as ITGβ1 internalization time period (Figure 4.36). ITGβ1 recycling potential of four RCC cell lines were compared to each other in order to demonstrate integrin trafficking potential of the cell lines. Recycling experiments were performed using 10μg/ml soluble fibronectin as described in Section 3.7.2. Since each cell line possess different levels of cell surface integrin ß1, the percentage of ITGβ1 found for the 12G10 labeled cells without acid rinse was considered as 100 per cent and the per cent of recycled integrin was determined by normalization using Quandard statistics. Experiments were conducted at least three times and statistical analyses were performed using GraphPad program (Section 3.9).

Results depicted form Figure 4.39 showed that primary site RCC cell lines were demonstrated a very low ITGβ1 recycling potential which was evaluated as 6.3 per cent for Caki-2 cells and 3.1 per cent in A-498 cells. In contrast to primary site cells, metastatic RCC cells demonstrated a significantly higher ITGβ1 recycling which then was calculated as 46.1 per cent for Caki-1 cells and 32 per cent for ACHN cells (Figure 40).

It was obviously seen that Caki-1 cells have the highest potential for the internalization and recycling of ß1 integrins. β1 integrin internalization rate was detected as 36.4 per cent for Caki-1 Wt cells while 46.15 per cent ITGβ1 recycling was detected in Caki-1 Wt cells which indicates that nearly 100 per cent of the internalized ITGβ1 was recycled by Caki-1 cells. Therefore, the possible collaborative role of SDC4 with TG2 on ITGβ1 turn-over was investigated using Caki-1 cells as a model.

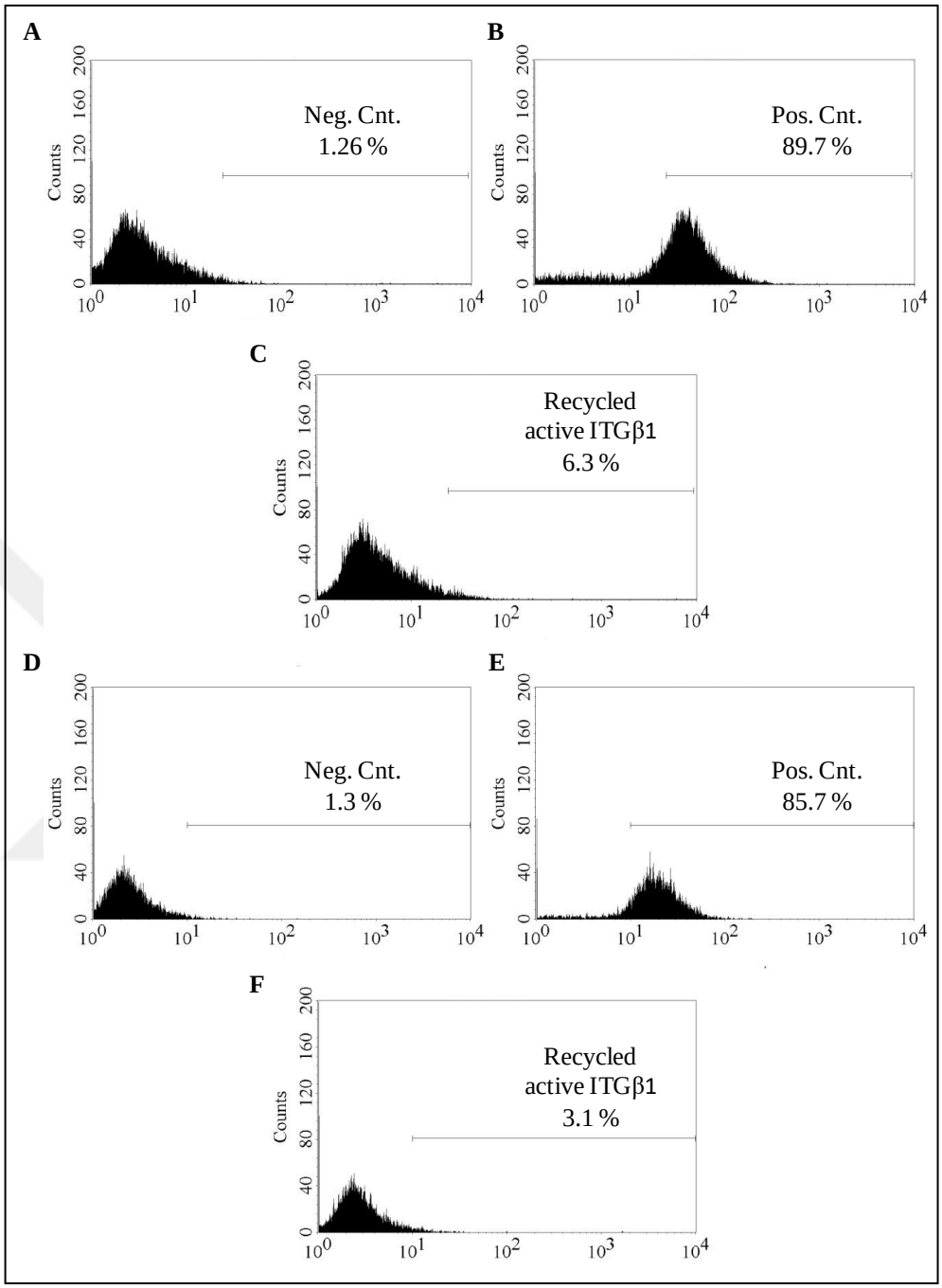

Figure 4.39. Detection of active ITβ1recycling in Caki-2 (**A-C**) and A-498 (**D-F**). Negative Control (Neg. Cnt) Caki-2 (**A**) and A-498 cells (**D**) labeled with mouse IgG isotype control respectively. Caki-2 (**B**) and A-498 cells (**E**) labeled with 12G10 followed by Alexa-488 secondary antibody without acid rinse. Recycled active ITGβ1 detected after acid rinse for Caki-2 (**C**) and A-498 (**F**) cells.

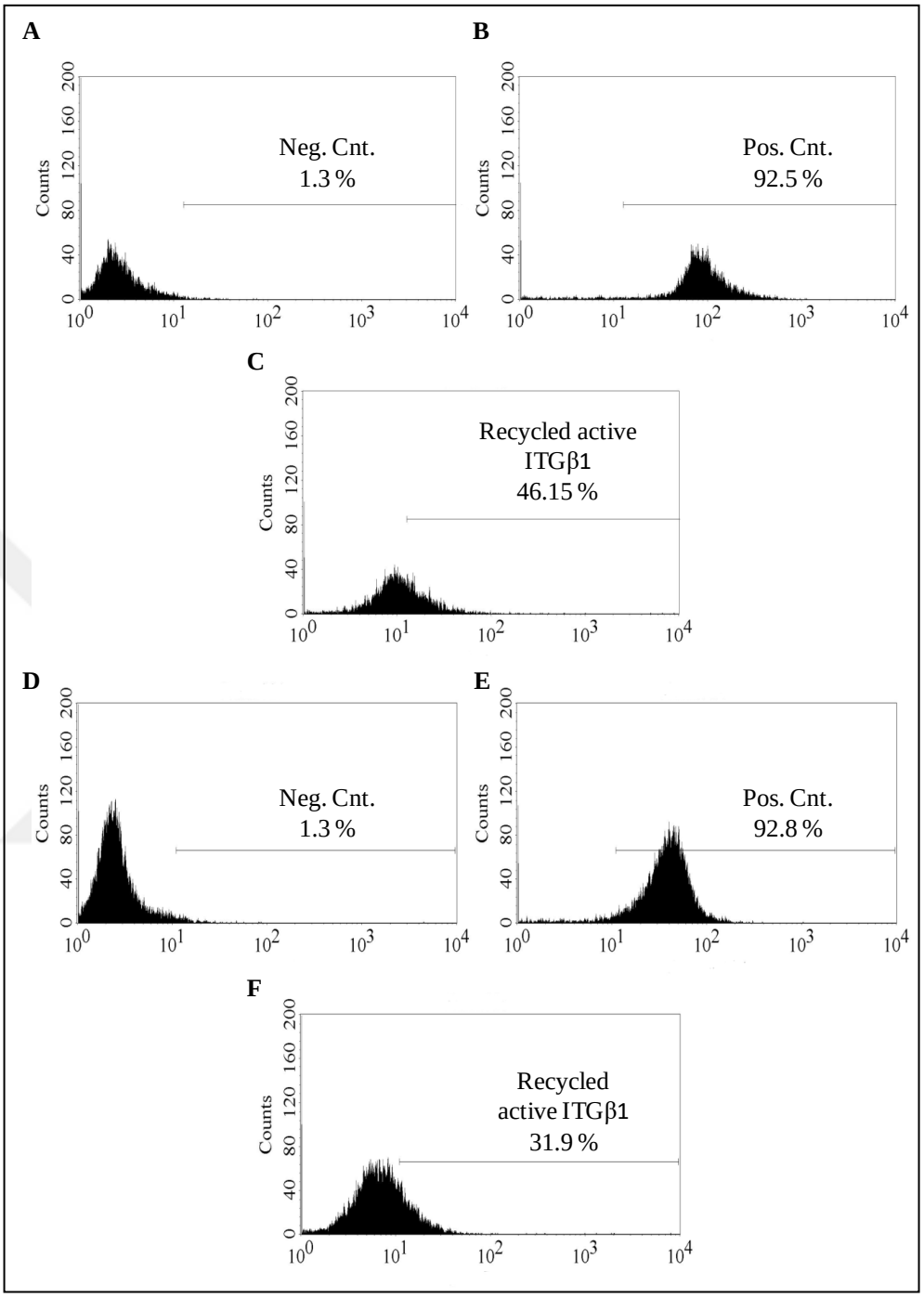

Figure 4.40. Detection of active ITβ1recycling in Caki-1 (**A**-**C**) and ACHN (**D**-**F**). Negative Control (Neg. Cnt) Caki-1 (**A**) and ACHN cells (**D**) labeled with mouse IgG isotype control respectively. Caki-1 (**B**) and ACHN cells (**E**) labeled with 12G10 followed by Alexa-488 secondary antibody without acetic rinse. Recycled active ITGβ1 detected after acid rinse for Caki-1 (**C**) and ACHN (**F**) cells.

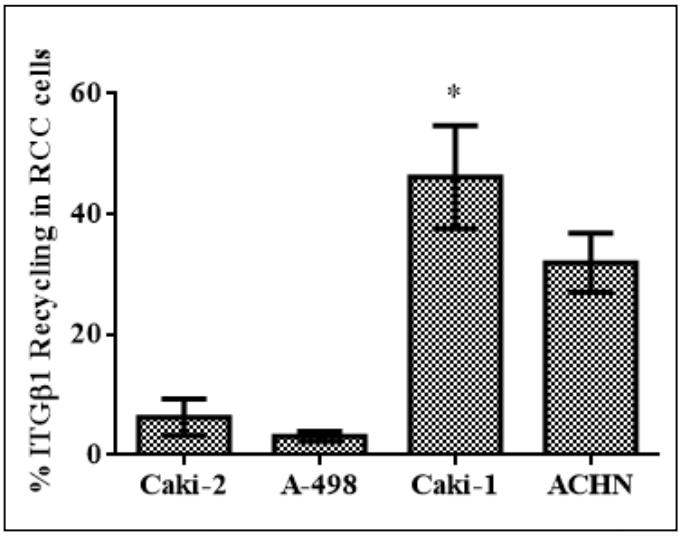

Figure 4.41. Analysis of ITGβ1 recycling of RCC cells using Flow Cytometry, * p< 0.05.

Recycling experiments were performed using 10µg/ml soluble fibronectin as described in Section 3.7.2. Owing to different cell surface integrin ß1 levels in each cell line, recycled integrins were determined by normalizing to that of cell surface integrins using Quandard statistics. Experiments were conducted at least three times and statistical analyses were performed using GraphPad program (Section 3.9). Results depicted form Figure 4.39 showed that primary site cell lines were demonstrated a very low ITGβ1 recycling potential which was evaluated as 6.3 per cent for Caki-2 cells and 3.1 per cent in A-498 cells. In contrast to primary site cells, metastatic cells demonstrated a significantly higher ITGβ1 recycling which then calculated as 46.1 per cent for Caki-1 cells and 32 per cent for ACHN cells.

It was obviously seen that Caki-1 cells have the highest potential during internalization and recycling of ß1 integrins. β1 integrin internalization rate was detected as 36.4 per cent for Caki-1 Wt cells whereas 46.15 per cent ITGβ1 recycling was detected in Caki-1 Wt cells which clearly showed that Caki-1 cells actively using the active integrin trafficking potential as a metastatic cell line. Therefore, progress of my experiments will be handled using Caki-1 cells to enlighten the importance of SDC4 in TG2 induced integrin ß1 internalization and recycling.

4.7.1 The effect of TG2 on β1 integrin internalization and recycling in Caki-1 cells

Internalization and recycling experiments in Caki-1 Scr, shTG2 and TG2 o/e cells were performed as described in Section 3.7.2 and 3.7.3. Cells were seeded on 6-well plate and serum starved using 0.01 per cent BSA (w/v) for 16 hours. Following the starvation, cell surface β1 integrins were labeled using NHS-SS biotin and then the labeled cell surface integrins were induced to be internalized using 10 per cent (v/v) FBS for 10, 20 and 30 mins.

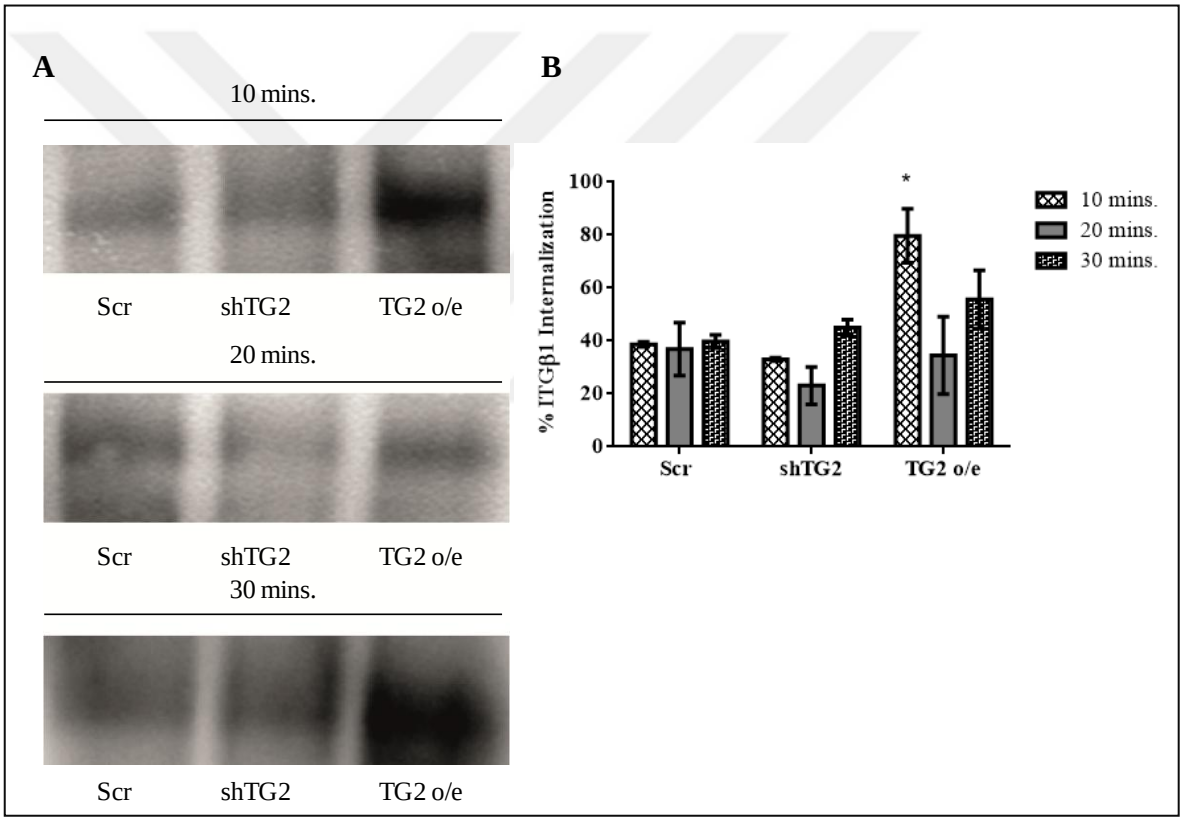

Figure 4.42. Biotin-based pull down of internalized active β1 integrins in Caki-1 cells. Western Blot images of biotin-based pull down of internalized active β1 integrins in Caki-1 cells (**A**). Density blot analysis of Western Blot images(**B**) .

Real time and Western Blot analysis (Figure 21A, B) showed no significant difference between Wt and Scr control by means of TG2 protein and mRNA expression, therefore: Caki-1 Scr cell was used as a control in order to investigate the integrin β1 internalization and recycling potential in Caki-1 clones, shTG2 and TG2 o/e.

A notable difference in the levels of internalized ITGβ1 was detected in Caki-1shTG2 and TG2 o/e cell lines in indicated the early time points of 10, 20 and 30 minutes when compared to that of Scr control. In 10 minutes, there is a slight difference in the β1 internalization rates of Scr control and shTG2 cells since they were calculated as 39.3 and 32.9, respectively, while TG2 o/e cells displayed a significant 33 per cent increase in the levels of ITGβ1 internalization when compared to Scr control cells. Further 10 minutes incubation showed a 10 per cent delay in β1 integrin internalization of shTG2 cells when compare to Scr cells (Figure 4.42A). Although at 10 mins, 79 per cent of β1 integrins were internalized in TG2 o/e cells, in 20 minutes only 45 per cent internalization was recorded for TG2 o/e cells compared to Scr suggesting that in TG2 o/e cell lines after 10 minutes the internalized integrins may be directed to membrane recycling (Figure 4.42A). In 30 minutes, integrin β1 internalization rates in Scr control cells was detected as 40 per cent whereas and shTG2 ITGβ1 internalization rates were evaluated as 45 and finally TG2 o/e cells showed a 55.6 per cent ITGβ1 internalization. (Figure 4.42A). Taken together, at the 20 mins and 30 mins, no evidence of significant difference in the internalization rates was detected between Scr, shTG2 and TG2 o/e cells due to possibly due to rapid start of integrin recycling after 10 minutes. This hypothesis also explain the unexpected decrease detected in ITGβ1 recycling for TG2 o/e cells (Figure 4.30) as it was seen from the internalization experiment (Figure 4.41A, 41B) TG2 o/e cells were able to internalize ITGβ1 faster than Scr, shTG2 cells therefore TG2 o/e cells might have recycled ITGβ1 rapidly compared to Scr and shTG2 cells. In the light of this new data, it was decided that the time point set for the recycling assay should be pull forward from 120 mins to 90 mins in order to detect the difference between Scr, shTG2 and TG2 o/e Caki-1 cells.

Following the 20 mins internalization using 10 per cent (v/v) FBS, recycling of ITGβ1 was stimulated using McCoy's 5A containing 10µg/ml soluble fibronectin for 90 mins (Figure 4.43). Results obtained from the experiment showed that in comparison to Scr Caki-1 cells a notable 10 per cent decrease in the level of recycled β1 integrins was detected in shTG2 cells, while a remarkable 16 per cent increase in integrin recycling was evident for Caki-1 TG2 o/e (Figure 4.43). Moreover a significant 24 per cent difference of recycled ITGβ1 was recorded between the shTG2 and TG2 o/e Caki-1 cells (Figure 43, 44).

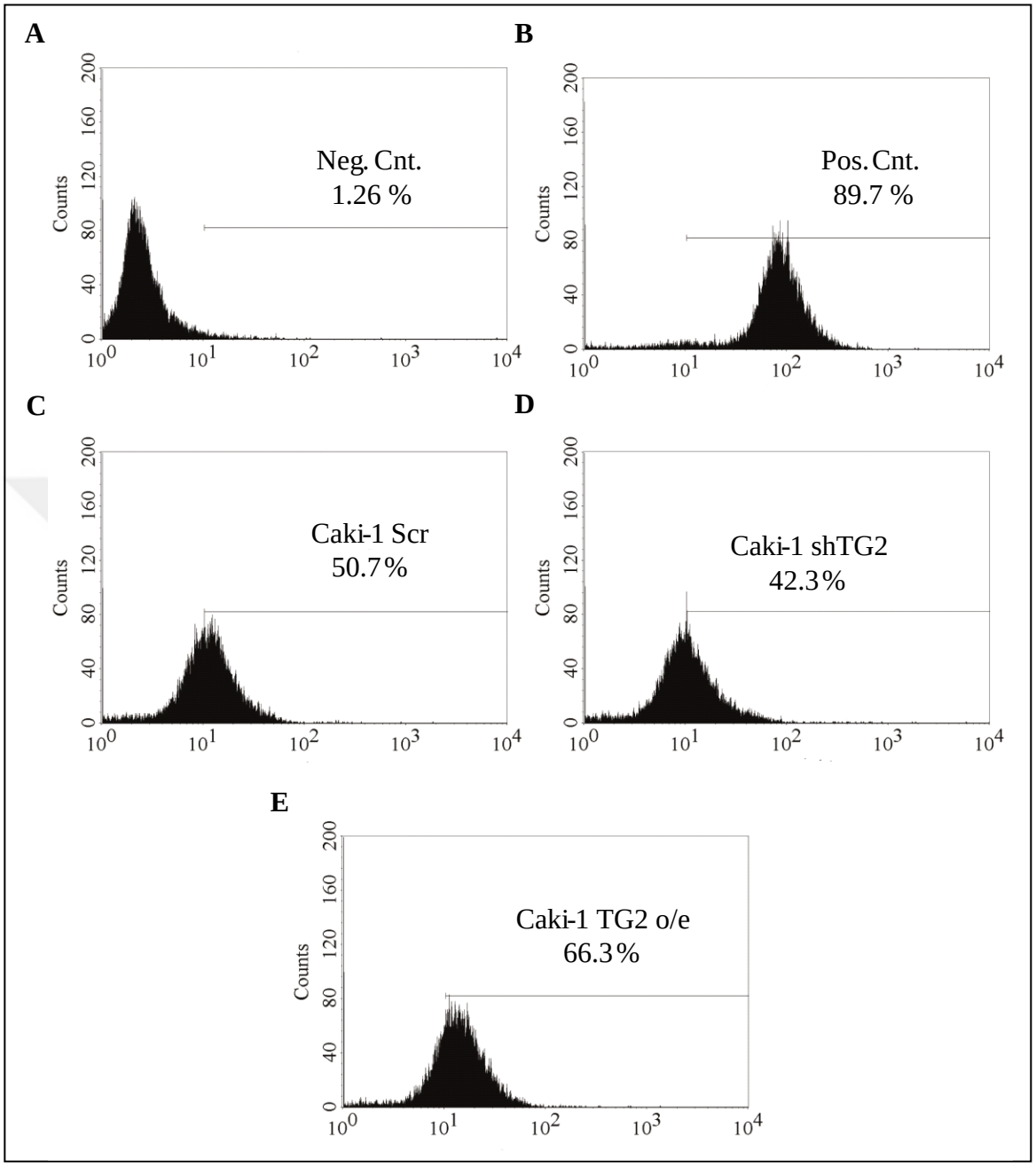

Figure 4.43. Detection of active ITβ1 recycling in metastatic site Caki-1 Scr, shTG2 and TG2 o/e cells. (**A**) Negative Control (Neg. Cnt) Caki-1 Scr cells labeled with mouse IgG isotype control (**B**) labeled with 12G10 followed by Alexa-488 secondary antibody without acid rinse (**C-D**) Recycled active ITGβ1 of Caki-1 Scr, shTG2 and TG2 o/e cells after acid rinse.

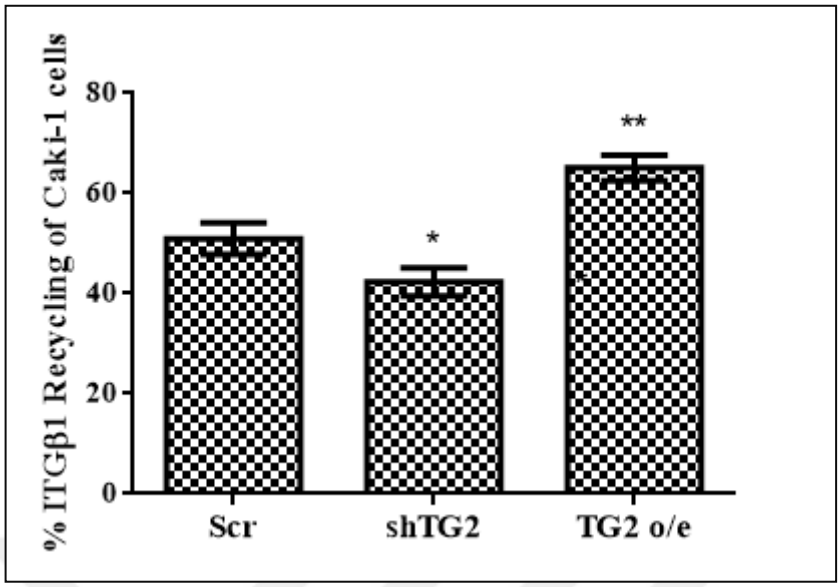

Figure 4.44. Flow cytometry analysis of active β1 integrin recycling in Caki-1 Scr, TG2 shTG2 and TG2 o/e cells using GraphPad program. Results were analyzed using ANOVA and confirmed by Tukey statistical analysis. * $p < 0.05$.

4.7.2 Detection of active β1 integrin internalization in SDC4 silenced (shSDC4) and SDC4 silenced TG2 overexpressed Caki-1 cells (shSDC4 TG2 o/e)

Previous reports showed that synergetic control of cell adhesion was maintained by SDC4 and ITGβ1 [53]. In addition to that, Telci *et al* demonstrated that TG-FN complex facilitated the adhesion and survival mechanism through activating integrins via SDC4 [113]. In the light of these evidences, SDC4 was stably silenced in TG2 o/e and Wt Caki-1 cells using shRNA technology in order to elucidate the role of SDC4 in TG2-dependent and independent internalization of β1 integrins. The previous internalization experiments showed that, only at the early time point of 10 mins a statistically significant difference between in internalized ITGβ1 levels were detected among Scr, shTG2 and TG2 o/e cells. Given that, in order to detect the importance of TG2 in SDC4 driven integrin β1 internalization, early time point of 10 mins was used during the ITGβ1 internalization.

In agreement with the previous experiment (Figure 42), TG2 o/e cells showed about 30 per cent increase in β1 integrin internalization when compared to Scr control cells at the early time point of 10 mins. A drastically 65 per cent decrease was detected in the ITGβ1

internalization of shSDC4 when compare to Wt, which showed the importance of SDC4 during integrin β1 internalization. A significant 79 per cent different was detected between shSDC4 and TG2 o/e cells in the ITGβ1 internalization while the difference between shSDC4 and shSDC4 TG2 o/e cells was recorded as 36 per cent by means of ITGβ1 internalization. These results clearly demonstrated that TG2 is the novel partner of SDC4 during integrin β1 internalization (Figure 45).

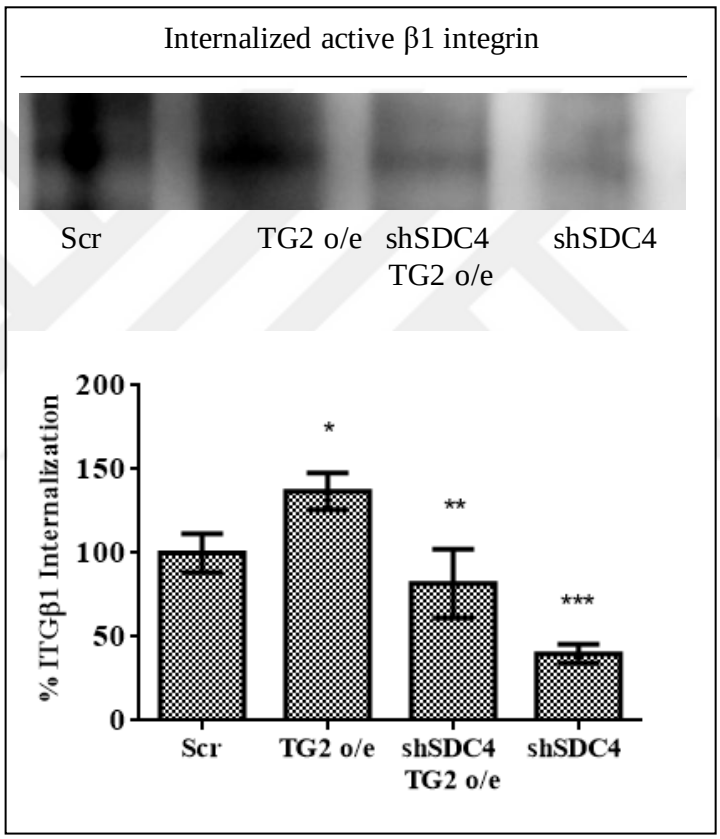

Figure 4.45. Detection of integrin β1 internalization using biotin-based IP method, in Caki-1 Scr, shTG2, TG2 o/e, shSDC4 TG2 o/e and shSDC4 cells. * $p < 0.05$.

5. DISCUSSION

cRCC, renal cortical tumor, is the most lethal urological cancer which is populated by tumorigenic epithelial cells. Since cRCC leads to a high mortality rate, which account 102.000 death per year, many different targeted therapies has been under investigation for a successful treatment [241].

ECM regulates the cellular adhesion and migration by controlling the signaling pathways, which determines whether a cell survives or undergoes into apoptosis. ECM leads to the transmission of the signals from extracellular environment to intracellular compartments though cell surface integral transmembrane proteins called integrins [10]. Although integrins do not have an intrinsic kinase activity, they are able to convey extra/intracellular stimuli by binding to adaptor proteins which pivot integrins to the cytoskeleton, cytosolic kinases and cell surface growth factor receptors [25]. Together with ECM, integrin-mediated cell adhesions regulate the disassembly and assembly of adhesions which takes role in the control of cell speed and directional persistence. There are 24 integrin heterodimers, which are able to recognize several ECM substrates. Once integrin associates with ECM, integrins become clustered at the cell membrane and facilitate actin filament assembly. Actin filaments reorganize into large stress fibers, which increases the integrin clustering on the cell membrane in order to increase cell-ECM binding [25]. When cells become cancerous they modulate their affinity and avidity against their ECM through phenotypic alterations that are primarily triggered by the changes in the integrin expression which is followed by the ECM remodeling and deposition of new ECM components. In response to these changes, signaling cascades are activated in order to regulate the cell adhesion and survival. As a result cancer cells become metastatic by increasing their invasion and migratory potential. Since elevated expression levels of integrins have been documented in many solid tumors such as, breast cancer, colon, prostate, ovarian, cervical, the increased expression of α5β1 integrin in melanoma and non-small lung cancer was found to in negative correlation with the patient survival [75]. In addition, the study on the integrin distribution in RCC showed that β1 integrin was found to be ubiquitously expressed in the tumor and stromal cells of RCC. On the basis of these findings, monoclonal antibodies has been developed against α5β1 integrins to be used as adjuvant therapy to treat advanced solid tumors, yet clinical trials showed minor responses against

patients with RCC and melanoma [101]. A recent study by Erdem *et al.* 2014 showed that together with ITGβ1 and SDC4, TG2 can be a prognostic marker for ccRCC due to its high level expression in the primary site tumor samples that has demonstrated metastatic properties [196]. When TG transamidating activity was investigated in randomly selected tumor and healthy kidney tissues, a lower TG activity was found in tumor tissues suggesting that function of TG2 can be interchangeable depending on the cells type and TG2 localization. Additionally, in this work primary site cell lines Caki-2 and A-498 demonstrated a higher TG2 transamidating activity when compared to the metastatic cells lines, albeit no statistical difference was detected among Caki-2, A-498, Caki-1 cells by means of *TGM2* mRNA expression except for ACHN cells which displayed a higher *TGM2* mRNA expression levels. Interestingly, results from this thesis showed that TG2 protein levels were lower in the metastatic site RCC cells Caki-1 and ACHN when compared to the primary site cells Caki-2 and A-498. The observed discrepancy between the TG2 mRNA and protein levels suggests that the TG2 protein somehow is exported out of the cell when it is translated. In support of this hypothesis, the 3.89 fold increase in *TGM2* mRNA levels in TG2 o/e cells translated to only 2.25 fold increase in the TG2 protein level. Although the exact mechanism for the externalization of TG2 is yet a recent study reported that TG2 together with FN could be packaged in cancer-derived microvesicles (MVs) and released from the cancer cells [227].

When the ITGβ1 and SDC4 protein levels were compared with the results from Erdem *et al.* 2014 Caki-1 cells similarly found to display higher ITGβ1 levels when compare to Caki-2, A-498 and ACHN cells. However, the same trend observed for TGM2 mRNA was also observed for SDC4 mRNA and protein levels suggesting that SDC4 might also be included in MLVs together with TG2 in the Caki-1 and ACHN. Given the strong interaction of TG2 with SDC4 [251] heparin sulphate chains and the fact that SDC4 is one of the proteins of exosomes released by MCF7 cells [172], it is quite possible that SDC4 is loaded together with TG2 into the exosomes.

Data from different research groups emphasized that TG2-SDC4 association is based on the interaction between TG2 and SDC4 heparan sulphate proteoglycan chains (HSPGs) on the cell surface, which was important not only in the regulation of cell adhesion and migration [113,220] but also that of cell survival. In order to show the TG2 association with ITGβ1 and SDC4 in RCC cell lines, co-IP experiments were performed. Although

Caki-1 cells expressed lower TG2 and SDC4 protein levels, among Caki-2, A-498 and ACHN cells, the highest interaction between TG2-ITGβ1 and TG2-SDC4 was demonstrated in Caki-1 cells. Akimov *et al*. 2001 showed that cell surface TG2 interacts with ITGβ1 and β3 through with 42 kDA gelatin binding domain of FN, which did not require integrin binding sites and this interaction regulated the integrin signaling [215]. Besides, Telci *et al*. 2008 demonstrated that TG2 in complex with the ITGβ1 integrin substrate FN was able to enhance cell adhesion and survival through SDC4 and/or ITGβ1 in a RGD independent manner [113]. Therefore, in this thesis in order to demonstrate the importance of TG2-ITGβ1 association in RCC cell adhesion TG2 silenced RCC cells were seeded on β1 integrin matrices; fibronectin (FN), collagen1 (Col1) and laminin (LM). Briefly, TG2 downregulation was achieved in Caki-2, ACHN and Caki-1 cells ~90 per cent whereas A-498 cells showed an average of 46 per cent decrease in *TGM2* mRNA levels. Telci *et al*. 2008 showed that no significant difference in ITGβ1 and β3 mRNA expression levels of SDC4 k/o MEF cells when compared to wild type MEF cells. In agreement with the study, qPCR analysis showed that *TGM2* gene silencing displayed no evidence of statistical difference in the mRNA expression levels of TG2 partners; SDC4 and ITGβ1 in RCC cell lines.

The importance of TG2 in cancer cell adhesion has been shown by different groups using various cancer models. For example, Malaga *et al*. 2007 demonstrated the role of TG2 in cell adhesion using a drug resistant MCF-7 cells where the attachment of TG2 expressing MCF-7 cells on FN brought about an acquired apoptotic resistance while the silencing of TG2 with siRNA impaired the cell attachment and survival of MCF-7 cells [263]. Another study performed by Satpathty *et al*. 2007 [189] showed that TG2 knockdown led to a decrease in the dissemination of the tumors in ovarian xenograft model, which was associated with the loss of β1 integrin-FN interaction while high expression of TG2 in ovarian tumors provide tumor dissemination by elevating the cell-ECM interactions due to increased β1 integrin and FN association. In the light of these data, the cell adhesion experiments performed in this thesis showed that among four NS treated RCC cell lines, Caki-1 cells showed the highest attachment and spreading potential on FN. Ku *et al* 2014 [247] showed that TG2 silencing led to apoptosis of 786-O, A-498, Caki-1, and ACHN cells however the silencing efficiency was not mentioned in this paper. In contrast to *Ku et al*. 2014 [247], *TGM2* silencing resulted in a significant decrease of RCC cell attachment

and spreading on β1 integrin substrates without any detectable decrease in the cell survival. Interestingly, the treatment with siRs did not lead to a significant decrease in the cell spreading of A-498 and ACHN cells on LM at the indicated early time point. It is not surprising that among the four RCC cell lines Caki-1 was the one whose adhesion on β1 integrin substrates was most drastically hampered by the TG2 downregulation since Caki-1 cells showed the highest interaction between TG2-ITGβ1 and TG2-SDC4.

In order to demonstrate the role of TG2 in β1 integrin trafficking, *TGM2* expression in Caki-1 Wt cells were stably silenced and overexpressed using lentiviral particles. TG2 silencing did not lead to a significant difference in ITGβ1 and SDC4 mRNA expression levels. Accumulating evidences showed that the changes in the adhesion traits of neoplastic cells lead to increase in the invasiveness and migration capability. The alterations in the expression and function of integrins are involved in each step of tumor development such as the dissociation of tumor cells from primary site, invasion through the surrounding basement membrane, penetration into bloodstream, spreading through circulation, extravasion into the parenchyma of distant organs and the formation of new metastatic colonies [109,264,265]. During the organization of cell polarity, adhesion, migration and regulation of related signaling pathways, these mechanisms progress in harmony under the control of integrin endocytosis and recycling pathways. Elevated expressions of certain integrin levels leads to the deregulation of endocytosis and recycling pathways consequently leading to the formation of aggressive, invasive, motile cancer cell formation. Among 24 integrin heterodimers, α5β1, α6β4, αvβ3, and αvβ6 have been associated with the cancer progression, except for α6β4, α5β1, αvβ3 and αvβ6 which recognizes the RGD sequences and function as a fibronectin receptor [112]. Among from α6β4, αvβ3 and αvβ6 integrins, a fibronectin receptor α5β1 facilitates the cancer invasion, metastasis, anti-cancer drug resistance and associated with decreased survival in patients [266].

In the light of these evidences, detection of β1 integrin internalization and recycling assays were optimized in order to demonstrate the role of TG2 in ITGβ1 trafficking. Jovic *et al*. 2006 [255] demonstrated the importance of C-terminal Eps15-homology (EH) domain-containing protein called EHD1 in β1 integrin trafficking using HeLa cells [255]. In contrast to the results observed by Jovic *et al*. 2006, using the same methodology efficient β1 recycling was not observed in Caki-1 Wt, Scr, shTG2 and TG2 o/e cells due to two

different problems in the conditions of internalization and antibody stripping suggesting for the further optimization of these parameters. Therefore conditions used by Liu 2007 *et al*. and Cera 2009 *et al*. were applied in our experimental model of Caki-1 cells [259]. In agreement with Lui *et al*. 2007, 0.1M glycine, 0.5M NaCl pH 3.0 was efficient in the rinsing off non-internalized ITGβ1 labeled β1 integrins on the cell surface [260]. Akimov *et al*. 2001 showed the role of TG2 in the migration of monocytic cells on FN using AIM-V medium also Balklava *et al*. 2002 used AIM-V medium in order to analyze the secreted TG2 into the growth medium in fibroblast cells by avoiding from possible interaction of secreted TG2 with the serum FN [267]. FBS was used by Arjonen *et al*. 2012 to demonstrate the distinct recycling of active and inactive β1 integrins in NCI-H46, PC3 and MDA-MB-231 cancer cell lines [141]. Huveneers *et al*. 2008 showed the reciprocal signaling between fibronectin and actin cytoskeleton through integrin α5β1 which led to focal adhesion formation and Rho-mediated contractility by binding to soluble FN [268]. In the light of these evidences to achieve an efficient integrin β1 internalization Caki-1 Wt cells were subjected to AIM-V, FBS and soluble fibronectin, all of which led to an average of 30 per cent β1 internalization in Caki-1 Wt cells. Powelka *et al*. 2004 demonstrated the stimulation dependent integrin β1 trafficking in HeLa and MDA-MB-231 by overnight serum starvation of these cells using bovine serum albumin (BSA) [140]. Similar to this study, in our experimental set up an efficient β1 integrin internalization was achieved by serum starving the cells using BSA; however, 10 per cent FBS was used as an inducer for the integrin internalization. In parallel with these experiments, integrin recycling was induced using either soluble FN or immobilized FN placed on tissue culture plates. However, recycling of β1 integrins through immobilized FN showed lower rates when compared to soluble FN. Since during the recycling experiments FBS was used to stimulate β1 integrin internalization, it is quite possible that proteins in the might interact with the FN coated matrices and lead to unspecific signaling changing the dynamics of the β1 integrin recycling. In comparison to immobilized FN, soluble FN showed ~a 50 per cent recycling in Caki-1 Wt cells which were acceptable when compared to PDGF which also induced 50 per cent recycling of β1 integrins in Swiss 3T3 cells [254]. In addition, Roberts *et al*. 2001 developed a capture-ELISA method in order to detect PDGF induced αvβ3 and α5β1 internalization and recycling cycles [254]. In contrast to this study β1 integrin internalization was not clearly detected in Caki-1 cells therefore immunoprecipitation

method was introduced into the experimental set up of the thesis to detect β1 integrin internalization. In comparison to Caki-2, ACHN and A-498 cells, Caki-1 cells displayed the highest potential for the internalization and recycling of ß1 integrins. Therefore for the further experiments Caki-1 cells were chosen as a cell model to investigate the role of TG2 in β1 integrin traffic. To further elucidate the role of TG2 in integrin β1 traffic, the levels of ITGβ1 internalization and recycling was analyzed between TG2 silenced (shTG2) and overexpressed (TG2 o/e) Caki-1 cells. Results showed that the downregulation of TG2 caused a drastic decrease in the internalization and hence recycling of ITGβ1 while the over expression of TG led to a significant increase in these processes suggesting that TG2 takes a role in the control of β1 integrin internalization and recycling in the metastatic RCC cancer cell line Caki-1.

Preliminarily experiments were performed by Ng *et al*. 1999 who demonstrated that PKCα regulates the integrin β1 internalization in mammary epithelial cells [269]. Further studies showed the upstream stimulator of PKCα, SDC4 served as a phosphorylation point during integrin αvβ3 and α5β1 traffic [161,167]. In addition to these evidences Telci *et al*. 2008 revealed that together with ITGβ1 integrin substrate FN, TG2 was able to increase cell adhesion and survival through SDC4 and/or ITGβ1 [113]. In addition to the evidence from above studies Bass *et al*. 2007 demonstrated that SDC4 is an essential component of integrin recycling pathway [127], a finding which proposed that SDC4 might also play an important role in the TG2 mediated ITGβ1 recycling pathway. In order to test this possibility, SDC4 silencing was achieved in Wt and TG2 o/e Caki-1 cells. Results internalization experiments showed that when SDC4 was silenced the ITGβ1 internalization levels were drastically decreased confirming the essential role of SDC4 in the grand scheme of integrin recycling pathway [127]. The fact that SDC4 downregulation in TG2 o/e Caki-1 cells decreased the level of internalized ITGβ1 to the same level as the Caki-1 Scr cells suggested that TG2 induced ITGβ1 internalization is mediated by SDC4 hence TG2 can be a novel partner of SDC4 in the regulation of β1 integrin traffic in RCC.

6. CONCLUSION AND FUTURE PROSPECTS

Regardless from its enzymatic activity, elevated levels of TG2 was obtained in primary and metastatic site RCC cells and TG2 together with FN and SDC4 was found to be able to restore integrin clustering and induce survival signaling pathways [113,196]. In the light of these evidences, this thesis was aimed to show (i) the importance of TG2 in the cell adhesion of primary (Caki-2&A-498) and metastatic site (Caki-1&ACHN) cRCC cancer cells on β1 integrin matrices by focusing on the interplay between the cell surface TG2 partners ITGβ1 and SDC4, (ii) the role of TG2 in ITGβ1 internalization and recycling using metastatic Caki-1 cells where TG2 was downregulated or overexpressed and (iii) TG2 induced SDC4 driven ITGβ1 internalization using SDC4 downregulated Wt and TG2 o/e cells.

Western Blot analysis showed that among four RCC cell lines, A-498 showed the higher TG2 and SDC4 protein expression levels while Caki-1 cells displayed a higher ITGβ1 protein levels compared to other RCC cell lines. However, Caki-1 cells displayed the highest interaction between TG2-ITGβ1 and TG2-SDC4. The importance of TG2-ITGβ1 association in RCC cell adhesion was demonstrated in TG2 silenced RCC cells using β1 integrin matrices; fibronectin (FN), collagen1 (Col1) and laminin (LM). In comparison to other cells lines, TG2 downregulation drastically reduce the cell attachment and spreading potential of Caki-1 cells on each β1 integrin matrix substrates. Biotin based integrin β1 internalization experiments and following integrin β1 recycling experiments have elucidated that Caki-1 cells have the highest potential for the internalization and recycling of β1 integrins. Therefore in order to investigate the possible collaborative role of SDC4 with TG2 and ITGβ1 turnover, Caki-1 cells were used as a cell model. Although integrin internalization exerts a minute to minute control, at the early time points of 10,20 and 30 mins the effect of TG2 on ITGβ1 internalization was observed. TG2 dowenregulation and overexpression showed a significant difference in β1 integrin internalization. In agreement with the internalization experiments, a remarkable 24 per cent difference of recycled ITGβ1 was recorded between shTG2 and TG2 o/e Caki-1 cells.

In order to reveal the role of SDC4 in TG2 dependent or independent internalization of ITGβ1 integrins, SDC4 was stably silenced in Caki-1 Wt and TG2 o/e cells and results

obtained from the experiments showed that ITGβ1 internalization was under control of SDC4 dominantly, and TG2 overexpression compensated the almost 40 per cent of the active ITGβ1 internalization.

Since integrins are the main regulators of cell adhesion, migration and proliferation events, deregulation or altered expression of integrins play a decisive role in tumor progression and metastasis by improving cancer cell migration and survival. From the literature it was obviously seen that integrin endo/exco cytosis mechanism is necessary to modulate integrin function and distribution [112]. This thesis showed that TG2, as a cell adhesion protein, modulates active integrin internalization and recycling mechanisms in metastatic site RCC cell Caki-1. Another important issue was obtained from this study that the overexpression of TG2 is able to restore integrin internalization in SDC4 downregulated cells, so that TG2 might be introduced as a novel partner of SDC4 during ITGβ1 internalization.

For further studies, it is important to reveal the internalization mechanisms of TG2 induced active β1 integrins. Caki-1 Scr, shTG2 and TG2 o/e cells might be treated with MitMab II, a Dynamin inhibitor in order to show whether TG2 induces integrin β1 internalization through dynamin-dependent or independent manner. According to the results obtained from this experiment will drive us to investigate the role of TG2 in clathrin dependent/independent β1 integrin internalization. One of the chemical clathrin inhibitors is monodensyl cadaverin (MDC), which has been widely used to disrupt clathrin-coated pit formation during receptor internalization from cell membrane, yet MDC is also a primary amine and a well-known TG2 activity inhibitor. Therefore, another inhibitor chlorpromazine which selectively inhibits clathrin-dependent endocytosis might be used during the internalization experiments. In the previous studies, Telci *et al.* 2008 demonstrated that α5β1 binding to ECM was impaired in response to RGD-containing peptides. TG2-FN complex can restore this function together with HSGCs of SDC4 and rescue the cell from anoikis [113]. In order to demonstrate the role of TG2 in active β1 integrin recycling or clustering in cells membrane, β1 integrin recycling experiments can be performed using guinea pig TG2-FN heterocomplex. The recycling of integrins from endosomal compartments can be organized through a long-loop pathway, which requires Rab11, or a short-loop pathway, which is controlled by Rab4. These pathways show the

delivery rate of integrins to cell surface, which can be correlated with the migration potential of the metastatic cells [131]. Following the downregulation of Rab4 and Rab11 using specific siRNAs, the recycling pathway of TG2 induced SDC4 driven active β1 can be elucidated in metastatic Caki-1 cells.

Overall, the main reason to reveal the importance of TG2 during integrin exco/enocytosis is to introduce a new therapeutic target protein which could be involved in the regulation of the internalization and recycling mechanism from the cell membrane. More durable and effective inhibitors can be developed in order to reduce integrin trafficking in metastatic cells.

REFERENCES

1. S. H. Kim, J. Turnbull and S. Guimond. Extracellular Matrix and Cell Signalling: the Dynamic Cooperation of Integrin, Proteoglycan and Growth Factor Receptor. *Journal of Endocrinology*, 209:139-151, 2011.

2. D. J. Hulmes. Building Collagen Molecules, Fibrils, and Suprafibrillar Structures. *Journal of Structural Biology*, 137:2-10, 2002.

3. C. M. Ferrier, W. L. van Geloof, H. Straatman, F. J. van de Molengraft, G. N. van Muijen and D. J. Ruiter. Spitz Naevi may Express Components of the Plasminogen Activation System. *The Journal of Pathology*, 198:92-99, 2002.

4. D. S. Harburger and D. A. Calderwood. Integrin Signalling at a Glance. *Journal of Cell Science*, 122:159-163, 2009.

5. C. Jean, P. Gravelle, J. Fournie and G. Laurent. Influence of Stress on Extracellular Matrix and Integrin Biology. *Oncogene*, 30:2697-2706, 2011.

6. S. Johansson, G. Svineng, K. Wennerberg, A. Armulik and L. Lohikangas. Fibronectin Integrin Interactions. *Frontiers Bioscience*, 2:126-146, 1997.

7. P. Friedl and S. Alexander. Cancer Invasion and the Microenvironment: Plasticity and Reciprocity. *Cell*, 147:992-1009, 2011.

8. K. Moissoglu and M. A. Schwartz. Integrin Signalling in Directed Cell Migration. *Biology of the Cell*, 98:547-555, 2006.

9. J. W. Tamkun, D. W. DeSimone, D. Fonda, R. S. Patel, C. Buck, A. F. Horwitz and R. O. Hynes. Structure of Integrin, a Glycoprotein Involved in the Transmembrane Linkage Between Fibronectin and Actin. *Cell*, 46:271-282, 1986.

10. R. O. Hynes. Integrins: Bidirectional, Allosteric Signaling Machines. *Cell*, 110:673-687, 2002.

11. I. D. Campbell and M. J. Humphries. Integrin Structure, Activation and Interactions. *Cold Spring Harbor Perspectives in Biology*, 3:1-15, 2011.

12. M. S. Johnson, N. Lu, K. Denessiouk, J. Heino and D. Gullberg. Integrins During Evolution: Evolutionary Trees and Model Organisms. *Biochimica et Biophysica Acta* 1788:779-789, 2009.

13. D. Calderwood. Talin Controls Integrin Activation. *Biochemical Society Transactions*, 32:434-437, 2004.

14. D. Valdramidou, M. J. Humphries and A. P. Mould. Distinct Roles of β1 MIDAS, ADMIDAS and Limbs Cation Binding Sites in Ligand Recognition by Integrin α2β1. *Journal of Biological Chemistry*, 2008.

15. A. P. Mould, S. J. Barton, J. A. Askari, S. E. Craig and M. J. Humphries. Role of ADMIDAS Cation Binding Site in Ligand Recognition by Integrin α5β1. *Journal of Biological Chemistry*, 278:51622-51629, 2003.

16. N. J. Anthis and I. D. Campbell. The Tail of Integrin Activation. *Trends in Biochemical Sciences*, 36:191-198, 2011.

17. Y. Takada, X. Ye and S. Simon. The Integrins. *Genome Biology*, 8:1-9, 2007.

18. B. D. Adair and M. Yeager. Three Dimensional Model of the Human Platelet Integrin αIIbβ3 Based on Electron Cryomicroscopy and X-Ray Crystallography. *Proceedings of the National Academy of Sciences*, 99:14059-14064, 2002.

19. A. Armulik, I. Nilsson, G. von Heijne and S. Johansson. Determination of the Border Between the Transmembrane and Cytoplasmic Domains of Human Integrin Subunits. *Journal of Biological Chemistry*, 274:37030-37034, 1999.

20. M. J. Williams, P. E. Hughes, T. E. O'Toole and M. H. Ginsberg. The Inner World of Cell Adhesion: Integrin Cytoplasmic Domains. *Trends in Cell Biology*, 4:109-112, 1994.

21. J. P. Xiong, T. Stehle, S. L. Goodman and M. A. Arnaout. New Insights into the Structural Basis of Integrin Activation. *Blood*, 102:1155-1159, 2003.

22. R. Li, C. R. Babu, J. D. Lear, A. J. Wand, J. S. Bennett and W. F. DeGrado. Oligomerization of the Integrin αIIbβ3: Roles of the Transmembrane and Cytoplasmic Domains. *Proceedings of the National Academy of Sciences*, 98:12462-12467, 2001.

23. A. Czuchra, H. Meyer, K. R. Legate, C. Brakebusch and R. Fässler. Genetic Analysis of β1 Integrin Activation Motifs in Mice. *The Journal of Cell Biology*, 174:889-899, 2006.

24. K. R. Legate and R. Fässler. Mechanisms that Regulate Adaptor Binding to β Integrin Cytoplasmic Tails. *Journal of Cell Science*, 122:187-198, 2009.

25. F. G. Giancotti and E. Ruoslahti. Integrin Signaling. *Science*, 285:1028-1033, 1999.

26. D. A. Calderwood, I. D. Campbell and D. R. Critchley. Talins and Kindlins: Partners in Integrin Mediated Adhesion. *Nature Reviews Molecular Cell Biology*, 14:503-517, 2013.

27. F. Ulrich and C. P. Heisenberg. Trafficking and Cell Migration. *Traffic*, 10:811-818, 2009.

28. K. L. Wegener, A. W. Partridge, J. Han, A. R. Pickford, R. C. Liddington, M. H. Ginsberg and I. D. Campbell. Structural Basis of Integrin Activation by Talin. *Cell*, 128:171-182, 2007.

29. S. J. Shattil and M. H. Ginsberg. Perspectives Series: Cell Adhesion in Vascular Biology. Integrin Signaling in Vascular Biology. *Journal of Clinical Investigation*, 100:1-5, 1997.

30. Z. Li, M. K. Delaney, K. A. O'Brien and X. Du. Signaling During Platelet Adhesion and Activation. *Arteriosclerosis, Thrombosis, and Vascular biology*, 30:2341-2349, 2010.

31. T. A. Haas and E. F. Plow. Development of a Structural Model for the Cytoplasmic Domain of an Integrin. *Protein Engineering*, 10:1395-1405, 1997.

32. A. Banno and M. H. Ginsberg. Integrin Activation. *Biochemical Society Transactions*, 36:229-234, 2008.

33. B. Franke, M. van Triest, K. M. de Bruijn, G. van Willigen, H. K. Nieuwenhuis, C. Negrier, J. W. N. Akkerman and J. L. Bos. Sequential Regulation of the Small GTPase Rap1 in Human Platelets. *Molecular and Cellular Biology*, 20:779-785, 2000.

34. B. Boettner and L. Van Aelst. Control of Cell Adhesion Dynamics by Rap1 Signaling. *Current Opinion in Cell Biology*, 21:684-693, 2009.

35. S. Tadokoro, S. J. Shattil, K. Eto, V. Tai, R. C. Liddington, J. M. de Pereda, M. H. Ginsberg and D. A. Calderwood. Talin Binding to Integrin ß tails: A Final Common Step in Integrin Activation. *Science*, 302:103-106, 2003.

36. D. A. Calderwood, R. Zent, R. Grant, D. J. G. Rees, R. O. Hynes and M. H. Ginsberg. The Talin Head Domain Binds to Integrin Beta Subunit Cytoplasmic Tails and Regulates Integrin Activation. *Journal of Biological Chemistry*, 274:28071-28074, 1999.

37. G. Di Paolo, L. Pellegrini, K. Letinic, G. Cestra, R. Zoncu, S. Voronov, S. Chang, J. Guo, M. R. Wenk and P. De Camilli. Recruitment and Regulation of Phosphatidylinositol Phosphate Kinase Type 1γ by the FERM Domain of Talin. *Nature*, 420:85-89, 2002.

38. C. Margadant, H. N. Monsuur, J. C. Norman and A. Sonnenberg. Mechanisms of Integrin Activation and Trafficking. *Current Opinion in Cell Biology*, 23:607-614, 2011.

39. D. H. Siegel, G. H. Ashton, H. G. Penagos, J. V. Lee, H. S. Feiler, K. C. Wilhelmsen, A. P. South, F. J. Smith, A. R. Prescott and V. Wessagowit. Loss of Kindlin 1, a Human Homolog of the *Caenorhabditis elegans* Actin–Extracellular-Matrix Linker Protein UNC 112, Causes Kindler Syndrome. *The American Journal of Human Genetics*, 73:174-187, 2003.

40. A. Meves, C. Stremmel, K. Gottschalk and R. Fässler. The Kindlin Protein Family: New Members to The Club of Focal Adhesion Proteins. *Trends in Cell Biology*, 19:504-513, 2009.

41. S. Ussar, H.-V. Wang, S. Linder, R. Fässler and M. Moser. The Kindlins: Subcellular Localization and Expression During Murine Development. *Experimental Cell Research*, 312:3142-3151, 2006.

42. E. Karaköse, H. B. Schiller and R. Fässler. The Kindlins at a Glance. *Journal of Cell Science*, 123:2353-2356, 2010.

43. E. Montanez, S. Ussar, M. Schifferer, M. Bösl, R. Zent, M. Moser and R. Fässler. Kindlin 2 Controls Bidirectional Signaling of Integrins. *Genes and Development*, 22:1325-1330, 2008.

44. M. Moser, B. Nieswandt, S. Ussar, M. Pozgajova and R. Fässler. Kindlin 3 is Essential for Integrin Activation and Platelet Aggregation. *Nature Medicine*, 14:325-330, 2008.

45. Y. Q. Ma, J. Qin, C. Wu and E. F. Plow. Kindlin 2 (Mig 2): A Co-activator of β3 Integrins. *The Journal of Cell Biology*, 181:439-446, 2008.

46. H. Hirata, K. Ohki and H. Miyata. Mobility of integrin α5β1 Measured on the Isolated Ventral Membranes of Human Skin Fibroblasts. *Biochimica et Biophysica Acta* 1723:100-105, 2005.

47. M. Vicente-Manzanares, C. K. Choi and A. R. Horwitz. Integrins in Cell Migration the Actin Connection. *Journal of Cell Science*, 122:199-206, 2009.

48. D. Bouvard, J. Pouwels, N. De Franceschi and J. Ivaska. Integrin Inactivators: Balancing Cellular Functions In Vitro and In Vivo. *Nature Reviews Molecular Cell Biology*, 14:430-442, 2013.

49. R. Zaidel-Bar, C. Ballestrem, Z. Kam and B. Geiger. Early Molecular Events in The Assembly of Matrix Adhesions at The Leading Edge of Migrating Cells. *Journal of Cell Science*, 116:4605-4613, 2003.

50. M. C. Wodnicka and K. Burridge. Rho-Stimulated Contractility Drives the Formation of Stress Fibers and Focal Adhesions. *The Journal of Cell Biology*, 133:1403-1415, 1996.

51. E. Goksoy, Y. Q. Ma, X. Wang, X. Kong, D. Perera, E. F. Plow and J. Qin. Structural Basis for the Autoinhibition of Talin in Regulating Integrin Activation. *Molecular Cell*, 31:124-133, 2008.

52. A. Carisey, R. Tsang, A. M. Greiner, N. Nijenhuis, N. Heath, A. Nazgiewicz, R. Kemkemer, B. Derby, J. Spatz and C. Ballestrem. Vinculin Regulates the Recruitment and Release of Core Focal Adhesion Proteins in a Force Dependent Manner. *Current Biology*, 23:271-281, 2013.

53. M. R. Morgan, M. J. Humphries and M. D. Bass. Synergistic Control of Cell Adhesion by Integrins and Syndecans. *Nature Reviews Molecular Cell Biology*, 8:957-969, 2007.

54. A. Huttenlocher and A. R. Horwitz. Integrins in Cell Migration. *Cold Spring Harbor Perspectives in Biology*, 3:1-17, 2011.

55. M. A. Wozniak, K. Modzelewska, L. Kwong and P. J. Keely. Focal Adhesion Regulation of Cell Behavior. *Biochimica et Biophysica Acta Molecular Cell Research*, 1692:103-119, 2004.

56. A. Nayal, D. J. Webb, C. M. Brown, E. M. Schaefer, M. Vicente-Manzanares and A. R. Horwitz. Paxillin Phosphorylation at Ser273 Localizes a GIT1 PIX PAK Complex and Regulates Adhesion and Protrusion Dynamics. *The Journal of Cell Biology*, 173:587-589, 2006.

57. P. W. Reddien and H. R. Horvitz. CED-2, CrkII and CED-10, Rac Control Phagocytosis and Cell Migration in *Caenorhabditis elegans*. *Nature Cell Biology*, 2:131-136, 2000.

58. M. D. Schaller and J. T. Parsons. pp125FAK dependent Tyrosine Phosphorylation of Paxillin Creates a High Affinity Binding Site for Crk. *Molecular and Cellular Biology*, 15:2635-2645, 1995.

59. E. Manser, T. H. Loo, C.-G. Koh, Z.-S. Zhao, X.-Q. Chen, L. Tan, I. Tan, T. Leung and L. Lim. PAK Kinases are Directly Coupled to the PIX Family of Nucleotide Exchange Factors. *Molecular Cell*, 1:183-192, 1998.

60. R.I. Manabe, M. Kovalenko, D. J. Webb and A. R. Horwitz. GIT1 Functions in a Motile, Multi-Molecular Signaling Complex that Regulates Protrusive Activity and Cell Migration. *Journal of Cell Science*, 115:1497-1510, 2002.

61. L. C. Sanders, F. Matsumura, G. M. Bokoch and P. de Lanerolle. Inhibition of Myosin Light Chain Kinase by p21 Activated Kinase. *Science*, 283:2083-2085, 1999.

62. V. D. Delorme Walker, J. R. Peterson, J. Chernoff, C. M. Waterman, G. Danuser, C. DerMardirossian and G. M. Bokoch. Pak1 Regulates Focal Adhesion Strength, Myosin IIA Distribution, and Actin Dynamics to Optimize Cell Migration. *The Journal of Cell Biology*, 193:1289-1303, 2011.

63. M. B. Srichai and R. Zent. Integrin Structure and Function. In: *Cell-Extracellular Matrix Interactions in Cancer*, pp 19-41. Springer, USA, 2010.

64. J. D. Hood and D. A. Cheresh. Role of Integrins in Cell Invasion and Migration. *Nature Reviews Cancer*, 2:91-100, 2002.

65. Y. Shen and M. D. Schaller. Focal Adhesion Targeting: The Critical Determinant of FAK Regulation and Substrate Phosphorylation. *Molecular Biology of the Cell*, 10:2507-2518, 1999.

66. K. Vuori, H. Hirai, S. Aizawa and E. Ruoslahti. Introduction of p130Cas Signaling Complex Formation Upon Integrin-Mediated Cell Adhesion: A Role For Src Family Kinases. *Molecular and Cellular Biology*, 16:2606-2613, 1996.

67. P. C. Brooks, R. Clark and D. A. Cheresh. Requirement of Vascular Integrin αVβ3 for Angiogenesis. *Science*, 264:569-571, 1994.

68. F. Echtermeyer, P. C. Baciu, S. Saoncella, Y. Ge and P. F. Goetinck. Syndecan4 Core Protein is Sufficient for the Assembly of Focal Adhesions and Actin Stress Fibers. *Journal of Cell Science*, 112:3433-3441, 1999.

69. M. L. Hibbs, S. Jakes, S. A. Stacker, R. W. Wallace and T. A. Springer. The Cytoplasmic Domain of the Integrin Lymphocyte Function Associated Antigen 1 Beta Subunit: Sites Required for Binding to Intercellular Adhesion Molecule 1 and the Phorbol Ester Stimulated Phosphorylation Site. *The Journal of Experimental Medicine*, 174:1227-1238, 1991.

70. K. Wennerberg, R. Fassler, B. Warmegard and S. Johansson. Mutational Analysis of the Potential Phosphorylation Sites in the Cytoplasmic Domain of Integrin β1. Requirement for Threonines 788, 789 in Receptor Activation. *Journal of Cell Science*, 111:1117-1126, 1998.

71. L. Pecorino. *Molecular biology of cancer: mechanisms, targets, and therapeutics*. Oxford University Press, U.K., 2012.

72. D. Hanahan and R. A. Weinberg. Hallmarks of cancer: the next generation. *Cell*, 144:646-674, 2011.

73. M. J. Bissell and D. Radisky. Putting Tumours in Context. *Nature Reviews Cancer*, 1:46-54, 2001.

74. B. S. Wiseman and Z. Werb. Stromal Effects on Mammary Gland Development and Breast Cancer. *Science*, 296:1046-1049, 2002.

75. W. Guo and F. G. Giancotti. Integrin Signalling During Tumour Progression. *Nature Reviews Molecular Cell Biology*, 5:816-826, 2004.

76. J. S. Desgrosellier and D. A. Cheresh. Integrins in Cancer: Biological Implications and Therapeutic Opportunities. *Nature Reviews Cancer*, 10:9-22, 2010.

77. T. R. Geiger and D. S. Peeper. Metastasis Mechanisms. *Biochimica et Biophysica Acta* 1796:293-308, 2009.

78. V. M. Weaver, O. W. Petersen, F. Wang, C. Larabell, P. Briand, C. Damsky and M. J. Bissell. Reversion of the Malignant Phenotype of Human Breast Cells in Three-Dimensional Culture and In vivo by Integrin Blocking Antibodies. *The Journal of Cell Biology*, 137:231-245, 1997.

79. C. Gimond, A. Van Der Flier, S. Van Delft, C. Brakebusch, I. Kuikman, J. G. Collard, R. Fässler and A. Sonnenberg. Induction of Cell Scattering by Expression of β1 Integrins in β1 Deficient Epithelial Cells Requires Activation of Members of the Rho Family of GTPases and Downregulation of Cadherin and Catenin Function. *The Journal of Cell Biology*, 147:1325-1340, 1999.

80. S. Pece and J. S. Gutkind. E Cadherin and Hakai: Signalling, Remodeling or Destruction. *Nature Cell Biology*, 4:72-74, 2002.

81. E. Avizienyte, A. W. Wyke, R. J. Jones, G. W. McLean, M. A. Westhoff, V. G. Brunton and M. C. Frame. Src Induced De-regulation of E Cadherin in Colon Cancer Cells Requires Integrin Signalling. *Nature Cell Biology*, 4:632-638, 2002.

82. P. E. Gleizes, J. S. Munger, I. Nunes, J. G. Harpel, R. Mazzieri, I. Noguera and D. B. Rifkin. TGFβ Latency: Biological Significance and Mechanisms of Activation. *Stem Cells*, 15:190-197, 1997.

83. G. Thomas, I. Hart, P. Speight and J. Marshall. Binding of TGFβ1 Latency-Associated Peptide (LAP) to αvβ6 Integrin Modulates Behaviour of Squamous Carcinoma Cells. *British Journal of Cancer*, 87:859-867, 2002.

84. D. Mu, S. Cambier, L. Fjellbirkeland, J. L. Baron, J. S. Munger, H. Kawakatsu, D. Sheppard, V. C. Broaddus and S. L. Nishimura. The Integrin αvβ8 Mediates Epithelial Homeostasis through MT1 MMP dependent Activation of TGFβ1. *The Journal of Cell Biology*, 157:493-507, 2002.

85. D. J. Webb, J. T. Parsons and A. F. Horwitz. Adhesion Assembly, Disassembly and Turnover in Migrating Cells Over and Over and Over Again. *Nature Cell Biology*, 4:97-100, 2002.

86. E. Sahai and C. J. Marshall. Differing Modes of Tumour Cell Invasion have Distinct Requirements for Rho ROCK Signalling and Extracellular Proteolysis. *Nature Cell Biology*, 5:711-719, 2003.

87. R. L. Klemke, S. Cai, A. L. Giannini, P. J. Gallagher, P. De Lanerolle and D. A. Cheresh. Regulation of Cell Motility by Mitogen Activated Protein Kinase. *The Journal of Cell Biology*, 137:481-492, 1997.

88. M. D. Sternlicht and Z. Werb. How Matrix Metalloproteinases Regulate Cell Behavior. *Annual Review of Cell and Developmental Biology*, 17:463-516, 2001.

89. H. A. Chapman and Y. Wie. Protease Crosstalk with Integrins: The Urokinase Receptor Paradigm. *Thrombosis and Haemostasis*, 86:124-129, 2001.

90. F. Blasi and P. Carmeliet. uPAR: A Versatile Signalling Orchestrator. *Nature Reviews Molecular Cell Biology*, 3:932-943, 2002.

91. C. L. Gladson and D. Cheresh. Glioblastoma Expression of Vitronectin and the αvβ3 Integrin. Adhesion Mechanism for Transformed Glial Cells. *Journal of Clinical Investigation*, 88:1924-1932, 1991.

92. O. Crociani, F. Zanieri, S. Pillozzi, E. Lastraioli, M. Stefanini, A. Fiore, A. Fortunato, M. D'Amico, M. Masselli and E. De Lorenzo. hERG1 Channels Modulate Integrin

Signaling to Trigger Angiogenesis and Tumor Progression in Colorectal Cancer. *Scientific Reports*, 3:1-13, 2013.

93. M. J. Reginato, K. R. Mills, J. K. Paulus, D. K. Lynch, D. C. Sgroi, J. Debnath, S. K. Muthuswamy and J. S. Brugge. Integrins and EGFR Coordinately Regulate the Pro Apoptotic Protein Bim to Prevent Anoikis. *Nature Cell Biology*, 5:733-740, 2003.

94. M. De la Fuente, B. Casanova, M. Garcia-Gila, A. Silva and A. Garcia-Pardo. Fibronectin Interaction with α4β1 Integrin Prevents Apoptosis in B Cell Chronic Lymphocytic Leukemia: Correlation with Bcl2 and Bax. *Leukemia* 13:266-274, 1999.

95. F. Aoudjit and K. Vuori. Matrix Attachment Regulates Fas induced Apoptosis in Endothelial Cells a Role for c-Flip and Implications for Anoikis. *The Journal of Cell Biology*, 152:633-644, 2001.

96. D. Ilić, E. A. Almeida, D. D. Schlaepfer, P. Dazin, S. Aizawa and C. H. Damsky. Extracellular Matrix Survival Signals Transduced by Focal Adhesion Kinase Suppress P53 Mediated Apoptosis. *The Journal of Cell Biology*, 143:547-560, 1998.

97. Y. Liu and X. Cao. Organotropic Metastasis: Role of Tumor Exosomes. *Cell Research*, 2015.

98. E. H. Danen. Integrin Signaling as a Cancer Drug Target. *ISRN Cell Biology*, 2013:1-14, 2013.

99. S. Kim, K. Bell, S. A. Mousa and J. A. Varner. Regulation of Angiogenesis In Vivo by Ligation of Integrin α5β1 with the Central Cell Binding Domain of Fibronectin. *The American Journal of Pathology*, 156:1345-1362, 2000.

100. Y. F. Caras, D. McDonald, D. Johnson, R. Murray and U. Jeffry. Preclinical Evaluation of an anti-α5β1 Integrin Antibody as a Novel Anti Angiogenic Agent. *Journal of Experimental Therapeutics and Oncology*, 5:273-286, 2006.

101. A. D. Ricart, A. W. Tolcher, G. Liu, K. Holen, G. Schwartz, M. Albertini, G. Weiss, S. Yazji, C. Ng and G. Wilding. Volociximab, A Chimeric Monoclonal Antibody that Specifically Binds α5β1 Integrin: A Phase I, Pharmacokinetic and Biological Correlative Study. *Clinical Cancer Research*, 14:7924-7929, 2008.

102. K. M. Bell-McGuinn, C. M. Matthews, S. N. Ho, M. Barve, L. Gilbert, R. T. Penson, E. Lengyel, R. Palaparthy, K. Gilder and A. Vassos. A phase II, Single Arm Study of the Anti α5β1 Integrin Antibody Volociximab as Monotherapy in Patients With Platinum Resistant Advanced Epithelial Ovarian or Primary Peritoneal Cancer. *Gynecologic Oncology*, 121:273-279, 2011.

103. D. Gao, D. J. Nolan, A. S. Mellick, K. Bambino, K. McDonnell and V. Mittal. Endothelial Progenitor Cells Control the Angiogenic Switch in Mouse Lung Metastasis. *Science*, 319:195-198, 2008.

104. Y. Shaked, A. Ciarrocchi, M. Franco, C. R. Lee, S. Man, A. M. Cheung, D. J. Hicklin, D. Chaplin, F. S. Foster and R. Benezra. Therapy Induced Acute Recruitment of Circulating Endothelial Progenitor Cells to Tumors. *Science*, 313:1785-1787, 2006.

105. J. Mateo, J. Berlin, J. De Bono, R. Cohen, V. Keedy, G. Mugundu, L. Zhang, A. Abbattista, C. Davis and C. G. Stampino. A First-in Human Study of the anti-alpha5 β1 Integrin Monoclonal Antibody PF-04605412 Administered Intravenously to Patients with Advanced Solid Tumors. *Cancer Chemotherapy and Pharmacology*, 74:1039-1046, 2014.

106. P. Friedl and D. Gilmour. Collective Cell Migration in Morphogenesis, Regeneration and Cancer. *Nature Reviews Molecular Cell Biology*, 10:445-457, 2009.

107. C. Gaggioli, S. Hooper, C. Hidalgo-Carcedo, R. Grosse, J. F. Marshall, K. Harrington and E. Sahai. Fibroblast led Collective Invasion of Carcinoma Cells with Differing Roles for RhoGTPases in Leading and Following Cells. *Nature Cell Biology*, 9:1392-1400, 2007.

108. V. Sanz-Moreno, G. Gadea, J. Ahn, H. Paterson, P. Marra, S. Pinner, E. Sahai and C. J. Marshall. Rac Activation and Inactivation Control Plasticity of Tumor Cell Movement. *Cell*, 135:510-523, 2008.

109. N. Makrilia, A. Kollias, L. Manolopoulos and K. Syrigos. Cell Adhesion Molecules: Role and Clinical Significance in Cancer. *Cancer Investigation*, 27:1023-1037, 2009.

110. N. R. Paul, G. Jacquemet and P. T. Caswell. Endocytic Trafficking of Integrins in Cell Migration. *Current Biology*, 25:1092-1105, 2015.

111. P. T. Caswell, H. J. Spence, M. Parsons, D. P. White, K. Clark, K. W. Cheng, G. B. Mills, M. J. Humphries, A. J. Messent and K. I. Anderson. Rab 25 Associates with α5β1 Integrin to Promote Invasive Migration in 3D Microenvironments. *Developmental Cell*, 13:496-510, 2007.

112. S. Shin, L. Wolgamott and S. O. Yoon. Integrin Trafficking and Tumor Progression. *International Journal of Cell Biology*, 2012, 2011.

113. D. Telci, Z. Wang, X. Li, E. A. Verderio, M. J. Humphries, M. Baccarini, H. Basaga and M. Griffin. Fibronectin Tissue Transglutaminase Matrix Rescues RGD Impaired Cell Adhesion through Syndecan 4 and Beta 1 Integrin Co Signaling. *Journal of Biochemistry*, 283:20937-209347, 2008.

114. M. D. Bass and M. J. Humphries. Cytoplasmic Interactions of Syndecan4 Orchestrate Adhesion Receptor and Growth Factor Receptor Signalling. *Biochemical Journal*, 368:1, 2002.

115. J. R. Henley, E. W. Krueger, B. J. Oswald and M. A. McNiven. Dynamin Mediated Internalization of Caveolae. *The Journal of Cell Biology*, 141:85-99, 1998.

116. J. Swanson and C. Watts. Trends Cell Biology. *Macropinocytosis*, 5:424-428, 1995.

117. E. J. Ezratty, M. A. Partridge and G. G. Gundersen. Microtubule Induced Focal Adhesion Disassembly is Mediated by Dynamin and Focal Adhesion Kinase. *Nature Cell Biology*, 7:581-590, 2005.

118. S. K. Mishra, P. A. Keyel, M. J. Hawryluk, N. R. Agostinelli, S. C. Watkins and L. M. Traub. Disabled 2 Exhibits the Properties of a Cargo Selective Endocytic Clathrin Adaptor. *The EMBO Journal*, 21:4915-4926, 2002.

119. T. Nishimura and K. Kaibuchi. Numb Controls Integrin Endocytosis for Directional Cell Migration with aPKC and PAR-3. *Developmental Cell*, 13:15-28, 2007.

120. Y. Wang, H. Cao, J. Chen and M. A. McNiven. A Direct Interaction Between the Large GTPase Dynamin 2 and FAK Regulates Focal Adhesion Dynamics in Response to Active Src. *Molecular Biology of the Cell*, 22:1529-1538, 2011.

121. W. T. Chao, F. Ashcroft, A. C. Daquinag, T. Vadakkan, Z. Wei, P. Zhang, M. E. Dickinson and J. Kunz. Type I Phosphatidylinositol Phosphate Kinase Beta Regulates Focal Adhesion Disassembly by Promoting β1 Integrin Endocytosis. *Molecular and Cellular Biology*, 30:4463-4479, 2010.

122. A. Teckchandani, N. Toida, J. Goodchild, C. Henderson, J. Watts, B. Wollscheid and J. A. Cooper. Quantitative Proteomics Identifies a Dab2/Integrin Module Regulating Cell Migration. *The Journal of Cell Biology*, 186:99-111, 2009.

123. A. Eskova, B. Knapp, D. Matelska, S. Reusing, A. Arjonen, T. Lisauskas, R. Pepperkok, R. Russell, R. Eils and J. Ivaska. An RNAi Screen Identifies KIF15 As a Novel Regulator of The Endocytic Trafficking of Integrin. *Journal of Cell Science*, 127:2433-2447, 2014.

124. R. Moravec, K. K. Conger, R. D'Souza, A. B. Allison and J. E. Casanova. BRAG2/GEP100/IQSec1 Interacts with Clathrin and Regulates α5β1 Integrin Endocytosis through Activation of ADP Ribosylation Factor 5 (Arf5). *Journal of Biological Chemistry*, 287:31138-31147, 2012.

125. I. R. Nabi and P. U. Le. Caveolae and Raft Dependent Endocytosis. *The Journal of Cell Biology*, 161:673-677, 2003.

126. L. Svensson, P. Stanley, F. Willenbrock and N. Hogg. The Gαq/11 Proteins Contribute to T lymphocyte Migration by Promoting Turnover of Integrin LFA 1 through Recycling. *Plos One*, 7:1-12, 2012.

127. M. D. Bass, R. C. Williamson, R. D. Nunan, J. D. Humphries, A. Byron, M. R. Morgan, P. Martin and M. J. Humphries. A Syndecan4 Hair Trigger Initiates Wound Healing Through Caveolin and Rhog Regulated Integrin Endocytosis. *Developmental Cell*, 21:681-693, 2011.

128. J. P. Lim and P. A. Gleeson. Macropinocytosis: an Endocytic Pathway for Internalising Large Gulps. *Immunology and Cell Biology*, 89:836-843, 2011.

129. Z. Gu, E. H. Noss, V. W. Hsu and M. B. Brenner. Integrins Traffic Rapidly via Circular Dorsal Ruffles and Macropinocytosis During Stimulated Cell Migration. *The Journal of Cell Biology*, 193:61-70, 2011.

130. M. Skalski, N. Sharma, K. Williams, A. Kruspe and M. G. Coppolino. SNARE mediated Membrane Traffic is Required for Focal Adhesion Kinase Signaling and Src Regulated Focal Adhesion Turnover. *Biochimica et Biophysica Acta*, 1813:148-158, 2011.

131. T. Pellinen and J. Ivaska. Integrin Traffic. *Journal of Cell Science*, 119:3723-3731, 2006.

132. A. Mai, S. Veltel, T. Pellinen, A. Padzik, E. Coffey, V. Marjomäki and J. Ivaska. Competitive Binding of Rab21 and p120RasGAP to Integrins Regulates Receptor Traffic and Migration. *The Journal of Cell Biology*, 194:291-306, 2011.

133. P. Mendoza, R. Ortiz, J. Díaz, A. F. Quest, L. Leyton, D. Stupack and V. A. Torres. Rab5 Activation Promotes Focal Adhesion Disassembly, Migration and Invasiveness in Tumor Cells. *Journal of Cell Science*, 126:3835-3847, 2013.

134. N. De Franceschi, H. Hamidi, J. Alanko, P. Sahgal and J. Ivaska. Integrin Traffic The Update. *Journal of Cell Science*, 128:839-852, 2015.

135. M. A. Dozynkiewicz, N. B. Jamieson, I. MacPherson, J. Grindlay, P. V. van den Berghe, A. von Thun, J. P. Morton, C. Gourley, P. Timpson and C. Nixon. Rab25 and CLIC3 Collaborate to Promote Integrin Recycling From Late Endosomes or Lysosomes and Drive Cancer Progression. *Developmental Cell*, 22:131-145, 2012.

136. R. T. Böttcher, C. Stremmel, A. Meves, H. Meyer, M. Widmaier, H.-Y. Tseng and R. Fässler. Sorting Nexin 17 Prevents Lysosomal Degradation of [Beta] 1 Integrins By Binding To The [Beta] 1-Integrin Tail. *Nature cell biology*, 14:584-592, 2012.

137. H. Y. Tseng, N. Thorausch, T. Ziegler, A. Meves, R. Fässler and R. T. Böttcher. Sorting Nexin 31 Binds Multiple β Integrin Cytoplasmic Domains and Regulates β1

Integrin Surface Levels and Stability. *Journal of Molecular Biology*, 426:3180-3194, 2014.

138. T. Zech, S. D. Calaminus, P. Caswell, H. J. Spence, M. Carnell, R. H. Insall, J. Norman and L. M. Machesky. The Arp2/3 Activator WASH Regulates α5β1 Integrin Mediated Invasive Migration. *Journal of Cell Science*, 124:3753-3759, 2011.

139. R. E. Bridgewater, J. C. Norman and P. T. Caswell. Integrin Trafficking at a Glance. *Journal of Cell Science*, 125:3695-3701, 2012.

140. A. M. Powelka, J. Sun, J. Li, M. Gao, L. M. Shaw, A. Sonnenberg and V. W. Hsu. Stimulation Dependent Recycling of Integrin β1 Regulated by ARF6 and Rab11. *Traffic*, 5:20-36, 2004.

141. A. Arjonen, J. Alanko, S. Veltel and J. Ivaska. Distinct Recycling of Active and Inactive β1 Integrins. *Traffic*, 13:610-625, 2012.

142. T. Pellinen, S. Tuomi, A. Arjonen, M. Wolf, H. Edgren, H. Meyer, R. Grosse, T. Kitzing, J. K. Rantala and O. Kallioniemi. Integrin Trafficking Regulated by Rab21 is Necessary for Cytokinesis. *Developmental Cell*, 15:371-385, 2008.

143. J. R. Couchman. Syndecans: Proteoglycan Regulators of Cell Surface Microdomains. *Nature Reviews Molecular Cell Biology*, 4:926-938, 2003.

144. C. Kim, O. Goldberger, R. Gallo and M. Bernfield. Members of the Syndecan Family of Heparan Sulfate Proteoglycans are Expressed in Distinct Cell, Tissue, and Development Specific Patter. *Molecular Biology of the Cell*, 5:797-805, 1994.

145. D. J. Carey, D. M. Evans, R. C. Stahl, V. K. Asundi, K. J. Conner, P. Garbes and G. Cizmeci-Smith. Molecular Cloning and Characterization of N Syndecan, a Novel Transmembrane Heparan Sulfate Proteoglycan. *The Journal of Cell Biology*, 117:191-201, 1992.

146. G. David, B. van der Schueren, P. Marynen, J.-J. Cassiman and H. Van den Berghe. Molecular Cloning of Amphiglycan, a Novel Integral Membrane Heparan Sulfate Proteoglycan Expressed by Epithelial and Fibroblastic Cells. *The Journal of Cell Biology*, 118:961-969, 1992.

147. P. Zimmermann and G. David. The Syndecans, Tuners of Transmembrane Signaling. *The Faseb Journal*, 13:91-100, 1999.

148. R. D. Sanderson and M. Bernfield. Molecular Polymorphism of a Cell Surface Proteoglycan: Distinct Structures on Simple and Stratified Epithelia. *Proceedings of the National Academy of Sciences*, 85:9562-9566, 1988.

149. E. Tkachenko, J. M. Rhodes and M. Simons. Syndecans New Kids on the Signaling Block. *Circulation Research*, 96:488-500, 2005.

150. T. W. Chittenden, F. Claes, A. A. Lanahan, M. Autiero, R. T. Palac, E. V. Tkachenko, A. Elfenbein, C. R. de Almodovar, E. Dedkov and R. Tomanek. Selective Regulation of Arterial Branching Morphogenesis by Synectin. *Developmental Cell*, 10:783-795, 2006.

151. T. Szatmári, R. Ötvös, A. Hjerpe and K. Dobra. Syndecan 1 in Cancer: Implications for Cell Signaling, Differentiation, and Prognostication. *Disease markers*, 2015:1-13, 2015.

152. A. Elfenbein and M. Simons. Syndecan4 Signaling At a Glance. *Journal of Cell Science*, 126:3799-3804, 2013.

153. S. Brule, N. Charnaux, A. Sutton, D. Ledoux, T. Chaigneau, L. Saffar and L. Gattegno. The Shedding of Syndecan4 and Syndecan1 from HeLa Cells and Human Primary Macrophages is Accelerated by SDF1/CXCL12 and Mediated by the Matrix Metalloproteinase 9. *Glycobiology*, 16:488-501, 2006.

154. E. Tkachenko and M. Simons. Clustering Induces Redistribution of Syndecan 4 Core Protein into Raft Membrane Domains. *Journal of Biological Chemistry*, 277:19946-19951, 2002.

155. M. Kan, F. Wang, J. Xu, J. W. Crabb, J. Hou and W. L. McKeehan. An Essential Heparin-Binding Domain in the Fibroblast Growth Factor Receptor Kinase. *Science*, 259:1918-1921, 1993.

156. K. Forsten-Williams, C. C. Chua and M. A. Nugent. The Kinetics of FGF2 Binding to Heparan Sulfate Proteoglycans and MAP Kinase Signaling. *Journal of Theoretical Biology*, 233:483-499, 2005.

157. C. C. Chua, N. Rahimi, K. Forsten-Williams and M. A. Nugent. Heparan Sulfate Proteoglycans Function as Receptors for Fibroblast Growth Factor 2 Activation of Extracellular Signal Regulated Kinases 1 and 2. *Circulation Research*, 94:316-323, 2004.

158. A. Woods and J. R. Couchman. Syndecan 4 Heparan Sulfate Proteoglycan is a Selectively Enriched and Widespread Focal Adhesion Component. *Molecular Biology of the Cell*, 5:183-192, 1994.

159. A. Horowitz and M. Simons. Phosphorylation of the Cytoplasmic Tail of Syndecan 4 Regulates Activation of Protein Kinase Cα. *Journal of Biological Chemistry*, 273:25548-25551, 1998.

160. A. Horowitz, M. Murakami, Y. Gao and M. Simons. Phosphatidylinositol 4, 5 bisphosphate Mediates the Interaction of Syndecan 4 with Protein Kinase C. *Biochemistry*, 38:15871-15877, 1999.

161. T. Ng, D. Shima, A. Squire, P. I. Bastiaens, S. Gschmeissner, M. J. Humphries and P. J. Parker. PKCα Regulates β1 integrin Dependent Cell Motility Through Association and Control of Integrin Traffic. *The EMBO Journal*, 18:3909-3923, 1999.

162. S.-T. Lim, R. L. Longley, J. R. Couchman and A. Woods. Direct Binding of Syndecan 4 Cytoplasmic Domain to the Catalytic Domain of Protein Kinase Cα (PKCα) Increases Focal Adhesion Localization of PKCα. *Journal of Biological Chemistry*, 278:13795-13802, 2003.

163. M. Murakami, A. Horowitz, S. Tang, J. A. Ware and M. Simons. Protein Kinase C (PKC) δ Regulates PKCα Activity in a Syndecan 4 Dependent Manner. *Journal of Biological Chemistry*, 277:20367-20371, 2002.

164. B. S. Kang, D. R. Cooper, F. Jelen, Y. Devedjiev, U. Derewenda, Z. Dauter, J. Otlewski and Z. S. Derewenda. PDZ Tandem of Human Syntenin: Crystal Structure and Functional Properties. *Structure*, 11:459-468, 2003.

165. A. Woods and J. R. Couchman. Syndecan 4 and Focal Adhesion Function. *Current Opinion in Cell Biology*, 13:578-583, 2001.

166. S. A. Wilcox-Adelman, F. Denhez and P. F. Goetinck. Syndecan 4 Modulates Focal Adhesion Kinase Phosphorylation. *Journal of Biological Chemistry*, 277:32970-32977, 2002.

167. M. R. Morgan, H. Hamidi, M. D. Bass, S. Warwood, C. Ballestrem and M. J. Humphries. Syndecan 4 Phosphorylation is a Control Point for Integrin Recycling. *Developmental Cell*, 24:472-485, 2013.

168. M. A. Schwartz and S. J. Shattil. Signaling Networks Linking Integrins and Rho Family GTPases. *Trends in Biochemical Sciences*, 25:388-391, 2000.

169. C. Partovian, R. Ju, Z. W. Zhuang, K. A. Martin and M. Simons. Syndecan 4 Regulates Subcellular Localization of mTOR Complex2 and Akt Activation in a PKCα-dependent Manner in Endothelial Cells. *Molecular Cell*, 32:140-149, 2008.

170. R. Brooks, R. C. Williamson and M. D. Bass. Syndecan4 Independently Regulates Multiple Small GTPases to Promote Fibroblast Migration During Wound Healing. *Small GTPases*, 3:73-79, 2012.

171. T. Kawauchi. Cell Adhesion and Its Endocytic Regulation in Cell Migration During Neural Development and Cancer Metastasis. *International Journal of Molecular Sciences*, 13:4564-4590, 2012.

172. M. F. Baietti, Z. Zhang, E. Mortier, A. Melchior, G. Degeest, A. Geeraerts, Y. Ivarsson, F. Depoortere, C. Coomans and E. Vermeiren. Syndecan, Syntenin, Alix Regulates the Biogenesis of Exosomes. *Nature Cell Biology*, 14:677-685, 2012.

173. H. Katoh and M. Negishi. RhoG activates Rac1 by Direct Interaction with the Dock180 binding Protein Elmo. *Nature*, 424:461-464, 2003.

174. R. Pankov, Y. Endo, S. Even-Ram, M. Araki, K. Clark, E. Cukierman, K. Matsumoto and K. M. Yamada. A Rac Switch Regulates Random Versus Directionally Persistent Cell Migration. *The Journal of Cell Biology*, 170:793-802, 2005.

175. A. Elfenbein, A. Lanahan, T. X. Zhou, A. Yamasaki, E. Tkachenko, M. Matsuda and M. Simons. Syndecan4 Regulates FGFR1 Signaling in Endothelial Cells by Directing Macropinocytosis. *Science Signaling*, 5:1-25, 2012.

176. M. Simons and G. Raposo. Exosomes Vesicular Carriers for Intercellular Communication. *Current Opinion in Cell Biology*, 21:575-581, 2009.

177. A. Hoshino, B. Costa-Silva, T.-L. Shen, G. Rodrigues, A. Hashimoto, M. T. Mark, H. Molina, S. Kohsaka, A. Di Giannatale and S. Ceder. Tumour Exosome Integrins Determine Organotropic Metastasis. *Nature*, 527:329-335, 2015.

178. L. Lorand and R. M. Graham. Transglutaminases: Crosslinking Enzymes with Pleiotropic Functions. *Nature Reviews Molecular Cell Biology*, 4:140-156, 2003.

179. J. Pisano, J. Finlayson and M. P. Peyton. Cross link in Fibrin Polymerized by Factor XIII: ε (γ glutamyl) Lysine. *Science*, 160:892-893, 1968.

180. P. Grenard, M. K. Bates and D. Aeschlimann. Evolution of Transglutaminase Genes: Identification of a Transglutaminase Gene Cluster on Human Chromosome 15q15 Structure Of The Gene Encoding Transglutaminase X and a Novel Gene Family Member, Transglutaminase Z. *Journal of Biological Chemistry*, 276:33066-33078, 2001.

181. D. Aeschlimann, M. K. Koeller, B. L. Allen-Hoffmann and D. F. Mosher. Isolation of a cDNA Encoding a Novel Member of The Transglutaminase Gene Family from Human Keratinocytes Detection and Identification of Transglutaminase Gene Products Based on Reverse Transcription-Polymerase Chain Reaction with Degenerate Primers. *Journal of Biological Chemistry*, 273:3452-3460, 1998.

182. M. Griffin, R. Casadio and C. M. Bergamini. Transglutaminases: Nature's Biological Glues. *Biochemical Journal*, 368:377-396, 2002.

183. R. L. Eckert, M. T. Kaartinen, M. Nurminskaya, A. M. Belkin, G. Colak, G. V. Johnson and K. Mehta. Transglutaminase Regulation of Cell Function. *Physiological Reviews*, 94:383-417, 2014.

184. M. Aleanzi, A. M. Demonte, C. Esper, S. Garcilazo and M. Waggener. Celiac Disease Antibody Recognition against Native and Selectively Deamidated Gliadin Peptides. *Clinical Chemistry*, 47:2023-2028, 2001.

185. G. Melino, M. Annicchiarico-Petruzzelli, L. Piredda, E. Candi, V. Gentile, P. Davies and M. Piacentini. Tissue Transglutaminase and Apoptosis: Sense and Antisense

Transfection Studies with Human Neuroblastoma Cells. *Molecular and Cellular Biology*, 14:6584-6596, 1994.

186. M. Lesort, J. Tucholski, M. L. Miller and G. V. Johnson. Tissue Transglutaminase: a Possible Role in Neurodegenerative Diseases. *Progress in Neurobiology*, 61:439-463, 2000.

187. L. Fesus and M. Piacentini. Transglutaminase 2 : An Enigmatic Enzyme with Diverse Functions. *Trends in Biochemical Sciences*, 27:534-539, 2002.

188. A. Verma, H. Wang, B. Manavathi, J. Y. Fok, A. P. Mann, R. Kumar and K. Mehta. Increased Expression of Tissue Transglutaminase in Pancreatic Ductal Adenocarcinoma and Its Implications in Drug Resistance and Metastasis. *Cancer Research*, 66:10525-10533, 2006.

189. M. Satpathy, L. Cao, R. Pincheira, R. Emerson, R. Bigsby, H. Nakshatri and D. Matei. Enhanced Peritoneal Ovarian Tumor Dissemination by Tissue Transglutaminase. *Cancer Research*, 67:7194-7202, 2007.

190. J. Y. Hwang, L. S. Mangala, J. Y. Fok, Y. G. Lin, W. M. Merritt, W. A. Spannuth, A. M. Nick, D. J. Fiterman, P. E. Vivas-Mejia and M. T. Deavers. Clinical and Biological Significance of Tissue Transglutaminase in Ovarian Carcinoma. *Cancer Research*, 68:5849-5858, 2008.

191. J. Y. Fok, S. Ekmekcioglu and K. Mehta. Implications of Tissue Transglutaminase Expression in Malignant Melanoma. *Molecular Cancer Therapeutics*, 5:1493-1503, 2006.

192. K. S. Park, H.-K. Kim, J.-H. Lee, Y.-B. Choi, S.-Y. Park, S.-H. Yang, S.-Y. Kim and K.-M. Hong. Transglutaminase 2 as a Cisplatin Resistance Marker in Non-Small Cell Lung Cancer. *Journal of Cancer Research and Clinical Oncology*, 136:493-502, 2010.

193. L. Yuan, M. Siegel, K. Choi, C. Khosla, C. Miller, E. Jackson, D. Piwnica-Worms and K. Rich. Transglutaminase 2 Inhibitor, KCC009, Disrupts Fibronectin Assembly in The Extracellular Matrix and Sensitizes Orthotopic Glioblastomas to Chemotherapy. *Oncogene*, 26:2563-2573, 2007.

194. K. Mehta, J. Fok, F. R. Miller, D. Koul and A. A. Sahin. Prognostic Significance of Tissue Transglutaminase in Drug Resistant and Metastatic Breast Cancer. *Clinical Cancer Research*, 10:8068-8076, 2004.

195. J. S. Chen, N. Agarwal and K. Mehta. Multidrug-Resistant MCF 7 Breast Cancer Cells Contain Deficient Intracellular Calcium Pools. *Breast Cancer Research and Treatment*, 71:237-247, 2002.

196. M. Erdem, S. Erdem, O. Sanli, H. Sak, I. Kilicaslan, F. Sahin and D. Telci. Up-Regulation of TGM2 with ITGβ1 and SDC4 is Important in the Development and Metastasis of Renal Cell Carcinoma. In: *Urologic Oncology: Seminars and Original Investigations*, 2014. vol 1. Elsevier, pp 13-20,

197. S. Erdem, G. Yegen, D. Telci, I. Yildiz, T. Tefik, H. Issever, I. Kilicaslan and O. Sanli. The Increased Transglutaminase 2 Expression Levels During Initial Tumorigenesis Predict Increased Risk of Metastasis and Decreased Disease-Free and Cancer-Specific Survivals in Renal Cell Carcinoma. *World Journal of Urology*, 33:1553-1560, 2015.

198. J. S. Chen and K. Mehta. Tissue Transglutaminase: An Enzyme with a Split Personality. *The International Journal of Biochemistry and Cell biology*, 31:817-836, 1999.

199. Z. Wang and M. Griffin. TG2, A Novel Extracellular Protein with Multiple Functions. *Amino acids*, 42:939-949, 2012.

200. S. Gundemir, G. Colak, J. Tucholski and G. V. Johnson. Transglutaminase 2 : A Molecular Swiss Army Knife. *Biochimica et Biophysica Acta* 1823:406-419, 2012.

201. C. M. Bergamini. GTP Modulates Calcium Binding and Cation Induced Conformational Changes in Erythrocyte Transglutaminase. *FEBS letters*, 239:255-258, 1988.

202. M. S. Pavlyukov, N. V. Antipova, M. V. Balashova and M. I. Shakhparonov. Detection of Transglutaminase 2 Conformational Changes in Living Cell. *Biochemical and Biophysical Research Communications*, 421:773-779, 2012.

203. X. Jin, J. Stamnaes, C. Klöck, T. R. DiRaimondo, L. M. Sollid and C. Khosla. Activation of Extracellular Transglutaminase 2 By Thioredoxin. *Journal of Biological Chemistry*, 286:37866-37873, 2011.

204. S. M. Jung, S. Jandu, J. Steppan, A. Belkin, S. S. An, A. Pak, E. Y. Choi, D. Nyhan, M. Butlin and K. Viegas. Increased Tissue Transglutaminase Activity Contributes to Central Vascular Stiffness in eNOS Knockout Mice. *American Journal of Physiology-Heart and Circulatory Physiology*, 305:803-810, 2013.

205. S. Mishra, G. Melino and L. J. Murphy. Transglutaminase 2 Kinase Activity Facilitates Protein Kinase a Induced Phosphorylation of Retinoblastoma Protein. *Journal of Biological Chemistry*, 282:18108-18115, 2007.

206. G. Hasegawa, S. Motoi, Y. Ichikawa, T. Ohtsuka, S. Kumagai, M. Kikuchi, S. Yoshitaka and Y. Saito. A Novel Function of Tissue Type Transglutaminase: Protein Disulphide Isomerase. *Biochemical Journal*, 373:793-803, 2003.

207. P. G. Mastroberardino, M. G. Farrace, I. Viti, F. Pavone, G. M. Fimia, G. Melino, C. Rodolfo and M. Piacentini. Tissue Transglutaminase Contributes to the Formation of Disulphide Bridges in Proteins of Mitochondrial Respiratory Complexes. *Biochimica et Biophysica Acta* 1757:1357-1365, 2006.

208. W. Malorni, M. Farrace, P. Matarrese, A. Tinari, L. Ciarlo, P. Mousavi-Shafaei, M. D'Eletto, G. Di Giacomo, G. Melino and L. Palmieri. The Adenine Nucleotide Translocator 1 Acts As a Type 2 Transglutaminase Substrate: Implications for Mitochondrial-Dependent Apoptosis. *Cell Death and Differentiation*, 16:1480-1492, 2009.

209. V. Gentile, V. Thomazy, M. Piacentini, L. Fesus and P. Davies. Expression of tissue transglutaminase in Balb-C 3T3 fibroblasts: effects on cellular morphology and adhesion. *The Journal of Cell Biology*, 119:463-474, 1992.

210. R. Jones, B. Nicholas, S. Mian, P. Davies and M. Griffin. Reduced Expression of Tissue Transglutaminase in A Human Endothelial Cell Line Leads to Changes in Cell Spreading, Cell Adhesion And Reduced Polymerisation of Fibronectin. *Journal of Cell Science*, 110:2461-2472, 1997.

211. E. Verderio, B. Nicholas, S. Gross and M. Griffin. Regulated Expression of Tissue Transglutaminase in Swiss 3T3 Fibroblasts: Effects on the Processing of Fibronectin, Cell Attachment, and Cell Death. *Experimental Cell Research*, 239:119-138, 1998.

212. D. Menter, J. Patton, T. Updyke, R. Kerbel, M. Maamer, L. McIntire and G. Nicolson. Transglutaminase Stabilizes Melanoma Adhesion Under Laminar Flow. *Cell Biophysics*, 18:123-143, 1991.

213. E. K. LeMosy, H. P. Erickson, W. F. Beyer, J. T. Radek, J. M. Jeong, S. Murthy and L. Lorand. Visualization of Purified Fibronectin Transglutaminase Complexes. *Journal of Biological Chemistry*, 267:7880-7885, 1992.

214. P. Turner and L. Lorand. Complexation of Fibronectin with Tissue Transglutaminase. *Biochemistry*, 28:628-635, 1989.

215. S. S. Akimov, D. Krylov, L. F. Fleischman and A. M. Belkin. Tissue Transglutaminase is an Integrin Binding Adhesion Coreceptor for Fibronectin. *The Journal of Cell Biology*, 148:825-838, 2000.

216. J. T. Radek, J. M. Jeong, S. Murthy, K. C. Ingham and L. Lorand. Affinity of Human Erythrocyte Transglutaminase for a 42 kDA Gelatin Binding Fragment of Human Plasma Fibronectin. *Proceedings of the National Academy of Sciences*, 90:3152-3156, 1993.

217. L. Lorand, J. Dailey and P. Turner. Fibronectin as a Carrier for the Transglutaminase from Human Erythrocytes. *Proceedings of the National Academy of Sciences*, 85:1057-1059, 1988.

218. A. Janiak, E. A. Zemskov and A. M. Belkin. Cell Surface Transglutaminase Promotes RhoA Activation via Integrin Clustering and Suppression of the Src p190RhoGAP Signaling Pathway. *Molecular Biology of the Cell*, 17:1606-1619, 2006.

219. X. Xian, S. Gopal and J. R. Couchman. Syndecans as Receptors and Organizers of the Extracellular Matrix. *Cell and Tissue Research*, 339:31-46, 2010.

220. H. Lortat-Jacob, I. Burhan, A. Scarpellini, A. Thomas, A. Imberty, R. R. Vives, T. Johnson, A. Gutierrez and E. A. Verderio. Transglutaminase 2 Interaction with Heparin

Identification of a Heparin Binding Site That Regulates Cell Adhesion To Fibronectin-Transglutaminase 2 Matrix. *Journal of Biological Chemistry*, 287:18005-18017, 2012.

221. Z. Wang, R. J. Collighan, S. R. Gross, E. H. Danen, G. Orend, D. Telci and M. Griffin. RGD-Independent Cell Adhesion via A Tissue Transglutaminase-Fibronectin Matrix Promotes Fibronectin Fibril Deposition and Requires Syndecan-4/2 and α5β1 Integrin co-signaling. *Journal of Biological Chemistry*, 285:40212-40229, 2010.

222. E. A. Zemskov, E. Loukinova, I. Mikhailenko, R. A. Coleman, D. K. Strickland and A. M. Belkin. Regulation of Platelet Derived Growth Factor Receptor Function by Integrin Associated Cell Surface Transglutaminase. *Journal of Biological Chemistry*, 284:16693-16703, 2009.

223. R. Dardik and A. Inbal. Complex Formation Between Tissue Transglutaminase II (tTG) and Vascular Endothelial Growth Factor Receptor 2 : Proposed Mechanism for Modulation of Endothelial Cell Response to Vascular Endothelial Growth Factor. *Experimental Cell Research*, 312:2973-2982, 2006.

224. R. Dardik, J. Loscalzo, R. Eskaraev and A. Inbal. Molecular Mechanisms Underlying the Proangiogenic Effect of Factor XIII. *Arteriosclerosis, Thrombosis, and Vascular Biology*, 25:526-532, 2005.

225. L. Faverman, L. Mikhaylova, J. Malmquist and M. Nurminskaya. Extracellular Transglutaminase 2 Activates β-catenin Signaling in Calcifying Vascular Smooth Muscle Cells. *FEBS letters*, 582:1552-1557, 2008.

226. L. Xu, S. Begum, J. D. Hearn and R. O. Hynes. GPR56, an Atypical G Protein-Coupled Receptor, Binds Tissue Transglutaminase, TG2, and Inhibits Melanoma Tumor Growth And Metastasis. *Proceedings of the National Academy of Sciences*, 103:9023-9028, 2006.

227. M. Antonyak, L. Bo, K. Lindsey, J. Johnson, J. Druso, K. Bryant, D. Holowka, R. Cerione and L. Boroughs. Cancer Cell Derived Microvesicles Induce Transformation by Transferring Tissue Transglutaminase and Fibronectin to Recipient Cells. *Proceedings of the National Academy of Sciences*, 108:17569-17569, 2011.

228. M. B. Atkins, M. Hidalgo, W. M. Stadler, T. F. Logan, J. P. Dutcher, G. R. Hudes, Y. Park, S.-H. Liou, B. Marshall and J. P. Boni. Randomized Phase II Study Of Multiple Dose Levels of Cci-779, a Novel Mammalian Target of Rapamycin Kinase Inhibitor, in Patients with Advanced Refractory Renal Cell Carcinoma. *Journal of Clinical Oncology*, 22:909-918, 2004.

229. P. H. Patel, R. S. Chaganti and R. J. Motzer. Targeted Therapy for Metastatic Renal Cell Carcinoma. *British Journal of Cancer*, 94:614-619, 2006.

230. R. M. Bukowski, T. Olencki, Q. Wan, D. Peereboom, G. T. Budd, P. Elson, K. Sandstrom, L. Tuason, P. Rayman and R. Tubbs. Phase II Trial of Interleukin 2 and Interferon Ce in Patients with Renal Cell Carcinoma: Clinical Results and Immunologic Correlates of Response. *Journal of Immunotherapy*, 20:301-311, 1997.

231. J. D. Hunt, O. L. Van der Hel, G. P. McMillan, P. Boffetta and P. Brennan. Renal Cell Carcinoma in Relation to Cigarette Smoking: Meta Analysis of 24 Studies. *International Journal of Cancer*, 114:101-108, 2005.

232. B. A. Van Dijk, L. J. Schouten, L. A. Kiemeney, R. A. Goldbohm and P. A. Van den Brandt. Vegetable and Fruit Consumption and Risk of Renal Cell Carcinoma: Results from the Netherlands Cohort Study. *International Journal of Cancer*, 117:648-654, 2005.

233. I. Ishikawa, Y. Saito, M. Asaka, N. Tomosugi, T. Yuri, M. Watanabe and R. Honda. Twenty-Year Follow Up of Acquired Renal Cystic Disease. *Clinical Nephrology*, 59:153-159, 2003.

234. F. Latif, K. Tory, J. Gnarra, M. Yao, F.-M. Duh, M. L. Orcutt, T. Stackhouse, I. Kuzmin, W. Modi and L. Geil. Identification of the Von Hippel Lindau Disease Tumor Suppressor Gene. *Science*, 260:1317-1320, 1993.

235. A. G. Knudson. Mutation and Cancer: Statistical Study of Retinoblastoma. *Proceedings of the National Academy of Sciences*, 68:820-823, 1971.

236. Brian I Rini and M. B. Atkins. Resistance to Targeted Therapy in Renal Cell Carcinoma. *Lancet Oncology*, 10:992-1000, 2009

237. T. Kamura, D. Koepp, M. Conrad, D. Skowyra, R. Moreland, O. Iliopoulos, W. Lane, W. Kaelin, S. Elledge and R. Conaway. Rbx1, A Component of the VHL Tumor Suppressor Complex and SCF Ubiquitin Ligase. *Science*, 284:657-661, 1999.

238. D. Shweiki, A. Itin, D. Soffer and E. Keshet. Vascular Endothelial Growth Factor Induced by Hypoxia may Mediate Hypoxia Initiated Angiogenesis. *Nature*, 359:843-845, 1992.

239. J. I. Bárdos and M. Ashcroft. Hypoxia Inducible Factor α1 and Oncogenic Signalling. *Bioessays*, 26:262-269, 2004.

240. N. J. Vogelzang and W. M. Stadler. Kidney Cancer. *The Lancet*, 352:1691-1696, 1998.

241. Brian I Rini, Steven C Campbell and B. Escudier. Renal Cell Carcinoma. *Lancet*, 373:1119–1132, 2009.

242. R. J. Motzer, B. Escudier, S. Oudard, T. E. Hutson, C. Porta, S. Bracarda, V. Grünwald, J. A. Thompson, R. A. Figlin and N. Hollaender. Phase 3 Trial of Everolimus for Metastatic Renal Cell Carcinoma. *Cancer*, 116:4256-4265, 2010.

243. G. Sonpavde, T. E. Hutson and B. I. Rini. Axitinib for Renal Cell Carcinoma. *Expert Opinion on Investigational Drugs*, 17:741-748, 2008.

244. A. A. Elfiky and G. Sonpavde. Novel Molecular Targets for the Therapy of Renal Cell Carcinoma. *Discovery Medicine*, 13:461-471, 2012.

245. M. J. Park, H. W. Baek, Y.-Y. Rhee, C. Lee, J. W. Park, H. W. Kim and K. C. Moon. Transglutaminase 2 Expression and Its Prognostic Significance in Clear Cell Renal Cell Carcinoma. *Journal of Pathology and Translational Medicine*, 49:37-43, 2015.

246. B. Min, H. Park, S. Lee, Y. Li, J. Choi, J. Lee, J. Kim, Y. Choi, Y. Kwon and H. Lee. CHIP Mediated Degradation of Transglutaminase 2 Negatively Regulates Tumor Growth and Angiogenesis in Renal Cancer. *Oncogene*, 15:1-11, 2015.

247. B. M. Ku, D.-S. Kim, K.-H. Kim, B. C. Yoo, S.-H. Kim, Y. D. Gong and S. Y. Kim. Transglutaminase 2 Inhibition Found to Induce p53 Mediated Apoptosis in Renal Cell Carcinoma. *The Faseb Journal*, 27:3487-3495, 2013.

248. J. Kang, J. Lee, D. Hong, S. Lee, N. Kim, W. Lee, T. Sung, Y. Gong and S. Kim. Renal Cell Carcinoma Escapes Death by p53 Depletion Through Transglutaminase 2 Chaperoned Autophagy. *Cell Death and Disease*, 7:2163-2175, 2016.

249. B. Messner, I. Zeller, C. Ploner, S. Frotschnig, T. Ringer, A. Steinacher-Nigisch, A. Ritsch, G. Laufer, C. Huck and D. Bernhard. Ursolic Acid Causes DNA Damage, P53 Mediated, Mitochondria and Caspase Dependent Human Endothelial Cell Apoptosis, and Accelerates Atherosclerotic Plaque Formation In Vivo. *Atherosclerosis*, 219:402-408, 2011.

250. E. A. Verderio, D. Telci, A. Okoye, G. Melino and M. Griffin. A Novel RGD-Independent Cell Adhesion Pathway Mediated by Fibronectin Bound Tissue Transglutaminase Rescues Cells from Anoikis. *Journal of Biological Chemistry*, 278:42604-42614, 2003.

251. D. Y. Chau, R. J. Collighan, E. A. Verderio, V. L. Addy and M. Griffin. The Cellular Response to Transglutaminase Cross-Linked Collagen. *Biomaterials*, 26:6518-6529, 2005.

252. Z. Wang, D. Telci and M. Griffin. Importance of Syndecan4 and Syndecan2 in Osteoblast Cell Adhesion and Survival Mediated by a Tissue Transglutaminase Fibronectin Complex. *Experimental Cell Research*, 317:367-381, 2011.

253. C. Nadalutti, K. Viiri, K. Kaukinen, M. Mäki and K. Lindfors. Extracellular Transglutaminase 2 has a Role in Cell Adhesion, whereas Intracellular Transglutaminase 2 is Involved in Regulation of Endothelial Cell Proliferation and Apoptosis. *Cell Proliferation*, 44:49-58, 2011.

254. M. Roberts, S. Barry, A. Woods, P. van der Sluijs and J. Norman. PDGF Regulated Rab4 Dependent Recycling of αvβ3 Integrin from Early Endosomes is Necessary for Cell Adhesion and Spreading. *Current Biology*, 11:1392-1402, 2001.

255. M. Jović, N. Naslavsky, D. Rapaport, M. Horowitz and S. Caplan. EHD1 Regulates β1 Integrin Endosomal Transport: Effects on Focal Adhesions, Cell Spreading and Migration. *Journal of Cell Science*, 120:802-814, 2007.

256. R. T. Böttcher, C. Stremmel, A. Meves, H. Meyer, M. Widmaier, H.-Y. Tseng and R. Fässler. Sorting Nexin 17 Prevents Lysosomal Degradation of β1 Integrins by Binding to the β1 Integrin Tail. *Nature Cell Biology*, 14:584-592, 2012.

257. A. P. Mould, A. N. Garratt, J. A. Askari, S. K. Akiyama and M. J. Humphries. Identification of a Novel Anti Integrin Monoclonal Antibody that Recognises a Ligand Induced Binding Site Epitope on the β1 Subunit. *Febs Letters*, 363:118-122, 1995.

258. R. Pardi, G. Bossi, L. Inverardi, E. Rovida and J. R. Bender. Conserved Regions in the Cytoplasmic Domains of the Leukocyte Integrin Alpha L Beta 2 are Involved in Endoplasmic Reticulum Retention, Dimerization, and Cytoskeletal Association. *The Journal of Immunology*, 155:1252-1263, 1995.

259. M. R. Cera, M. Fabbri, C. Molendini, M. Corada, F. Orsenigo, M. Rehberg, C. A. Reichel, F. Krombach, R. Pardi and E. Dejana. JAM A Promotes Neutrophil Chemotaxis by Controlling Integrin Internalization and Recycling. *Journal of Cell Science*, 122:268-277, 2009.

260. L. Liu, B. He, W. M. Liu, D. Zhou, J. V. Cox and X. A. Zhang. Tetraspanin CD151 Promotes Cell Migration by Regulating Integrin Trafficking. *Journal of Biological Chemistry*, 282:31631-31642, 2007.

261. J. Du, X. Chen, X. Liang, G. Zhang, J. Xu, L. He, Q. Zhan, X.-Q. Feng, S. Chien and C. Yang. Integrin Activation and Internalization on Soft ECM as a Mechanism of Induction of Stem Cell Differentiation by ECM Elasticity. *Proceedings of the National Academy of Sciences*, 108:9466-9471, 2011.

262. E. Rainero, J. D. Howe, P. T. Caswell, N. B. Jamieson, K. Anderson, D. R. Critchley, L. Machesky and J. C. Norman. Ligand Occupied Integrin Internalization Links Nutrient Signaling to Invasive Migration. *Cell Reports*, 10:398-413, 2015.

263. L. Mangala, J. Fok, I. Zorrilla-Calancha, A. Verma and K. Mehta. Tissue Transglutaminase Expression Promotes Cell Attachment, Invasion and Survival in Breast Cancer Cells. *Oncogene*, 26:2459-2470, 2007.

264. B. Felding-Habermann, T. E. O'Toole, J. W. Smith, E. Fransvea, Z. M. Ruggeri, M. H. Ginsberg, P. E. Hughes, N. Pampori, S. J. Shattil and A. Saven. Integrin Activation Controls Metastasis in Human Breast Cancer. *Proceedings of the National Academy of Sciences*, 98:1853-1858, 2001.

265. P. C. Brooks, S. Strömblad, L. C. Sanders, T. L. von Schalscha, R. T. Aimes, W. G. Stetler-Stevenson, J. P. Quigley and D. A. Cheresh. Localization of Matrix Metalloproteinase MMP2 to the Surface of Invasive Cells by Interaction with Integrin αvβ3. *Cell*, 85:683-693, 1996.

266. K. Friedrichs, P. Ruiz, F. Franke, I. Gille, H. J. Terpe and B. A. Imhof. High Expression Level of α6 Integrin in Human Breast Carcinoma is Correlated with Reduced Survival. *Cancer Research*, 55:901-906, 1995.

267. Z. Balklava, E. Verderio, R. Collighan, S. Gross, J. Adams and M. Griffin. Analysis of Tissue Transglutaminase Function In The Migration of Swiss 3t3 Fibroblasts The Active-State Conformation of the Enzyme does not Affect Cell Motility but is Important for Its Secretion. *Journal of Biological Chemistry*, 277:16567-16575, 2002.

268. S. Huveneers, H. Truong, R. Fässler, A. Sonnenberg and E. H. Danen. Binding of Soluble Fibronectin to Integrin α5β1 Link to Focal Adhesion Redistribution and Contractile Shape. *Journal of Cell Science*, 121:2452-2462, 2008.

269. T. Ng, D. Shima, A. Squire, P. I. H. Bastiaens, S. Gschmeissner, M. J.Humphries and P. J. Parker. PKCα Regulates β1 Integrin Dependent Cell Motility Through Association and Control of Integrin Traffic. *The EMBO Journal*, 18:3909–3923, 1999.